



Faculteit Farmaceutische, Biomedische en Diergeneeskundige Wetenschappen  
Departement Farmaceutische Wetenschappen  
Medicinale Chemie

**Structural investigation of two novel classes of  
quinoloxycetamide- and hydantoin-based  
antimycobacterials guided by phenotypic screening and  
targeted approaches**

Structurele exploratie van nieuwe quinoloxycetamide- en  
hydantoïne-gebaseerde antimycobacteriële verbindingen,  
gestuurd door fenotypische screening en target-specifieke  
benaderingen

Proefschrift voorgelegd tot het behalen van de graad  
van doctor in de Farmaceutische Wetenschappen  
aan de Universiteit Antwerpen, te verdedigen door

**Eleni Pitta**

**Promotoren:**  
**Prof. dr. Pieter Van der Veken**  
**Dr. Robert Bates**  
**Prof. dr. Koen Augustyns**

Antwerpen, 2017



To my family



# Table of contents

---

List of abbreviations .....	vii
1. Introduction.....	3
1.1. Background.....	3
1.2. Epidemiology .....	3
1.3. Mechanism .....	4
1.3.1. Transmission.....	4
1.3.2. Pathogenesis.....	5
1.4. Development of drug-resistant TB .....	7
1.5. TB treatment and vaccines.....	9
1.5.1. First-line treatment for drug-susceptible (DS) active TB.....	10
1.5.2. Second-line treatment for rifampicin-resistant (RR) or multidrug-resistant (MDR)-TB.....	11
1.5.2.1. Fluoroquinolones (Group A).....	12
1.5.2.2. Second-line injectable agents (Group B) .....	13
1.5.2.3. Other core second-line agents (Group C).....	14
1.5.2.4. Add-on agents (Group D).....	15
1.5.3. Vaccines.....	18
1.6. Drug discovery and hit identification .....	19
1.7. General thesis objectives.....	20
2. Quinoloxycetamide inhibitors: aims and objectives .....	25
2.1. Structure-Activity Relationship (SAR).....	27
2.2. Optimization of physicochemical properties .....	28
2.3. Elimination of toxicity.....	28
2.4. Improvement of metabolic stability.....	28

3.	Quinoloxycetamides as antimycobacterial agents .....	31
3.1.	Introduction .....	31
3.2.	Library design .....	32
3.3.	Chemistry .....	33
3.3.1.	Modification of the quinolone core .....	34
3.3.1.1.	Modification of the quinoline substitution pattern .....	34
3.3.1.2.	Replacement of quinoline with related aza-aromatic systems .....	36
3.3.1.3.	Structure elucidation .....	38
3.3.2.	Modification of the linker .....	47
3.3.3.	Modification of the northern aryl fragment .....	50
3.3.4.	Amide bond replacements .....	51
3.4.	Results and discussion .....	52
3.4.1.	Antimycobacterial activity, cytotoxicity and physicochemical properties .....	52
3.4.1.1.	Modification of the quinoline substitution pattern .....	52
3.4.1.2.	Replacement of quinoline with related aza-aromatic systems .....	54
3.4.1.3.	Modification of the linker .....	55
3.4.1.4.	Modification of the northern aryl fragment .....	57
3.4.2.	Metabolic stability studies .....	60
3.4.3.	Antimycobacterial activity, physicochemical properties and metabolic stability of compounds containing amide bond replacements .....	62
3.4.4.	Intracellular <i>M. tuberculosis</i> activity .....	63
3.4.5.	Cardiotoxicity (hERG binding assay) .....	64
3.5.	Conclusion .....	66
3.6.	Experimental section .....	67
4.	DprE1 inhibitors: aims and objectives .....	125
4.1.	DprE <sub>1</sub> as drug target .....	125
4.2.	Aims and objectives .....	127

---

4.2.1.	Improvement of safety and metabolic stability .....	130
4.2.2.	Enhancement of potency and affinity .....	131
4.2.3.	Improvement of physicochemical properties .....	131
4.2.4.	<i>In vivo</i> proof of concept.....	131
5.	DprE <sub>1</sub> inhibitors .....	135
5.1.	Design .....	135
5.2.	First round of Hit-to-Lead optimization .....	136
5.2.1.	Chemistry.....	136
5.2.1.1.	Linker modification.....	136
5.2.1.2.	Hydantoin core replacements .....	138
5.2.1.3.	Carbonitrile replacement .....	144
5.2.1.4.	Structure elucidation .....	145
5.2.2.	Results and discussion.....	148
5.2.2.1.	Linker modification.....	148
5.2.2.2.	Hydantoin modification.....	150
5.2.2.3.	Carbonitrile replacement .....	152
5.2.3.	Conclusion of the first round of Hit-to-Lead optimization .....	157
5.3.	Second round of Hit-to-Lead optimization.....	158
5.3.1.	Chemistry.....	158
5.3.2.	Results and discussion.....	159
5.3.3.	Conclusions for the second round of Hit-to-Lead optimization .....	163
5.4.	Intracellular <i>M. tuberculosis</i> activity .....	164
5.5.	Metabolic stability.....	165
5.6.	Cardiotoxicity (hERG binding assay).....	166
5.7.	General antimicrobial activity profile.....	168
5.8.	Mode of action .....	169

## Table of contents

---

5.8.1.	Evaluation against <i>M. tuberculosis</i> DprE1 overexpressor strain.....	169
5.8.2.	Evaluation against <i>M. tuberculosis</i> DprE1 mutant strains .....	171
5.8.3.	Time course curves .....	171
5.9.	Therapeutic efficacy.....	172
5.10.	Conclusion.....	173
5.11.	Experimental section .....	174
6.	Conclusions and outlook.....	205
6.	Outlook .....	205
6.1.	Quinoloxycetamide series.....	205
6.2.	Hydantoin series .....	207
7.	Summary.....	211
7.1.	Introduction .....	211
7.2.	Discovery and SAR exploration of QOA-based antimycobacterial compounds.....	211
7.3.	Identification and exploration of the hydantoins series as DprE1 inhibitors .....	214
7.3.1.	First round of Hit-to-Lead optimization .....	214
7.3.2.	Second round of Hit-to-Lead optimization .....	215
7.3.3.	Further evaluation of selected compounds.....	215
8.	Samenvatting .....	219
8.1.	Inleiding.....	219
8.2	Discovery en Structuur-Activiteitsrelatie (SAR) onderzoek op quinoloxycetamide-gebaseerde antimycobacteriële verbindingen. ....	219
8.3.	Identificatie en exploratie van een hydantoïne-gebaseerde serie DprE1 inhibitoren. ....	222
8.3.1.	Eerste cyclus van Hit-to-Lead optimalisatie.....	222
8.3.2	Tweede cyclus van Hit-to-Lead optimalisatie .....	223
8.3.3.	Uitgebreide evaluatie van geselecteerde verbindingen .....	223
	Acknowledgements.....	227



References.....	231
Curriculum Vitae.....	249



# List of abbreviations

---

$\delta$	chemical shift in parts per million
$\mu$	micro
$^{\circ}\text{C}$	degrees Celsius
1D	one-dimensional
2D	two-dimensional
3D	three-dimensional
ADME	absorption, distribution, metabolism and excretion
AIBN	2,2'-azobis(2-methylpropionitrile)
anhyd.	anhydrous
Am	amikacin
AMP	artificial membrane permeability
ATP	adenosine triphosphate
BCG	Bacillus Calmette–Guérin
Bdq	bedaquiline
br	broad signal (spectral)
calcd	calculated
CFU	colony forming unit
Cfz	clofazimine
CHI	chromatographic hydrophobicity index
chrom	chromatographic
$\text{Cl}_{\text{int}}$	intrinsic clearance
CLND	chemiluminescent nitrogen detection
Cm	capreomycin
compd	compound
COSY	correlation spectroscopy

## List of abbreviations

---

Cs	cycloserine
Cs <sub>2</sub> CO <sub>3</sub>	cesium carbonate
CuI	copper (I) iodide
d	day (s); doublet (spectral)
DCM	dichloromethane
dd	doublet of doublets (spectral)
ddd	doublets of doublets of doublets (spectral)
Ddn	F <sub>420</sub> -deazaflavin-dependent nitroreductase
DDW	Diseases of the Developing World
DHFR	dihydrofolate reductase
DHFS	dihydrofolate synthase
DHPS	dihydropteroate synthase
Dlm	delamanid
DMF	<i>N,N</i> -dimethylformamide
DMSO	dimethyl sulfoxide
DNA	deoxyribonucleic acid
DOT	directly observed therapy
DPA	decaprenylphosphoryl- $\beta$ -D-arabinofuranose
DPR	decaprenylphosphoryl- $\beta$ -D-ribose
DprE <sub>1</sub>	decaprenylphosphoryl- $\beta$ -D-ribose oxidase
DPX	decaprenylphosphoryl- $\beta$ -D-2'-keto-erythro-pentafuranose
DS	drug susceptible
DST	drug susceptibility testing
E	ethambutol
EBA	early bactericidal activity
EDTA	ethylenediaminetetraacetic acid

e.g.	for example (exempli gratia)
equiv.	equivalent
ESI	electrospray ionization
Et	ethyl
Et <sub>3</sub> N	triethylamine
Eto	ethionamide
EtOAc	ethyl acetate
EU	European Union
FAD	flavin adenine dinucleotide
FBS	fetal bovine serum
FDA	Food and Drug Administration
FPR	farnesylphosphoryl- $\beta$ -D-ribose
FPX	farnesylphosphoryl- $\beta$ -D-2'-keto-erythro-pentafuranose
g	gram(s)
Gfx	gatifloxacin
GSK	GlaxoSmithKline
h	hour(s); human
H	isoniazid
H2L	Hit-to-Lead
HCl	hydrochloric acid
HepG2	human liver hepatocellular carcinoma cell line
hERG	human Ether-à-go-go-Related Gene
HIV	human immunodeficiency virus
HRMS	high resolution mass spectrometry
HPLC	high-performance liquid chromatography; high-pressure liquid chromatography
HSAB	Hard and Soft Acids and Bases

## List of abbreviations

---

HSQC	heteronuclear single-quantum correlation spectroscopy
HMBC	heteronuclear multiple-bond correlation spectroscopy
HTS	high throughput screening
Hz	hertz
IC <sub>50</sub>	half maximal inhibitory concentration
Imp	imipenem
<i>J</i>	coupling constant (in NMR spectrometry)
K <sub>2</sub> CO <sub>3</sub>	potassium carbonate
Km	kanamycin
Lfx	levofloxacin
L	liter(s)
LC-MS	liquid chromatography-mass spectrometry
LLE	lipophilic ligand efficiency
logD	distribution coefficient
LTBI	latent tuberculosis infection
Lzd	linezolid
m	multiplet (spectral); meter(s); milli; meta
M	molar (moles per liter)
M <sup>+</sup>	parent molecular ion
max	maximum
MBC	minimal bactericidal concentration
MDR-TB	multidrug-resistant tuberculosis
MDT	multidrug therapy
Me	methyl
MEM	Minimum Essential Medium
MeOH	methanol

---

Mfx	moxifloxacin
MIC	minimal inhibitory concentration
min	minute(s); minimum
mL	milliliter
mM	millimolar (millimoles per liter)
MOE	molecular operating environment
mol	mole(s); molecular (as in mol wt)
mp	melting point
Mpm	meropenem
<i>Mtb</i>	<i>Mycobacterium tuberculosis</i>
<i>M. tuberculosis</i>	<i>Mycobacterium tuberculosis</i>
MW	molecular weight
m.w.	microwave irradiation
<i>m/z</i>	mass-to-charge ratio
NEAA	Non-Essential Amino Acid
nm	nanometer(s)
NMR	nuclear magnetic resonance
NOE	nuclear Overhauser effect spectroscopy
<i>o</i>	ortho
OD600	optical density at 600 nm
q	quartet (spectral)
quint	quintet (spectral)
<i>p</i>	para
PAS	<i>p</i> -aminosalicylic acid
PBr <sub>3</sub>	phosphorus tribromide
PBS	phosphate buffered saline

## List of abbreviations

---

Ph	phenyl
pIC <sub>50</sub>	-log <sub>10</sub> (IC <sub>50</sub> )
PMA	phorbol myristate acetate
ppm	part(s) per million
Pr	propyl
Pto	prothionamide
R	rifampicin
R&D	research and development
R <sub>f</sub>	retention factor (in chromatography)
RNA	ribonucleic acid
RPMI medium	Roswell Park Memorial Institute medium
RR-TB	rifampicin-resistant tuberculosis
rt	room temperature
RT	retention time
s	singlet (spectral); second(s)
S	streptomycin
SAR	structure-activity relationship
t	triplet (spectral)
T	thioacetazone
t <sub>1/2</sub>	half-life time
TB	tuberculosis
TEA	trimethylamine
TFA	trifluoroacetic acid
THF	tetrahydrofuran
THP-1	human acute monocytic leukemia cell line
TLC	thin layer chromatography



TMEDA	tetramethylethylenediamine
Trz	terizidone
XDR-TB	extensively drug-resistant tuberculosis
WHO	World Health Organization
Z	pyrazinamide



# Chapter 1

---

*Introduction*



## 1. Introduction

### 1.1. Background

Tuberculosis (TB), in the past also called phthisis, phthisis pulmonalis, or consumption, is a widespread, and in many cases fatal, infectious disease caused by *Mycobacterium tuberculosis*.<sup>1</sup> It is an ancient scourge that has plagued humankind throughout known history and human prehistory.<sup>2</sup> In the beginning of the 19<sup>th</sup> century people began to understand the pathogenesis of TB with the work of Theophile Laennec. In 1865, Jean-Antoine Villemin demonstrated the transmissibility of *M. tuberculosis* infection, while in 1882 Robert Koch identified the tubercle bacillus as the etiologic agent for TB.<sup>2</sup> *M. tuberculosis* is an aerobic, acid-fast, non-motile, non-encapsulated, non-spore forming bacillus. It grows most successfully in tissues with high oxygen content, such as the lungs.<sup>3</sup> The classic clinical features of pulmonary TB include chronic cough, sputum production, appetite loss, weight loss, fever, night sweats and hemoptysis.<sup>3,4</sup>

The discovery of the first anti-TB drugs (streptomycin, *p*-aminosalicylic acid, isoniazid) in the 1940s and 50s followed by combination chemotherapy, made TB a curable disease. However, hopes of completely eliminating TB from the population were dashed after the rise of drug-resistant strains in the 1980s.<sup>5</sup> In that time, it was realized that TB had not only ceased to decline in the developed countries, notably the USA, but was actually increasing, particularly in major cities.<sup>6</sup> It was also soon realized that the disease was out of control and increasing at an alarming rate across most of the poorest regions of the world especially Africa due to human immunodeficiency virus (HIV) co-infection.<sup>7</sup> The subsequent resurgence of TB resulted in the declaration of a global health emergency by the World Health Organization (WHO) in 1993.<sup>8</sup> Hopes of totally controlling the disease have been dramatically dampened because of a number of factors, including the difficulty of developing an effective vaccine, the expensive and time-consuming diagnostic process, the necessity of many months of treatment, the increase in HIV-associated TB, and the emergence of drug-resistant cases in the 1980s.<sup>3</sup>

### 1.2. Epidemiology

The WHO estimates that one-third of the world's population is infected with *M. tuberculosis*, however, most infections do not cause TB disease and 90–95% of infections remain asymptomatic.<sup>8,9</sup>

Although TB mortality has fallen 47% since 1990, with nearly all of that improvement taking place since 2000, and TB incidence has fallen to 18% lower than the level of 2000, TB still remains one of the world's biggest health threats. In 2015, an estimated 10.4 million people developed TB (including 1.2 million among HIV-positive people) (Figure 1.1, A) and 1.4 million died from the disease.<sup>10</sup>

The Global Project on Anti-Tuberculosis Drug Resistance Surveillance has been gathering data since 1994. The percentage of new TB cases with multidrug-resistant (MDR) TB as well as any other patient with TB resistant to rifampicin (RR), referred as MDR/RR-TB, are shown in Figure 1.1, B. As the data indicate, almost every region of the world has reported MDR/RR-TB cases. Globally in 2015, there were an estimated 580 000 incident cases of MDR/RR-TB and approximately 250 000 deaths from MDR/RR-TB. On average, an estimated 9.5% of patients with MDR-TB had extensively drug-resistant TB (XDR-TB).<sup>10</sup>

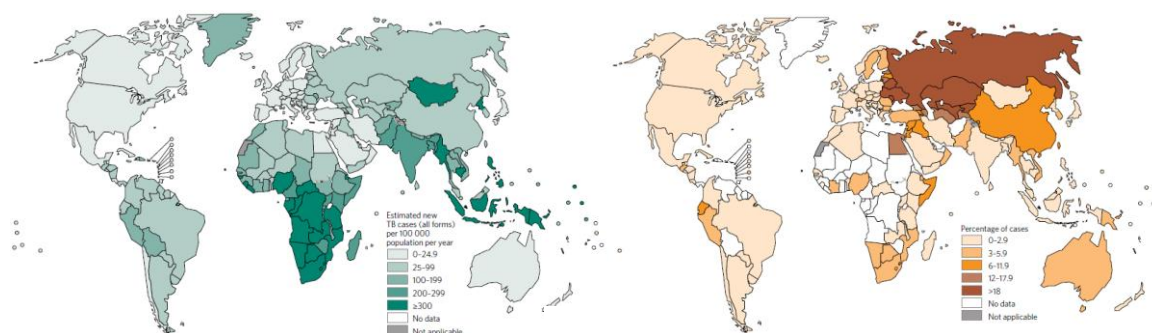


**Figure 1.1. (A) Estimated TB incidence rates in 2015; (B) Percentage of new TB cases with MDR/RR-TB (the most recent year for which data have been reported).<sup>10</sup>**

From 2016, the End TB Strategy will be implemented with the goal to end the global TB epidemic. In May 2014, the World Health Assembly adopted this strategy to reduce the number of TB deaths by 90% by 2030 (compared with 2015 levels), cut new cases by 80% and ensure that no family is burdened with catastrophic costs due to TB.

## 1.3.Mechanism

### 1.3.1. Transmission

*M. tuberculosis* is transmitted when a patient with pulmonary TB expels droplet nuclei into the air (usually by coughing), which are then inhaled by a susceptible person.<sup>11</sup> The diameter of an infectious droplet nucleus is approximately 1 to 3  $\mu\text{m}$  and its content is one to three bacilli. It was demonstrated that particles so small remain airborne as droplet nuclei with a half-life of about 6 h.<sup>12</sup>

There are three distinct outcomes to this inhalation. The best outcome is that the bacteria do not establish infection or the initial infection is completely eradicated by the host's immune system. Alternatively, the bacteria are not fully eradicated but controlled in a dormant state, called latent TB infection (LTBI) which is by definition asymptomatic. The third possible outcome is progression to active TB.<sup>11</sup> This progression occurs anytime from immediately to decades after infection. Approximately 5-10% of people with LTBI eventually progress to active TB, but patients with an impaired immune response (e.g. HIV/AIDS) have a much higher risk of progression to active TB. In other words, there is only a 5-10% lifetime chance that the latent infection will progress to active tuberculous disease.

### 1.3.2. Pathogenesis

*M. tuberculosis* usually enters the alveolar passages of exposed humans in an aerosol droplet exhaled into the atmosphere by an individual with active disease. *M. tuberculosis* is taken up by phagocytic cells and transported across the alveolar epithelium into the lung.<sup>13</sup> The process of phagocytosis is initiated by bacterial contact with macrophage multiple cell surface receptors such as mannose receptor, complement receptors, and Fc receptors.<sup>14</sup> On entry into a host macrophage, *M. tuberculosis* initially resides in an endocytic vacuole called the phagosome.<sup>15</sup> However, in contrast to the normal course of events during which the phagocytosed cargo is shuttled to lysosomes where it is efficiently destroyed, following uptake, mycobacteria are able to block their delivery to lysosomes.<sup>16</sup> By escaping phagosome-lysosome fusion, the intracellular bacilli are able to avoid killing and continue to multiply, eventually leading to lysis of the infected cells.

Infected macrophages recruit additional macrophages and other immune cells from neighbouring blood vessels to form dynamic, organized structures called granulomas, which are a pathological hallmark of TB (Figure 1.2).<sup>13</sup> The granuloma consists of a kernel of infected macrophages surrounded by foamy macrophages and other mononuclear phagocytes, with a mantle of lymphocytes in association with a fibrous cuff of vessel collagen and other extracellular matrix components that delineate the periphery of the structure.<sup>17</sup> If the infection is successfully contained, the granuloma shrinks and may eventually calcify.<sup>18</sup>

If however, the immune response does not successfully control the bacterial replication, the granulomas increase in size and cellularity. In the later stages, granuloma develops central areas of necrosis (called caseum, from the word 'cheese'), resulting in the death of the majority of the bacteria and destruction of the surrounding host tissue.<sup>16</sup> The caseum initially forms in the centre of the granuloma and spreads outwards, eventually compressing the surrounding lung tissue and

destroying the vasculature (Figure 1.2).<sup>19</sup> Although *M. tuberculosis* bacilli are postulated to be unable to multiply within this caseous tissue due to its acidic pH, the low availability of oxygen, and the presence of toxic fatty acids, some organisms may remain dormant but alive for decades.<sup>15</sup> The strength of the host cellular immune response determines whether an infection is arrested here or progresses to the next stages.

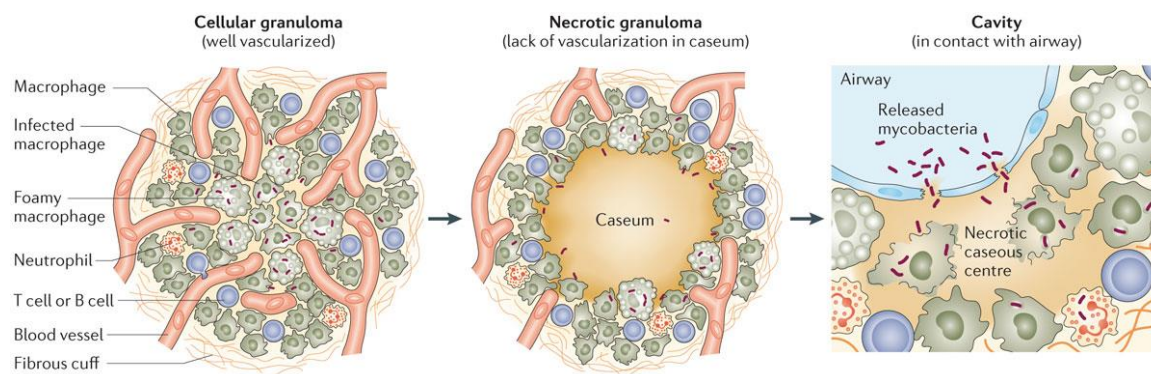


**Figure 1.2. Morphology of cellular granuloma, necrotic granuloma and cavity.**<sup>13</sup>

Containment usually fails when the immune status of the host changes, which is usually a consequence of old age, malnutrition or co-infection with HIV - basically any condition that reduces the number, or impairs the function, of CD4+ T cells. If the granuloma is close to the surface of the lung, the tissue destruction caused by necrosis can breach the mucosal surface, giving rise to the prototypic symptom of TB, a persistent cough with blood in the sputum, a process referred to as cavitation (Figure 1.2). At this point the patient is highly infectious, spreading the bacteria by aerosol.<sup>18</sup>

Granuloma formation is commonly referred to as a host-protective strategy to limit mycobacterial replication and prevent the spread of infection. However, within the granulomatous environment, *M. tuberculosis* may be shielded from immune-based killing mechanisms, and anti-TB drugs may have limited penetration into this compartment. Recent molecular studies indicate that *M. tuberculosis* possesses mechanisms that deliberately promote cellular recruitment to the nascent granuloma, suggesting that granuloma formation is part of a pathogen-directed virulence programme.<sup>20</sup> This tissue response typifies the 'containment' phase of the infection in which there are no overt signs of disease and the host does not transmit the infection to others.



## 1.4. Development of drug-resistant TB

Although the etiologic agent for TB was found in 1882, more than 130 years ago, the disease still remains a public health concern. One of the main reasons is mycobacterium's ability to adapt easily to different environments. As a consequence of genetic transformation, drug resistance is frequently encountered after exposure to a certain medicine.<sup>21</sup> In 1947, shortly after the introduction of streptomycin as monotherapy for TB, high rates of treatment failure were observed as a result of the development of streptomycin-resistant strains.<sup>22</sup> Therapy with a single drug results into rapid selection of drug-resistant mutants, which will dominate and eventually will lead to relapse. Simultaneous occurrence of multiple resistance mutations in cells is less probable with an increased number of combined drugs. In other words, the risk of selecting resistant mutants in a susceptible population of *M. tuberculosis* is reduced effectively by combining two or more anti-TB drugs. The recognition of this phenomenon led to the principle of multi-agent chemotherapy for TB in 1950,<sup>23</sup> which efficiently controlled TB pandemic for the next decades. However, in the early 90s, the emergence of MDR-TB in the United States reawakened public concern.<sup>24</sup> In subsequent years, drug-resistant TB has been recognized as a potentially catastrophic challenge to global public health.<sup>5</sup>

Molecular genetic studies showed that resistance to anti-TB drugs in *M. tuberculosis* arises from naturally occurring spontaneous chromosomal mutations at low frequency.<sup>25</sup> The presence of an anti-TB drug exhibits selective pressure that favors multiplication only of the resistant bacilli. Mutations in genes encoding drug targets or drug activating enzymes have been found in drug-resistant strains against all first-line drugs and some second-line drugs.<sup>26</sup> MDR-TB strains could arise by sequential acquisition of single drug resistances.<sup>27</sup>

Drug resistance is divided into 2 types: primary drug resistance and acquired drug resistance. Primary resistance arises in people who have never taken anti-TB drugs and apparently were infected with a resistant strain of *M. tuberculosis*. Acquired resistance develops during therapy for TB and some of the common causes are misuse of anti-TB drugs, prescription of inadequate treatment regimen, irregular drug supply, poor drug quality with low bioavailability and poor compliance.<sup>5</sup>

Global efforts to control the TB pandemic have been challenged by the emergence and spread of strains that are resistant to the commonly used first-line anti-TB drugs isoniazid (H), rifampicin (R), ethambutol (E) and pyrazinamide (Z).

MDR-TB is defined as TB caused by *M. tuberculosis* bacilli that are resistant to at least isoniazid and rifampicin. MDR-TB treatment is rather complicated as it requires second-line drugs. Some of these can only be administered parenterally and most are less efficacious, more toxic and/or more expensive than the first-line agents and treatment generally lasts from 9-12 months to 18 months or more.<sup>28</sup> Only around 50-60% of MDR-TB patients will be cured, in comparison with 95%–97% cure rate for patients with drug-susceptible (DS) strains treated with first-line drugs.<sup>29</sup> Globally, in 2015 an estimated 3.9% of new cases and 21% of previously treated cases have MDR-TB.<sup>10</sup> The recent emergence of XDR-TB has further complicated the problem. XDR-TB is caused by *M. tuberculosis* bacilli that are resistant to rifampicin, isoniazid, plus any fluoroquinolone and at least one of the three injectable second-line drugs: amikacin, kanamycin and capreomycin. In 2015, the average proportion of MDR-TB cases with XDR-TB was 9.5%.<sup>10</sup>

The TB situation has also worsened since the appearance of HIV. Co-infection with HIV can weaken the host immune system and induce both endogenous reactivation and exogenous re-infection with TB. Drug-resistant TB and HIV co-infection is a lethal combination that presents a serious challenge for effective TB control.<sup>25</sup>

Drug susceptibility testing (DST) is an *in vitro* assay that determines resistance to a given drug. Universal DST is essential to ensure that patients are correctly diagnosed and have access to the appropriate treatment. DST for TB is divided in two different types, phenotypic or genotypic testing. As the standard method for diagnosing active TB, phenotypic testing involves sputum microscopy and culture of *M. tuberculosis* in the presence of anti-TB drugs in order to detect growth (indicating drug resistance) or inhibition (indicating drug susceptibility).<sup>4</sup> Because of the slow growth of *M. tuberculosis*, conventional drug susceptibility testing takes 3-12 weeks to complete.<sup>27</sup> Genotypic based assays include two main types, the Line-probe Hybridization Assays and Molecular Beacon Assays. The newly introduced Xpert MTB/RIF Assay is a diagnostic test that utilizes molecular beacon technology and can be used with minimal technical expertise, enabling rapid diagnosis of TB and simultaneous assessment of rifampicin resistance within 2 hours.<sup>11,30</sup> According to WHO recommendations, it should be used as an initial diagnostic test for people at risk of drug-resistant TB and HIV-positive individuals.<sup>31</sup>

Containment of MDR- and XDR-TB will be extremely difficult without treatment regimens that are shorter, safer, more effective, and less expensive than those that are available.<sup>32</sup> New drugs with novel mechanisms of action are needed for the effective management of MDR- and XDR-TB.

## 1.5.TB treatment and vaccines

There was no known anti-TB chemotherapy until the 1940s. In that decade, introduction of streptomycin and p-aminosalicylic acid (PAS) as anti-TB drugs led to a TB chemotherapy revolution, as TB mortality rates were considerably reduced.<sup>33</sup> Subsequently, other anti-TB drugs were also developed, such as isoniazid, ethambutol and rifampicin, among others. The introduction of rifampicin into clinical practice in the 1960s was a major breakthrough that allowed treatment duration to be shortened to 9 months, and when used in a regimen that also contained pyrazinamide, to 6 months.<sup>30</sup>

The discovery of the antitubercular drugs is presented chronologically in Figure 1.3.

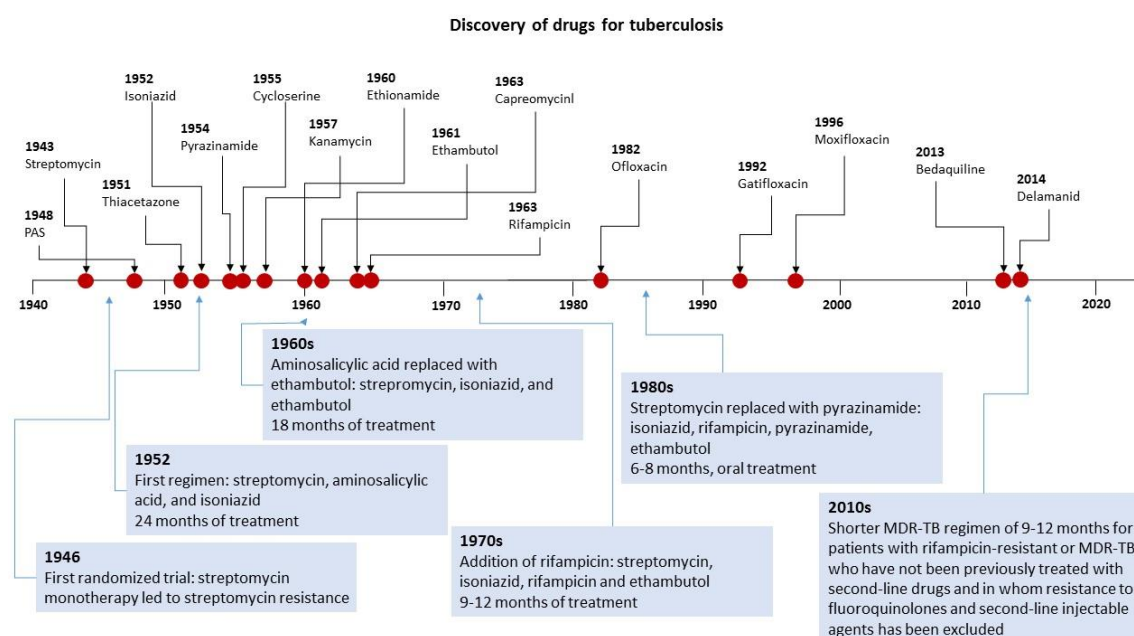


**Figure 1.3. History of drug discovery and development of treatment regimens for TB (adopted from ref. <sup>32</sup>)**

Since 1950 and the widespread use of chemotherapy, the annual risk of infection had been declining at a rate of nearly 10% per year.<sup>33</sup> During the same period, the anti-TB drug pipeline and TB drug Research and Development (R&D) were almost non-existent, since TB was perceived no longer to be a disease of significance. However, this attitude contrasts sharply with figures from the World Health Organization (WHO) after 1985. Increasing rates of drug resistance, co-infection with HIV, poor infection control practices, and the problems caused by international migration are among the issues of concern related to TB.<sup>34</sup> It becomes apparent that TB represents a major global health emergency and new anti-TB drugs are urgently required.

Nowadays, anti-TB drugs can be broadly categorized into 2 groups based on clinical uses, namely (i) first-line for drug-susceptible active TB and (ii) second-line drugs for drug-resistant TB.

### 1.5.1. First-line treatment for drug-susceptible (DS) active TB

Treatment of drug-susceptible (DS) active TB involves a short-course therapeutic regimen comprising first-line drugs (isoniazid, rifampicin, pyrazinamide and ethambutol, Figure 1.4) for the first 2 months followed by a continuation phase of isoniazid and rifampicin for the last 4 months. Up to 95% of people with DS-TB can be cured in 6 months.<sup>35</sup> Directly observed therapy (DOT) and follow-up support are necessary in order to ensure patient compliance and TB treatment.

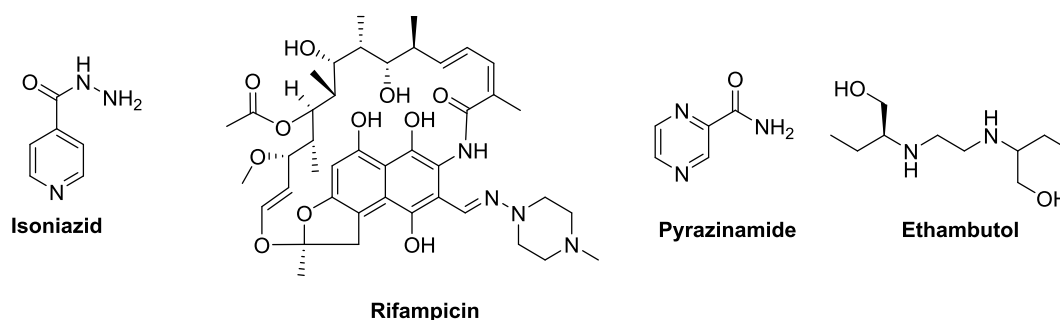


Figure 1.4. Chemical structures of first-line drugs against TB.

#### Isoniazid (H)

Since its introduction in 1952, it has been one of the most effective and key drugs for treatment of TB. Isoniazid is only active against growing tubercle bacilli and is not active against non-replicating bacilli or under anaerobic conditions.<sup>36</sup> Isoniazid is a prodrug and must be activated by a bacterial catalase-peroxidase enzyme in *M. tuberculosis* encoded KatG.<sup>37</sup> Its target is an enoyl-[acyl-carrier-protein] reductase which participates in mycolic acid synthesis.<sup>38</sup> The most significant adverse reactions associated with isoniazid administration are hepatotoxicity and neurotoxicity.<sup>36</sup>

#### Rifampicin (R)

Rifampicin is a semisynthetic derivative of the natural rifamycins (a large family of structurally related compounds), first synthesized in 1959.<sup>39</sup> In 1967, it was introduced in TB therapy which allowed a reduction in the duration of treatment from 18 to 9 months.<sup>40</sup> Rifampicin acts by binding to the  $\beta$ -subunit of RNA polymerase (rpoB), the enzyme responsible for transcription and expression of mycobacterial genes, resulting in inhibition of bacterial transcription activity.<sup>41</sup> An important characteristic of rifampicin is that it is active against actively growing and slowly metabolizing (non-growing) bacilli.<sup>36</sup> However, a major drawback of rifamycins is that they induce

cytochromes P-450 in the liver, which leads to drug–drug interactions with antiretroviral agents and other TB drug candidates.<sup>42</sup>

### **Pyrazinamide (Z)**

In 1972, it was found that pyrazinamide, an analogue of nicotinamide, has remarkable cidal activity. When added to regimens containing rifampicin, it is responsible for much of the killing of persisting tubercle bacilli allowing treatment to be shortened from 9 months to 6 months.<sup>43</sup> It is also a cornerstone drug for the treatment of MDR-TB. Pyrazinamide inhibits protein and RNA synthesis and serine uptake as well as disruption of membrane potential at acidic pH.<sup>44</sup>

### **Ethambutol (E)**

Ethambutol, discovered in 1961, is a first-line drug for treating all forms of TB. The primary mode of action of ethambutol appears to be inhibition of arabinogalactan synthesis by targeting arabinosyl transferases.<sup>45</sup> Soon after its introduction for TB treatment, it was found that its main adverse effect is ‘toxic amblyopia’.<sup>46</sup> Because of the potentially serious nature of this complication there has been considerable reluctance to use ethambutol in young children.

## **1.5.2. Second-line treatment for rifampicin-resistant (RR) or multidrug-resistant (MDR)-TB**

Second-line drugs are used for treatment of TB that is resistant to first-line drugs, and can be further categorized as shown in Table 1.1.

**Table 1.1. Medicines recommended for the treatment of rifampicin-resistant and multidrug-resistant TB.<sup>28</sup>**

<b>A. Fluoroquinolones<sup>a</sup></b>	Levofloxacin Moxifloxacin Gatifloxacin	Lfx Mfx Gfx
<b>B. Second-line injectable agents</b>	Amikacin Capreomycin Kanamycin (Streptomycin)	Am Cm KM (S)
<b>C. Other core second-line agents<sup>a</sup></b>	Ethionamide / Prothionamide Cycloserine / Terizidone Linezolid Clofazimine	Eto / Pto Cs/Trd Lzd Cfz

<b>D. Add-on agents</b>	<b>D1</b>	Pyrazinamide Ethambutol High-dose isoniazid	Z E H <sup>h</sup>
	<b>D2</b>	Bedaquiline Delamanid	Bdq Dlm
	<b>D3</b>	p-aminosalicylic acid Imipenem-cilastatin <sup>b</sup> Meropenem <sup>b</sup> Amoxicillin-clavulanate <sup>b</sup> (Thioacetazone) <sup>c</sup>	PAS Ipm Mpm Amx-Clv (T)

<sup>a</sup>Medicines in Groups A and C are shown by decreasing order of usual preference for use

<sup>b</sup>Carbapenems and clavulanate are meant to be used together; clavulanate is only available in formulations combined with amoxicillin

<sup>c</sup>HIV-status must be tested and confirmed to be negative before thioacetazone is started

### 1.5.2.1. Fluoroquinolones (Group A)

Fluoroquinolones are a family of broad spectrum, systemic antibacterial agents that have been used widely as therapy of respiratory and urinary tract infections. This group of drugs is considered to be the most important component of the core MDR-TB regimen and the benefits from their use outweighs potential risks: they should therefore always be included unless there is an absolute contra-indication for their use.

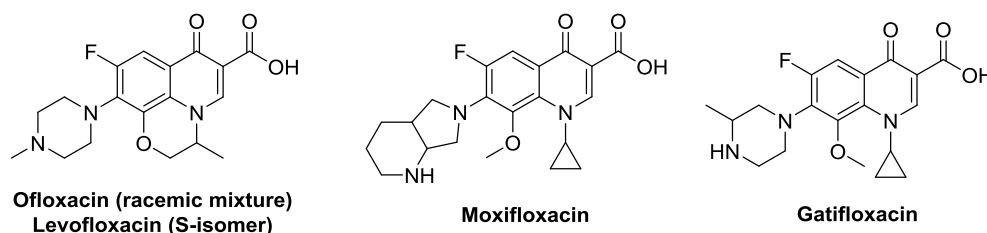


**Figure 1.5. Chemical structures of fluoroquinolones (Group A).**

High dose of levofloxacin (Lfx), moxifloxacin (Mfx), and gatifloxacin (Gfx) (Figure 1.5) are the most common used for MDR-TB treatment. This class of antibiotics inhibits DNA gyrases and thus prevents bacterial DNA synthesis.<sup>47</sup> Overall these drugs are well tolerated and have a generally good safety record in long-term administration, although moxifloxacin has potential to prolong the QT interval and this has raised concerns especially when used in combination with other medications which have a similar effect (including bedaquiline and delamanid). There are fewer concerns about the cardiotoxicity of levofloxacin and gatifloxacin, an important consideration given that several other second-line drugs have QT-prolonging potential.<sup>28,48</sup>

Concerns about dysglycaemia reported in 2006 in patients treated with gatifloxacin for conditions other than TB led the producing company to suspend manufacture of the drug,<sup>49</sup> and a global shortage in quality-assured formulations of this drug ensued. A trial of a four-month standardised

regimen for drug-susceptible TB which included gatifloxacin (400 mg once daily) published in 2014 reported no significant risk of hyperglycaemia associated with exposure to gatifloxacin.<sup>50</sup> Although adverse events were poorly recorded, the data for this review showed that there was a lower risk of serious adverse events (defined as grade 3-4 adverse events or drugs stopped due to adverse event) in patients taking gatifloxacin (3.6%) than in those who did not, including those receiving no fluoroquinolones (8%; not statistically significant). The frequency of SAEs associated with gatifloxacin was thus comparable to the that associated with fluoroquinolones on the meta-analysis level.<sup>28</sup>

### 1.5.2.2. Second-line injectable agents (Group B)

Since the discovery of streptomycin's (S) bactericidal activity against *M. tuberculosis*, aminoglycosides have been utilized to treat TB. Today, the aminoglycosides kanamycin (Km) and amikacin (Am) are used to treat MDR-TB (Figure 1.6).<sup>51</sup>

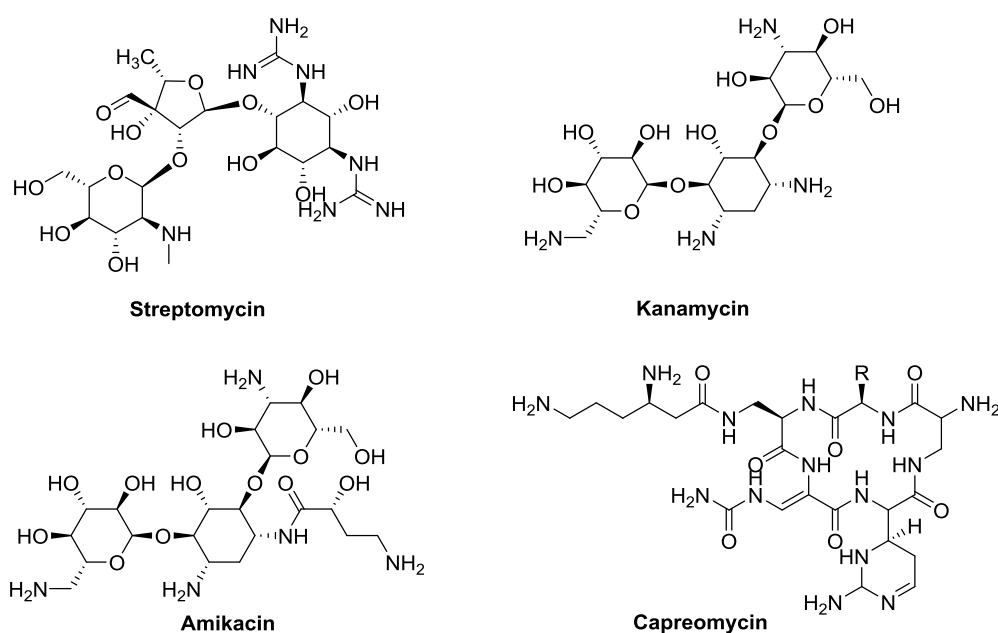


**Figure 1.6. Chemical structures of injectable aminoglycosides and polypeptides (group B).**

All aminoglycosides exhibit similar mechanism of action by binding to the 30S ribosomal subunit and thereby inhibiting protein synthesis. Capreomycin (Cm), a cyclic peptide, does not belong to aminoglycosides but shares a similar mechanism of action and this is the reason that it is commonly grouped with them. In the long-term treatment of TB with aminoglycosides, hearing loss and nephrotoxicity are among the most frequent and most severe adverse effects; however, skin rash, hypersensitivity and peripheral neuropathy may also occur.<sup>52</sup>

Based on the available evidence, second-line injectable agents were associated with an increased likelihood of treatment success when included in a conventional MDR-TB treatment regimen. It is therefore recommended that adults with rifampicin-resistant or multidrug-resistant TB always receive a second-line injectable agent as part of their regimen unless there is an important contraindication. In children with mild forms of disease, however, the harms associated with this group of medications may outweigh potential benefits and therefore injectable agents may be excluded in this group.<sup>28</sup>

### 1.5.2.3. Other core second-line agents (Group C)

This group encompasses agents from four drug classes extensively evaluated in clinical efficacy studies: the thioamides (ethionamide (Eto) and prothionamide (Pto)), cycloserine (Cs) or terizidone (Trd), linezolid (Lzd), and clofazimine (Cfz) (Figure 1.7). Usually they are used in this order of preference, unless the balance of benefits-to-harms for the individual patient demands otherwise.

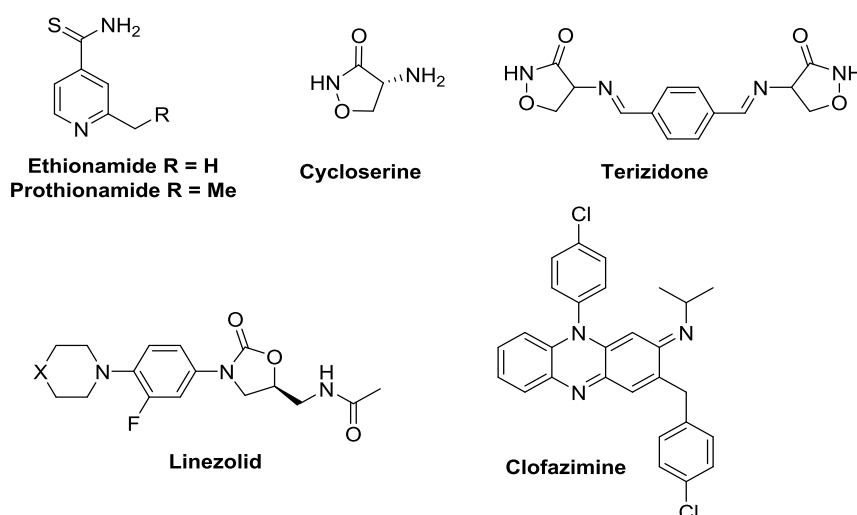


Figure 1.7. Chemical structures of the other core second-line agents (Group C).

#### Thioamides: ethionamide (Eto), prothionamide (Pto)

Thioamides are by far the best of the Group C drugs, as documented by numerous studies showing their efficacy and ability to cure.<sup>47</sup> Thioamides target enoyl-[acyl-carrier-protein] reductase and thereby inhibit oxygen dependent mycolic acid synthesis.<sup>30</sup> Ethionamide and prothionamide can cause gastro-intestinal disturbance, in particular vomiting, which can limit their tolerability.

#### Cycloserine (Cs), Terizidone (Trz)

Cs is only bacteriostatic and competitively blocks the enzyme that incorporates alanine into an alanyl-alanine dipeptide, an essential component of the mycobacterial cell wall.<sup>53</sup> Cs has become



a basic drug in MDR-TB and XDR-TB treatment regimens in spite of its lower activity and adverse effects. Cycloserine has a well-established association with neuropsychiatric adverse effects. The main reason for Cs's extensive use worldwide is that there are currently no better drugs to include in MDR-TB regimens. Terizidone is a combination of two molecules of cycloserine and might be less toxic, although studies of this drug are scarce.<sup>36</sup>

### **Oxazolidinones**

Oxazolidinones are a newer class of antibiotics that act by inhibiting protein synthesis via binding to the 23S rRNA in the 50S ribosomal subunit of bacteria, and they are active against a large spectrum of Gram-positive bacteria.<sup>54</sup> Linezolid has been found to be active against XDR-TB, however, some significant adverse effects such as inhibition of mitochondrial protein synthesis, thrombocytopenia and myelosuppression were observed.<sup>55</sup> Its modified versions, sutezolid (PNU-100480) and AZD-5847 with better activity against *M. tuberculosis*, currently in phase I studies, should address in their clinical development plan the known toxicity issues of linezolid.<sup>35</sup>

### **Clofazimine (Cfz)**

Clofazimine is a drug that has been used in combination with rifampicin and dapson as multidrug therapy (MDT) for the treatment of leprosy. Repurposing it for TB treatment has shown that it could play a significant role in the treatment of MDR-TB. Using a murine model of MDR-TB, the clofazimine-containing regimen was significantly more active in achieving culture conversion and preventing relapse in comparison with mice treated without clofazimine-containing regimen.<sup>56</sup> Taking into account that clofazimine is a safe drug for long-term use, a more close evaluation for its use in the treatment of drug-resistant TB is in progress.

#### **1.5.2.4. Add-on agents (Group D)**

Drugs that belong to this group are not recommended by WHO for routine use in MDR-TB treatment and they are not part of the core MDR-TB regimen.<sup>57</sup> Although all of them have demonstrated some activity at least *in vitro* or in animal models, the quality of the evidence of their efficacy and safety in humans for the treatment of drug-resistant TB varies. As such, some of the drugs in these groups are generally reserved for patients with MDR-TB for whom options available in forming an adequate treatment regimen are limited. This group of medicines is split into three subgroups.

**Subgroup D1** consists of pyrazinamide, ethambutol and high-dose of isoniazid. These agents are usually added to the core second-line medications, unless the risks from confirmed resistance, pill burden, intolerance or drug-drug interaction outweigh potential benefits.

**Subgroup D2** is made up of bedaquiline and delamanid (Figure 1.8), two new drugs which have been released in recent years.

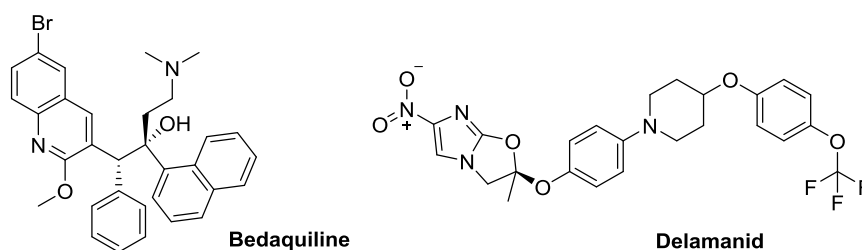


**Figure 1.8. Chemical structures of bedaquiline and delamanid (subgroup D2).**

Bedaquiline is a newly approved drug of a novel class of compounds that inhibit the *c* subunit of ATP synthase, in that way decreasing intracellular ATP levels.<sup>58</sup> In 2012, FDA provisionally approved it for treatment of MDR-TB as part of combination therapy when there is no alternative.<sup>31</sup> Its discovery was a result of phenotypic screening and for its target identification whole-genome sequencing was used.<sup>30</sup> It possesses some unique characteristics such as potency against both replicating and dormant *M. tuberculosis* bacilli and both drug-susceptible and drug-resistant strains.<sup>59,60</sup> However, side effects like nausea, diarrhea, hemoptysis and hyperuricemia were reported.<sup>61</sup> Moreover, it has been shown to accumulate in tissues and therefore carry-over effects should be taken into account.<sup>62</sup> Its potential to induce arrhythmia still remains unclear and further investigation is necessary.<sup>63</sup>

Delamanid belongs to the nitroimidazoles, together with the older metronidazole and the newer pretomanid (PA-824). Delamanid has showed activity against slow, rapidly replicating, drug-susceptible as well as resistant strains of *M. tuberculosis*.<sup>64</sup> Delamanid is a prodrug activated intracellularly by an F<sub>420</sub>-deazaflavin-dependent nitroreductase (Ddn).<sup>65</sup> It inhibits mycolic acid biosynthesis, thus preventing formation of the mycobacterial cell envelope.<sup>66,67</sup> Evaluation of delamanid in clinical trials against XDR-TB showed that patients had a higher rate of 2-month sputum-culture conversion and lower mortality.<sup>68</sup> In 2014, delamanid received provisional approval for the treatment of MDR-TB in the European Union (EU), for use in combination with optimised background therapy.<sup>67</sup> However, QT prolongation was reported at a significantly higher frequency in patients receiving delamanid, thus suggesting that there is a risk of cardiotoxicity.<sup>30</sup>

**Group D3** consists of p-aminosalicylic acid (PAS), imipenem-cilastatin or meropenem plus clavulanate and thioacetazone (Figure 1.9). These drugs are only to be used when a MDR-TB regimen with at least 5 effective drugs (i.e. primarily 4 core second-line medicines plus pyrazinamide) cannot be otherwise composed.

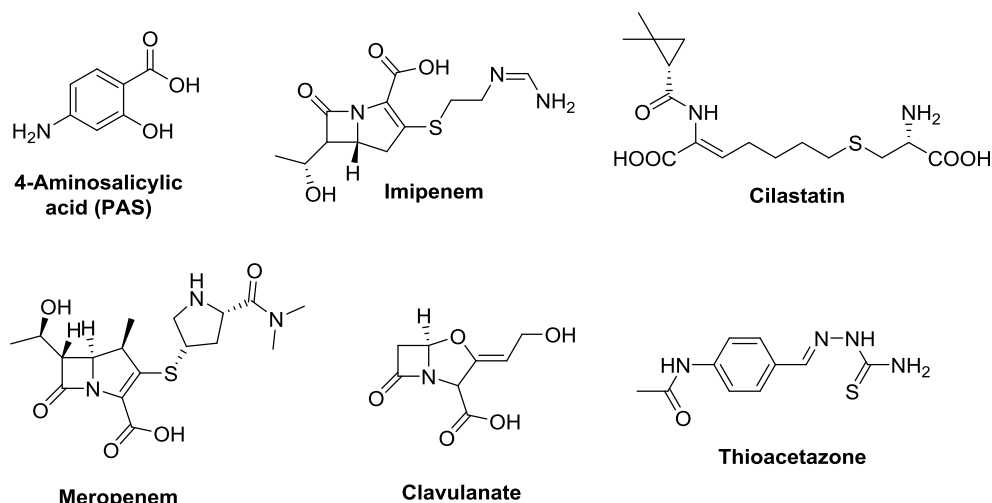


**Figure 1.9. Chemical structures of add-on agents (subgroup D3).**

### ***p*-Aminosalicylic acid (PAS)**

PAS is incorporated into the folate pathway by dihydropteroate synthase (DHPS) and dihydrofolate synthase (DHFS) to generate a hydroxyl dihydrofolate antimetabolite, which in turn inhibits dihydrofolate reductase (DHFR) enzymatic activity.<sup>69</sup> Although PAS is quite weak, has only bacteriostatic activity and is very poorly tolerated (particularly gastric adverse effects), it is still in use as one of the last options during drug selection for drug-resistant TB treatment plans.<sup>47</sup>

### **Carbapenems, imipenem-cilastin or meropenem plus clavulanate combination**

$\beta$ -Lactams were previously thought to be ineffective against *M. tuberculosis*, primarily due to the endogenous mycobacterial BlaC enzyme which effectively hydrolyzes them.<sup>70</sup> However, recently, it was shown that BlaC inhibition by clavulanate could lead to *M. tuberculosis* becoming susceptible to imipenem-cilastin or meropenem. Their combination was proven to be efficient against drug-susceptible, MDR and XDR clinical strains.<sup>71</sup> Amoxicillin-clavulanate has shown poor results in *in vitro* studies and in early bactericidal activity (EBA) studies.

### **Thioacetazone (T)**

Thioacetazone has been used extensively in the past as part of first-line combination therapy for TB. However, use of the drug in TB treatment has been restricted since the early 1990s due to the severe skin reactions it causes, including Stevens-Johnson syndrome and toxic epidermal necrolysis (which can lead to death, especially in people living with HIV). If thioacetazone is being considered as part of a MDR-TB treatment regimen, close monitoring for severe skin reactions is required and it is imperative that the patient be tested for HIV, and that the drug should not be used if the patient is HIV seropositive.

Conventional regimen in patients with MDR/RR-TB includes a regimen with at least five effective anti-TB medicines during the intensive phase, including pyrazinamide and four core second-line anti-TB medicines. This regimen can be further strengthened with high-dose isoniazid and/or ethambutol. Conventional MDR-TB regimens last 18 months or more and may be standardised or individualised.

According to recent WHO treatment guidelines in 2016 for drug-resistant TB,<sup>28</sup> for patients with rifampicin-resistant or multidrug-resistant TB who have not been previously treated with second-line drugs and in whom resistance to fluoroquinolones and second-line injectable agents has been excluded or is considered highly unlikely, a shorter MDR-TB regimen of 9-12 months may be used instead of a conventional regimen. Firstly, an intensive phase of 4 months (extended to 6 months in case of lack of sputum smear conversion) is given including the following drugs: gatifloxacin (or moxifloxacin), kanamycin, prothionamide, clofazimine, high-dose isoniazid, pyrazinamide, and ethambutol. This is followed by a continuation phase of 5 months with the following medicines: gatifloxacin (or moxifloxacin), clofazimine, ethambutol, and pyrazinamide (prothionamide was kept in the continuation phase in earlier studies).

The analyses performed for the evidence assessment showed that patients who met specific inclusion criteria for receiving the shorter MDR-TB treatment regimens had a significantly higher likelihood of treatment success than those who received longer conventional regimens (89.9% vs. 78.3% respectively when success was compared with treatment failure/relapse/death and 83.4% vs. 61.7% when compared with treatment failure/relapse/death/loss to follow-up).<sup>28</sup>

### 1.5.3. Vaccines

*M. bovis* Bacille-Calmette-Guérin (BCG), the only licensed TB vaccine, was first given to infants in 1921 and still continues to be administered in newborns in most regions where TB is endemic.<sup>3,4</sup> Vaccination with BCG was significantly associated with a reduction in the incidence of pulmonary TB and extrapulmonary disease via reducing the risk of TB by an average of 50%.<sup>72</sup> BCG gives significant protection, but only for a limited period of time (at best 10 to 20 years), and in addition, it is not effective in populations already sensitized to mycobacterial antigens (whether by prior BCG vaccination, exposure to environmental mycobacteria, or latent TB infection). Therefore, BCG seems to be effective at reducing the rate of pediatric TB if given to infants (who have no prior immunity to interfere with the vaccination). Neonatal vaccination with BCG seems to consistently provide significant protection against the most severe childhood manifestations of the disease, such as TB meningitis. However, neonatal vaccination has had little effect on the rate of TB in adults.<sup>18</sup> Since BCG has not managed to control TB efficiently, the necessity to develop new more

effective vaccines against *M. tuberculosis* has become apparent. In August 2015, the global pipeline of TB vaccine candidates in clinical trials contained 15 vaccines, including recombinant BCGs, attenuated *M. tuberculosis* strains, recombinant viral-vectored platforms, protein/adjuvant combinations and mycobacterial extracts.<sup>31</sup>

## 1.6. Drug discovery and hit identification

Despite the number of drugs mentioned above, there is an urgent need for the discovery and development of new antitubercular agents. It is especially desirable to identify new types of anti-TB drugs acting on novel drug targets and biochemical pathways with no cross-resistance to existing drugs.

To address this need over the past decade, high-throughput screening (HTS) of corporate compound decks has become the major paradigm for hit or lead discovery in big Pharma.<sup>73</sup> Therefore, HTS of drug-like libraries are used as a tool to discover a variety of new active scaffolds that will stimulate new biological research and drug discovery. The philosophy behind these efforts rests on the statistically driven belief that with large enough libraries of chemically diverse molecules, one will find compounds that can serve as good starting points for drug optimization efforts. The goal of HTS campaigns is not to identify drugs but rather to identify starting points (hits) for medicinal chemistry efforts towards lead optimization.<sup>74</sup>

Assays developed for HTS can be divided broadly into two categories: biochemical assays (target-based) and cell-based assays and each of them is accompanied by advantages and disadvantages.<sup>75</sup> If the goal of a HTS is to identify a molecular structure that selectively binds to and modulates the activity of a biological target (e.g., a protein) of interest, then it is called target-based. On the other hand, if the goal of a HTS is to identify a molecule that selectively induces a desired phenotype in a cell population or organism of interest, it is called cell-based or phenotypic. Cell-based HTS have the potential to immediately identify compounds with sufficient permeability. However, one of the drawbacks of the whole-cell screening approach is that upfront knowledge regarding the mechanism of action remains largely lacking, thereby preventing any input from structural biology into medicinal chemistry efforts around drug design.<sup>35</sup> Subsequent identification of the corresponding cellular targets using genetic, genomic, and/or proteomic tools is important in order to facilitate advancement of the cell-based hit. Target-based screening is an alternative method that has the advantage of the possibility to rationalize structure–activity relationships (SAR). However, the main drawback of this method is the frequently encountered lack of activity against the whole cell (MIC) as penetration issues can limit their entrance.

## 1.7. General thesis objectives

The present thesis about antimycobacterial drug discovery was performed as part of the OpenMedChem project at the University of Antwerp (Antwerp, Belgium) and GlaxoSmithKline (GSK) (Tres Cantos, Spain) funded by Marie Skłodowska-Curie Initial Training Networks. The OpenMedChem project comprised collaboration between a major industrial R&D unit and academia with the common goal to find new chemical entities to battle *M. tuberculosis*.

As fellow of the OpenMedChem group, I was part of a multidisciplinary drug discovery team, in which we were responsible for the design and synthesis of novel antimycobacterials. The biological evaluation data sets for these compounds were generated by the industrial team members. Working in iterative optimization cycles allowed us to maximally valorize the biological data for the design of compounds with an improved antimycobacterial and/or biopharmaceutical profile.

GlaxoSmithKline regularly performs HTS campaigns to identify new hits for antimycobacterial drug discovery. These efforts have produced a number of compound families that require in depth investigation to assess their potential for lead generation.

Within this thesis, two chemical families were chosen for further investigation. Their general chemical structures are shown in Figure 1.10. The whole-cell HTS approach was used for the identification of the quinoloxycetamide hits of the first sub-project described in chapters 2 and 3, while the target-based approach was used for the identification of the hydantoin-based decaprenylphosphoryl- $\beta$ -D-ribose oxidase (DprE1) inhibitors described in chapters 4 and 5.

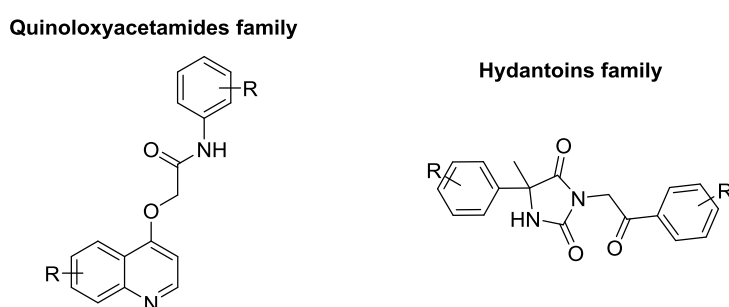


**Figure 1.10. General chemical structures of the families under investigation.**

For the first family of quinoloxycetamides, it was found that the primary hits possessed high cellular potency against *M. tuberculosis* H37Rv strain and that they were selective for mycobacteria. However, clear warnings were available for key physicochemical properties such as solubility and permeability, CYP inhibition and metabolic stability. Therefore, this family required

further optimization before being ready for an *in vivo* proof-of-concept assay. Furthermore, since this family was identified by a whole-cell HTS, its target was unknown.

The second family selected for further studies was hydantoin. It was identified by a target-based HTS campaign offering the advantage of target engagement. The cellular activity of the primary hit was within satisfactory ranges, although further optimization was necessary. Moreover, it possessed the advantages of being metabolically stable and had a promising physicochemical profile. Main areas of concern were structural features such as the hydantoin ring, the carbonitrile group and the benzylic keto function.

Using the initial screening data as a starting point, the general thesis objectives can be summarized as follows:

- Lead generation for both families and deliverance of *in vivo* proof-of-concept.
- SAR investigation around the initial hits.
- MIC optimization and further improvement of physicochemical properties and toxicological profile (cytotoxicity, hepG2 and cardiotoxicity, hERG).
- Validation of the gross mode of action (where possible).

Table 1.2 summarizes the parameters and desired values that are taken into account in order to classify a compound as a Lead (usually after optimization of a hit obtained by HTS).

**Table 1.2. Parameters for characterization of a compound as Lead.**

Parameter	Desirable	Acceptable	Undesirable
<b>MW</b>	≤350	350 < MW < 450	≥450
<b>MIC (μM)</b>	<1	1 ≤ MIC ≤ 10	>10
<b>HepG2</b>	pIC <sub>50</sub> ≤ 4		pIC <sub>50</sub> > 4
<b>hERG</b>	pIC <sub>50</sub> ≤ 5	5 < pIC <sub>50</sub> < 6	pIC <sub>50</sub> ≥ 6
<b>CLND Solubility (μM)</b>	> 200	30 ≤ CLND ≤ 200	<30
<b>Permeability (cm/sec)</b>	>100	10 ≤ AMP ≤ 100	<10
<b>ChromLogD</b>	≤ 4	4 < chromlogD < 5	≥ 5
<b><i>in vitro</i> Cl<sub>int</sub> (mL/min/g)</b>	≤1	1 < Cl <sub>int</sub> < 6	≥6





# Chapter 2

---

*Quinoloxycetamide inhibitors: Aims and Objectives*

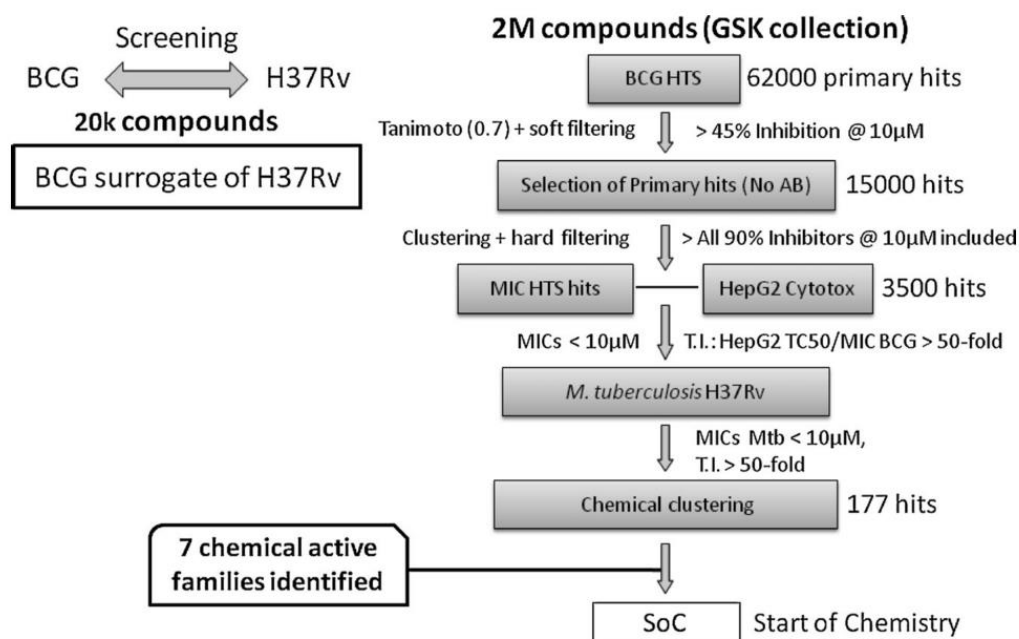


## 2. Quinoloxycetamide inhibitors: aims and objectives

Currently, the development of an effective anti-TB drug is an objective with significant challenges.<sup>35</sup> Any emerging entity is required to satisfy a range of factors relating to: safety, efficacy, a new mode of action and activity against resistant strains.

GSK performed a whole-cell high throughput screening (HTS) campaign against *M. bovis* BCG with hit confirmation in *M. tuberculosis* H37Rv and the results became publically available in 2013.<sup>76</sup> *M. bovis* BCG was used as an *M. tuberculosis* surrogate to overcome that challenges related with the use of a virulent strain during the initial screening of more than 2 million chemical entities present in GSK's corporate compound collection. The initial HTS BCG primary hit list was narrowed after the application of a number of similarity and physicochemical property filters, such as calculated  $\log P < 6$  and MW < 600 Da. Structures containing reactive functional groups together with compounds that exhibited cytotoxic effects (HepG2) were also eliminated. The remaining 777 compounds were further progressed to MIC determination against *M. tuberculosis* H37Rv. Applying a threshold of MIC < 10  $\mu$ M and therapeutic index of (HepG2 IC<sub>50</sub>/MIC) > 50 resulted in 177 compounds among which 7 clustered chemical families were identified. An overall description of that process can be found in Figure 2.1.

During the initial phase of the OpenMedChem project, a further examination of the 777 compound subset was performed. Combined Molecular Operating Environment (MOE) and visual clustering of the final selection provided a number of highly potent structural clusters in agreement with GSK clustering. Furthermore, literature search was performed to check for prior reports on the selected classes and their potential targets (if known).

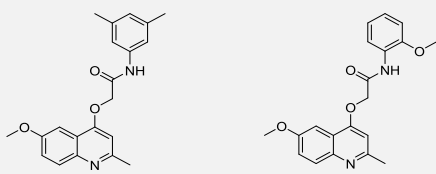


**Figure 2.1. HTS progression cascade leading to 177 confirmed *M. tuberculosis* H37Rv positive compounds.<sup>76</sup>**

The quinoloxycetamides (QOA) constituted one of the identified families and the two most active hit compounds (**2.1** and **2.2**, shown in Table 2.1) were selected for further SAR studies and optimization of their properties. Quinolines have notable value for drug discovery since they often display drug-like properties. They can be found in many drugs such as antibiotics, antimalarials, antifungal etc.<sup>77–81</sup> Moreover, quinoline represents a common substructure of several known anti-tubercular drugs, e.g., bedaquiline and fluoroquinolones such as moxifloxacin and gatifloxacin.<sup>82–86</sup>

As shown in Table 2.1, the hit compounds **2.1** and **2.2** were found to possess significant anti-mycobacterial activity with minimum inhibitory concentration (MIC) values 1.9 μM and 1.4 μM respectively against *M. tuberculosis* (H37Rv). Moreover, two key physicochemical parameters (solubility and permeability) were investigated, revealing workable, but suboptimal properties of **2.1** and **2.2**. ChromlogD values were measured at pH 7.4 indicating that the hit compounds are rather lipophilic molecules. The cytotoxicity (HepG2) of the initial hits was also evaluated and hit **2.1** displayed a level of cytotoxicity ( $IC_{50} = 20 \mu\text{M}$ ) while hit **2.2** did not exhibit cytotoxic effects. Cardiotoxicity (hERG) was also measured where hit **2.1** did not display any hERG interactions while hit **2.2** displayed some interaction ( $IC_{50} = 10 \mu\text{M}$ ). Also, murine and human microsomal stabilities were determined, and the results indicated that further optimization was required before progressing to an *in vivo* proof-of-concept.<sup>76</sup>

Table 2.1. Biological profile for the hit compounds 2.1 and 2.2.<sup>[a]</sup>

Structure			
Compound	2.1	2.2	
	Molecular weight	350	352
<b>Activity</b>	MIC ( $\mu\text{M}$ ) <sup>[b]</sup>	1.9	1.4
<b>Physicochemical properties</b>	Permeability (nm/sec) <sup>[c]</sup>	180	120
	Solubility CLND ( $\mu\text{M}$ ) <sup>[d]</sup>	26	38
	ChromlogD (pH 7.4)	5.64	4.74
<b>Toxicity</b>	Cytotoxicity HepG2 IC <sub>50</sub> ( $\mu\text{M}$ ) <sup>[e]</sup>	20	>100
	Cardiotoxicity hERG IC <sub>50</sub> ( $\mu\text{M}$ )	>50	10
<b>Metabolic stability<sup>[f]</sup></b>	Cl <sub>int</sub> (mL min <sup>-1</sup> g <sup>-1</sup> tissue) mouse	18.9	>30
	Cl <sub>int</sub> (mL min <sup>-1</sup> g <sup>-1</sup> tissue) human	1.3	5.4
	t <sub>1/2</sub> (min) mouse	<5	<3
	t <sub>1/2</sub> (min) human	>30	16

<sup>a</sup>upon re-testing the obtained data were found to differ in some cases from the data published in reference <sup>76</sup>; <sup>b</sup>MIC against *M. tuberculosis* (H37Rv); <sup>c</sup>artificial membrane permeability; <sup>d</sup>*in vitro* profiling for kinetic aqueous solubility (CLND, chemiluminescent nitrogen detection); <sup>e</sup>HepG2, human caucasian hepatocyte carcinoma; <sup>f</sup>*in vitro* microsomal fraction stability (mouse and human) results: intrinsic clearance (Cl<sub>int</sub>) and half-life time (t<sub>1/2</sub>) are reported; imidazolam was used as control with Cl<sub>int</sub> = 27.5 ± 0.4 and 6.4 mL min<sup>-1</sup>g<sup>-1</sup> in mouse and human, respectively; and t<sub>1/2</sub> ≤ 5 and 9 min in mouse and human, respectively.

Summarizing, compounds **2.1** and **2.2** had a satisfactory hit-profile. However, further optimization was necessary to produce a high-quality lead. The primary objective of this work was to perform a SAR exploration around the initial hits with the aim to discover even more potent inhibitors than the hit compounds against *M. tuberculosis*. The second complementary objective was the improvement of the physicochemical properties and toxicity of the series. The third goal was to improve the metabolic stability of the series.

The main goals for this part of the thesis are discussed below:

### 2.1. Structure-Activity Relationship (SAR)

Based on the promising initial data, a set of novel analogues was designed and synthesized, relying on iterative logic-based SAR exploration of the chemical space around the hits. The aim of this SAR exploration was to identify more potent compounds and to determine the structural components that are necessary for the activity. Of course, development of efficient synthetic methods for

preparation of the proposed compounds was a supplementary goal during the whole PhD program.

## **2.2.Optimization of physicochemical properties**

Along with identifying the structural parameters that govern the anti-mycobacterial properties of these molecules, a primary goal of this project was to optimize the physicochemical properties of the series. The hit compounds **2.1** and **2.2** possessed good permeability (>100 nm/sec), but they exhibited low solubility. During the optimization process, we aimed to increase the solubility values more than 100  $\mu$ M. Moreover, chromlogD was used as indicator of the overall lipophilicity of the molecules with the goal to reach values less than 4.

## **2.3.Elimination of toxicity**

The cytotoxicity data from the HepG2 assay for the hit compounds **2.1** and **2.2** displayed some cytotoxic effects only for compound **2.1**. Conversely, measurement of the hERG interactions, as a preliminary cardiotoxicity estimation, reveal some interactions only with hit **2.2**. Both parameters are decisive for the progression of a compound, therefore special attention was paid to them.

## **2.4.Improvement of metabolic stability**

Last but not least, another goal of this project was to identify metabolically labile groups of the reference compound **2.1**. Once identified, attempts to replace this group with other appropriate groups would follow with aim to retain the antimycobacterial activity.

Practically, the process of compound optimization was organized around iterative cycles of design, synthesis and evaluation. At each stage, experimentally obtained anti-mycobacterial, physicochemical, and *in vitro* toxicity data were used to refine the decision model used for synthetic planning.

# Chapter 3

---

## *Quinoloxycetamides as antimycobacterial agents*

The content in this chapter is based on:

1. Pitta, E.; Rogacki, M. K.; Balabon, O.; Huss, S.; Cunningham, F.; Lopez-Roman, E. M.; Joossens, J.; Augustyns, K.; Ballell, L.; Bates, R. H.; Van der Veken, P. Searching for New Leads for Tuberculosis: Design, Synthesis and Biological Evaluation of Novel 2-Quinolin-4-yloxyacetamides. *J. Med. Chem.* 2016, *59* (14), 6709–6728.
2. Pitta, E.; Balabon, O.; Rogacki, M. K.; Gómez, J.; Cunningham, F.; Augustyns, K.; Joossens, J.; Van der Veken, P.; Bates, R. H. Differential characterization using readily accessible NMR experiments of novel *N*- and *O*-alkylated quinolin-4-ol, 1,5-naphthyridin-4-ol and quinazolin-4-ol derivatives with antimycobacterial activity. *Eur. J. Med. Chem.* 2017; *125*, 890-901.





### 3. Quinoloxacetamides as antimycobacterial agents

#### 3.1. Introduction

Quinoline represents a common substructure of several known anti-tubercular drugs with the most recent successful example, bedaquiline.<sup>82-85</sup> Fluoroquinolones also are known for their antimicrobial activity with characteristic example moxifloxacin and gatifloxacin which are used as second-line drugs against TB.<sup>86</sup> Therefore, quinoline-based scaffolds have attracted the attention of medicinal chemists for further exploration as potential starting points to develop more antimycobacterial drugs. This exploration of chemical space around quinoline scaffolds has led to the identification of several new series of compounds with notable antimycobacterial activity against *M. tuberculosis*.<sup>87</sup>

Quinolinone or quinolinol is the hydroxy/keto substituted derivative of quinoline and it can exhibit an ambident character due to its resonance isomers. Despite continuing advances in synthetic organic chemistry, regioselective alkylation of heterocyclic N/O ambident nucleophiles remains a challenging transformation. Many scientists have tried to identify reaction parameters and conditions (e.g., counteraction, solvent, temperature, electrophile) that influence the outcome in a predictive manner.<sup>88-91</sup> However, in general the outcome can still vary among different heterocycles and even between identical scaffolds depending on their substitution pattern.<sup>92</sup> Likewise, several theoretical approaches to offer insight in this matter have been proposed. Systematic investigations by Kornblum and Tieckelmann were integrated in Pearson's concept of "Hard and Soft Acids and Bases" (HSAB) which became the most popular approach to rationalize ambident reactivity.<sup>93,94</sup> The HSAB rationale was complemented with the Klopman-Salem theory of charge and orbital control of organic reactions.<sup>95,96</sup> Although these concepts have been widely accepted, they have also been criticized by Gompper and Wagner and by Mayer and co-workers.<sup>97,98</sup> More recently, Marcus analysis has been proposed by Breugst and co-workers as a more successful alternative to rationalize the behavior of ambident nucleophiles.<sup>99</sup>

As shown in Figure 3.1, 4-quinolinones/4-quinolinols have two potential alkylation sites, the nitrogen atom and the hydroxy group. Under alkylation conditions, they are expected to be mainly present in a deprotonated form, stabilized by resonance. Similarly, the related aza-heterocyclic scaffolds 4-quinazolinones/4-quinazolinols have three potential alkylation sites, i.e., the two nitrogen atoms and the hydroxy group which can lead to three possible regioisomers (*N*(1)-, *N*(3)- and *O*-).

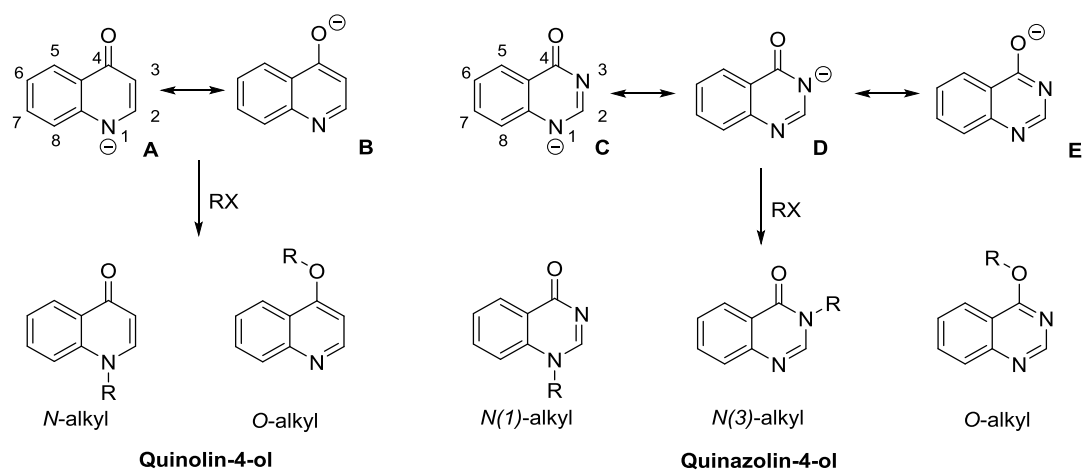


**Figure 3.1.** 4-Quinolinone and 4-quinazolinone anions, their resonance isomers and possible alkylation positions.

### 3.2. Library design

Based on the promising results obtained for the initial quinoline-based hits found at GSK by a whole-cell HTS campaign, we decided to explore the SAR of this novel class of antimycobacterials in greater detail. For practical reasons, the primary hit **2.1** was selected as a reference and divided into three substructures to help organize the SAR exploration: the quinoline, the linker and the northern aryl part (Figure 3.2).

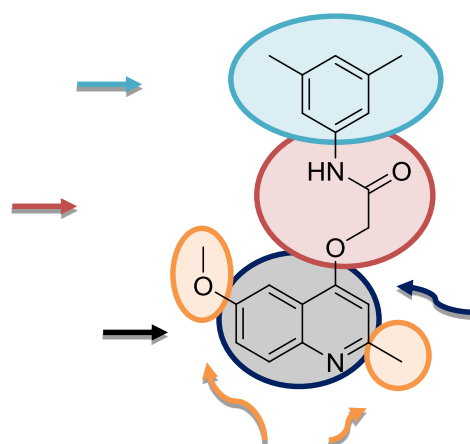


**Figure 3.2.** Primary hit 2.1 and structure division.

This was done by preparing three compound sub-series in which each of the substructures was modified separately, while keeping the rest of the molecule identical to the reference compound.

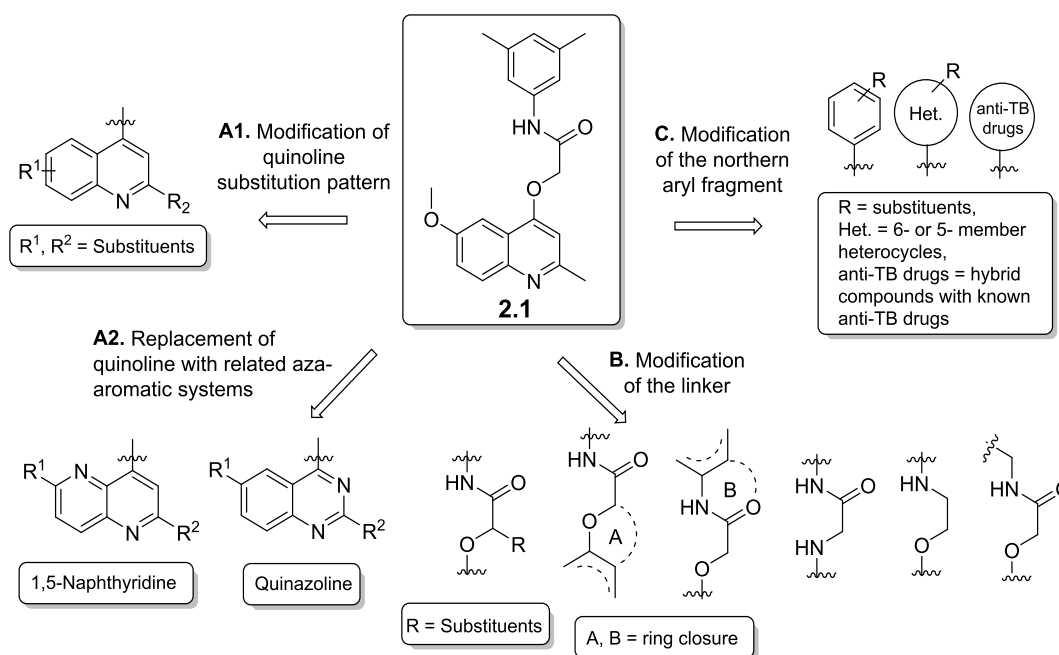
**A. Modifications on the quinoline core.** As shown in Scheme 3.1, they consisted of two types:

**A1. Modification of the substitution pattern.** Several groups replaced the initial 6-methoxy group or the methyl group at position 2.

**A2. Replacement with related bicyclics** such as naphthyridine and quinazoline. The rationale for the scaffold replacement approach was to decrease the lipophilicity of the molecules (chromlogD was used as an indicator of lipophilicity) and improve solubility by introducing additional nitrogen atoms.<sup>100,101</sup>

**B. Modification of the linker.** They included introduction of substituents on methylene group, conformational constraint, i.e., by introducing 5- or 6-membered cycles and other type of modifications.

**C. Modification of the northern aryl fragment.** They included variation of substituents on aryl residue, (un)substituted heterocycles and hybrid molecules with known anti-TB drugs.



**Scheme 3.1. Design of new compounds.**

### 3.3. Chemistry

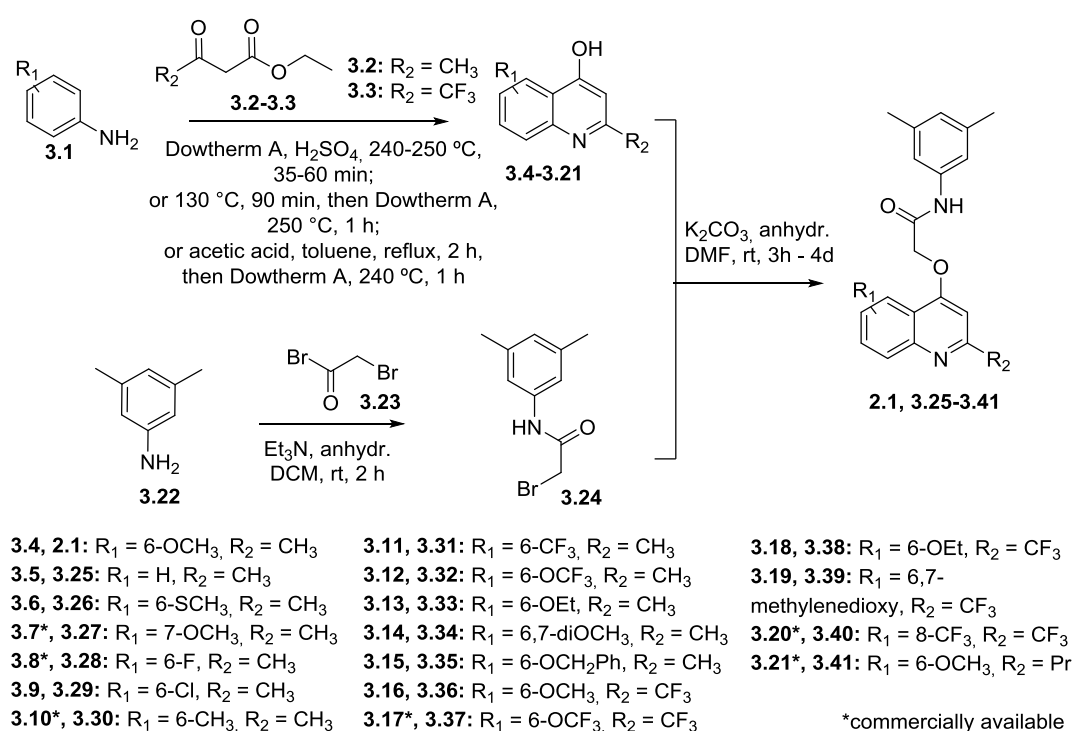
More than seventy novel compounds were synthesized for this study. The target compounds were clustered according to the modification type they contained, relative to reference compound **2.1**. Lastly, three compounds which contain amide bond replacements are presented.

### 3.3.1. Modification of the quinolone core

#### 3.3.1.1. Modification of the quinoline substitution pattern

An important goal of these compounds was to investigate the contribution to antimycobacterial activity of the 6-methoxy and 2-methyl quinoline substituents in **2.1**. The selection of substituents was carried out in a highly exploratory manner and comprised groups with widely differing impact on the sterics and electronics of the quinoline system.

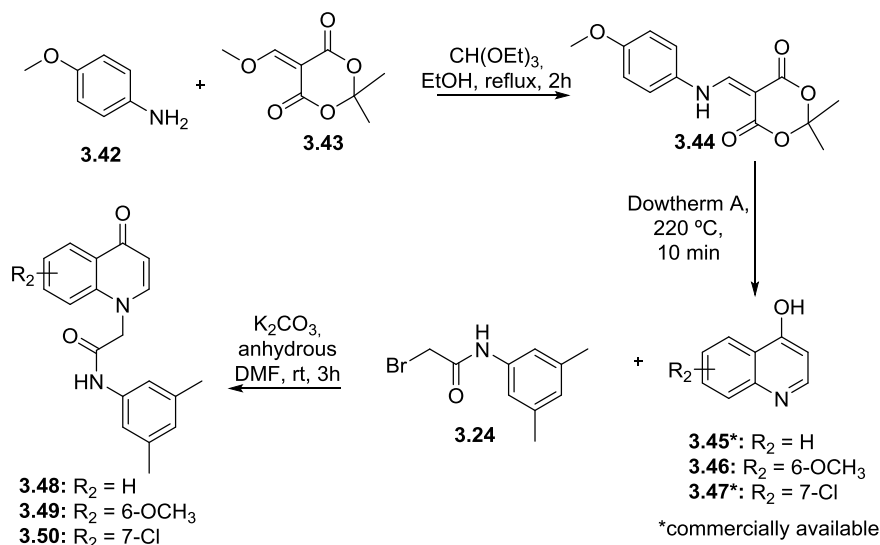
The general synthetic strategy to obtain the target compounds **2.1** and **3.25-3.41** consisted of coupling the modified quinoline core **3.4-3.21** to 2-bromo-*N*-(3,5-dimethylphenyl)acetamide **3.24** in the presence of potassium carbonate ( $K_2CO_3$ ) (Scheme 3.2). Construction of the 2-methyl and 2-trifluoromethyl quinolin-4-ols (**3.4-3.6**, **3.9**, **3.11-3.16**, **3.18**, **3.19**) was achieved by condensation of a number of commercially available anilines **3.1** with ethyl acetoacetate **3.2** or ethyl 4,4,4-trifluoroacetoacetate **3.3** following a Conrad-Limpach protocol.<sup>102,103,104</sup> The *N*-aryl haloacetamide building block **3.24** was obtained in excellent yield by acylation of aniline **3.22** with bromoacetyl bromide **3.23** in the presence of triethylamine (TEA).<sup>105</sup>



**Scheme 3.2. Synthesis of compounds with quinoline substitution modifications.**

For preparing the 2*H*-quinolin-4-ol core, the Conrad-Limpach strategy used earlier for the 2-substituted series was considered unsuitable because this methodology performs sluggishly for

the production of 2-unsubstituted derivatives.<sup>106</sup> The alternative condensation reaction that was used, involved two steps as shown in Scheme 3.3.<sup>107</sup> First, aniline **3.42** was added to Meldrum's acid derivative **3.43** in order to deliver enamine **3.44**. Afterwards, thermal cyclization of **3.44** gave the desired 2*H*-quinolin-4-ol **3.46**. Unexpectedly, alkylation of quinolinols **5.45-5.47** with alkyl halide **3.24** using the previously mentioned alkylation protocol exclusively rendered the *N*-alkylated products **3.48-3.50** (unambiguous structural identification was carried out as described in the next section, *Structure elucidation*).

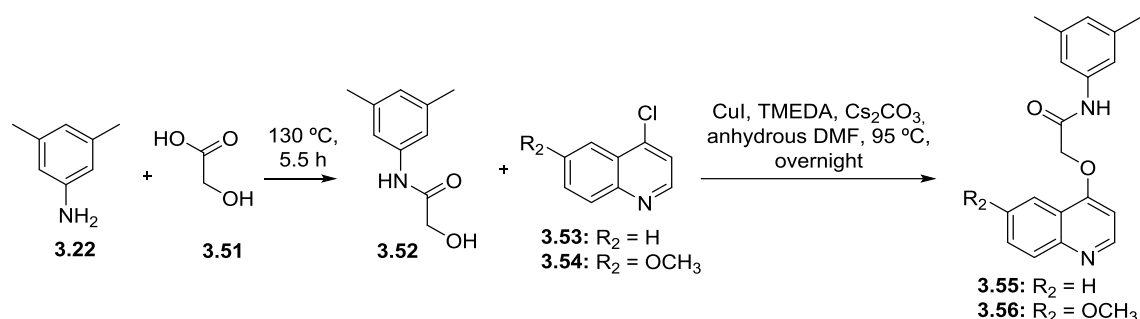


**Scheme 3.3. Synthesis of 2*H*-quinolin-4-ols and their *N*-alkylation.**

A likely explanation for this inverted regioselectivity could be that the 2-methyl substituent exerted sufficient steric hindrance around the quinoline ring nitrogen to render the oxygen more reactive. In agreement with our findings, Wang and co-workers in 1996 and Oyama *et al.* in 2015 reported exclusively *N*-alkylated products in case of 2*H*-quinolin-4-ols under the same experimental conditions.<sup>108,109</sup> Moreover, Pissinate *et al.*, working on the same series, obtained the *N*-alkylated product with high chemoselectivity when the 2-methyl group was substituted with hydrogen.<sup>110</sup> On the other hand, one can find publications where *O*-alkylated products were reported when applying the same protocol, although after careful examination, we found that they did not include full, unambiguous characterization data.<sup>111,112</sup>

A different synthetic approach was designed to obtain the originally desired *O*-alkylated analogues by employing a S<sub>N</sub>Ar reaction of the desired alcohols with 4-chloroquinoline. The synthesis (shown in Scheme 3.4) began with preparation of 2-hydroxyacetamide **3.52** by heating the corresponding aniline **3.22** and glycolic acid **3.51** at 130 °C without solvent according to a procedure described by Hung *et al.*<sup>113</sup> Subsequently, 2-hydroxyacetamide **3.52** was coupled with 4-chloroquinolines

**3.53** and **3.54**, in an Ullman-type reaction, catalysed by copper iodide/tetramethyl ethylenediamine (CuI/TMEDA), according with Zhou *et al.*<sup>114</sup> Cesium carbonate (Cs<sub>2</sub>CO<sub>3</sub>) was used as a base and dimethyl sulfoxide (DMSO) as a solvent. Heating the reaction mixture overnight at 95 °C afforded final products **3.55** and **3.56**.

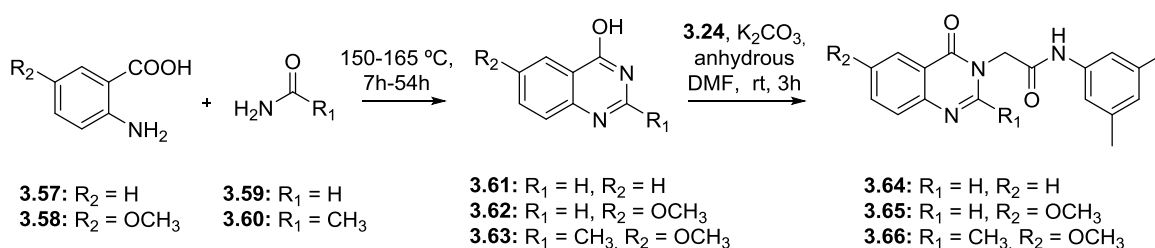


**Scheme 3.4.** Synthesis of *O*-alkylated 2*H*-quinolin-4-ols **3.55-3.56**.

### 3.3.1.2. Replacement of quinoline with related aza-aromatic systems

The second subset included compounds with related aza-aromatic systems such as quinazoline and naphthyridine instead of quinoline.

For the ring synthesis of 4-hydroxy quinazolines **3.61-3.63**, a Niementowski protocol was employed as shown in Scheme 3.5.<sup>115</sup> The appropriate anthranilic acids (**3.57-3.58**) and formamide (**3.59**) or acetamide (**3.60**) were heated at 150-165 °C to afford intermediates **3.61-3.63**. Afterwards, their alkylation with alkyl bromide **3.24** under the standard conditions (K<sub>2</sub>CO<sub>3</sub>, anhydrous DMF, r.t.) provided the *N*(3)-alkylated products **3.64-3.66** (unambiguous structural identification was carried out as described in the next section, *Structure Elucidation*) in all cases (2-substituted and 2-unsubstituted). Clearly in this case, steric factors can no longer reasonably explain the observed regioselectivity.

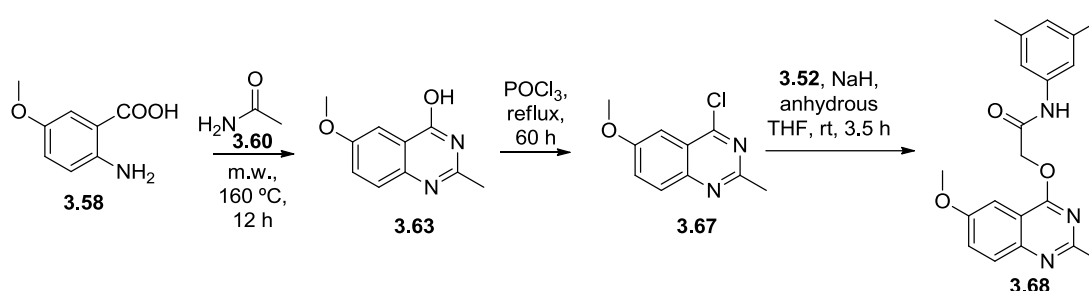


**Scheme 3.5.** Synthesis of quinazolinone intermediates **3.61-3.63** and their *N*(3)-alkylation.

It is known that 4-quinazolinones react normally with alkyl halides at *N*(3) of the quinazolinone ring and occasionally at the oxygen atom.<sup>92</sup> Therefore, the fact that we obtained *N*(3)-alkylated products (**3.64-3.66**) should not be surprising. As highlighted by Spulak *et al.*,<sup>116</sup> there is likely an

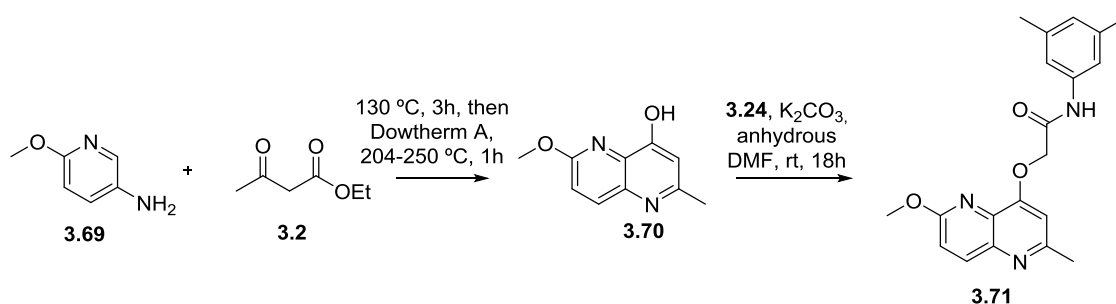
artificially high number of *O*-alkylated products in the literature due to mischaracterization or insufficient data which fully, unambiguously characterise the obtained products.<sup>117,118,119</sup>

As shown in Scheme 3.6, a different synthetic approach was selected to obtain the desired *O*-alkylated quinazolin-4-ol **3.68**. First, quinazolin-4-ol **3.36** was prepared using a modified Niementowski protocol by means of microwave irradiation.<sup>115</sup> Oxychloro-exchange was achieved by treatment with phosphoryl chloride (POCl<sub>3</sub>) under reflux for 60 h resulting in 4-chloroquinazolin-4-ol **3.67**. Subsequently, alcohol **3.52** was treated with sodium hydride (NaH) in tetrahydrofuran (THF) for 1 h and 4-chloroquinazolin-4-ol **3.67** was added to deliver the desired *O*-alkylated compound **3.68**.<sup>120</sup>



**Scheme 3.6. Synthesis of *O*-alkylated quinazolin-4-ol **3.68**.**

To obtain 6-methoxy-2-methyl-1,5-naphthyridin-4-ol **3.70**, a classical Conrad-Limpach protocol could be employed as shown in Scheme 3.7.<sup>102,121</sup> Thus, 6-methoxypyridin-3-amine **3.69** and ethyl acetoacetate (**3.2**) were heated at 130 °C for 3 h, followed by addition of Dowtherm A and heating at 240-250 °C for 1 h. Subsequently, intermediate **3.70** was subjected to the selected alkylation protocol with alkyl bromide **3.24** to obtain the desired *O*-alkylated analogue **3.71** (unambiguous structural identification was carried out as described in the next section, *Structure Elucidation*). As previously hypothesized, the presence of a substituent *ortho* to the ring-nitrogen likely accounts for the observed regioselectivity.



**Scheme 3.7. Synthesis of naphthyridin-4-ol analogue **3.71**.**

### 3.3.1.3. Structure elucidation

The routine analytical tools that are used for addressing structural identity and purity of compounds in most cases are incapable of unambiguously distinguishing *O*- versus *N*-alkylated analogues. Both regioisomers often produce similar  $^1\text{H}$  NMR spectra and have identical masses. IR spectroscopy has been demonstrated to be helpful to determine the alkylation position in structurally simple molecules.<sup>122</sup> In case of *N*-alkylation, a carbonyl-type group is preserved and its characteristic stretching bands are potentially easy to recognize in a relatively isolated spectral region.<sup>123</sup> However, this is not always true for more complex molecules, especially if other carbonyl groups are present, leading to possible overlap of the key IR signals.

During the course of our investigation we were surprised to find that *N*-, *O*- selectivity of our compounds was not always as expected and therefore each scaffold was carefully examined using NMR techniques to fully assign the structure and rationalise the selectivity of the core heterocycles. Therefore, we used a number of standard one-dimensional (1D) and two-dimensional (2D) NMR techniques which allowed the unambiguous characterization of these type of heterocyclic systems. All 1D and 2D NMR experiments described here are pre-programmed on standard, contemporary NMR spectrometers.

#### **$^{13}\text{C}$ NMR chemical shifts:**

The sensitivity of  $^{13}\text{C}$  chemical shifts to the carbon's environment has been commonly used for structure determination and differentiation between compounds, as reflected in many examples from the literature. We exploited the fact that the carbon atom of the methylene linker ( $-\text{CH}_2-$ ) directly bonded to an oxygen versus a nitrogen atom will possess a notably different  $^{13}\text{C}$  chemical shift as an initial indication of the obtained regioisomer. The desired *O*-analogues will produce a significant and predictable downfield shift of the methylene signal in comparison to the *N*-analogue. The examples provided in Table 3.1 and 3.2 demonstrate that typical  $^{13}\text{C}$  chemical shifts for *O*-analogues fall into the 50-80 ppm range, while in the case of *N*-analogues, they appear at higher field (typically 40-60 ppm).



Table 3.1. Comparison of  $^{13}\text{C}$ -NMR chemical shifts in  $\text{DMSO-}d_6$  of the methylene group ( $-\text{CH}_2-$ ) for the *N/O*-alkylated quinolinols 3.48-3.50 and 3.55-3.56.

	<i>N</i> -alkylated			<i>O</i> -alkylated		
	Compd	Structure	$^{13}\text{C}$ shifts (ppm)	Compd	Structure	$^{13}\text{C}$ shifts (ppm)
Quinolin-4-ols/ones	3.48		54.6	3.55		67.2
	3.49		54.7	3.56		67.1
	3.50		54.5			

Table 3.2. Comparison of  $^{13}\text{C}$ -NMR chemical shifts in  $\text{DMSO-}d_6$  of the methylene group ( $-\text{CH}_2-$ ) for the *N*-alkylated quinazolin-4-ones 3.64-3.66 and *O*-alkylated quinazolin-4-ol 3.68 and 1,5-naphthyridin-4-ol 3.71.

	<i>N</i> -alkylated			<i>O</i> -alkylated		
	Compd	Structure	$^{13}\text{C}$ shifts (ppm)	Compd	Structure	$^{13}\text{C}$ shifts (ppm)
Quinazolin-4-ols/ones	3.64		48.8			
	3.65		48.8			
	3.66		47.0	3.68		64.5
1,5-Naphthyridin-4-ol				3.71		67.3

A faster alternative to  $^{13}\text{C}$  NMR acquisition is a highly sensitive 2D NMR Heteronuclear Single Quantum Correlation (HSQC) experiment, which detects correlations between nuclei of two different types separated by one bond.<sup>124,125</sup> HSQC crosspeaks correlate protons of the methylene linker ( $-\text{CH}_2-$ ) with their attached carbon, facilitating the rapid determination of the  $^{13}\text{C}$  chemical shift of interest.

This methodology does not render definitive proof on atom connectivity. However, in a series of structurally related compounds, the complete assignment of some representatives allows a trend in the  $^{13}\text{C}$  chemical shifts to be established which can be utilised for preliminary assignment of target compounds.

#### **HSQC & HMBC:**

$^1\text{H}$ - $^{13}\text{C}$  HMBC (Heteronuclear Multi-Bond Connectivity) correlates coupled spins across multiple bonds, optimized in a way to detect proton-carbon correlation over two or three bonds.<sup>126,127</sup> Single-bond HSQC and multiple-bond HMBC experiments are complementary and their combination allows full resonance assignment and unambiguous structure determination.

As an example, relevant HMBC correlations of quinolin-4-ols/ones **3.48**, **3.55** are displayed in Figures **3.3-3.4** respectively, to demonstrate their appropriateness for confident differentiation between *N*- and *O*- analogues.

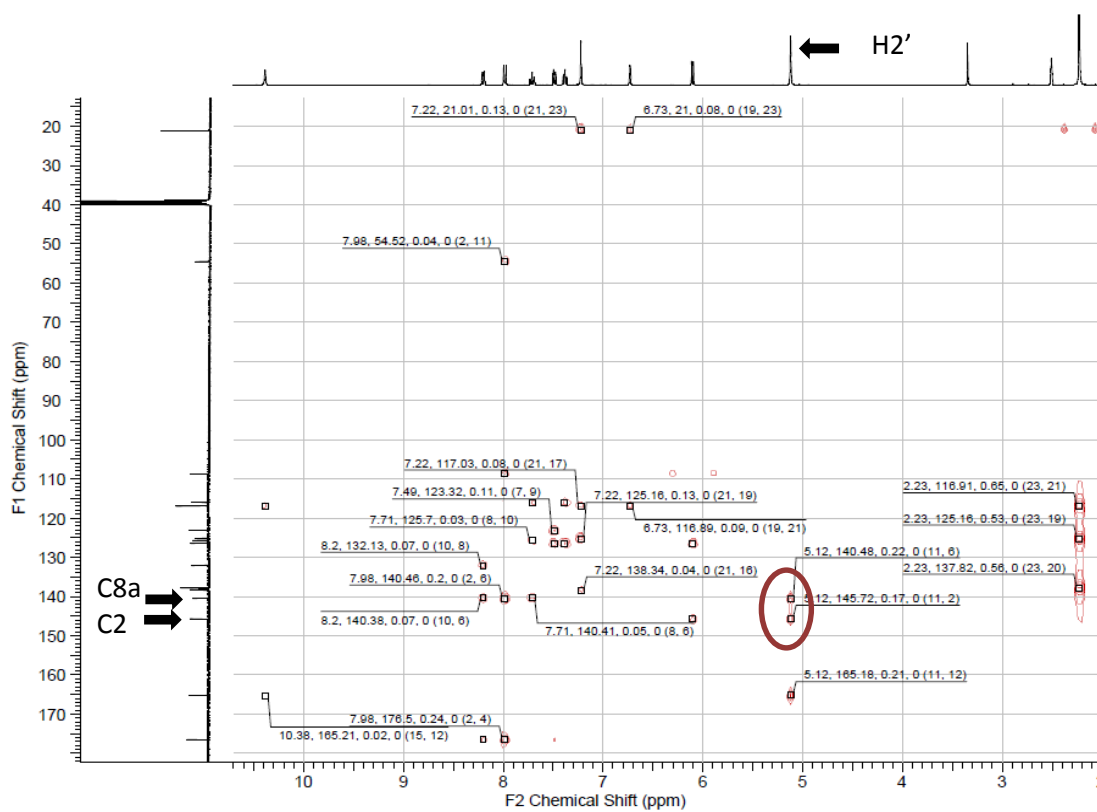


Figure 3.3. HMBC correlations of compound 3.48.

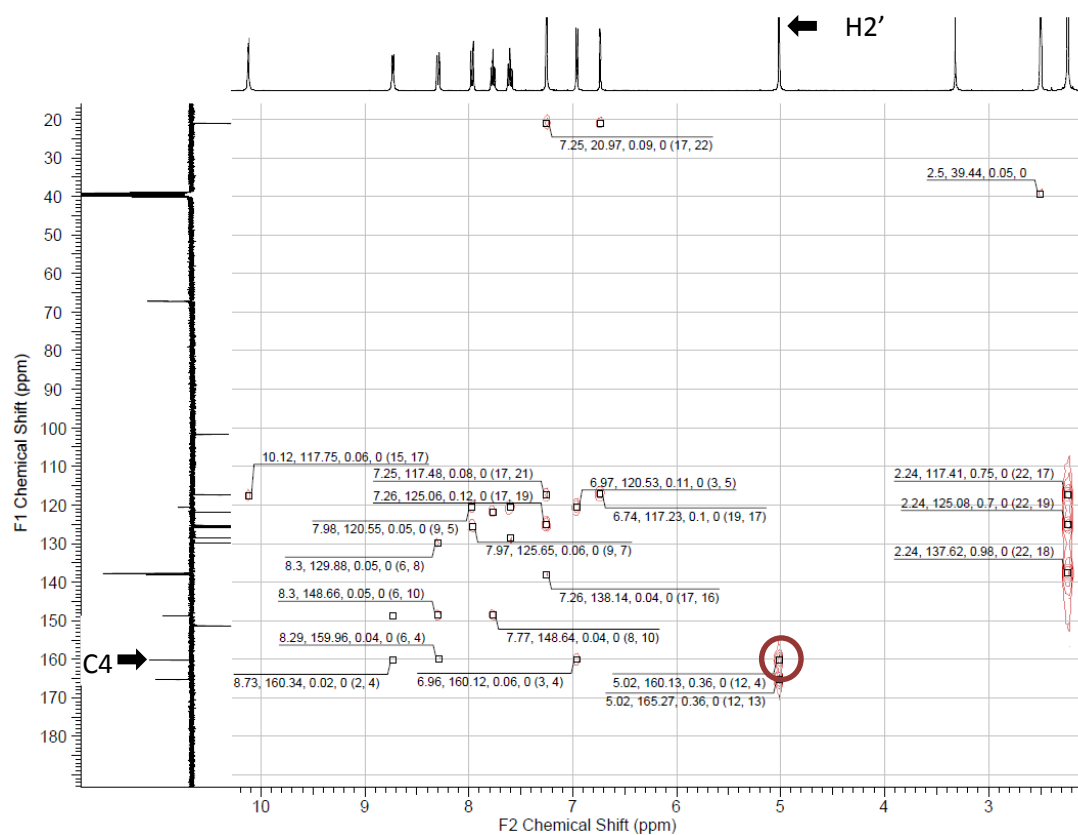
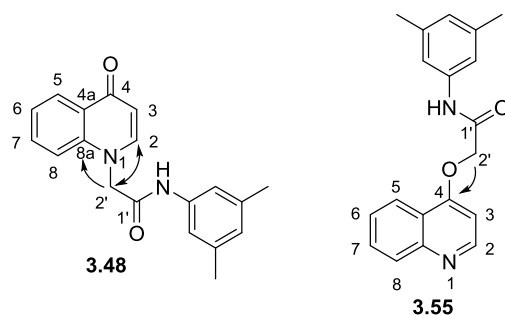


Figure 3.4. HMBC correlations of compound 3.55.

For compound **3.48**, consistency with an *N*-linked connectivity was clear due to the presence of H2'/C2 and H2'/C8a crosspeaks, meaning that H2' should be within two or three bond distances from C2 and C8a of the quinolin-4-ol core, as shown schematically in Figure 3.5. This pattern of correlations was impossible for the *O*-alkylated analogue. Instead, the acetyl protons H2' in compound **3.55** had a distinctive correlation with C4 of the core, indicating the formation of *O*-alkylated regioisomer (Figure 3.5).



**Figure 3.5.** Relevant HMBC connectivities in **3.48** and **3.55** for *N*- vs *O*- differentiation.

Another example of *N/O* differentiation is quinazolin-4-one **3.66** and quinazolin-4-ol **3.68**. Their relevant HMBC correlations are displayed in Figures 3.6 and 3.7.

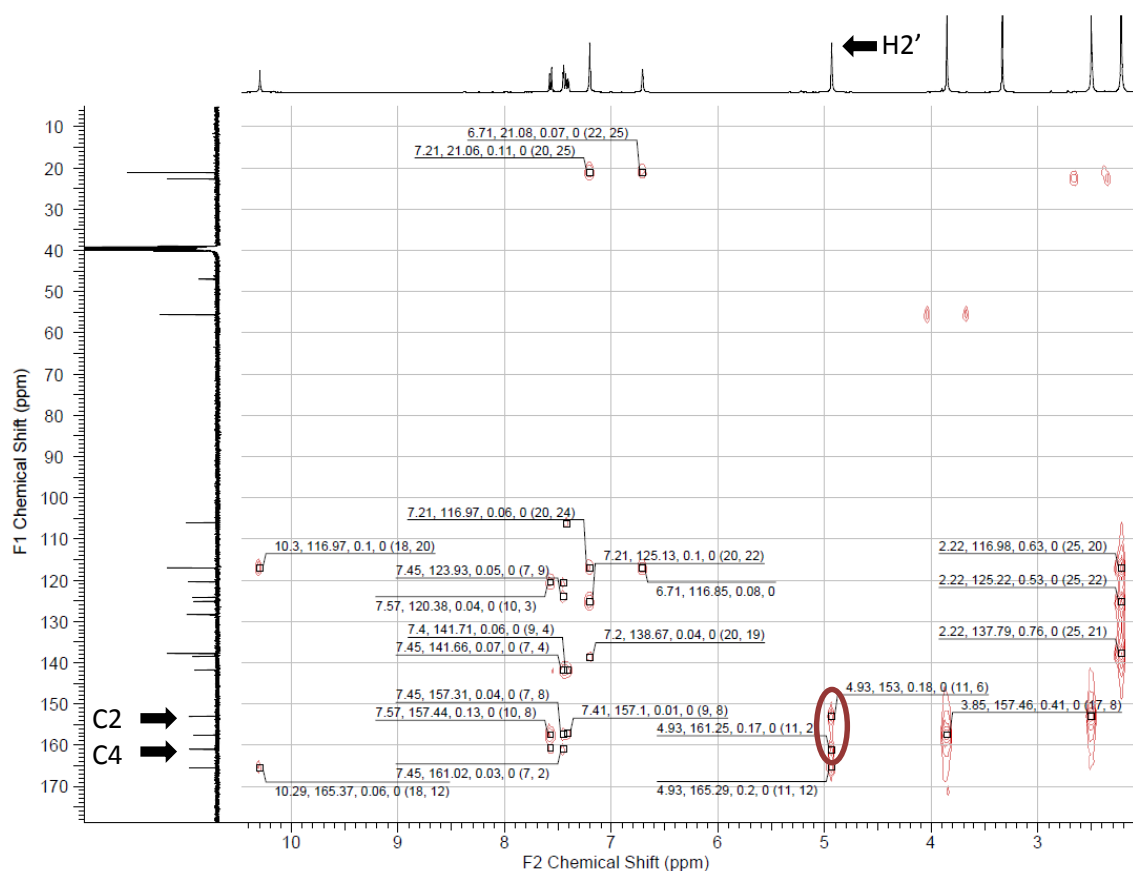


**Figure 3.6.** HMBC correlations of compound **3.66**.

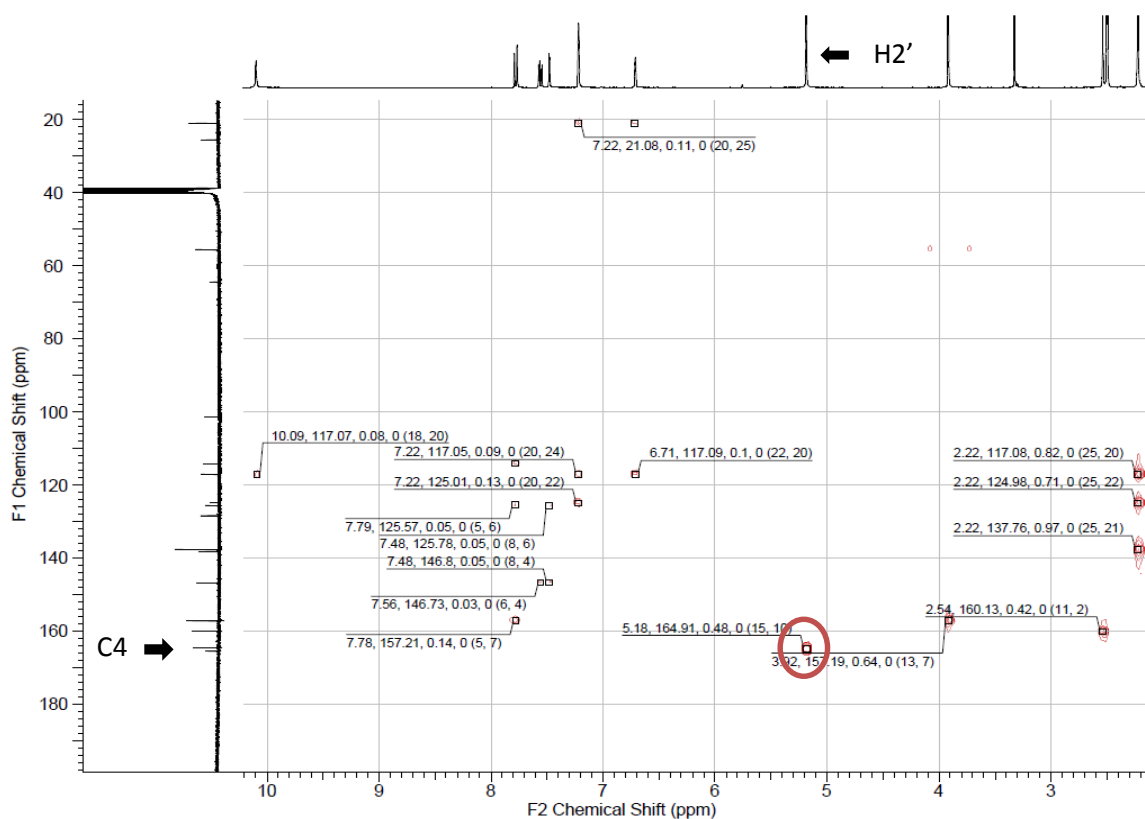


Figure 3.7. HMBC correlations of compound 3.68.

The HMBC spectrum of compound **3.66** demonstrated crosspeaks H2'/C2 and H2'/C4, which were consistent with alkylation on the nitrogen atom at position 3. It is worth noting that the correlation of H2' with C4 of the carbonyl group and absence of H2'/C8a crosspeak excluded the possibility of alkylation on nitrogen atom at position 1. In contrast, in the regioisomer **3.68** only one crosspeak was noted, which was proven to represent H2'/C4 correlation, consistent with the *O*-substituted analogue (Figure 3.8).

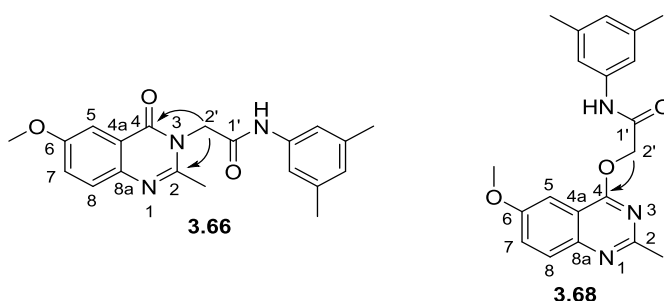


Figure 3.8. HMBC connectivity in 3.66 and 3.68 for *N*- vs *O*-differentiation.

**NOE:**

The Nuclear Overhauser Effect (NOE) is a transfer of nuclear spin polarization through space, not through chemical bonds. It provides valuable information on the intramolecular distances as the relaxation is strongly dependent on the distance between a pair of nuclei. In our studies, 1D NOE experiments were performed by irradiating the methylene linker to produce an intensive signal, while neighbouring nuclei were identified by weaker signals of the opposite phase. The peak to be irradiated should possess a relatively isolated signal in  $^1\text{H}$  NMR in order to produce a precise NOE. 2D NOESY experiments can be used as an alternative to 1D NOE, as it is a pre-programmed NMR experiment which gives connectivity through space for the whole molecule, not only for a selected signal.

In many cases an intrinsic limitation of the NOE approach arises from necessity of a previous full proton and carbon assignments (often by 2D HMBC) for correlation of the observed peaks with the compound structure. Nevertheless, when the groups neighbouring to the bond in question are easily assigned by  $^1\text{H}$  NMR, their chemical shifts can be used directly as references in 1D NOE. In such case, the NOE approach becomes the fastest unambiguous method to assess the compound structure.

We have used this method to confirm our findings from the previous methods in case of compounds **3.48** and **3.55**. NOE spectra are shown in Figures 3.9 and 3.10.

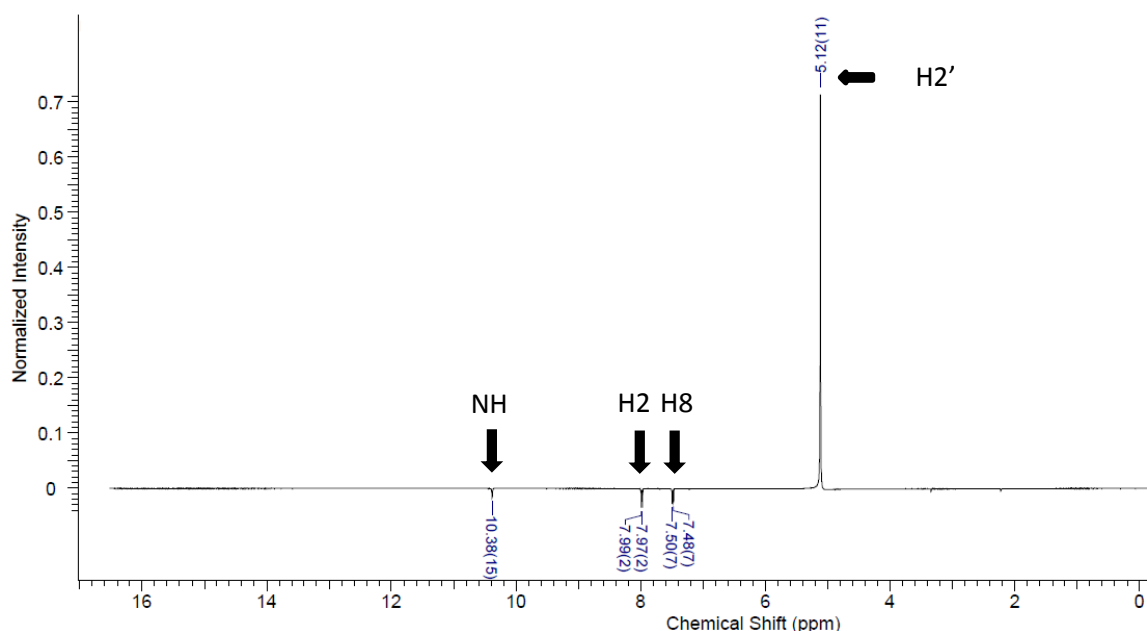


**Figure 3.9. NOE spectrum of compound 3.48 upon irradiation of methylene protons (H2').**

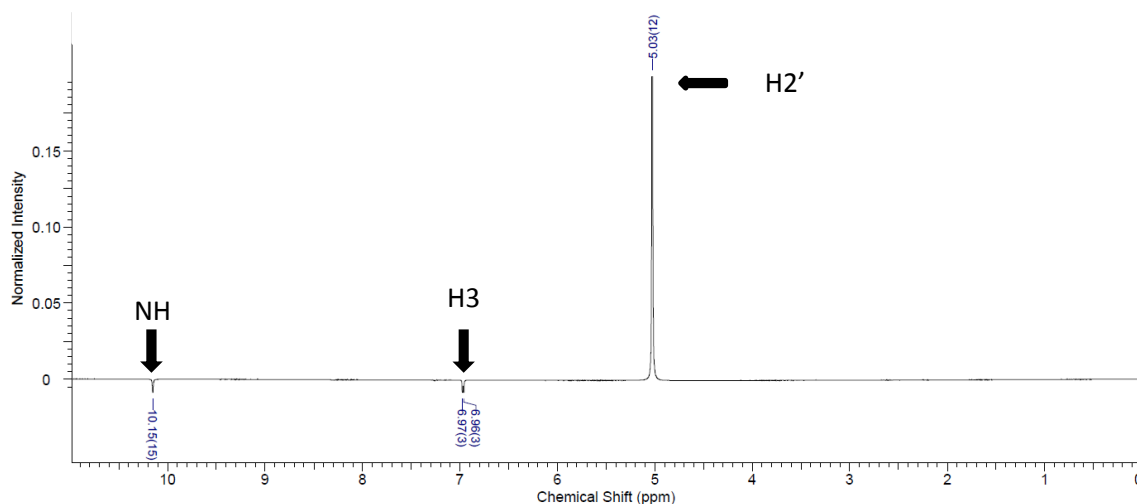


**Figure 3.10.** NOE spectrum of compound **3.55** upon irradiation of methylene protons ( $H_{2'}$ ).

The presence of  $H_2$ ,  $H_8$  and  $NH$  peaks in the NOE spectrum of the compound **3.48** upon irradiation of  $H_{2'}$ , indicated that  $H_{2'}$  is in proximity of those protons. This was consistent with the *N*-alkylated analogue. In contrast, the NOE data of compound **3.55** showed  $H_3$  and  $NH$  peaks upon irradiation of methylene protons  $H_{2'}$ , consistent with the *O*-alkylated analogue (Figure 3.11).

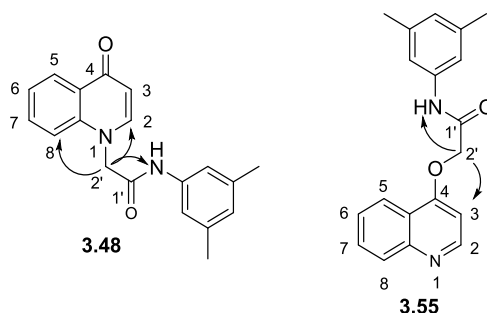


**Figure 3.11.** NOE correlations upon irradiation of  $H_{2'}$  in **3.48** and **3.55** for *N*- vs *O*-differentiation.

The quinazolin-4-ols **3.66** and **3.68** are an excellent demonstration of the NOE method's potential. The 2-methyl group was readily assigned from  $^1H$  NMR spectrum. In this case, no previous full assignment using HSQC and HMBC spectra was necessary. NOE spectra for **3.66** and **3.68** which are shown in Figures 3.12 and 3.13 respectively, offered sufficient proof of structure.

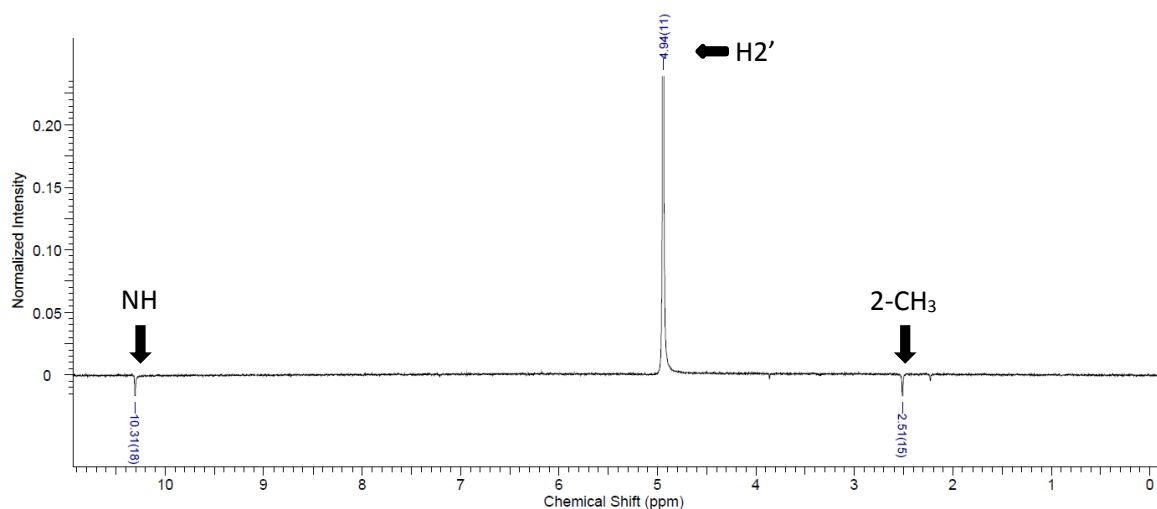


Figure 3.12. NOE spectrum of compound 3.66 upon irradiation of methylene protons (H2').

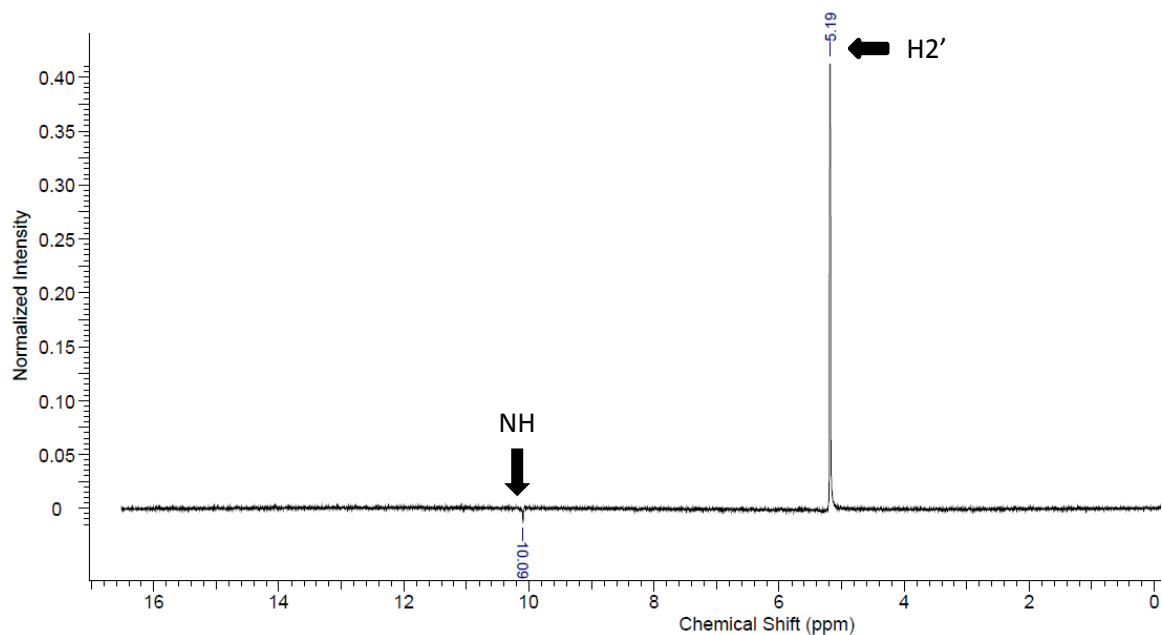
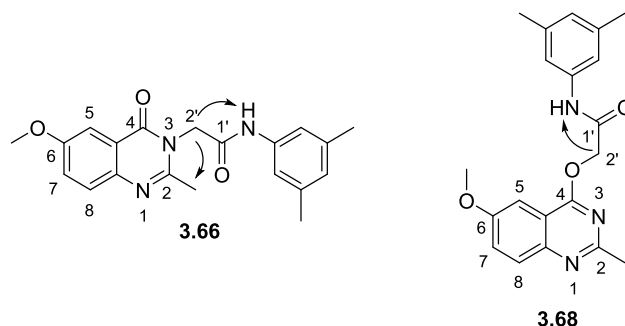


Figure 3.13. NOE spectrum of compound 3.68 upon irradiation of methylene protons (H2').

In case of quinazolin-4-ol derivative **3.66** irradiation of methylene protons H2' resulted in two peaks: NH (of the linker) and 2-CH<sub>3</sub>, which gave a direct indication of the linker proximity to the methyl group. This was consistent with alkylation on the nitrogen atom in position 3. It is worth noticing that no H8 peak was observed, which would be expected in case of alkylation on nitrogen atom in position 1. On the other hand, in **3.68** only a weak NH signal (amide) was registered upon irradiation of methylene proton H2', which was in a good agreement with the *O*-alkylated analogue (Figure 3.14).



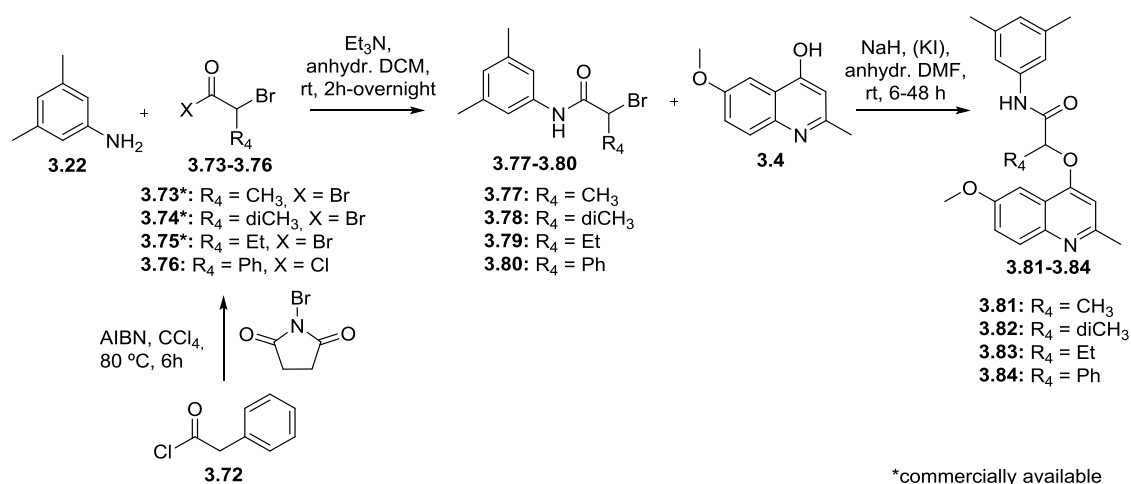


**Figure 3.14.** NOE correlations upon irradiation of H2' in **3.66** and **3.68** for N- vs O-differentiation.

### 3.3.2. Modification of the linker

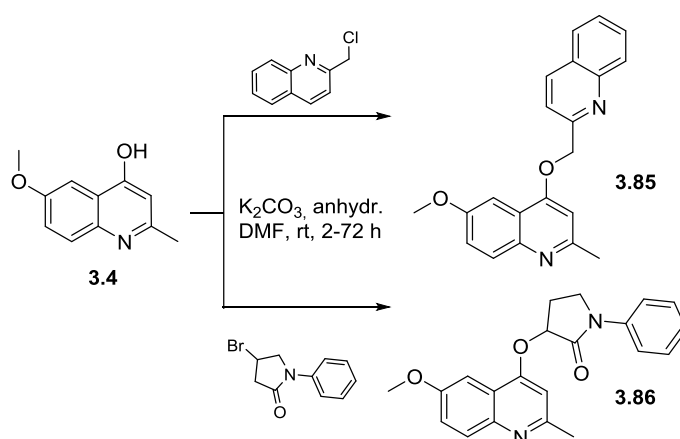
SAR investigation of the linker region was focused on three main approaches: (1) introduction of substituents on the acetyl's methylene group, (2) conformational constraint of the linker and (3) other modification types (Schemes 3.8, 3.9 and 3.10, respectively).

The synthetic approach to target compounds with the first modification type (**3.81-3.84**, summarized in Scheme 3.8), was analogous to the general strategy described earlier (Scheme 3.2). The reaction of 3,5-dimethylaniline **3.22** with acyl halides **3.73-3.76** gave intermediates **3.77-3.80**. The bromoalkylacyl bromides **3.73-3.75** were commercially available, while 2-bromo-2-phenylacetyl chloride **3.76** was prepared from phenylacetyl chloride **3.72** in the presence of *N*-bromosuccinimide and 2,2'-azobis(2-methylpropionitrile) (AIBN) according to a literature procedure.<sup>128</sup> The final products **3.81-3.84** were subsequently obtained by alkylation of 2-methyl-6-methoxy-quinolinol **3.4** with these halides (**3.77-3.80**) in the presence of sodium hydride (NaH).

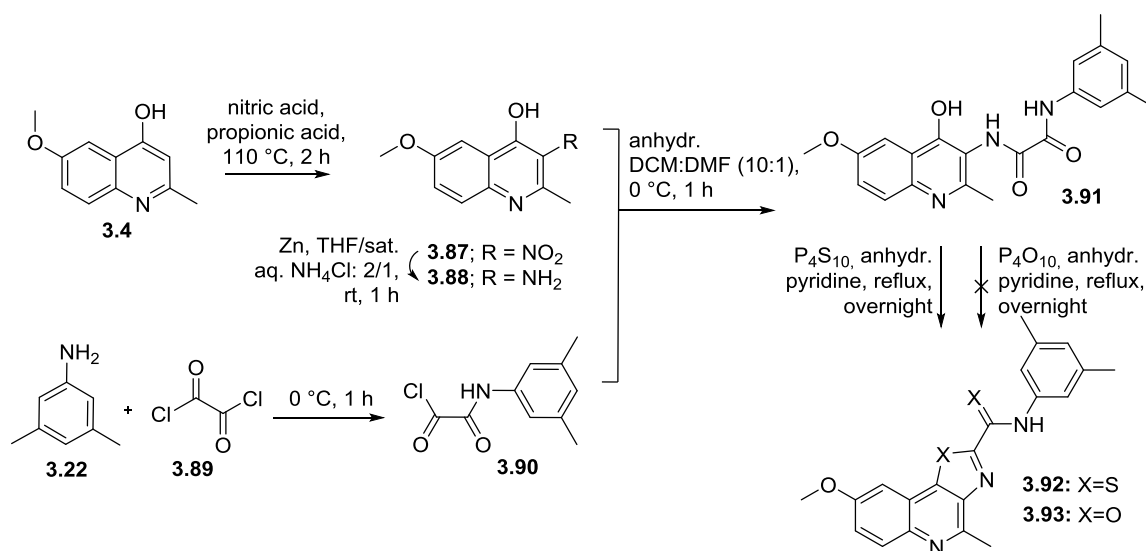


**Scheme 3.8.** Synthesis of compounds with introduction of substituents on the linker.

Next, four conformationally constrained analogues were prepared (compounds **3.85**, **3.86**, **3.92** and **3.95**). While the synthetic preparation of the target compounds **3.85** and **3.86** could be achieved using the general alkylation procedure (Scheme 3.9), a more lengthy approach was required for compound **3.92** (Scheme 3.10). Nitration and subsequent zinc/ammonium chloride ( $\text{Zn}/\text{NH}_4\text{Cl}$ ) reduction of 2-methyl-6-methoxyquinolin-4-ol (**3.4**) yielded 3-aminoquinolin-4-ol **3.88**.<sup>103</sup> The latter compound was *N*-acylated with intermediate **3.90**, which was prepared from oxalyl chloride **3.89** and 3,5-dimethylaniline **3.22**. Dehydration of the obtained intermediate **3.91** with phosphorus pentasulfide ( $\text{P}_4\text{S}_{10}$ ) led to the assembly of the annulated thiazole ring of thiazoloquinoline **3.92**. The associated formation of a thioamide in **3.92** during  $\text{P}_4\text{S}_{10}$ -mediated dehydration was not considered problematic, and the obtained compound was allowed to enter biological evaluation after purification. Comparable attempts to prepare the oxazole analogue of **3.92** (compound **3.93**) by dehydration of **3.91** with phosphorus pentoxide ( $\text{P}_4\text{O}_{10}$ ), were not successful.

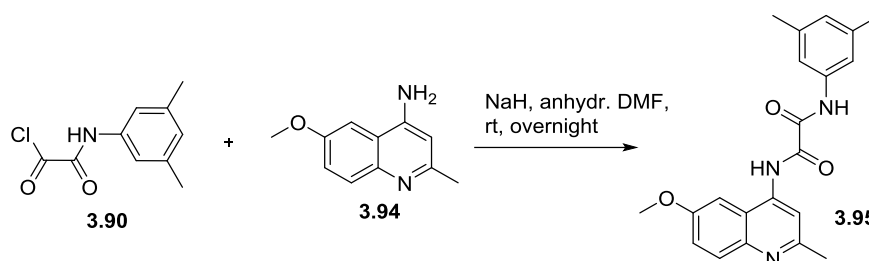


Scheme 3.9. Synthesis of compounds **3.85**, **3.86** with conformational constraint of the linker.



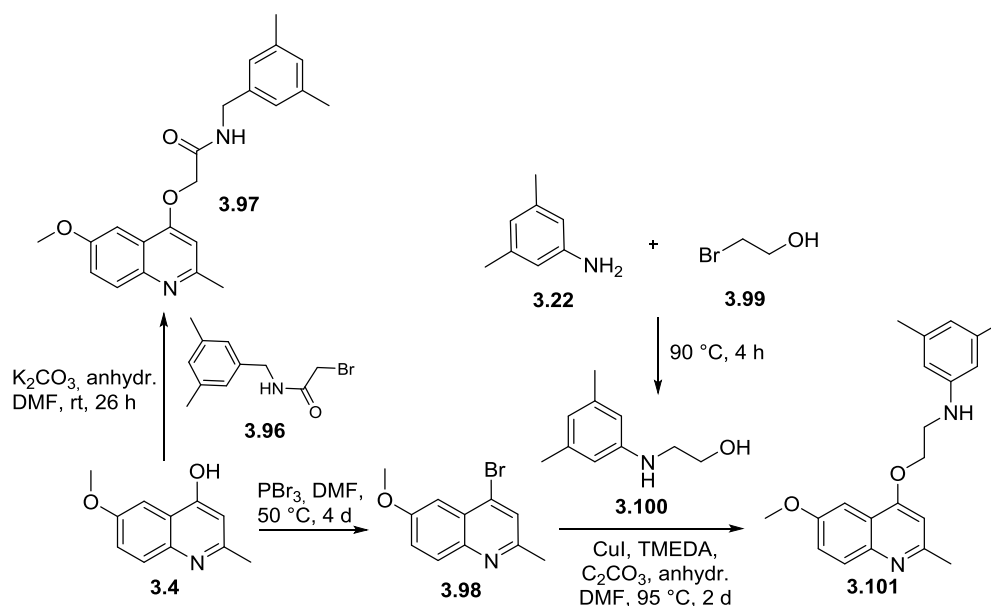
Scheme 3.10. Synthesis of compound **3.92** with a conformational constraint linker.

Compound **3.95** was obtained from the acylation reaction of intermediate **3.90** with the commercially available 2-methyl-4-amino-6-methyl quinoline **3.94**, as shown in Scheme 3.11.



**Scheme 3.11. Synthesis of compound 3.95 with a conformational constraint linker.**

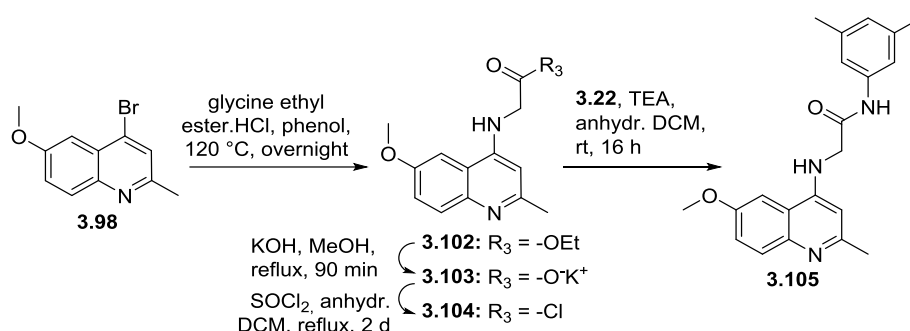
Subsequently, three more analogues (**3.97**, **3.101** and **3.105**) were prepared with linker modifications that were not covered in the aforementioned sets (Schemes 3.12 and 3.13). The synthetic approach to **3.97** was completely analogous to the general strategy mentioned earlier. While for the preparation of **3.101**, the hydroxy group of quinolinol **3.4** was converted to bromine by phosphorous tribromide ( $\text{PBr}_3$ ) leading to intermediate **3.98**. Separately, the reaction of 3,5-dimethylaniline **3.22** and 2-bromoethanol **3.99** resulted in intermediate **3.100**, which was subsequently coupled with **3.98** to yield the target compound **3.101** using Cu(I)-catalysis (Ullmann reaction).<sup>129,114</sup>



**Scheme 3.12. Synthesis of compounds 3.97 and 3.101 which contain other linker modification types.**

For the synthesis of **3.105**, intermediate **3.98** was coupled with glycine ethyl ester under nucleophilic aromatic substitution conditions to yield the carboxylic ester **3.102**.<sup>130</sup> After basic hydrolysis of **3.102** in methanol, carboxylate **3.103** was obtained in quantitative yield and then

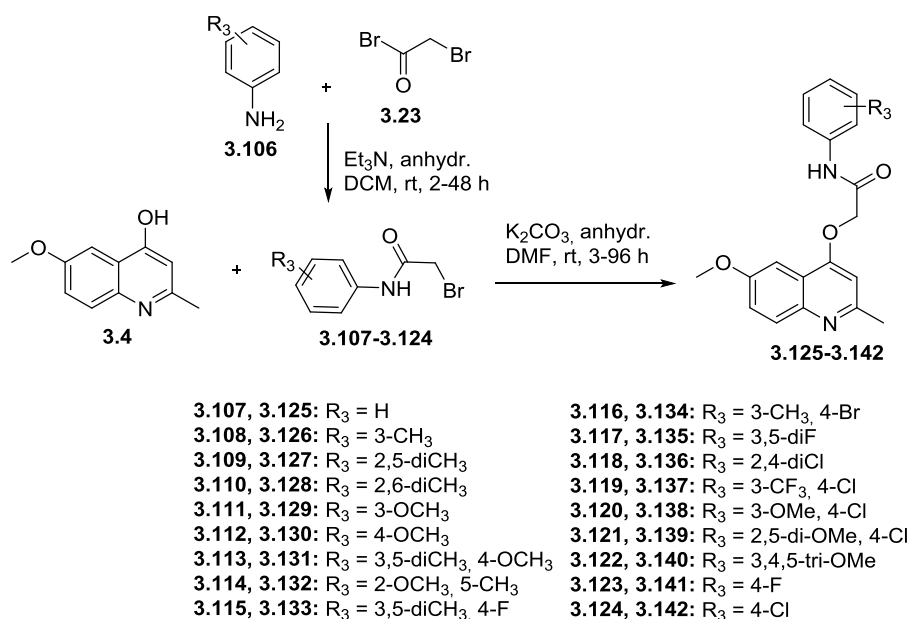
converted to the acyl chloride **3.104** using thionyl chloride (SOCl<sub>2</sub>). Amide bond formation between intermediate **3.104** and 3,5-dimethylaniline **3.22** was achieved using basic acylating conditions to afford final compound **3.105**.



**Scheme 3.13.** Synthesis of compound **3.105** which contain other linker modification types.

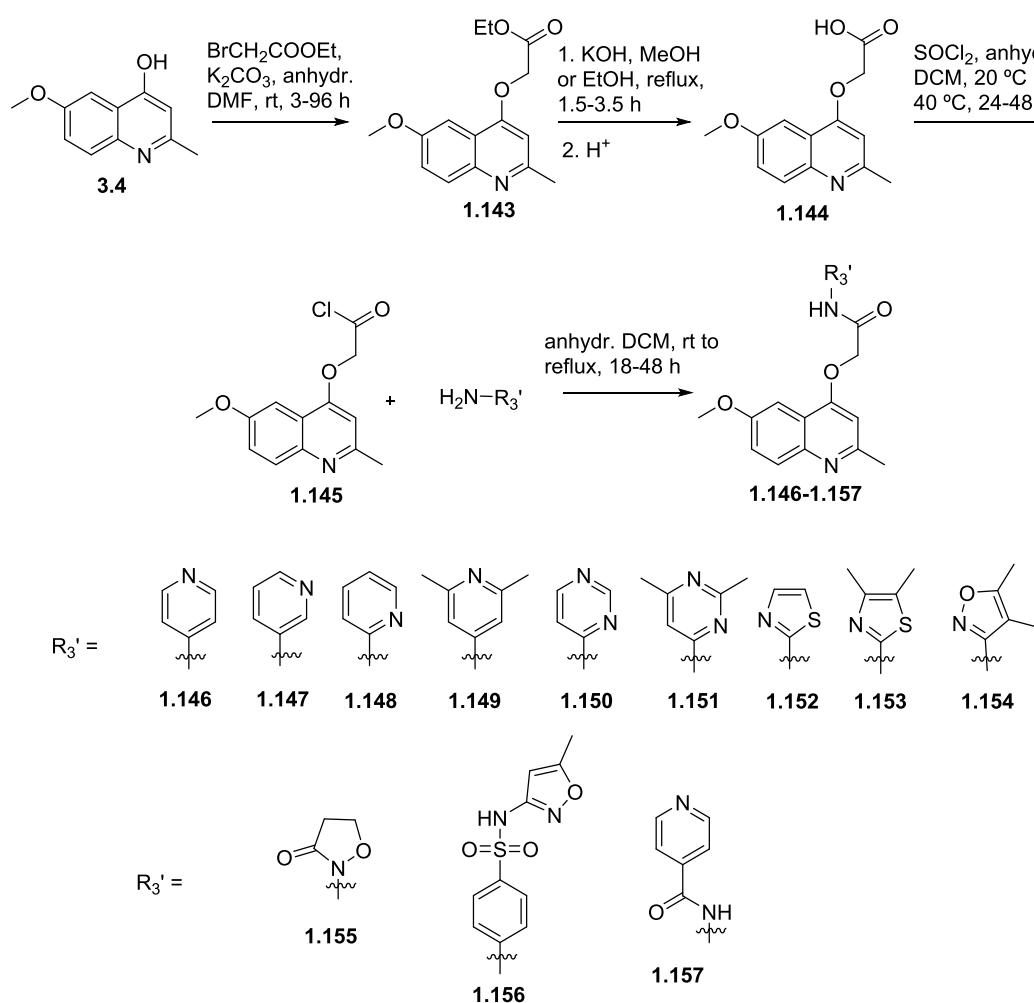
### 3.3.3. Modification of the northern aryl fragment

Analogue in this section are divided into three categories: (1) derivatives with modified phenyl substitution (**3.125-3.142**), (2) compounds with heteroaryl groups (**3.146-3.154**) and (3) hybrid molecules in which known anti-TB drugs replace the aniline of the initial hits (**3.155-3.157**). The synthesis of the first set of compounds (**3.125-3.142**) relied on the general alkylation-based methodology. Thus, haloacetamide intermediates **3.107-3.124** were first prepared by acylation of a number of commercially available anilines coupled with bromoacetyl bromide **3.23**, as depicted in Scheme 3.14 (Method A). Subsequently, *O*-alkylation of the quinolinol **3.4** with these halides (**3.107-3.124**) resulted in the final products **3.125-3.142**.



**Scheme 3.14.** Synthesis of compounds with modifications of the northern aryl fragment (Method A).

The target compounds **3.146-3.154** were obtained by an alternative route (Method B) shown in Scheme 3.15. According to this, quinolinol **3.4** was alkylated with ethyl 2-bromoacetate followed by hydrolysis of ester **3.143** under basic conditions and conversion of the corresponding carboxylic acid **3.144** to acyl chloride **3.145** using thionyl chloride (SOCl<sub>2</sub>). Subsequently, reaction with a number of commercially available heteroaromatic amines afforded the final compounds (**3.146-3.154**). Lastly, the same methodology (method B) was used to synthesize three “hybrid” compounds, in which the quinoloxacetamide core was covalently linked to known anti-TB drugs with available free amines: cycloserine (**3.155**), sulfamethoxazole (**3.156**) and isoniazid (**3.157**).<sup>131</sup>

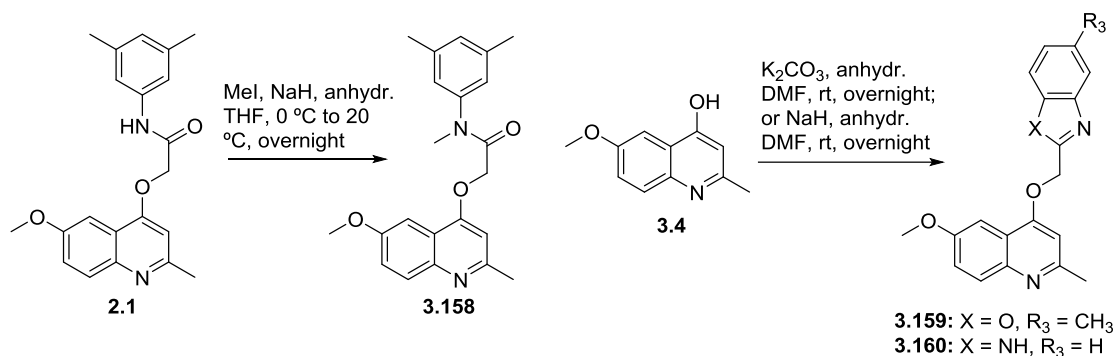


**Scheme 3.15. Synthesis of compounds with modifications of the northern aryl fragment (Method B).**

### 3.3.4. Amide bond replacements

Lastly, three compounds (**3.158-3.160**) which could avoid amide bond hydrolysis were prepared and their synthesis is shown in Scheme 3.16. Deprotonation of compound **2.1** using sodium hydride (NaH) and subsequent methylation with methyl iodide (MeI) afforded the target

compound **3.158**. Preparation of compounds **3.159** and **3.160** was similar to the general alkylation method described previously.



**Scheme 3.16. Synthesis of compounds with amide bond replacements.**

### 3.4. Results and discussion

The hit compound **2.1** obtained from high throughput screening (HTS) was resynthesized to confirm its activity and evaluated together with 72 novel derivatives.

#### 3.4.1. Antimycobacterial activity, cytotoxicity and physicochemical properties

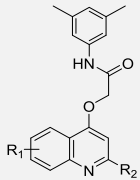
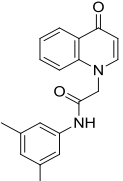
All final compounds were first assayed for their antimycobacterial activity against *M. tuberculosis* H37Rv strain, which showed that several compounds were potent antimycobacterials, with micromolar levels of activity. To better understand the properties of these compounds beyond their antimycobacterial activity, cytotoxicity in HepG2 cells was evaluated. In parallel, physicochemical measurements were obtained to further explore the profiles of these molecules, and in particular, artificial membrane permeability (AMP), kinetic aqueous solubility (CLND, chemiluminescent nitrogen detection) and the hydrophobicity was measured using the chromatography technique to generate ChromlogD (pH 7.4) values.<sup>132,100</sup>

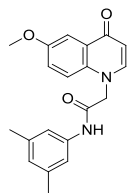
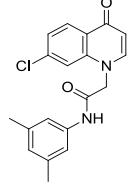
##### 3.4.1.1. Modification of the quinoline substitution pattern

Table 3.3 presents the results for the reference compound **2.1** and the first set of compounds possessing variations to the substitution pattern of the quinoline system (**3.25-3.41**). The main goal was to investigate the contribution to antimycobacterial activity of the 6-methoxy and 2-methyl quinoline substituents. Therefore, the 6-methoxy substituent was removed or replaced with halides, methylthio, alkyl or alkoxy substituents (**3.25, 3.26, 3.28-3.33, 3.35**, Table 3.3). In addition, a regio-isomer of compound **2.1** with the methoxy group shifted from position 6 to 7 was prepared (**3.27**, Table 3.3). Compound **3.34** possessed two methoxy groups at positions 6 and

7. Since the 2-methyl substituent of hits **2.1** and **2.2** was suspected to be a metabolically labile site, a few analogues possessing a trifluoromethyl group were synthesized (**3.36-3.40**, Table 3.3). Additionally, the 2-methyl group was replaced by a propyl group in an attempt to explore the available space (**3.41**).

**Table 3.3. Biological profile of the compounds with a modified quinoline part.**

Compd			MIC ( $\mu\text{M}$ ) <sup>[a]</sup>	TOX <sub>50</sub> ( $\mu\text{M}$ ) <sup>[b]</sup>	Permeability (nm/sec) <sup>[c]</sup>	Solubility ( $\mu\text{M}$ ) <sup>[d]</sup>	Chrom logD <sup>[e]</sup>
	R <sub>1</sub>	R <sub>2</sub>					
<b>2.1</b>	6-OCH <sub>3</sub>	-CH <sub>3</sub>	1.9	20	180	26	5.64
<b>3.25</b>	-H	-CH <sub>3</sub>	24	>100	370	55	5.39
<b>3.26</b>	6-SCH <sub>3</sub>	-CH <sub>3</sub>	>125	>100	n.d. <sup>[f]</sup>	3	6.42
<b>3.27</b>	7-OCH <sub>3</sub>	-CH <sub>3</sub>	>250	50	n.d. <sup>[f]</sup>	n.d. <sup>[f]</sup>	5.59
<b>3.28</b>	6-F	-CH <sub>3</sub>	15.6	63	310	28	5.79
<b>3.29</b>	6-Cl	-CH <sub>3</sub>	40	>100	n.d. <sup>[f]</sup>	8	6.38
<b>3.30</b>	6-CH <sub>3</sub>	-CH <sub>3</sub>	3.9	16	520	83	5.95
<b>3.31</b>	6-CF <sub>3</sub>	-CH <sub>3</sub>	>250	>100	<30	10	6.67
<b>3.32</b>	6-OCF <sub>3</sub>	-CH <sub>3</sub>	>250	>100	<30	n.d. <sup>[f]</sup>	6.79
<b>3.33</b>	6-OEt	-CH <sub>3</sub>	>250	>100	<30	n.d. <sup>[f]</sup>	5.98
<b>3.34</b>	6,7-diOCH <sub>3</sub>	-CH <sub>3</sub>	>250	10	605	n.d. <sup>[f]</sup>	4.84
<b>3.35</b>	6-OCH <sub>2</sub> Ph	-CH <sub>3</sub>	>250	>100	<10	<1	7.03
<b>3.36</b>	6-OCH <sub>3</sub>	-CF <sub>3</sub>	>250	>100	<10	15	7.02
<b>3.37</b>	6-OCF <sub>3</sub>	-CF <sub>3</sub>	>250	>100	<3	34	7.96
<b>3.38</b>	6-OEt	-CF <sub>3</sub>	>250	>100	<3	<1	7.55
<b>3.39</b>	6,7-methylen-dioxy	-CF <sub>3</sub>	>250	>100	<30	<1	6.73
<b>3.40</b>	8-CF <sub>3</sub>	-CF <sub>3</sub>	>250	>100	<10	<1	7.73
<b>3.41</b>	6-OCH <sub>3</sub>	-Pr	>250	13	n.d. <sup>[f]</sup>	12	6.44
<b>3.48</b>			>250	63	450	34	3.54

<b>3.49</b>			>250	>100	190	30	3.72
<b>3.50</b>			>250	100	260	86	4.39
<b>3.55</b>	6-H	-H	>80	>100	460	59	5.03
<b>3.56</b>	6-OCH <sub>3</sub>	-H	10	50	280	51	5.30

<sup>a</sup>MIC against *M. tuberculosis* (H37Rv), isoniazid was used as reference with MIC = 1.8 μM; <sup>b</sup>HepG2, human caucasian hepatocyte carcinoma; <sup>c</sup>artificial membrane permeability; <sup>d</sup>*in vitro* profiling for kinetic aqueous solubility (CLND, chemiluminescent nitrogen detection); <sup>e</sup>chromlogD values at pH = 7.4; <sup>f</sup>n.d. = not determined.

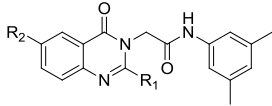
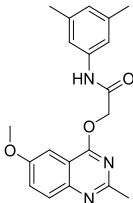
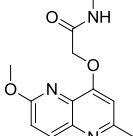
As shown in Table 3.3, SAR analysis of the quinoline part of the molecule showed that only a methyl can be considered an acceptable alternative for the original 6-methoxy group (**3.30**, MIC = 3.9 μM). This compound showed slightly better solubility (CLND) and high permeability, although it displayed similar cytotoxicity to **2.1**. The presence of fluorine or no substituent (-H) at the same position led to decreased activity (**3.28** and **3.25**; MIC = 15.6 and 24 μM, respectively). Chlorine resulted in a further drop of the potency (**3.29**, MIC = 40 μM). All the other substituents in the series were inactive. Steric limitations might be involved here, although other factors most likely contribute, as reflected by the absence of activity for the 6-trifluoromethyl containing analogue **3.32**.<sup>133</sup> Regarding the methyl group at position 2, its replacement with a trifluoromethyl or a propyl group led to inactive compounds (**3.36** and **3.41**). On the other hand, removal of the methyl group at position 2, preserved some of the antimycobacterial potency (**3.56**, MIC = 10 μM). For all the compounds (**3.36-3.40**) possessing a trifluoromethyl group in position 2, the extremely poor solubility, poor permeability and higher chromlogD values could play a role in the loss of potency. All *N*-alkylated compounds (**3.48-3.50**) completely lost their activity against *M. tuberculosis*, suggesting that alkylation at the *O*- is essential for the activity of this series. Removal of both substituents from the quinoline core led to the inactive compound **3.55**.

#### 3.4.1.2. Replacement of quinoline with related aza-aromatic systems

Table 3.4 presents the biological and physicochemical data obtained for compounds containing related aza-aromatic systems such as quinazoline and naphthyridine instead of quinoline together with the *N*(3)-alkyl quinazolines obtained.



**Table 3.4. Biological profile of the compounds with related aza-aromatic systems.**

Compd	Structure	MIC ( $\mu\text{M}$ ) <sup>[a]</sup>	TOX <sub>50</sub> ( $\mu\text{M}$ ) <sup>[b]</sup>	Permeability (nm/sec) <sup>[c]</sup>	Solubility ( $\mu\text{M}$ ) <sup>[d]</sup>	Chrom logD <sup>[e]</sup>
<b>3.64</b>	 <p>3.64: R<sub>1</sub> = H, R<sub>2</sub> = H            3.65: R<sub>1</sub> = H, R<sub>2</sub> = OCH<sub>3</sub>            3.66: R<sub>1</sub> = CH<sub>3</sub>, R<sub>2</sub> = OCH<sub>3</sub></p>	>250	79	600	20	4.29
<b>3.65</b>		>250	>100	n.d. <sup>[f]</sup>	8	4.50
<b>3.66</b>		250	>100	580	74	4.77
<b>3.68</b>		1.25	>100	370	4	5.59
<b>3.71</b>		3.8	>100	510	19	5.57

<sup>a</sup>MIC against *M. tuberculosis* (H37Rv), isoniazid was used as reference with MIC = 1.8  $\mu\text{M}$ ; <sup>b</sup>HepG2, human caucasian hepatocyte carcinoma; <sup>c</sup>artificial membrane permeability; <sup>d</sup>*in vitro* profiling for kinetic aqueous solubility (CLND, chemiluminescent nitrogen detection); <sup>e</sup>chromlogD values at pH = 7.4; <sup>f</sup>n.d. = not determined.

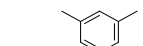
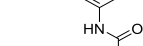
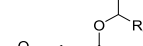
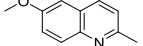
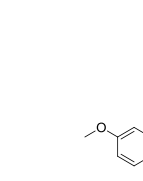
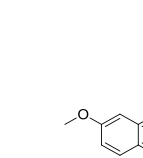
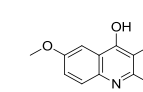
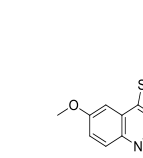
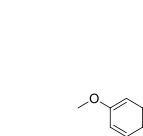
As before, all *N*-alkylated compounds (**3.64-3.66**) completely lost their activity against *M. tuberculosis*. The most interesting compounds, possessing a quinazolinone or naphthyridine core (**3.68, 3.71**), showed potent antimycobacterial activity with MIC values of 1.25 and 3.8  $\mu\text{M}$ , respectively, comparable with the reference compound **2.1**. Additionally, these compounds did not exhibit cytotoxicity against HepG2 cells, another improvement on the reference compound **2.1**. Unfortunately, chromlogD values for compounds **3.68** and **3.71** remained at the same level as **2.1**, while their solubility continued to be very poor (<30  $\mu\text{M}$ ).

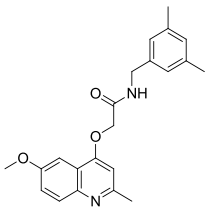
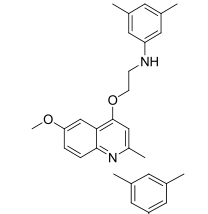
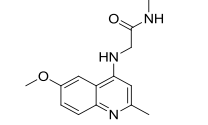
### 3.4.1.3. Modification of the linker

Table 3.5 presents the results for the second set of compounds possessing modifications of the linker. The first area of exploration was around the acetyl methylene group. Mono-substitution at this prochiral position is the most straightforward way of introducing a chiral center in these compounds without affecting the quinoloxacetamide basic framework. In addition, this site was also suspected of being a contributor to the fast (oxidative) metabolism observed for the hit compounds. In this initial proof-of-concept compound set, the substituent choice was limited to small aliphatic groups (methyl and ethyl) and a phenyl ring (**3.81-3.84**). Next, four

conformationally constrained analogues were prepared (**3.85**, **3.86**, **3.92** and **3.95**). In compounds **3.85**, **3.86** and **3.92** conformational locking was accomplished by an additional ring closure, while in the case of analogue **3.95** the oxalyl diamide fragment was expected to rigidify the linker region into a constrained conformation.<sup>134, 135</sup> Subsequently, three more analogues (**3.97**, **3.101**, **3.105**) were prepared with linker-modifications that were not covered in the aforementioned sets. Compound **3.97** contained a benzylamide function as a means to avoid potential toxicity and metabolic stability concerns that are associated with anilide groups. Compound **3.101** possesses a fully reduced linker, while in compound **3.105** the ether bridge between the linker region and the quinoline residue was replaced by an amine function.

**Table 3.5. Biological profile of the compounds with linker modifications.**

Compd	Structure	MIC ( $\mu\text{M}$ ) <sup>[a]</sup>	TOX <sub>50</sub> ( $\mu\text{M}$ ) <sup>[b]</sup>	Permeability (nm/sec) <sup>[c]</sup>	Solubility ( $\mu\text{M}$ ) <sup>[d]</sup>	Chrom logD <sup>[e]</sup>
<b>3.81</b>	 R <sub>4</sub> = CH <sub>3</sub>	125	40	320	61	5.76
<b>3.82</b>	 R <sub>4</sub> = diCH <sub>3</sub>	>250	>100	n.d. <sup>[f]</sup>	20	6.37
<b>3.83</b>	 R <sub>4</sub> = Et	>250	79	390	123	6.28
<b>3.84</b>	 R <sub>4</sub> = Ph	>125	>100	<30	2	7.13
<b>3.85</b>		32	32	470	21	5.48
<b>3.86</b>		125	100	550	215	4.99
<b>3.91</b>		>125	>100	n.d. <sup>[f]</sup>	10	3.76
<b>3.92</b>		>125	>100	<30	35	n.d. <sup>[f]</sup>
<b>3.95</b>		>125	>100	n.d. <sup>[e]</sup>	10	6.47

<b>3.97</b>		31	>100	<3	92	5.25
<b>3.101</b>		32	32	190	33	6.93
<b>3.105</b>		47	6	310	204	3.59

<sup>a</sup>MIC against *M. tuberculosis* (H37Rv), isoniazid was used as reference with MIC = 1.8 μM; <sup>b</sup>HepG2, human caucasian hepatocyte carcinoma; <sup>c</sup>artificial membrane permeability; <sup>d</sup>*in vitro* profiling for kinetic aqueous solubility (CLND, chemiluminescent nitrogen detection); <sup>e</sup>chromlogD values at pH = 7.4; <sup>f</sup>n.d. = not determined.

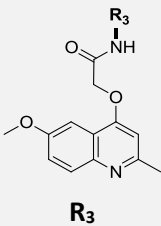
Antimycobacterial screening of the compounds with an *alpha*-substituted acetyl group (**3.81-3.84**) demonstrated that modifications of this type are detrimental to activity. Similarly, in the second group of compounds the activity was lost or significantly reduced in all cases, except from compound **3.85** which exhibited moderate activity. In the same way, compounds belonging to the third group (**3.97**, **3.101** and **3.105**) showed moderate potency giving MIC values of 31, 32 and 47 μM respectively.

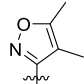
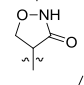
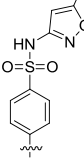
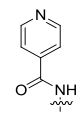
#### 3.4.1.4. Modification of the northern aryl fragment

To investigate the role of the hydrophobic phenyl ring in the northern part of the molecule, thirty compounds (**3.125-3.142**, **3.146-3.157**) possessing modifications on the northern aryl part were prepared and data from their biological and physicochemical evaluation is presented in Table 3.6. Analogues in this section are divided into three categories: (1) derivatives with modified phenyl substitution (**3.125-3.142**), (2) compounds with heteroaryl groups (**3.146-3.154**) and (3) hybrid molecules in which three known anti-TB drugs replaced the aniline of the hit compounds (**3.155-3.157**). For the first category, the initial goal was to introduce a diverse set of commercially available anilines. These molecules allowed a more thorough investigation of the role of the aryl substituents on the antimycobacterial properties of QOA-based molecules. Furthermore, the metabolic liability of the specific aryl residues present in **2.1** and **2.2** had also been proposed as a potential reason for the observed microsomal instability. Therefore, additional value for this series could come from its potential to deliver antimycobacterial products in which positions prone to

CYP-mediated oxidation have been blocked or modified. Similar to the substitutions discussed above, replacement of the phenyl ring with a heteroaryl (**3.146-3.154**) offered the possibility of improving the microsomal stability, at least partially, by reducing the overall lipophilicity of the molecule. Commercially available heteroaromatic amines with an identical or similar dimethyl-substitution pattern as present in reference **2.1** were included in the series to allow direct comparisons. Regarding the hybrid compounds, we hypothesized that the full hybrid constructs could still possess antimycobacterial properties. In addition, if metabolic cleavage of the amide would take place, either inside bacteria or mediated by host metabolism, a second antimycobacterial compound could be released.

**Table 3.6. Biological profile of the compounds with modifications on the northern aryl.**

Compd		MIC ( $\mu\text{M}$ ) <sup>[a]</sup>	TOX <sub>50</sub> ( $\mu\text{M}$ ) <sup>[b]</sup>	Permeability (nm/sec) <sup>[c]</sup>	Solubility ( $\mu\text{M}$ ) <sup>[d]</sup>	Chrom logD <sup>[e]</sup>
<b>3.125</b>	phenyl	2	40	370	63	4.28
<b>3.126</b>	3-CH <sub>3</sub> -phenyl	2	40	355	193	4.83
<b>3.127</b>	2,5-diCH <sub>3</sub> -phenyl	8	>100	810	45.5	5.05
<b>3.128</b>	2,6-diCH <sub>3</sub> -phenyl	125	>100	630	112	4.55
<b>2.2</b>	2-OCH <sub>3</sub> -phenyl	1.4	>100	120	38	4.68
<b>3.129</b>	3-OCH <sub>3</sub> -phenyl	6.4	>100	470	35	4.49
<b>3.130</b>	4-OCH <sub>3</sub> -phenyl	0.6	>100	420	108	4.22
<b>3.131</b>	3,5-diCH <sub>3</sub> , 4-OCH <sub>3</sub> -phenyl	1	8	320	17	4.99
<b>3.132</b>	2-OCH <sub>3</sub> , 5-CH <sub>3</sub> -phenyl	2.5	>100	n.d. <sup>[f]</sup>	9.5	5.65
<b>3.133</b>	3,5-diCH <sub>3</sub> , 4-F-phenyl	2	>100	210	31.5	5.50
<b>3.134</b>	3-CH <sub>3</sub> , 4-Br-phenyl	3.9	16	n.d. <sup>[f]</sup>	<1	5.95
<b>3.135</b>	3,5-diF-phenyl	3	>100	n.d. <sup>[f]</sup>	13	5.13
<b>3.136</b>	2,4-diCl-phenyl	2	>100	n.d. <sup>[f]</sup>	20.5	6.40
<b>3.137</b>	3-CF <sub>3</sub> , 4-Cl-phenyl	47	79	n.d. <sup>[f]</sup>	17	6.22
<b>3.138</b>	3-OMe, 4-Cl-phenyl	>125	>100	570	13	5.09
<b>3.139</b>	2,5-di-OMe, 4-Cl-phenyl	>125	>100	n.d. <sup>[f]</sup>	3	5.80
<b>3.140</b>	3,4,5-tri-OMe-phenyl	62	>100	620	34	3.95
<b>3.141</b>	4-F-phenyl	12	63	230	104	4.49

<b>3.142</b>	4-Cl-phenyl	3	>100	n.d. <sup>[f]</sup>	9	5.15
<b>3.146</b>	pyridin-2-yl	15.65	>100	480	29	3.49
<b>3.147</b>	pyridin-3-yl	62.5	>100	330	32	2.46
<b>3.148</b>	pyridin-4-yl	>250	>100	560	91.5	2.50
<b>3.149</b>	2,6-diCH <sub>3</sub> -pyridin-4-yl	>250	13	n.d. <sup>[f]</sup>	12	3.01
<b>3.150</b>	pyrimidin-4-yl	>250	>100	525	27.5	2.53
<b>3.151</b>	2,6-diCH <sub>3</sub> -pyrimidin-4-yl	>250	>100	12	5	3.24
<b>3.152</b>	thiazol-2-yl	>250	>100	1120	54	3.20
<b>3.153</b>	4,5-diCH <sub>3</sub> -thiazol-2-yl	62	>100	440	31.5	4.24
<b>3.154</b>		187	>100	625	195.5	3.30
<b>3.155</b>		>125	>100	<10	≥166	0.79
<b>3.156</b>		125	>100	15	≥381	2.20
<b>3.157</b>		62	>100	33	≥375	1.48

<sup>a</sup>MIC against *M. tuberculosis* (H37Rv), isoniazid was used as reference with MIC = 1.8 μM; <sup>b</sup>HepG2, human caucasian hepatocyte carcinoma; <sup>c</sup>artificial membrane permeability; <sup>d</sup>*in vitro* profiling for kinetic aqueous solubility (CLND, chemiluminescent nitrogen detection); <sup>e</sup>chromlogD values at pH = 7.4; <sup>f</sup>n.d. = not determined.

Modification of the substitution pattern on the phenyl ring resulted in a number of active compounds with MIC values in the low micromolar range. Elimination of one or both methyl groups (**3.126**, **3.125**) did not affect the activity (MIC = 2 μM), indicating that the methyl groups are not critical for potency. Moreover, solubility and chromlogD values were improved, although cytotoxicity remained at similar levels as **2.1**. It is worth noting that shifting one methyl group from position 3 to 2 led to decreased activity (**3.127**, MIC = 8 μM), while shifting both methyls from 3,5 to 2,6 positions led to the inactive compound **3.128** (MIC = 125 μM).

Exploration of the position of the methoxy group of the hit compound **2.2** indicated that the *para*-position (compound **3.130**, MIC = 0.6 μM) is more favourable than the *ortho*- (hit compound **2.2**, 1.4 μM) or *meta*- substitution (compound **3.129**, MIC = 6.4 μM). Compound **3.130**, apart from excellent activity, also possessed an improved profile in comparison with the reference compound **2.1**. More specifically, it did not exhibit cytotoxic effects (IC<sub>50</sub> >100 μM), had good permeability

(420 nm/sec), improved kinetic aqueous solubility (CLND = 108  $\mu$ M) and chromlogD value (4.22). Compound **3.131**, where we preserved both methyl groups at positions 3 and 5 (as the reference compound **2.1**) and a methoxy group at position 4 (as compound **3.130**), showed very good activity (MIC = 1  $\mu$ M) but high cytotoxicity (IC<sub>50</sub> = 8  $\mu$ M) and low solubility (17  $\mu$ M). Several compounds possessing mono-, di- or tri- substituted phenyl rings (**3.132-3.136**, **3.142**) exhibited very good potencies, comparable or slightly less active than the reference compounds. Most of them did not show cytotoxic effects (**3.132**, **3.133**, **3.135**, **3.136**, **3.142**), but, chromlogD values were generally high (>5) and solubility low (<32  $\mu$ M).

Introduction of more hydrophilic rings such as pyridine, pyrimidine, thiazole, isoxazolidinone or dimethylisoxazole did not provide the desired solubility improvement although the chromlogD values (2.46-4.24) were lower than the phenyl derivatives, and the antitubercular activity was lost for most of them. Comparison among compounds **3.146-3.148** revealed that 2-pyridine (**3.146**) is the most favourable, however still less active than the hit compounds (**2.1** and **2.2**). The last subset of compounds which include three hybrid molecules (**3.155-3.157**), unfortunately, led to loss of activity too.

### 3.4.2. Metabolic stability studies

In view of the fact that microsomal instability was identified as a possible liability of the initial hits, six compounds were selected and evaluated for their stability in murine and human microsomal fractions before continuing with further synthetic efforts. The selection of compounds was driven by structural criteria in an attempt to identify the metabolic liabilities of the series. Four possible metabolic sites were explored: the methoxy group, the amide bond, the methylene linker, and the phenyl ring of the reference compound **2.1**. Therefore, compound **3.30** which possessed a methyl group instead of methoxy group was selected in order to evaluate the first metabolic point under exploration. Compounds **3.82** and **3.101**, which had a sterically hindered amide by substitution of the methylene linker and an amine, respectively, were chosen to evaluate the amide and methylene linker metabolic stability. Lastly, compounds **3.126**, **3.127** and **3.133** were selected to explore the metabolic stability of the phenyl ring.

The six selected compounds together with the reference compound **2.1** that were evaluated for their stability in murine and human microsomal fractions, and the obtained data are presented in Table 3.7. All tested compounds proved to be highly unstable, when incubated with murine microsomal fractions, while they exhibited moderate Cl<sub>int</sub> when incubated with human microsomal fractions. Comparison of the obtained data with the control without co-factor data

(not shown) indicated that cytochrome P-450 metabolism was not determinant for all the tested compounds apart from compound **3.101**, signifying that the amide bond may be the most susceptible group of the series and that the esterase hydrolysis might be involved.

In order to confirm that esterases were responsible for the rapid metabolism of the compounds, the selected compounds were incubated in fresh whole CD1 murine blood. A parallel run, after pretreatment of the blood with pan-esterase inhibitor sodium fluoride (NaF), was performed and the obtained results are depicted in Table 3.8. As expected and in accordance with the no-cofactor control in the microsomal stability experiment, nearly all the compounds possessing an amide bond were highly unstable. On the other hand, compounds **3.101** and **3.82**, which possess an amine or a sterically hindered amide, were stable. In addition, the instability was mitigated after NaF pretreatment suggesting that it is mainly due to the hydrolysis of the amide. Microsomal stability in human fractions was better, which is in agreement with the hypothesis of esterase hydrolysis, since esterases in rodents are more active.<sup>136</sup>

**Table 3.7. Stability of selected compounds in murine/human microsomal fractions and blood.**

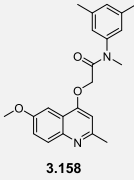
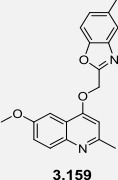
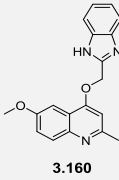
Compd	Microsomal fraction stability <sup>[a]</sup>				Blood stability <sup>[b]</sup>	
	Mouse		Human		NaF	$t_{1/2}$ (min)
	$Cl_{int}$ (mL min <sup>-1</sup> g <sup>-1</sup> )	$t_{1/2}$ (min)	$Cl_{int}$ (mL min <sup>-1</sup> g <sup>-1</sup> )	$t_{1/2}$ (min)		
<b>2.1</b>	18.9	<5	1.3	>30	Partially stabilized	<5
<b>3.30</b>	21.9	<5	1.6	>30	Partially stabilized	<5
<b>3.82</b>	27.3	<5	2.7	19	Stable	96
<b>3.101</b>	86.5	<5	6.3	>30	Stable	>120
<b>3.125</b>	18.1	<5	2.5	23	Partially stabilized	<5
<b>3.127</b>	50.2	<5	2.3	24	Partially stabilized	<5
<b>3.133</b>	19.3	<5	1.1	>30	Partially stabilized	<5

<sup>a</sup>*in vitro* murine and human microsomal fraction stability results: intrinsic clearance ( $Cl_{int}$ ) and half-life time ( $t_{1/2}$ ) are reported; imidazolam was used as control with  $Cl_{int} = 27.5 \pm 0.4$  and  $6.4$  mL min<sup>-1</sup>g<sup>-1</sup> in mouse and human, respectively and  $t_{1/2} = <5$  and  $9$  min in mouse and human, respectively; <sup>b</sup>blood stability results: half-life time ( $t_{1/2}$ ) and effect in presence of NaF are reported.

### 3.4.3. Antimycobacterial activity, physicochemical properties and metabolic stability of compounds containing amide bond replacements

In light of this evidence, further medicinal chemistry efforts led to methylation of the amide bond (**3.158**) and replacement of the *N*-phenyl amide with benzoxazole (**3.159**) or benzimidazole (**3.160**) rings in an effort to overcome the rapid clearance observed in murine microsomal fractions. *N*-methylation of the reference compound **2.1** (compound **3.158**) was explored as a classic approach to reduce amide hydrolysis. The ring closure could potentially stabilize the metabolic liability of the series, in theory rendering an improved profile over the previous scaffold. Table 3.8 presents the obtained data for compounds **3.158**, **3.159** and **3.160**.

**Table 3.8. Biological profile of compounds 3.158, 3.159 and 3.160.**

Structure Compd			
	3.158	3.159	3.160
<b>MIC (μM)<sup>[a]</sup></b>	109.3	5.5	16
<b>Cytotoxicity IC<sub>50</sub> (μM)<sup>[b]</sup></b>	50	>100	>100
<b>Permeability (nm/sec)<sup>[c]</sup></b>	300	86	n.d. <sup>[d]</sup>
<b>Solubility (μM)<sup>[e]</sup></b>	373	1	13
<b>ChromlogD<sup>[f]</sup></b>	5.47	6.12	3.59
<b>Microsomal fraction stability<sup>[g]</sup></b>			
Cl <sub>int</sub> [mL min <sup>-1</sup> g <sup>-1</sup> ] mouse	n.d. <sup>[d]</sup>	46.8	n.d. <sup>[d]</sup>
Cl <sub>int</sub> [mL min <sup>-1</sup> g <sup>-1</sup> ] human	n.d. <sup>[d]</sup>	3.5	n.d. <sup>[d]</sup>
t <sub>1/2</sub> (min) mouse	n.d. <sup>[d]</sup>	<5	n.d. <sup>[d]</sup>
t <sub>1/2</sub> (min) human	n.d. <sup>[d]</sup>	15.7	n.d. <sup>[d]</sup>
<b>Blood stability</b>			
t <sub>1/2</sub> (min)	n.d. <sup>[d]</sup>	>240	n.d. <sup>[d]</sup>

<sup>a</sup>MIC against *M. tuberculosis* (H37Rv), isoniazid was used as reference with MIC = 1.8 μM; <sup>b</sup>HepG2, human caucasian hepatocyte carcinoma; <sup>c</sup>artificial membrane permeability; <sup>d</sup>n.d. = not determined; <sup>e</sup>*in vitro* profiling for kinetic aqueous solubility (CLND, chemiluminescent nitrogen detection); <sup>f</sup>chromlogD values at pH = 7.4; <sup>g</sup>*in vitro* microsomal fraction stability results; clearance (Cl<sub>int</sub>) and half-life time (t<sub>1/2</sub>) is reported; imidazolam was used as control with Cl<sub>int</sub> = 27.5 ± 0.4 and 6.4 mL min<sup>-1</sup>g<sup>-1</sup> in mouse and human, respectively and t<sub>1/2</sub> = <5 and 9 min in mouse and human, respectively.

Compound **3.159**, which possessed a benzoxazole ring instead of anilide, showed significant anti-tubercular activity with an MIC value of 5.5 μM. Moreover, this compound did not exhibit

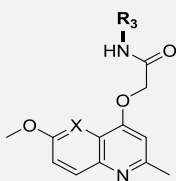
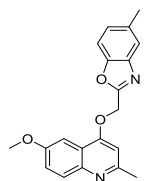


cytotoxic effects. Subsequent testing for blood and microsomal stability revealed the expected improvement in blood stability due to the removal of the labile amide bond. However, solubility of compound **3.159** was very poor and *in vitro* microsomal clearance was high, suggesting that further medicinal chemistry effort is required in order to overcome these problems.

#### 3.4.4. Intracellular *M. tuberculosis* activity

Additionally, the intracellular activity for the hit compounds **2.1** and **2.2** and the most active, non-cytotoxic synthesized compounds (**3.71**, **3.130**, **3.132**, **3.133**, **3.135**, **3.136**, **3.142** and **3.159**) was evaluated. This assay determines the effect of the compounds on mycobacteria growing inside macrophages. Activity in this assay is considered highly desirable as many of the bacteria during an active *M. tuberculosis* infection are found intracellularly in phagocytotic cell types. The obtained results are shown in Table 3.9.

**Table 3.9. Intracellular IC<sub>50</sub> and IC<sub>90</sub> values for selected compounds.**

Compd			MIC ( $\mu\text{M}$ )	Intracellular	
	R <sub>3</sub>	X		IC <sub>50</sub> ( $\mu\text{M}$ ) <sup>[a]</sup>	IC <sub>90</sub> ( $\mu\text{M}$ ) <sup>[a]</sup>
<b>2.1</b>	3,5-diCH <sub>3</sub> -phenyl	C	1.9	0.05	0.21
<b>2.2</b>	2-OCH <sub>3</sub> -phenyl	C	1.4	0.50	1.58
<b>3.71</b>	3,5-diCH <sub>3</sub> -phenyl	N	3.8	2.51	6.31
<b>3.130</b>	4-OCH <sub>3</sub> -phenyl	C	0.6	0.03	0.25
<b>3.132</b>	2-OCH <sub>3</sub> , 5-CH <sub>3</sub> -phenyl	C	2.5	0.16	0.63
<b>3.133</b>	3,5-diCH <sub>3</sub> , 4-F-phenyl	C	2	0.08	0.25
<b>3.135</b>	3,5-diF-phenyl	C	3	0.40	2.51
<b>3.136</b>	2,4-diCl-phenyl	C	2	0.79	>50
<b>3.142</b>	4-Cl-phenyl	C	3	0.16	0.50
<b>3.159</b>			5.5	3.16	5.01

<sup>[a]</sup>IC<sub>50</sub> and IC<sub>90</sub> against infected Human THP-1 macrophages with *M. tuberculosis* (H37Rv).

It is worth noting that 7 out of 10 tested compounds showed excellent intracellular IC<sub>90</sub> values, ranging from 0.21 to 2.51 μM. More specifically, hit compound **2.1**, compound **3.130**, which had also shown the highest MIC value, and compound **3.133** exhibited the highest intracellular potencies with IC<sub>90</sub> values of 0.21-0.25 μM. They were followed by compounds **3.142** and **3.132** with IC<sub>90</sub> values 0.50 and 0.63 μM, respectively. Less active but still very potent compounds were the hit compound **2.2** and compounds **3.135**, **3.159** and **3.71** (IC<sub>90</sub> = 1.58, 2.51, 5.01 and 6.31 μM, respectively). Lastly, compound **3.136**, despite having shown good MIC values, did not reach 90% inhibition at 50 μM (IC<sub>90</sub> >50 μM) in the intracellular assay. This could be due to poor permeability of the compounds through the cell membrane, to bacterial efflux pumps activated by the macrophage or to inactivation of the compounds by host cell derived metabolites such as reactive species.<sup>137</sup>

Direct comparison of the intracellular values (IC<sub>90</sub>) with the “extracellular” values (MIC) is not reliable, since they depend on different readouts and are calculated differently. Even so, a qualitative comparison between them could give some useful information on their properties for macrophage penetration. Compounds **3.71** and **3.136** seem to be less potent in macrophages than the “extracellular” MIC values would suggest. This could be due to poor permeability of the compounds through the cell membrane, to bacterial efflux pumps activated by the macrophage or to inactivation of the compounds by host cell-derived metabolites such as reactive species.<sup>137</sup> On the other hand, compounds **2.1**, **3.130**, **3.132**, **3.133** and **3.142** exhibited better intracellular IC<sub>90</sub> values than “extracellular” MIC values indicating that these compounds might be targeting pathways, either in the bacteria or in the macrophage, that are essential during infection but not for *in vitro* growth or they are accumulating inside the macrophages.<sup>138</sup> Lastly, compounds **2.2**, **3.135** and **3.159** showed comparable activities in both assays.

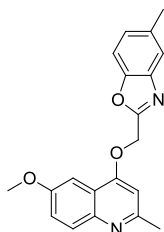
#### 3.4.5. Cardiotoxicity (hERG binding assay)

Lastly, a preliminary safety evaluation of the cardiovascular risk of the series was performed by measuring the human Ether-à-go-go-Related Gene (hERG) potassium channel binding of selected compounds. hERG is a gene (KCNH<sub>2</sub>) that codes for a protein known as Kv11.1, the *alpha* subunit of a potassium ion (K<sup>+</sup>) channel.<sup>139</sup> This ion channel is best known for its contribution to the electrical activity of the heart that coordinates the heart's beating (i.e., the hERG channel mediates the repolarizing I<sub>Kr</sub> current in the cardiac action potential). When this channel's ability to conduct electrical current across the cell membrane is inhibited or compromised, either by application of drugs or by rare mutations in some families, it can result in a potentially fatal disorder called long

QT syndrome, in which delayed repolarization of the heart following a heartbeat increases the risk of episodes of *torsades de pointes* (TdP, a form of irregular heartbeat that originates from the ventricles).<sup>139</sup> These episodes may lead to palpitations, fainting, and sudden death due to ventricular fibrillation.<sup>140</sup>

A number of clinically successful drugs in the market were later found to inhibit hERG channel, and create a concomitant risk of sudden death, which has made hERG inhibition an important off-target that must be avoided during drug development.<sup>140</sup> Therefore, measurement of hERG channel binding of selected compounds was performed with the purpose to identify cardiovascular risks early in our optimization program. The obtained results are presented in Table 3.10.

**Table 3.10. Results of hERG binding of selected compounds.**

Compd	Structure			hERG IC <sub>50</sub> (μM)
	R <sub>1</sub>	R <sub>3</sub>	X	
<b>2.1</b>	6-CH <sub>3</sub> O-	3,5-diCH <sub>3</sub> -phenyl	C	>50
<b>2.2</b>	6-CH <sub>3</sub> O-	2-OCH <sub>3</sub> -phenyl	C	10
<b>3.30</b>	6-CH <sub>3</sub> -	3,5-diCH <sub>3</sub> -phenyl	C	>50
<b>3.68</b>	6-CH <sub>3</sub> O-	3,5-diCH <sub>3</sub> -phenyl	N	>50
<b>3.130</b>	6-CH <sub>3</sub> O-	4-OCH <sub>3</sub> -phenyl	C	6
<b>3.132</b>	6-CH <sub>3</sub> O-	2-OCH <sub>3</sub> , 5-CH <sub>3</sub> -phenyl	C	5
<b>3.133</b>	6-CH <sub>3</sub> O-	3,5-diCH <sub>3</sub> , 4-F-phenyl	C	>50
<b>3.142</b>	6-CH <sub>3</sub> O-	4-Cl-phenyl	C	6
<b>3.159</b>				>50

4 out of 9 tested compounds interacted with hERG channel, while the rest of them showed no activity in the hERG binding assay up to the maximum concentration tested (IC<sub>50</sub> >50 μM). Interestingly, 3 out of 4 compounds (**2.2**, **3.130** and **3.132**) which showed some interaction possessed a methoxy substituent on the phenyl ring. However, the small size of the dataset does not allow decisive conclusions about a possible correlation between the presence of a methoxy

group and hERG channel inhibition. Compound **3.159** which is of particular interest due to its blood stability did not show any interaction with hERG.

### 3.5. Conclusion

In the presented work, the synthesis of more than seventy novel quinoloxycetamide derivatives and their biological evaluation against *M. tuberculosis* (H37Rv) is reported. Apart from the SAR exploration around the initial hits, the optimization processes focused on the improvement of the physicochemical properties, cytotoxicity (HepG2) and metabolic stability of the series.

During our antimycobacterial research on quinoloxycetamides, several synthetic routes were explored. Furthermore, we studied the alkylation position of heterocyclic *N/O*-ambident nucleophilic scaffolds such as quinolin-4-ol, naphthyridin-4-ol and quinazolin-4-ol. When *N*-alkylated products were obtained, the desired alkoxy- analogues were prepared via alternative methods. Given the lack of commonly applied methods (<sup>1</sup>H-NMR and mass spectroscopy) for the unambiguous assignment of *N/O*-ambident alkylation reaction products, three more advanced NMR methods (<sup>13</sup>C-NMR chemical shifts, 2D HSQC/HMBC and 1D NOE) were applied for structure determination.

Several compounds showed potent anti-tubercular activities with MICs in the low micromolar range with the best compound (**3.130**) exhibiting a MIC value of 0.6 μM and no measurable cytotoxicity. This compound and other potent, non-cytotoxic analogues also showed excellent intracellular IC<sub>90</sub> values ranging from 0.21 to 2.51 μM.

Furthermore, the metabolic stability of the series was investigated and it was shown that the amide bond was the most labile group. Thus, further synthetic efforts were focused on amide replacement and compound **3.159** which possessed a benzoxazole was identified as a good alternative to improve blood stability ( $t_{1/2} > 240$  min).

Evaluation of the human ether-a-go-go-related gene (hERG) channel binding indicated that compounds mainly possessing a methoxy phenyl substituent (including compound **3.130**) showed some interactions with hERG, while the optimized compound **3.159** displayed no activity in this assay.

Further medicinal chemistry effort is necessary to increase solubility and microsomal stability of the series in order to provide a strong lead for a new anti-tubercular drug discovery program.

## 3.6. Experimental section

### 3.6.1. General Information

Unless otherwise stated, laboratory reagent grade solvents were used. Reagents were purchased from Sigma-Aldrich, Acros Organics, TCI or Enamine and were used without further purification unless otherwise mentioned. Reactions were monitored by TLC on silica gel with detection by UV light (254 nm). TLC analysis was performed using Polygram® precoated silica gel TLC sheets SIL G/UV<sub>254</sub>.

Characterization of all compounds was done using <sup>1</sup>H NMR and <sup>13</sup>C-NMR spectroscopy and mass spectrometry. <sup>1</sup>H NMR (400 MHz) and <sup>13</sup>C-NMR (100 MHz) spectra were recorded on a Bruker Avance III Nanobay Ultrashield 400 or a Bruker DPX 400 spectrometer. The chemical shift ( $\delta$ ) values are expressed in parts per million (ppm) and coupling constants are in Hertz (Hz). Minor rotamers of the amide bond, which were less than 10% of the major rotamer, are not reported in the NMR data. CDCl<sub>3</sub>, CD<sub>3</sub>OD or DMSO-*d*<sub>6</sub> were used as the standard NMR solvents. Legend: s = singlet, d = doublet, t = triplet, q = quartet, quint = quintet, m = multiplet, dd = doublet of doublets, ddd = doublets of doublets of doublets, br = broad signal. For the measurement of melting points, a Technoterm 7300 (Reichert-Jung Optische Werke) microscope was used.

Purity and mass were verified using a UPLC-MS system and purities of all final products were found to be >95%. UPLC-MS involved the following: Waters Acquity UPLC system coupled to a Waters TQD ESI mass spectrometer and Waters TUV detector. A Waters Acquity UPLC BEH C18 1.7  $\mu$ m, 2.1 mm  $\times$  50 mm column was used. Solvent A consisted of water with 0.1% formic acid. Solvent B consisted of acetonitrile with 0.1% formic acid. Method A involved the following: flow 0.4 mL/min, 0.15 min isocratic elution (95% A, 5% B), followed by gradient elution during 1.85 min (from 95% A, 5% B to 95% B, 5% A), then 0.25 min (0.350 mL/min) isocratic elution (95% B, 5% A). The wavelength for UV detection was 254 nm. Method B: flow 0.4 mL/min, 0.25 min isocratic elution (95% A, 5% B), followed by gradient elution during 4.75 min (95% B, 5% A, then isocratic 0.25 min of isocratic elution (95% B, 5% A) followed by 0.75 min isocratic elution (95% A, 5% B). The wavelength for UV detection was 214 nm. For method C, a Waters Acquity UPLC system was coupled to a Waters SQ detector and an Acquity UPLC BEH C18 1.7  $\mu$ m, 3x50 mm column was used. The concentration of the measured samples was 0.1 mg/mL and flow 0.8 mL/min. The method involved the following: Ammonium acetate (NH<sub>4</sub>CH<sub>3</sub>CO<sub>2</sub>) 25mM + 10% ACN at pH 6.6 /ACN, 0.0-0.2 min 99.9: 0.1, 0.2-1.0 min 10:90, 1.0-1.8 min 10:90, 1.9-2.0 min 99.9:0.1 at temperature 40 °C. The UV detection was an averaged signal from wavelength of 210 nm to 400

nm. The quasi-molecular ions  $[M+H]^+$  or  $[M-H]^-$  were detected. Retention time (RT) was indicated for the described method.

For the High Resolution Mass Spectrometry (HRMS) measurements: Positive ion mass spectra were acquired using a QSTAR Elite (AB Sciex Instruments) mass spectrometer, equipped with a turbospray source, over a mass range of 250–700.

Where necessary, flash purification was performed on a Biotage ISOLERA One flash system equipped with an internal variable dual-wavelength diode array detector (200-400 nm). For normal phase purifications SNAP cartridges (10-100 g, flow rate of 10-100 mL/min) were used, and reverse-phase purifications were done making use of KP-C18 containing cartridges. Dry sample loading was done by self-packing samplet cartridges using silica or Celite 545, respectively, for normal and reversed phase purifications. Gradients used varied for each purification. However, typical gradients used for normal phase were gradient of 0–100% ethyl acetate in *n*-heptane or 0–15% methanol in ethyl acetate. For reverse phase a gradient of 5% MeCN in water to 50% MeCN in water was used.

The following section comprises the synthetic procedures and analytical data for all final compounds and intermediates reported in this thesis. Synthetic procedures that were used in the preparation of several products are summarized here as “General Procedures”.

### 3.6.2. General procedures

For the synthesis of the quinolin-4-ols, three related methods were used (General procedure A, B and C).

**General procedure A. Formation of 2-methyl-quinolin-4-ols 3.4, 3.15 and 2-trifluoromethyl-quinolin-4-ols 3.16, 3.18, 3.19.** According to Brouet *et al.*, the appropriate substituted aniline (1 equiv.) and ethyl acetoacetate or ethyl 4,4,4-trifluoroacetoacetate (1.25-2.5 equiv.) were dissolved in Dowtherm A (molarity: 0.5 M) and concentrated sulfuric acid (1-3 drops) was added to the stirred mixture.<sup>1</sup> The reaction vessel was equipped with a short distillation apparatus. The reaction mixture was heated gradually to 240-250 °C for 35-60 min and the produced water/ethanol were removed by distillation as the reaction progressed. Subsequently, the reaction mixture was cooled down to room temperature and poured into *n*-heptane to give a precipitate. The precipitate was collected by filtration and washed with *n*-heptane and ethyl acetate. If necessary, the product was further purified by recrystallization or silica gel flash chromatography.

**General procedure B. Formation of 2-methyl-quinolin-4-ols 3.4, 3.6, 3.9, 3.11-3.14, 3.70.** In accordance with the second method described by Tantrizos *et al.*, the appropriate aniline (1 equiv.) and ethylacetoacetate (1 equiv.) were stirred at 130 °C for 90 min to form the corresponding imine.<sup>104</sup> Then, Dowtherm A (molarity: 0.7-2.3 M) was added to the reaction mixture and it was heated at 250 °C for 1 h. Then, the reaction mixture was cooled down to room temperature and poured into *n*-heptane to give a (sticky) precipitate. The precipitate was collected by filtration and washed with *n*-heptane and ethyl acetate. If necessary, the product was further purified by recrystallization or silica gel flash chromatography.

**General procedure C. Formation of 2-methyl-quinolin-4-ols 3.4, 3.5.** In line with Escribano *et al.*, acetic acid (1.3 equiv.) was added to a solution of the appropriate aniline (1 equiv.) and ethylacetoacetate (1.2 equiv.) in toluene (molarity: 0.5 M).<sup>103</sup> The reaction mixture was held at reflux for 2 h with azeotropic removal of water by means of a Dean-Stark apparatus. The solvent was evaporated under reduced pressure, the liquid residue was dissolved in Dowtherm A (molarity: 0.1 M) and heated at 240 °C for 1 h. A Dean-Stark apparatus was used to remove the ethanol produced during the reaction. The reaction mixture was cooled down to room temperature and poured into *n*-heptane to give a (sticky) precipitate. The precipitate was collected by filtration and washed with *n*-heptane and EtOAc. If necessary, the product was further purified by recrystallization or silica gel flash chromatography.

**General Procedure D. Preparation of 2-bromo-*N*-substituted-acetamides (3.24, 3.77-3.80, 3.96, 3.107-3.124).** 2-Bromoacetyl bromide (1.2 equiv.) was slowly added dropwise to a mixture of arylamines (1 equiv.) and triethylamine (1.2 mmol) in anhydrous DCM (molarity: 1M) at 0 °C. The reaction mixture was warmed to room temperature and stirred for additional 2-48 h. After the solvent was removed under reduced pressure, the residue was washed with ice water and separated by filtration. If necessary, the product was purified by recrystallization or silica gel column chromatography.

**General Procedure E. *O*-alkylation of 4-quinolinols with primary halides (2.1, 3.25-3.41, 3.48-3.50, 3.64-3.66, 3.71, 3.85, 3.97, 3.125-3.143, 3.159, 3.160).** To a solution of the appropriate 4-quinolinol (1 equiv.) in anhydrous DMF under nitrogen atmosphere was added K<sub>2</sub>CO<sub>3</sub> (3 equiv.) and a solution of the suitable halide (1-1.2 equiv.) in anhydrous DMF. The reaction mixture was stirred for 3h-4d at room temperature before being poured into water (50 mL) and extracted with ethyl acetate (3 x 50 mL) or filtered in case of precipitation. The combined organic extracts were dried over MgSO<sub>4</sub>, filtered, concentrated in vacuo and purified by silica gel flash chromatography, if necessary.

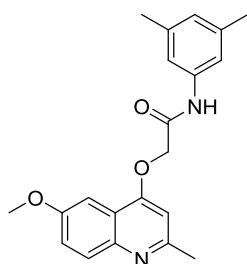
**General Procedure F. O-alkylation of deprotonated 4-quinolinols with secondary or tertiary halides (3.81-3.84, 3.86).** Sodium hydride (NaH), 60% suspended in mineral oil (1 equiv.) was added to a solution of intermediate **3.4** in anhydrous DMF under nitrogen atmosphere, and the resulting suspension was stirred for 30 min. Subsequently, a solution of the suitable halide (1 equiv.) and in some cases potassium iodide (KI) (1 equiv.) in anhydrous DMF was added to the reaction mixture and left stirring for 3 h – 4 d at room temperature. Afterwards, the reaction mixture was poured into water (50 mL) and extracted with ethyl acetate (3 x 50 mL) or filtered in case of precipitation. The combined organic extracts were dried over magnesium sulfate, concentrated under reduced pressure and purified by flash chromatography, if necessary.

**General Procedure G. Formation of the acyl chlorides (3.104, 3.145).** The appropriate carboxylic acid/carboxylate (1 equiv.) was dissolved in anhydrous DCM (Molarity: 0.04-0.3 M) and thionyl chloride was added (1.2-45 equiv.) dropwise. The reaction mixture was left stirring for 1-3 days at room temperature or under reflux. The volatiles of the reaction mixture were evaporated under reduced pressure and the obtained acyl chlorides were directly used for next step.

**General Procedure H. Formation of the amide bond (3.105, 3.146-3.157).** The acyl chlorides (**3.104, 3.145**) were dissolved in anhydrous DCM (Molarity: 0.04-0.5 M) and the suitable amine (1-2.5 equiv.) was added to the solution. In some cases, triethylamine (1-1.2 equiv.) was also added to the reaction mixture. Then, the reaction mixture was stirred at room temperature for 7-72 h. If triethylamine was used, DCM was evaporated and the obtained residue was purified by column chromatography. If triethylamine was not used, the volatiles were evaporated under reduced pressure and the residue was dissolved in water. The solution was basified to pH 8-9 using an aqueous solution of NaOH (2 N), and the obtained crystals were collected by filtration, washed with water and dried to obtain in most cases the pure product. If necessary, the crude product was recrystallized from ethyl acetate or purified by column chromatography.

### 3.6.3. Chemistry

#### ***N*-(3,5-dimethylphenyl)-2-((6-methoxy-2-methylquinolin-4-yl)oxy)acetamide (2.1).**

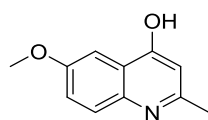


The title compound was prepared according to the general procedure E using 6-methoxy-2-methyl-4-quinolinol (150 mg, 0.793 mmol), 2-bromo-*N*-(3,5-dimethylphenyl)acetamide (230 mg, 0.951 mmol) and potassium carbonate (329 mg, 2.38 mmol) in anhydrous DMF (9 mL) and the reaction time was 3 h.



White solid; yield 85% (237 mg, 0.676 mmol); mp 189-191 °C; TLC,  $R_f$  0.71 (ethyl acetate/methanol: 90/10).  $^1\text{H}$  NMR (400 MHz,  $\text{CDCl}_3$ )  $\delta$  8.16 (s, 1H), 7.91 (d,  $J = 9.0$  Hz, 1H), 7.42 – 7.32 (m, 2H), 7.18 (s, 2H), 6.80 (s, 1H), 6.60 (s, 1H), 4.80 (s, 2H), 3.96 (s, 3H), 2.64 (s, 3H), 2.29 (s, 6H).  $^{13}\text{C}$  NMR (101 MHz,  $\text{CDCl}_3$ )  $\delta$  165.3, 159.0, 157.6, 157.3, 145.0, 139.1, 136.6, 130.1, 127.0, 122.2, 119.9, 118.0, 102.3, 99.6, 67.9, 55.7, 25.7, 21.5. UPLC-MS (A) (ESI) RT 1.58 min,  $m/z$  351.5  $[\text{M}+\text{H}]^+$  (>95%). HRMS (ESI)  $m/z$  calcd for  $\text{C}_{21}\text{H}_{23}\text{N}_2\text{O}_3$   $[\text{M}+\text{H}]^+$ : 351.1703; found: 351.1694.

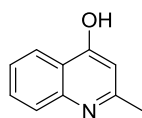
#### 6-Methoxy-2-methylquinolin-4-ol (3.4).



The title compound was prepared according to the general procedures A, B and C. According to procedure A, 4-methoxyaniline (1.00 g, 8.12 mmol), ethylacetoacetate (2.6 mL, 20 mmol) and concentrated sulfuric acid (1-2 drops) in Dowtherm A (15 mL) were used and the reaction time was 35 min. According to procedure B, 4-methoxyaniline (500 mg, 4.06 mmol) and ethylacetoacetate (0.5 mL, 4.1 mmol) were used and the reaction time was 90 min. Then, diphenyl ether (5 mL) was added to the reaction mixture and heated at 250 °C for 1 h. According to procedure C, 4-methoxyaniline (9.2 mL, 80 mmol), ethylacetoacetate (12 mL, 94 mmol) and acetic acid (6 mL, 0.1 mol) in toluene (150 mL) were used. The reaction mixture was held at reflux for 2 h. Then, the solvent was evaporated under reduced pressure and the liquid residue was dissolved in Dowtherm A and heated at 240 °C for 1 h.

Off-white solid; yield 7% (100 mg, 0.529 mmol, procedure A), 20% (153 mg, 0.809 mmol, procedure B), 41% (6.237 g, 32.96 mmol, procedure C).  $^1\text{H}$  NMR (400 MHz,  $\text{DMSO}-d_6$ )  $\delta$  11.53 (br s, 1H), 7.45 (dd,  $J = 5.9, 2.9$  Hz, 2H), 7.24 (dd,  $J = 9.0, 2.9$  Hz, 1H), 5.86 (s, 1H), 3.81 (s, 3H), 2.32 (s, 3H).  $^{13}\text{C}$  NMR (101 MHz,  $\text{DMSO}-d_6$ )  $\delta$  176.1, 155.2, 148.5, 134.7, 125.5, 121.7, 119.4, 107.4, 104.2, 55.3, 19.3. UPLC-MS (A) (ESI) RT 1.06 min,  $m/z = 190.1$   $[\text{M}+\text{H}]^+$  (>95%).

#### 2-Methylquinolin-4-ol (3.5).

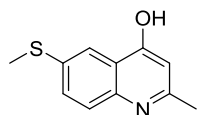


The title compound was prepared according to the general procedure C using aniline (1.000 g, 10.74 mmol), ethylacetoacetate (1.6 mL, 13 mmol) and acetic acid (0.8 mL, 14 mmol) in toluene (20 mL). The reaction mixture was held at reflux for 2 h with azeotropic removal of water by means of a Dean-Stark apparatus. The solvent was evaporated under reduced pressure, the liquid residue was dissolved in Dowtherm A (5 mL) and heated at 240 °C for 1 h. A Dean-Stark apparatus was used to remove the ethanol produced during the reaction.

White solid; yield 31% (569 mg, 3.36 mmol).  $^1\text{H}$  NMR (400 MHz,  $\text{DMSO}$ )  $\delta$  11.55 (s, 1H), 8.02 (ddd,  $J = 8.0, 1.5, 0.4$  Hz, 1H), 7.60 (ddd,  $J = 8.4, 7.0, 1.6$  Hz, 1H), 7.48 (dd,  $J = 8.3, 0.5$  Hz, 1H), 7.26 (ddd,

$J = 8.1, 7.0, 1.1$  Hz, 1H), 5.90 (s, 1H), 2.33 (s, 3H).  $^{13}\text{C}$  NMR (101 MHz, DMSO)  $\delta$  176.7, 149.6, 140.1, 131.4, 124.8, 124.5, 122.7, 117.7, 108.4, 39.5, 19.5. UPLC-MS (A) (ESI) RT 0.38 min,  $m/z$  160.2  $[\text{M}+\text{H}]^+$  (94%).

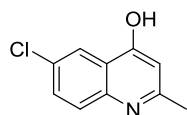
### 2-Methyl-6-(methylthio)quinolin-4-ol (3.6).



The title compound was prepared according to the general procedure B using p-(methylmercapto)aniline (1.500 g, 10.77 mmol) and ethylacetoacetate (1.4 mL, 11 mmol). The mixture was heated at 130 °C for 90 min. Then, Dowtherm A (5 mL) was added to the reaction mixture and heated at 250 °C for 1 h.

White solid; yield 11% (233 mg, 1.14 mmol).  $^1\text{H}$  NMR (400 MHz, DMSO)  $\delta$  11.59 (s, 1H), 7.82 (d,  $J = 2.2$  Hz, 1H), 7.53 (dd,  $J = 8.7, 2.3$  Hz, 1H), 7.45 (d,  $J = 8.7$  Hz, 1H), 5.91 (s, 1H), 2.52 (s, 3H), 2.32 (s, 3H). UPLC-MS (A) (ESI) RT 1.21 min,  $m/z$  205.9  $[\text{M}+\text{H}]^+$  (>95%).

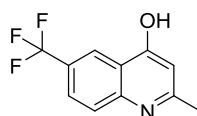
### 6-Chloro-2-methylquinolin-4-ol (3.9).



The title compound was prepared according to the general procedure B using 4-chloroaniline (1.500 g, 11.76 mmol) and ethylacetoacetate (1.5 mL, 12 mmol). The mixture was heated at 130 °C for 90 min. Then, Dowtherm A (5 mL) was added to the reaction mixture and heated at 250 °C for 1 h.

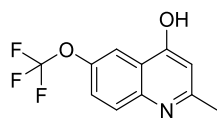
Orange solid; yield 13% (300 mg, 1.55 mmol).  $^1\text{H}$  NMR (400 MHz, DMSO)  $\delta$  11.73 (s, 1H), 7.95 (d,  $J = 2.5$  Hz, 1H), 7.64 (dd,  $J = 8.8, 2.5$  Hz, 1H), 7.52 (d,  $J = 8.8$  Hz, 1H), 5.95 (s, 1H), 2.34 (s, 3H). UPLC-MS (A) (ESI) RT 1.21 min,  $m/z$  194.0, 196.0 (3:1)  $[\text{M}+\text{H}]^+$  (83%).

### 2-Methyl-6-(trifluoromethyl)quinolin-4-ol (3.11).



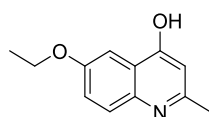
The title compound was prepared according to the general procedure B using p-trifluoromethylaniline (1.00 g, 6.21 mmol) and ethylacetoacetate (0.8 mL, 6 mmol). The mixture was heated at 130 °C for 2 h. Then, Dowtherm A (5 mL) was added to the reaction mixture and heated at 250 °C for 1 h.

White solid; yield 16% (224 mg, 0.986 mmol).  $^1\text{H}$  NMR (400 MHz, DMSO)  $\delta$  11.91 (s, 1H), 8.30 (s, 1H), 7.91 (dd,  $J = 8.7, 2.3$  Hz, 1H), 7.68 (d,  $J = 8.7$  Hz, 1H), 6.03 (s, 1H), 2.37 (s, 3H).  $^{13}\text{C}$  NMR (101 MHz, DMSO)  $\delta$  176.1, 151.0, 142.2, 127.5 (q,  $^3J_{\text{CF}} = 3.3$  Hz), 124.4 (q,  $^1J_{\text{CF}} = 248.1$  Hz), 123.7, 122.9 (q,  $^2J_{\text{CF}} = 9.2$  Hz), 122.4 (q,  $^3J_{\text{CF}} = 4.4$  Hz), 119.4, 19.5. UPLC-MS (A) (ESI) RT 1.37 min,  $m/z$  228.1  $[\text{M}+\text{H}]^+$  (>95%).

**2-Methyl-6-(trifluoromethoxy)quinolin-4-ol (3.12).**

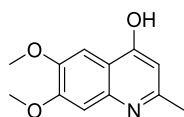
The title compound was prepared according to the general procedure B using 4-(trifluoromethoxy)aniline (0.8 mL, 5.7 mmol) and ethylacetoacetate (0.7 mL, 6 mmol). The mixture was heated at 130 °C for 90 min. Then, Dowtherm A (5 mL) was added to the reaction mixture and heated at 250 °C for 1 h.

Light pink solid; yield 15% (210 mg, 0.864 mmol). <sup>1</sup>H NMR (400 MHz, DMSO) δ 11.80 (s, 1H), 7.87 (s, 1H), 7.63 (d, *J* = 1.5 Hz, 2H), 5.97 (s, 1H), 2.36 (s, 3H). <sup>13</sup>C NMR (101 MHz, DMSO) δ 175.8, 150.5, 143.7, 138.7, 125.2, 125.1, 120.4, 120.2 (q, <sup>1</sup>*J*<sub>CF</sub> = 256.3 Hz), 115.9, 108.4, 19.5. UPLC-MS (A) (ESI) RT 1.82 min, *m/z* 244.1 [M+H]<sup>+</sup> (>95%).

**6-Ethoxy-2-methylquinolin-4-ol (3.13).**

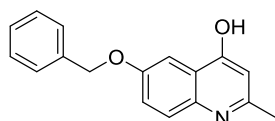
The title compound was prepared according to the general procedure B using phenetidine (500 mg, 3.64 mmol) and ethylacetoacetate (0.5 mL, 4 mmol). The mixture was heated at 130 °C for 90 min. Then, Dowtherm A (5 mL) was added to the reaction mixture and it was heated at 250 °C for 1 h.

Light brown solid; yield 41% (300 mg, 1.48 mmol). <sup>1</sup>H NMR (400 MHz, DMSO) δ 11.51 (s, 1H), 7.47 – 7.40 (m, 2H), 7.23 (dd, *J* = 8.9, 3.0 Hz, 1H), 5.85 (s, 1H), 4.07 (q, *J* = 6.9 Hz, 2H), 2.32 (s, 3H), 1.35 (t, *J* = 7.0 Hz, 3H). UPLC-MS (A) (ESI) RT 1.71 min, *m/z* 204.1 [M+H]<sup>+</sup> (94%).

**6,7-Dimethoxy-2-methylquinolin-4-ol (3.14).**

The title compound was prepared according to the general procedure B using 4-aminoveratrole (500 mg, 3.26 mmol) and ethylacetoacetate (0.8 mL, 7 mmol). The mixture was heated at 130 °C for 100 min. Then, Dowtherm A (5 mL) was added to the reaction mixture and heated at 250 °C for 1 h.

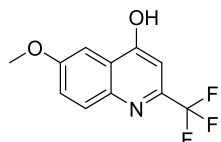
Light brown solid; yield 45% (323 mg, 1.47 mmol). <sup>1</sup>H NMR (400 MHz, MeOD) δ 7.57 (s, 1H), 6.95 (s, 1H), 6.15 (s, 1H), 4.59 (s, 1H), 3.95 (s, 3H), 3.92 (s, 3H), 2.44 (s, 3H). UPLC-MS (A) (ESI) RT 1.32 min, *m/z* 220.1 [M+H]<sup>+</sup> (94%).

**6-(Benzyloxy)-2-methylquinolin-4-ol (3.15).**

The title compound was prepared according to the general procedure A using 4-(phenylmethoxy)benzenamine hydrochloride (1.00 g, 4.24 mmol) and ethylacetoacetate (1.3 mL, 11 mmol) in Dowtherm A (8 mL) and the reaction time was 35 min.

Off-white solid; yield 12% (136 mg, 0.513 mmol).  $^1\text{H}$  NMR (400 MHz, DMSO)  $\delta$  11.53 (s, 1H), 7.54 (d,  $J = 2.9$  Hz, 1H), 7.52 – 7.22 (m, 8H), 5.86 (d,  $J = 1.0$  Hz, 1H), 5.16 (s, 2H), 2.32 (s, 3H).  $^{13}\text{C}$  NMR (101 MHz, DMSO)  $\delta$  175.9, 165.2, 155.5, 144.8, 138.3, 137.9, 135.1, 127.6, 125.2, 121.8, 117.9, 116.9, 107.6, 105.5, 55.4, 21.1. UPLC-MS (A) (ESI) RT 1.50 min,  $m/z$  266.4  $[\text{M}+\text{H}]^+$  (>95%).

**6-Methoxy-2-(trifluoromethyl)quinolin-4-ol (3.16).**

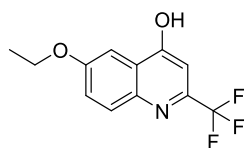


The title compound was prepared according to the general procedure A using *para*-anisidine (2.000 g, 16.24 mmol), ethyl 4,4,4-trifluoroacetoacetate (3 mL, 20 mmol) and concentrated sulfuric acid (1-2 drops) in Dowtherm A (32 mL).

The reaction mixture was heated gradually up to 240 °C for 30 min, followed by additional 35 min of heating at 240-250°C.

Brown solid; yield 55% (2.172 g, 8.931 mmol).  $^1\text{H}$  NMR (400 MHz, DMSO)  $\delta$  12.12 (s, br, 1H), 7.94 (d,  $J = 9.5$  Hz, 1H), 7.53 – 7.43 (m, 2H), 7.12 (s, br, 1H), 3.92 (s, 3H). UPLC-MS (A) (ESI) RT 1.52 min,  $m/z$  244.3  $[\text{M}+\text{H}]^+$  (>95%).

**6-Ethoxy-2-(trifluoromethyl)quinolin-4-ol (3.18).**

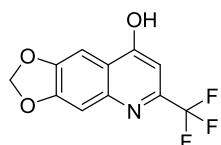


The title compound was prepared according to the general procedure A using phenetidine (500 mg, 3.64 mmol), ethyl 4,4,4-trifluoroacetoacetate (0.8 mL, 5 mmol) and concentrated sulfuric acid (2-3 drops) in Dowtherm A

(8 mL). The reaction mixture was heated gradually up to 240 °C for 15min, followed by additional 35 min of heating at 240-250°C.

White solid; yield 30% (279 mg, 1.09 mmol).  $^1\text{H}$  NMR (400 MHz, DMSO)  $\delta$  11.97 (br. s, 1H), 7.92 (d,  $J = 9.7$  Hz, 1H), 7.50 – 7.40 (m, 2H), 7.10 (s, 1H), 4.17 (q,  $J = 6.9$  Hz, 2H), 1.40 (t,  $J = 6.9$  Hz, 3H). UPLC-MS (A) (ESI) RT 1.68 min,  $m/z$  258.4  $[\text{M}+\text{H}]^+$  (>95%).

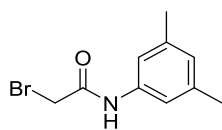
**6-(Trifluoromethyl)-[1,3]dioxolo[4,5-g]quinolin-8-ol (3.19).**



The title compound was prepared according to the general procedure A using 1,3-benzodioxol-5-amine (500mg, 3.65 mmol), ethyl 4,4,4-trifluoro aceto acetate (1.68 g, 9.12 mmol) and concentrated sulfuric acid (2-3 drops) in

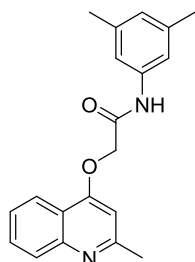
Dowtherm A (14 mL). The reaction mixture was heated gradually for 30 min up to 230°C.

Brown solid; yield 66% (618 mg, 2.40 mmol).  $^1\text{H}$  NMR (400 MHz, DMSO- $d_6$ ) (a mixture of isomers)  $\delta$  ppm 12.24 (br. s., 1 H), 7.34 - 7.47 (m, 1 H), 6.75 - 7.15 (m, 2 H), 6.11 - 6.33 (m, 2 H). UPLC-MS (A) (ESI) RT 1.53 min,  $m/z$  258.4  $[\text{M}+\text{H}]^+$  (>95%).

**2-Bromo-*N*-(3,5-dimethylphenyl)acetamide (3.24).**

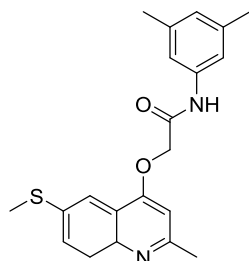
The title compound was prepared according to general procedure D using bromoacetic acid bromide (1.7 mL, 20 mmol), 3,5-xylidine (2.000 g, 16.5 mmol) and TEA (2.8 mL, 20 mmol) in anhydrous DCM (16.5 mL) and the reaction time was 2 h.

Brown solid; yield 97% (3.890 g, 16.07 mmol).  $^1\text{H}$  NMR (400 MHz, DMSO- $d_6$ )  $\delta$  10.20 (br. s, 1H), 7.20 (s, 2H), 6.73 (s, 1H), 4.00 (s, 2H), 2.24 (d,  $J=0.4$  Hz, 6H).  $^{13}\text{C}$  NMR (101 MHz, DMSO- $d_6$ ) (major cis/trans amide rotamers)  $\delta$  170.6, 138.3, 137.6, 125.0, 117.3, 61.8, 21.1; (minor cis/trans amide rotamers)  $\delta$  164.7, 138.5, 137.9, 125.4, 117.0, 30.5, 21.1. UPLC-MS (A) (ESI) RT 1.73 min,  $m/z$  242.3:244.3 (1:1)  $[\text{M}+\text{H}]^+$  (>95%).

***N*-(3,5-dimethylphenyl)-2-((2-methylquinolin-4-yl)oxy)acetamide (3.25).**

The title compound was prepared according to the general procedure E using 2-methylquinolin-4-ol (250 mg, 1.57 mmol), 2-bromo-*N*-(3,5-dimethylphenyl)acetamide (380 mg, 1.57 mmol) and potassium carbonate (651 mg, 4.71 mmol) in anhydrous DMF (15 mL) and the reaction time was 18 h.

White solid; yield 63% (318 mg, 0.992 mmol); TLC,  $R_f$  0.30 (ethyl acetate).  $^1\text{H}$  NMR (400 MHz, DMSO- $d_6$ )  $\delta$  10.10 (s, 1H), 8.24 (dd,  $J = 8.3, 1.0$  Hz, 1H), 7.87 (dd,  $J = 8.4, 0.5$  Hz, 1H), 7.72 (ddd,  $J = 8.4, 6.9, 1.5$  Hz, 1H), 7.53 (ddd,  $J = 8.2, 6.9, 1.2$  Hz, 1H), 7.27 (s, 2H), 6.89 (s, 1H), 6.75 (s, 1H), 4.99 (s, 2H), 2.60 (s, 3H), 2.25 (s, 6H).  $^{13}\text{C}$  NMR (101 MHz, DMSO- $d_6$ )  $\delta$  165.4, 160.2, 159.7, 148.4, 138.2, 137.8, 129.8, 127.9, 125.3, 124.8, 121.8, 119.2, 117.5, 102.0, 67.2, 25.4, 21.1. UPLC-MS (A) (ESI) RT 1.49 min,  $m/z$  321.4  $[\text{M}+\text{H}]^+$  (>95%).

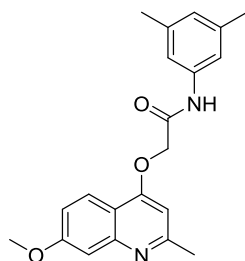
***N*-(3,5-dimethylphenyl)-2-((2-methyl-6-(methylthio)quinolin-4-yl)oxy)acetamide (3.26).**

The title compound was prepared according to the general procedure E using 2-methyl-6-(methylthio)quinolin-4-ol (200 mg, 0.974 mmol), 2-bromo-*N*-(3,5-dimethylphenyl)acetamide (236 mg, 0.975 mmol) and potassium carbonate (404 mg, 2.92 mmol) in anhydrous DMF (11 mL) and the reaction time was 4 h.

White solid; yield 48% (171 mg, 0.464 mmol); TLC,  $R_f$  0.43 (ethyl acetate).  $^1\text{H}$  NMR (400 MHz, DMSO- $d_6$ )  $\delta$  10.10 (s, 1H), 7.94 (d,  $J = 2.1$  Hz, 1H), 7.79 (d,  $J = 8.8$  Hz, 1H), 7.61 (dd,  $J = 8.8, 2.3$  Hz, 1H), 7.26 (s, 2H), 6.87 (s, 1H), 6.74 (s, 1H), 4.99 (s, 2H), 2.60 (s, 3H), 2.56 (s, 3H), 2.24 (s, 6H).  $^{13}\text{C}$  NMR (101 MHz, DMSO- $d_6$ )  $\delta$  165.4, 159.3, 158.8, 146.4, 138.2, 137.8, 134.9, 128.8, 128.4, 125.3,

119.6, 117.4, 116.7, 102.6, 67.1, 25.3, 21.1, 14.9. UPLC-MS (A) (ESI) RT 1.65 min,  $m/z$  367.1 [M+H]<sup>+</sup> (>95%).

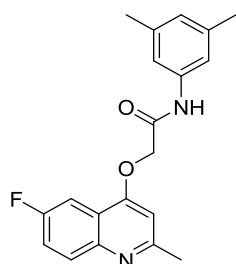
***N*-(3,5-dimethylphenyl)-2-((7-methoxy-2-methylquinolin-4-yl)oxy)acetamide (3.27).**



The title compound was prepared according to the general procedure E using 7-methoxy-2-methyl-4-quinolinol (150 mg, 0.792 mmol), 2-bromo-*N*-(3,5-dimethylphenyl)acetamide (192 mg, 0.793 mmol) and potassium carbonate (329 mg, 2.37 mmol) in anhydrous DMF (9 mL) and the reaction time was 5 h.

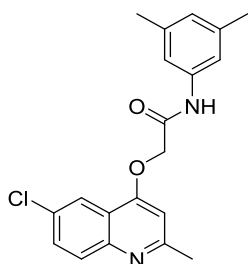
White solid; yield 34% (93 mg, 0.27 mmol); TLC,  $R_f$  0.38 (broad spot) (ethyl acetate/methanol: 90/10). <sup>1</sup>H NMR (400 MHz, CDCl<sub>3</sub>)  $\delta$  8.12 (br. s, 1H), 8.03 (d,  $J$  = 9.1 Hz, 1H), 7.38 (d,  $J$  = 2.5 Hz, 1H), 7.22 – 7.15 (m, 3H), 6.81 (s, 1H), 6.55 (s, 1H), 4.80 (s, 2H), 3.94 (s, 3H), 2.68 (s, 3H), 2.31 (s, 6H). <sup>13</sup>C NMR (101 MHz, CDCl<sub>3</sub>)  $\delta$  165.1, 161.7, 160.6, 160.2, 150.7, 139.1, 136.5, 127.1, 122.2, 118.5, 118.1, 113.8, 106.8, 100.5, 67.7, 55.7, 25.8, 21.5. UPLC-MS (A) (ESI) RT 1.63 min,  $m/z$  351.5 [M+H]<sup>+</sup> (>95%).

***N*-(3,5-dimethylphenyl)-2-(6-fluoro-2-methylquinolin-4-yloxy)acetamide (3.28).**



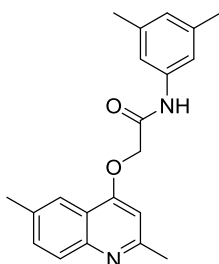
The title compound was prepared according to the general procedure E using 6-fluoro-4-hydroxy-2-methylquinoline (400 mg, 2.26 mmol), 2-bromo-*N*-(3,5-dimethylphenyl)acetamide (656 mg, 2.71 mmol) and potassium carbonate (936 mg, 6.77 mmol) in anhydrous DMF (25 mL) and the reaction time was 3.5 h.

White solid; yield 84% (643 mg, 1.90 mmol); TLC,  $R_f$  0.56 (ethyl acetate/methanol: 90/10). <sup>1</sup>H NMR (400 MHz, CDCl<sub>3</sub>)  $\delta$  8.07 – 7.97 (m, 2H), 7.75 (dd,  $J$  = 9.2, 2.8 Hz, 1H), 7.48 (ddd,  $J$  = 9.2, 8.2, 2.9 Hz, 1H), 7.20 (s, 2H), 6.82 (s, 1H), 6.69 (s, 1H), 4.82 (s, 2H), 2.70 (s, 3H), 2.31 (s, 6H). <sup>13</sup>C NMR (101 MHz, CDCl<sub>3</sub>)  $\delta$  164.8, 160.2 (d, <sup>1</sup> $J_{C-F}$  = 246.8 Hz), 159.6 (d, <sup>4</sup> $J_{C-F}$  = 2.6 Hz), 146.0, 139.2, 136.4, 131.0 (d, <sup>3</sup> $J_{C-F}$  = 8.7 Hz), 127.2, 120.4 (d, <sup>2</sup> $J_{C-F}$  = 25.3 Hz), 119.9 (d, <sup>3</sup> $J_{C-F}$  = 9.5 Hz), 118.2, 118.0, 105.2 (d, <sup>2</sup> $J_{C-F}$  = 23.6 Hz), 102.6, 67.9, 25.8, 21.5. UPLC-MS (A) (ESI) RT 1.58 min,  $m/z$  339.4 [M+H]<sup>+</sup> (>95%).

**2-((6-Chloro-2-methylquinolin-4-yl)oxy)-N-(3,5-dimethylphenyl)acetamide (3.29).**

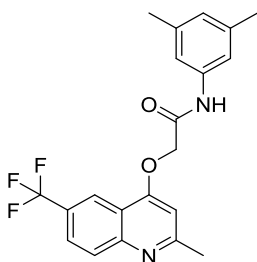
The title compound was prepared according to the general procedure E using 6-chloro-2-methylquinolin-4-ol (200 mg, 1.03 mmol), 2-bromo-*N*-(3,5-dimethylphenyl)acetamide (250 mg, 1.03 mmol) and potassium carbonate (428 mg, 3.10 mmol) in anhydrous DMF (12 mL) and the reaction mixture was stirred overnight.

White solid; yield 31% (113 mg, 0.318 mmol); TLC,  $R_f$  0.43 (ethyl acetate).  $^1\text{H}$  NMR (400 MHz, DMSO- $d_6$ )  $\delta$  10.10 (s, 1H), 8.22 (d,  $J$  = 2.3 Hz, 1H), 7.88 (d,  $J$  = 9.0 Hz, 1H), 7.72 (dd,  $J$  = 9.0, 2.5 Hz, 1H), 7.25 (s, 2H), 6.97 (s, 1H), 6.74 (s, 1H), 5.00 (s, 2H), 2.59 (s, 3H), 2.24 (s, 6H).  $^{13}\text{C}$  NMR (101 MHz, DMSO- $d_6$ )  $\delta$  165.3, 160.6, 159.5, 146.8, 138.1, 137.8, 130.2, 130.1, 129.4, 125.4, 120.8, 120.0, 117.7, 103.0, 67.3, 25.4, 21.1. UPLC-MS (A) (ESI) RT 1.67 min,  $m/z$  355.1, 357.1 (3:1)  $[\text{M}+\text{H}]^+$  (>95%).

***N*-(3,5-dimethylphenyl)-2-((2,6-dimethylquinolin-4-yl)oxy)acetamide (3.30).**

The title compound was prepared according to the general procedure E using 2,6-dimethyl-4-hydroxyquinoline (200 mg, 1.16 mmol), 2-chloro-*N*-(3,5-dimethylphenyl)acetamide (308 mg, 1.27 mmol) and potassium carbonate (479 mg, 3.46 mmol) in anhydrous DMF (13 mL) and the reaction time was 3 h.

White solid; yield 95% (365 mg, 1.09 mmol); mp 208-210 °C; TLC,  $R_f$  0.7 (ethyl acetate/methanol: 80/20).  $^1\text{H}$  NMR (400 MHz, DMSO- $d_6$ )  $\delta$  10.10 (s, 1H), 7.99 (s, 1H), 7.76 (d,  $J$  = 8.5 Hz, 1H), 7.55 (dd,  $J$  = 8.6, 2.0 Hz, 1H), 7.27 (s, 2H), 6.83 (s, 1H), 6.75 (s, 1H), 4.97 (s, 2H), 2.57 (s, 3H), 2.25 (s, 6H).  $^{13}\text{C}$  NMR (101 MHz, DMSO- $d_6$ )  $\delta$  165.4, 159.9, 158.6, 146.9, 138.2, 137.8, 134.1, 131.7, 127.7, 125.3, 120.5, 119.0, 117.4, 101.9, 67.1, 25.3, 21.2, 21.1. UPLC-MS (A) (ESI) RT 1.64 min,  $m/z$  335.5  $[\text{M}+\text{H}]^+$  (>95%). HRMS (ESI)  $m/z$  calcd for  $\text{C}_{21}\text{H}_{23}\text{N}_2\text{O}_2$   $[\text{M}+\text{H}]^+$ : 335.1754; found: 335.1739.

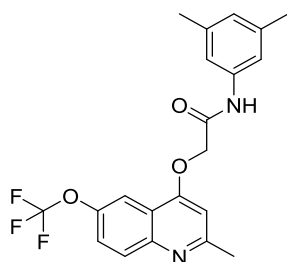
***N*-(3,5-dimethylphenyl)-2-((2-methyl-6-(trifluoromethyl)quinolin-4-yl)oxy)acetamide (3.31).**

The title compound was prepared according to the general procedure E using 2-methyl-6-(trifluoromethyl)quinolin-4-ol (200 mg, 0.880 mmol), 2-bromo-*N*-(3,5-dimethylphenyl)acetamide (213 mg, 0.880 mmol) and potassium carbonate (365 mg, 2.64 mmol) in anhydrous DMF (10 mL) and the reaction mixture was stirred overnight.

White solid; yield 66% (226 mg, 0.582 mmol); mp >210 °C; TLC,  $R_f$  0.45 (ethyl acetate).  $^1\text{H}$  NMR (400 MHz, DMSO- $d_6$ )  $\delta$  10.14 (s, 1H), 8.54 (s, 1H), 8.07 (d,  $J$  = 8.8 Hz, 1H), 7.98 (dd,  $J$  = 8.9, 2.1 Hz,

1H), 7.24 (s, 2H), 7.06 (s, 1H), 6.74 (s, 1H), 5.06 (s, 2H), 2.64 (s, 3H), 2.24 (s, 6H). <sup>13</sup>C NMR (101 MHz, DMSO-*d*<sub>6</sub>) δ 165.2, 163.0, 160.8, 149.5, 138.1, 137.8, 125.3, 125.2 (q, <sup>3</sup>J<sub>C-F</sub> = 3.1 Hz), 125.0 (q, <sup>2</sup>J<sub>C-F</sub> = 32.1 Hz), 124.3 (q, <sup>1</sup>J<sub>C-F</sub> = 272.2 Hz), 120.0 (q, <sup>3</sup>J<sub>C-F</sub> = 4.5 Hz), 118.5, 117.5, 103.4, 67.3, 25.6, 21.1. UPLC-MS (A) (ESI) RT 2.08 min, *m/z* 389.2 [M+H]<sup>+</sup> (>95%). HRMS (ESI) *m/z* calcd for C<sub>21</sub>H<sub>20</sub>F<sub>3</sub>N<sub>2</sub>O<sub>2</sub> [M+H]<sup>+</sup>: 389.1471; found: 389.1478.

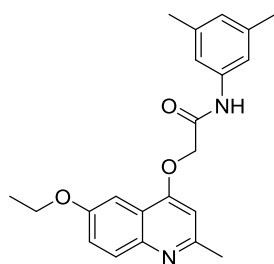
***N*-(3,5-dimethylphenyl)-2-((2-methyl-6-(trifluoromethoxy)quinolin-4-yl)oxy)acetamide (3.32).**



The title compound was prepared according to the general procedure E using 2-methyl-6-(trifluoromethoxy)quinolin-4-ol (200 mg, 0.822 mmol), 2-bromo-*N*-(3,5-dimethylphenyl)acetamide (199 mg, 0.822 mmol) and potassium carbonate (341 mg, 2.47 mmol) in anhydrous DMF (11 mL) and the reaction mixture was stirred overnight.

White solid; yield 47% (157 mg, 0.388 mmol); mp 241 °C; TLC, R<sub>f</sub> 0.36 (ethyl acetate), 0.83 (ethyl acetate/methanol: 90/10). <sup>1</sup>H NMR (400 MHz, DMSO-*d*<sub>6</sub>) δ 10.12 (s, 1H), 8.09 (d, *J* = 1.4 Hz, 1H), 8.00 (d, *J* = 9.1 Hz, 1H), 7.71 (dd, *J* = 9.1, 2.1 Hz, 1H), 7.24 (s, 2H), 7.00 (s, 1H), 6.74 (s, 1H), 5.03 (s, 2H), 2.61 (s, 3H), 2.24 (s, 6H). <sup>13</sup>C NMR (101 MHz, DMSO-*d*<sub>6</sub>) δ 165.2, 161.0, 160.2, 146.8, 144.9, 138.1, 137.8, 130.6, 125.3, 123.7, 120.2 (q, <sup>1</sup>J<sub>C-F</sub> = 256.9 Hz), 119.4, 117.5, 112.8, 103.1, 67.2, 25.4, 21.1. UPLC-MS (A) (ESI) RT 2.08 min, *m/z* 405.2 [M+H]<sup>+</sup> (>95%). HRMS (ESI) *m/z* calcd for C<sub>21</sub>H<sub>20</sub>F<sub>3</sub>N<sub>2</sub>O<sub>3</sub> [M+H]<sup>+</sup>: 405.1421; found: 405.1418.

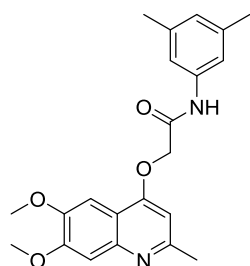
***N*-(3,5-dimethylphenyl)-2-((6-ethoxy-2-methylquinolin-4-yl)oxy)acetamide (3.33).**



The title compound was prepared according to the general procedure E using 6-ethoxy-2-methylquinolin-4-ol (200 mg, 0.984 mmol), 2-bromo-*N*-(3,5-dimethylphenyl)acetamide (238 mg, 0.984 mmol) and potassium carbonate (408 mg, 2.95 mmol) in anhydrous DMF (11 mL) and the reaction time was 3h.

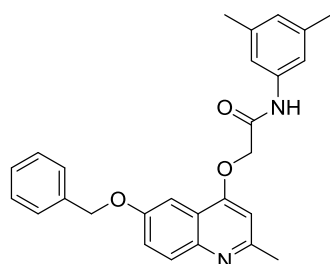
White solid; yield 9% (32 mg, 0.088 mmol); TLC, R<sub>f</sub> 0.67 (ethyl acetate/methanol: 90/10), fluorescence. <sup>1</sup>H NMR (400 MHz, DMSO-*d*<sub>6</sub>) δ 10.10 (s, 1H), 7.77 (d, *J* = 9.1 Hz, 1H), 7.48 (d, *J* = 2.8 Hz, 1H), 7.34 (dd, *J* = 9.1, 2.9 Hz, 1H), 7.25 (s, 2H), 6.82 (s, 1H), 6.74 (s, 1H), 4.97 (s, 2H), 4.15 (q, *J* = 7.0 Hz, 2H), 2.54 (s, 3H), 2.24 (s, 6H), 1.40 (t, *J* = 7.0 Hz, 3H). <sup>13</sup>C NMR (101 MHz, DMSO-*d*<sub>6</sub>) δ 165.5, 159.4, 156.8, 155.5, 144.1, 138.2, 137.8, 129.5, 125.3, 121.8, 119.8, 117.4, 102.1, 100.7, 67.1, 63.4, 25.1, 21.1, 14.6. UPLC-MS (B) (ESI) RT 4.08 min, *m/z* 365.2 [M+H]<sup>+</sup> (>95%).



**2-((6,7-Dimethoxy-2-methylquinolin-4-yl)oxy)-N-(3,5-dimethylphenyl)acetamide (3.34).**

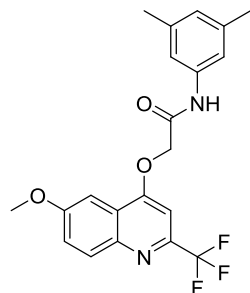
The title compound was prepared according to the general procedure E using 6,7-dimethoxy-2-methylquinolin-4-ol (200 mg, 0.912 mmol), 2-bromo-*N*-(3,5-dimethylphenyl)acetamide (221 mg, 0.912 mmol) and potassium carbonate (378 mg, 2.74 mmol) in anhydrous DMF (11 mL) and the reaction time was 3 h.

White solid; yield 70% (244 mg, 0.641 mmol); TLC,  $R_f$  0.5 (ethyl acetate/methanol: 80/20).  $^1\text{H}$  NMR (400 MHz,  $\text{DMSO-}d_6$ )  $\delta$  10.09 (s, 1H), 7.44 (s, 1H), 7.26 (s, 1H), 7.26 (s, 2H), 6.73 (s, 1H), 6.72 (s, 1H), 4.96 (s, 2H), 3.90 (s, 6H), 2.52 (s, 3H), 2.24 (s, 6H).  $^{13}\text{C}$  NMR (101 MHz,  $\text{DMSO-}d_6$ )  $\delta$  165.6, 159.3, 157.0, 152.1, 148.1, 145.3, 138.2, 137.8, 125.2, 117.3, 113.2, 107.4, 100.6, 99.9, 67.0, 55.6, 55.5, 25.1, 21.1. UPLC-MS (A) (ESI) RT 1.94 min,  $m/z$  381.3  $[\text{M}+\text{H}]^+$  (>95%).

**2-(6-(Benzyloxy)-2-methylquinolin-4-yloxy)-N-(3,5-dimethylphenyl)acetamide (3.35).**

The title compound was prepared according to the general procedure E using 6-(benzyloxy)-2-methylquinolin-4-ol (130 mg, 0.490 mmol), 2-bromo-*N*-(3,5-dimethylphenyl)acetamide (130 mg, 0.536 mmol) and potassium carbonate (203 mg, 1.47 mmol) in anhydrous DMF (5.5 mL) and the reaction time was 3 h.

White solid; yield 48% (100 mg, 0.234 mmol); TLC,  $R_f$  0.49 (ethyl acetate/methanol: 90/10).  $^1\text{H}$  NMR (400 MHz,  $\text{DMSO-}d_6$ )  $\delta$  10.09 (s, 1H), 7.80 (d,  $J = 9.1$  Hz, 1H), 7.63 (d,  $J = 2.8$  Hz, 1H), 7.54 – 7.49 (m, 2H), 7.45 – 7.31 (m, 4H), 7.27 (s, 2H), 6.84 (s, 1H), 6.74 (s, 1H), 5.24 (s, 2H), 4.98 (s, 2H), 2.55 (s, 3H), 2.24 (s, 6H).  $^{13}\text{C}$  NMR (101 MHz,  $\text{DMSO-}d_6$ )  $\delta$  165.5, 159.5, 157.0, 155.3, 144.3, 138.2, 137.8, 136.8, 129.6, 128.4, 127.9, 127.8, 125.3, 121.9, 119.7, 117.4, 102.2, 101.6, 69.6, 67.1, 25.1, 21.1. UPLC-MS (A) (ESI) RT 1.82 min,  $m/z$  427.5  $[\text{M}+\text{H}]^+$  (>95%).

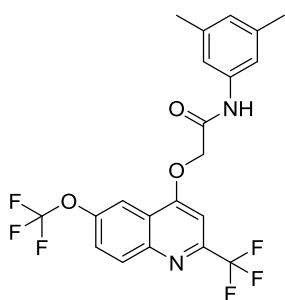
***N*-(3,5-dimethylphenyl)-2-(6-methoxy-2-(trifluoromethyl)quinolin-4-yloxy)acetamide (3.36).**

The title compound was prepared according to the general procedure E using 6-methoxy-2-(trifluoromethyl)quinolin-4-ol (500 mg, 2.06 mmol), 2-bromo-*N*-(3,5-dimethylphenyl)acetamide (548 mg, 2.26 mmol) and potassium carbonate (852 mg, 6.17 mmol) in anhydrous DMF (23 mL) and the reaction time was 3 h.

Off-white solid; yield 72% (597 mg, 1.48 mmol); mp 201-202 °C; TLC,  $R_f$  0.61 (n-heptane/EtOAc: 50/50).  $^1\text{H}$  NMR (400 MHz,  $\text{DMSO-}d_6$ )  $\delta$  10.18 (s, 1H), 8.05 (d,  $J = 9.2$  Hz, 1H), 7.61 (d,  $J = 2.8$  Hz, 1H), 7.57 (dd,  $J = 9.2, 2.9$  Hz, 1H), 7.36 (s, 1H), 7.24 (s, 2H), 6.75 (s, 1H), 5.20 (s,

2H), 3.97 (s, 3H), 2.24 (s, 6H).  $^{13}\text{C}$  NMR (101 MHz, DMSO- $d_6$ )  $\delta$  165.1, 161.3, 158.6, 145.1 (q,  $^2J_{\text{C-F}} = 33.5$  Hz), 143.4, 138.1, 137.9, 130.8, 125.3, 123.8, 122.3, 121.7 (q,  $^1J_{\text{C-F}} = 275.4$  Hz), 117.3, 99.9, 98.2, 67.6, 55.7, 21.1. UPLC-MS (B) (ESI) RT 4.60 min,  $m/z$  405.6  $[\text{M}+\text{H}]^+$  (>95%). HRMS (ESI)  $m/z$  calcd for  $\text{C}_{21}\text{H}_{20}\text{F}_3\text{N}_2\text{O}_3$   $[\text{M}+\text{H}]^+$ : 405.1421; found: 405.1426.

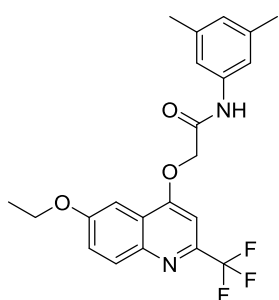
***N*-(3,5-dimethylphenyl)-2-(6-(trifluoromethoxy)-2-(trifluoromethyl)quinolin-4-yloxy)acetamide (3.37).**



The title compound was prepared according to the general procedure E using 4-hydroxy-6-(trifluoromethoxy)-2-(trifluoromethyl)quinoline (300 mg, 1.01 mmol), 2-bromo-*N*-(3,5-dimethylphenyl)acetamide (269 mg, 1.11 mmol) and potassium carbonate (419 mg, 3.03 mmol) in anhydrous DMF (19 mL) and the reaction time was 3 h.

White solid; yield 39% (182 mg, 0.397 mmol); TLC,  $R_f$  0.79 (n-heptane/ethyl acetate: 50/50).  $^1\text{H}$  NMR (400 MHz, DMSO- $d_6$ )  $\delta$  10.18 (s, 1H), 8.30 (d,  $J = 9.2$  Hz, 1H), 8.24 (bs, 1H), 7.95 (dd,  $J = 8.8, 2.3$  Hz, 1H), 7.54 (s, 1H), 7.23 (s, 2H), 6.75 (s, 1H), 5.25 (s, 2H), 2.24 (s, 6H).  $^{13}\text{C}$  NMR (101 MHz, DMSO- $d_6$ )  $\delta$  164.8, 162.7, 148.5 (q,  $^2J_{\text{C-F}} = 33.9$  Hz), 147.1, 145.9, 138.1, 137.9, 132.1, 125.5, 125.4, 121.6, 121.3 (q,  $^1J_{\text{C-F}} = 275.9$  Hz), 120.1 (q,  $^1J_{\text{C-F}} = 258.5$  Hz), 117.4, 112.8, 99.1, 67.9, 21.1. UPLC-MS (A) (ESI) RT 2.51 min,  $m/z$  459.4  $[\text{M}+\text{H}]^+$  (>95%).

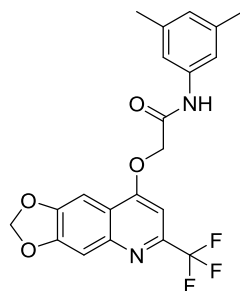
***N*-(3,5-dimethylphenyl)-2-(6-ethoxy-2-(trifluoromethyl)quinolin-4-yloxy)acetamide (3.38).**



The title compound was prepared according to the general procedure E using 6-ethoxy-2-(trifluoromethyl)quinolin-4-ol (150 mg, 0.583 mmol), 2-bromo-*N*-(3,5-dimethylphenyl)acetamide (169 mg, 0.698 mmol) and potassium carbonate (242 mg, 1.75 mmol) in anhydrous DMF (6.5 mL) and the reaction time was 4.5 h.

White solid; yield 77% (189 mg, 0.452 mmol); TLC,  $R_f$  0.75 (n-heptane/ethyl acetate: 50/50).  $^1\text{H}$  NMR (400 MHz, DMSO- $d_6$ )  $\delta$  10.16 (s, 1H), 8.03 (d,  $J = 9.2$  Hz, 1H), 7.59 (d,  $J = 2.8$  Hz, 1H), 7.54 (dd,  $J = 9.2, 2.9$  Hz, 1H), 7.35 (s, 1H), 7.24 (s, 2H), 6.74 (s, 1H), 5.18 (s, 2H), 4.23 (q,  $J = 7.0$  Hz, 2H), 2.24 (s, 6H), 1.43 (t,  $J = 7.0$  Hz, 3H).  $^{13}\text{C}$  NMR (101 MHz, DMSO- $d_6$ )  $\delta$  165.1, 161.2, 157.8, 145.0 (q,  $^2J_{\text{C-F}} = 33.8$  Hz), 143.3, 138.1, 137.8, 130.8, 125.3, 124.0, 122.3, 121.7 (q,  $^1J_{\text{C-F}} = 274.7$  Hz), 117.3, 100.5, 98.1, 67.6, 63.8, 21.0, 14.5. UPLC-MS (A) (ESI) RT 2.28 min,  $m/z$  419.4  $[\text{M}+\text{H}]^+$  (>95%).

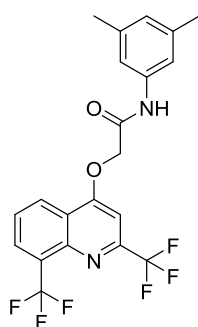
***N*-(3,5-dimethylphenyl)-2-((6-(trifluoromethyl)-[1,3]dioxolo[4,5-*g*]quinolin-8-yl)oxy)acetamide (3.39).**



The title compound was prepared according to the general procedure E using 6-(trifluoromethyl)-[1,3]dioxolo[4,5-*g*]quinolin-8-ol (309 mg, 1.20 mmol), 2-bromo-*N*-(3,5-dimethylphenyl)acetamide (291 mg, 1.20 mmol) and potassium carbonate (498 mg, 3.60 mmol) in anhydrous DMF (13 mL) and the reaction time was 19 h.

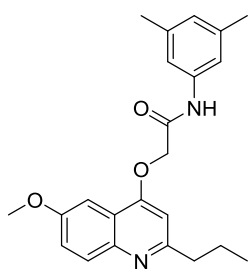
White solid; yield 43% (217 mg, 0.519 mmol); TLC,  $R_f$  0.49 (n-heptane/ethyl acetate: 50/50).  $^1\text{H}$  NMR (400 MHz, DMSO- $d_6$ )  $\delta$  10.11 (s, 1H), 7.63 (s, 1H), 7.47 (s, 1H), 7.29 (s, 1H), 7.23 (s, 2H), 6.74 (s, 1H), 6.29 (s, 2H), 5.12 (s, 2H), 2.24 (s, 6H).  $^{13}\text{C}$  NMR (101 MHz, DMSO- $d_6$ )  $\delta$  165.2, 161.3, 152.0, 149.0, 146.2, 145.4 (q,  $^2J_{\text{C-F}} = 33.8$  Hz), 138.1, 137.8, 125.4, 121.7 (q,  $^1J_{\text{C-F}} = 274.9$  Hz), 117.7, 117.6, 105.2, 102.8, 97.5 (q,  $^3J_{\text{C-F}} = 2.4$  Hz), 97.4, 67.6, 21.1. UPLC-MS (A) (ESI) RT 2.17 min,  $m/z$  419.4  $[\text{M}+\text{H}]^+$  (>95%).

***N*-(3,5-dimethylphenyl)-2-((2,8-bis(trifluoromethyl)quinolin-4-yl)oxy)acetamide (3.40).**



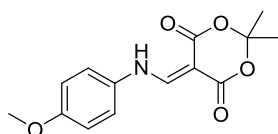
The title compound was prepared according to the general procedure E, using 2,8-bis(trifluoromethyl)-4-quinolinol (150 mg, 0.534 mmol), 2-bromo-*N*-(3,5-dimethylphenyl)acetamide (129 mg, 0.534 mmol) and potassium carbonate (221 mg, 1.60 mmol) in anhydrous DMF (12 mL) and the reaction mixture was stirred overnight.

White solid; yield 50% (118 mg, 0.267 mmol); TLC,  $R_f$  0.69 (n-heptane/ethyl acetate: 50/50).  $^1\text{H}$  NMR (400 MHz, DMSO- $d_6$ )  $\delta$  10.17 (s, 1H), 8.67 (d,  $J = 7.9$  Hz, 1H), 8.35 (d,  $J = 7.2$  Hz, 1H), 7.90 (t,  $J = 7.9$  Hz, 1H), 7.61 (s, 1H), 7.24 (s, 2H), 6.74 (s, 1H), 5.27 (s, 2H), 2.24 (s, 6H).  $^{13}\text{C}$  NMR (101 MHz, DMSO- $d_6$ )  $\delta$  164.8, 163.1, 148.4 (q,  $^2J_{\text{C-F}} = 33.8$  Hz), 143.7, 138.1, 137.8, 130.2 (q,  $^3J_{\text{C-F}} = 5.2$  Hz), 127.3, 127.1, 126.3 (q,  $^2J_{\text{C-F}} = 29.7$  Hz), 125.4, 123.7 (q,  $^1J_{\text{C-F}} = 273.5$  Hz), 121.8, 121.1 (q,  $^1J_{\text{C-F}} = 276.6$  Hz), 117.4, 99.4, 67.9, 21.0. UPLC-MS (A) (ESI) RT 2.35 min,  $m/z$  443.4  $[\text{M}+\text{H}]^+$  (>95%).

***N*-(3,5-dimethylphenyl)-2-((6-methoxy-2-propylquinolin-4-yl)oxy)acetamide (3.41).**

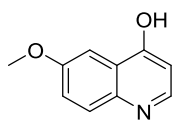
The title compound was prepared according to the general procedure E, using 6-methoxy-2-propylquinolin-4-ol (200 mg, 0.921 mmol), 2-bromo-*N*-(3,5-dimethylphenyl)acetamide (245 mg, 1.01 mmol) and potassium carbonate (382 mg, 2.76 mmol) in anhydrous DMF (9 mL) and the reaction mixture was stirred overnight.

White solid; yield 57% (197 mg, 0.521 mmol); TLC,  $R_f$  0.63, broad spot (ethyl acetate).  $^1\text{H}$  NMR (400 MHz,  $\text{DMSO-}d_6$ )  $\delta$  10.10 (s, 1H), 7.80 (d,  $J = 9.1$  Hz, 1H), 7.50 (d,  $J = 2.8$  Hz, 1H), 7.35 (dd,  $J = 9.1, 2.9$  Hz, 1H), 7.24 (s, 2H), 6.84 (s, 1H), 6.73 (s, 1H), 4.99 (s, 2H), 3.89 (s, 3H), 2.81 – 2.72 (m, 2H), 2.23 (s, 6H), 1.80 – 1.66 (m, 2H), 0.91 (t,  $J = 7.4$  Hz, 3H).  $^{13}\text{C}$  NMR (101 MHz,  $\text{DMSO-}d_6$ )  $\delta$  165.6, 160.6, 159.5, 156.3, 144.2, 138.2, 137.8, 129.7, 125.3, 121.5, 120.0, 117.4, 101.7, 100.0, 67.2, 55.4, 40.5, 22.3, 21.1, 13.8. UPLC-MS (A) (ESI) RT 2.01 min,  $m/z$  379.3  $[\text{M}+\text{H}]^+$  (>95%).

***5*-((4-Methoxyphenylamino)methylene)-2,2-dimethyl-1,3-dioxane-4,6-dione (3.44).**

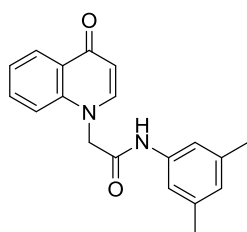
A solution of *para*-anisidine (1.00 g, 8.12 mmol), 2,2-dimethyl-1,3-dioxane-4,6-dione (meldrum's acid derivative) (1.38 g, 9.58 mmol) and triethoxymethane (1.6 mL, 9.6 mmol) in ethanol (10 mL) was heated under reflux for 2 h and then allowed to cool down to room temperature. Filtration, washing with cold absolute ethanol and drying under reduced pressure afforded the title compound.

White solid; yield 90% (2.03 g, 7.31 mmol); TLC,  $R_f$  0.6 (*n*-heptane/ethyl acetate: 50/50).  $^1\text{H}$  NMR (400 MHz,  $\text{CDCl}_3$ )  $\delta$  ppm 11.23 (d,  $J=14.6$  Hz, 1 H), 8.55 (d,  $J=14.3$  Hz, 1 H), 7.16 - 7.23 (m, 2 H), 6.93 - 6.98 (m, 2 H), 3.84 (s, 3 H), 1.76 (s, 6 H). UPLC-MS (ESI), RT 1.63 min,  $m/z$  278.4  $[\text{M}+\text{H}]^+$  (>95%).

***6*-Methoxyquinolin-4-ol (3.46).**

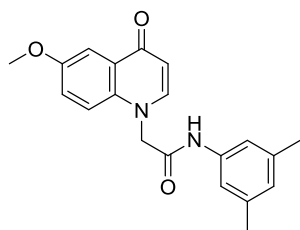
**3.44** (1.00 g, 3.61 mmol) was added portionwise to Dowtherm A (10 mL) at 220 °C. After bubbling stopped, the mixture was heated for additional 10 min and then allowed to cool down to room temperature. The mixture was poured into *n*-heptane, the brown solid was collected by filtration and washed with *n*-heptane. It was purified using silica gel column chromatography.

Off-white solid; yield 64% (403 mg, 2.30 mmol); TLC,  $R_f$  0.40 (ethyl acetate/methanol, 80/20). UPLC-MS (ESI) (A), RT 0.56 min,  $m/z$  176.4  $[\text{M}+\text{H}]^+$  (>95%).

***N*-(3,5-dimethylphenyl)-2-(4-oxoquinolin-1(4*H*)-yl)acetamide (3.48).**

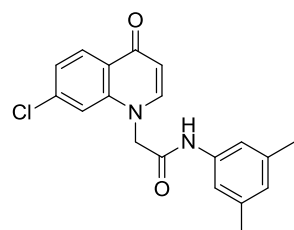
The title compound was prepared according to the general method E using 4-hydroxy-1-azanaphthalene (300 mg, 2.07 mmol), 2-bromo-*N*-(3,5-dimethylphenyl)acetamide (550 mg, 2.27 mmol) and potassium carbonate (857 mg, 6.20 mmol) in anhydrous DMF (24 mL) and the reaction time was 3 h.

White solid; yield 84% (553 mg, 1.74 mmol); TLC,  $R_f$  0.4 (ethyl acetate/methanol, 90/10).  $^1\text{H}$  NMR (400 MHz,  $\text{DMSO-}d_6$ )  $\delta$  ppm 10.38 (s, 1 H), 8.19 (dd,  $J=8.0, 1.4$  Hz, 1 H), 7.98 (d,  $J=7.6$  Hz, 1 H), 7.70 (ddd,  $J=8.6, 7.1, 1.5$  Hz, 1 H), 7.48 (d,  $J=8.6$  Hz, 1 H), 7.37 (t,  $J=7.5$  Hz, 1 H), 7.21 (s, 2 H), 6.72 (s, 1 H), 6.10 (d,  $J=7.8$  Hz, 1 H), 5.11 (s, 2 H), 2.22 (s, 6 H).  $^{13}\text{C}$  NMR (101 MHz,  $\text{DMSO-}d_6$ )  $\delta$  ppm 176.5, 165.2, 145.8, 140.5, 138.3, 137.9, 132.1, 126.4, 125.7, 125.2, 123.3, 116.9, 116.0, 108.7, 54.6, 21.0. UPLC-MS (ESI) (A), RT 1.64 min,  $m/z$  307.5  $[\text{M}+\text{H}]^+$  (>95%).

***N*-(3,5-dimethylphenyl)-2-(6-methoxy-4-oxoquinolin-1(4*H*)-yl)acetamide (3.49).**

The title compound was prepared according to the general method E using 6-methoxyquinolin-4-ol (400 mg, 2.28 mmol), 2-bromo-*N*-(3,5-dimethylphenyl)acetamide (608 mg, 2.51 mmol) and potassium carbonate (947 mg, 6.85 mmol) in anhydrous DMF (25 mL) and the reaction time was 3 h.

White solid; yield 51% (393 mg, 1.17 mmol); TLC,  $R_f$  0.35 (ethyl acetate/methanol: 90/10).  $^1\text{H}$  NMR (400 MHz,  $\text{DMSO-}d_6$ )  $\delta$  ppm 10.35 (s, 1 H), 7.92 (d,  $J=7.6$  Hz, 1 H), 7.61 (d,  $J=3.0$  Hz, 1 H), 7.45 (d,  $J=9.3$  Hz, 1 H), 7.34 (dd,  $J=9.1, 3.0$  Hz, 1 H), 7.20 (s, 2 H), 6.72 (s, 1 H), 6.05 (d,  $J=7.6$  Hz, 1 H), 5.10 (s, 2 H), 3.84 (s, 3 H), 2.22 (s, 6 H).  $^{13}\text{C}$  NMR (101 MHz,  $\text{DMSO-}d_6$ )  $\delta$  ppm 175.9, 165.2, 155.5, 144.8, 138.3, 137.9, 135.1, 127.6, 125.2, 121.8, 117.9, 116.9, 107.6, 105.5, 55.4, 54.7, 21.0. UPLC-MS (ESI) (A), RT 1.69 min,  $m/z$  337.6  $[\text{M}+\text{H}]^+$  (>95%).

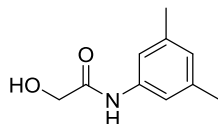
***2*-(7-Chloro-4-oxoquinolin-1(4*H*)-yl)-*N*-(3,5-dimethylphenyl) acetamide (3.50).**

The title compound was prepared according to the general method E using 7-chloro-4-hydroxyquinoline (500 mg, 2.78 mmol), 2-bromo-*N*-(3,5-dimethylphenyl)acetamide (674 mg, 2.78 mmol) and potassium carbonate (1.15 g, 8.35 mmol) in anhydrous DMF (31 mL) and the reaction time was 3 h.

White solid; yield 5% (45 mg, 0.13 mmol); TLC,  $R_f$  0.63 (ethyl acetate/methanol: 90/10).  $^1\text{H}$  NMR (400 MHz,  $\text{DMSO-}d_6$ )  $\delta$  ppm 10.33 (s, 1 H), 8.17 (d,  $J=8.6$  Hz, 1 H), 7.98 (d,  $J=7.8$  Hz, 1 H), 7.64 (s, 1

H), 7.41 (dd,  $J=8.6, 1.0$  Hz, 1 H), 7.21 (s, 2 H), 6.73 (s, 1 H), 6.12 (d,  $J=7.8$  Hz, 1 H), 5.12 (s, 2 H), 2.22 (s, 6 H).  $^{13}\text{C}$  NMR (101 MHz, DMSO- $d_6$ )  $\delta$  ppm 175.9, 165.0, 146.2, 141.5, 138.3, 137.9, 137.0, 127.9, 125.2, 125.0, 123.7, 116.9, 115.9, 109.4, 54.5, 21.0. UPLC-MS (ESI) (A), RT 1.81 min,  $m/z$  341.5, 343.5 (3:1)  $[\text{M}+\text{H}]^+$  (>95%).

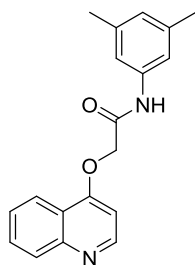
***N*-(3,5-dimethylphenyl)-2-hydroxyacetamide (3.52).**



A mixture of 3,5-dimethylaniline (1.00 g, 8.25 mmol) and glycolic acid (0.628 g, 8.25 mmol) were stirred at 130 °C for 5.5 h. The mixture was cooled to room temperature and dissolved in ethyl acetate (50 mL). The organic phase was washed with ammonium chloride (1N, 50 mL), saturated sodium bicarbonate (50 mL) and brine (50 mL). The organic phase was dried under magnesium sulfate and the solvent was removed under reduced pressure.

Brown solid; yield 81% (1.20 g, 6.70 mmol).  $^1\text{H}$  NMR (400 MHz, DMSO- $d_6$ )  $\delta$  ppm 9.42 (s, 1 H), 7.30 (s, 2 H), 6.70 (s, 1 H), 5.62 (t,  $J=5.9$  Hz, 1 H), 3.96 (d,  $J=5.8$  Hz, 2 H), 2.23 (s, 6 H).  $^{13}\text{C}$  NMR (101 MHz, DMSO- $d_6$ )  $\delta$  ppm 170.6, 138.3, 137.6, 124.9, 117.3, 61.8, 21.1. UPLC-MS (ESI) (B) RT 0.99 min,  $m/z$  180  $[\text{M}+\text{H}]^+$  (>95%).

***N*-(3,5-dimethylphenyl)-2-(quinolin-4-yloxy)acetamide (3.55).**

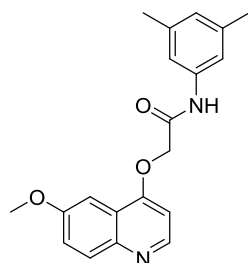


A mixture of 4-chloroquinoline (100 mg, 0.611 mmol), *N*-(3,5-dimethylphenyl)-2-hydroxyacetamide (110 mg, 0.611 mmol), *N,N,N',N'*-tetramethylethylenediamine (7.1 mg, 0.061 mmol), copper(I) iodide (11.6 mg, 0.06 mmol) and cesium carbonate (398 mg, 1.22 mmol) in anhydrous DMF (5 mL) were placed in a high pressure tube under nitrogen atmosphere. The reaction mixture was stirred at 95 °C overnight, cooled down and filtered using a nylon syringe filter. The filtrate was evaporated and the residue was dissolved in ethyl acetate (50 mL) and washed with brine (30 mL x 3). The organic layer was dried over magnesium sulfate and evaporated under reduced pressure. The residue was purified by HPLC using an X-bridge 30 column and as eluent ACN /H<sub>2</sub>O gradient from 40-100 (basic method).

Off-white solid; yield 21% (40 mg, 0.13 mmol); mp 162-163 °C; TLC,  $R_f$  0.40 (ethyl acetate).  $^1\text{H}$  NMR (400 MHz, DMSO- $d_6$ )  $\delta$  ppm 10.12 (s, 1 H), 8.73 (d,  $J=5.1$  Hz, 1 H), 8.30 (d,  $J=7.6$  Hz, 1 H), 7.97 (d,  $J=8.3$  Hz, 1 H), 7.77 (ddd,  $J=8.3, 6.9, 1.4$  Hz, 1 H), 7.61 (ddd,  $J=8.3, 6.9, 1.4$  Hz, 1 H), 7.25 (s, 2 H), 6.96 (d,  $J=5.3$  Hz, 1 H), 6.74 (s, 1 H), 5.02 (s, 2 H), 2.24 (s, 6 H).  $^{13}\text{C}$  NMR (101 MHz, DMSO- $d_6$ )  $\delta$  ppm 165.3, 160.2, 151.4, 148.8, 138.1, 137.7, 129.8, 128.5, 125.7, 125.3, 121.9, 120.6, 117.4, 101.8,

67.2, 21.0. UPLC-MS (ESI) (B), RT 1.18 min,  $m/z$  307  $[M+H]^+$  (>95%); HRMS (ESI)  $m/z$  calculated for  $C_{19}H_{19}N_2O_2$   $[M+H]^+$ : 307.1441; found: 307.1440.

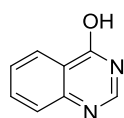
***N*-(3,5-dimethylphenyl)-2-((6-methoxyquinolin-4-yl)oxy)acetamide (3.56).**



A mixture of 4-chloro-6-methoxyquinoline (100 mg, 0.516 mmol), *N,N,N',N'*-tetramethylethylenediamine (6 mg, 0.05 mmol), copper(I) iodide (9.8 mg, 0.051 mmol) and cesium carbonate (337 mg, 1.03 mmol) in anhydrous DMF (5 mL) were placed in a high pressure tube under nitrogen atmosphere. The reaction mixture was stirred at 95 °C overnight. The reaction mixture was allowed to cool down and it was filtered through a nylon syringe filter. The filtrate was evaporated and the residue was dissolved in ethyl acetate (50 mL) and washed with brine (50 mL x 3). The organic layer was dried over sodium sulfate and evaporated under reduced pressure. The mixture was using silica gel column chromatography and then HPLC using an X-bridge 30 column and as eluent ACN/H<sub>2</sub>O gradient from 40/60-100/0 (basic method).

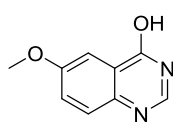
Off-white solid; yield 4% (7 mg, 0.02 mmol); mp 156-157 °C; TLC,  $R_f$  0.48 (ethyl acetate). <sup>1</sup>H NMR (400 MHz, DMSO-*d*<sub>6</sub>)  $\delta$  ppm 10.13 (s, 1 H), 8.58 (d,  $J=5.1$  Hz, 1 H), 7.88 (d,  $J=9.1$  Hz, 1 H), 7.55 (d,  $J=3.0$  Hz, 1 H), 7.41 (dd,  $J=9.1, 2.8$  Hz, 1 H), 7.25 (s, 2 H), 6.91 (d,  $J=5.3$  Hz, 1 H), 6.73 (s, 1 H), 5.02 (s, 2 H), 3.92 (s, 3 H), 2.24 (s, 6 H); <sup>13</sup>C NMR (101 MHz, DMSO-*d*<sub>6</sub>)  $\delta$  ppm 165.4, 159.3, 156.8, 148.7, 144.7, 138.2, 137.8, 130.2, 125.2, 121.9, 121.3, 117.3, 101.9, 99.9, 67.1, 55.5, 21.1; UPLC-MS (ESI) (B), RT 1.18 min,  $m/z$  337  $[M+H]^+$  (>95%); HRMS (ESI)  $m/z$  calculated for  $C_{20}H_{21}N_2O_3$   $[M+H]^+$ : 337.1547; found: 337.1540.

***Quinazolin-4-ol* (3.61).**



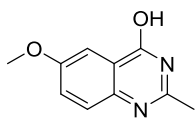
A 50 mL round bottom flask was charged with 2-aminobenzoic acid (1.00 g, 7.29 mmol) and formamide (4 mL, 101 mmol) and heated for 7 h at 150 °C. Then, the reaction mixture was cooled down to room temperature and a white precipitate was formed, filtered, washed with water to remove the excess of formamide and dried.

White solid, yield 56% (595 mg, 4.07 mmol); TLC,  $R_f$  0.48 (ethyl acetate),  $R_f$  0.83 (ethyl acetate/methanol: 90/10). <sup>1</sup>H NMR (400 MHz, Methanol-*d*<sub>4</sub>)  $\delta$  ppm 8.22 (dd,  $J=8.2, 1.4$  Hz, 1 H), 8.09 (s, 1 H), 7.83 (ddd,  $J=8.3, 7.2, 1.4$  Hz, 1 H), 7.70 (d,  $J=8.3$  Hz, 1 H), 7.55 (ddd,  $J=8.0, 7.1, 1.3$  Hz, 1 H). UPLC-MS (ESI) (A), RT 0.46 min,  $m/z$  147.3  $[M+H]^+$  (>95%).

**6-Methoxyquinazolin-4-ol (3.62).**

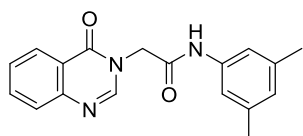
A 50 mL round bottom flask was charged with 2-amino-5-methoxybenzoic acid (500 mg, 2.99 mmol) and formamide (3 mL, 75 mmol) and heated for 7 h at 150 °C. Then, the reaction mixture was cooled down to room temperature and the precipitate was filtered, washed with water to remove the excess of formamide and dried.

Light brown solid; yield 65% (343 mg, 1.95 mmol); TLC,  $R_f$  0.66 (ethyl acetate/methanol: 90/10).  $^1\text{H}$  NMR (400 MHz, DMSO)  $\delta$  12.19 (s, 0.4H), 7.98 (s, 1H), 7.62 (d,  $J$  = 8.9 Hz, 1H), 7.50 (d,  $J$  = 3.0 Hz, 1H), 7.41 (dd,  $J$  = 8.9, 3.0 Hz, 1H), 4.04 (s, 0.6H), 3.86 (s, 3H).  $^{13}\text{C}$  NMR (101 MHz, DMSO)  $\delta$  157.8, 143.2, 143.1, 143.0, 129.0, 123.8, 123.5, 105.9, 55.6. UPLC-MS (ESI) (A), RT 1.11 min,  $m/z$  177.4  $[\text{M}+\text{H}]^+$  (>95%).

**6-Methoxy-2-methylquinazolin-4-ol (3.63).**

**Method A:** A 50 mL round bottom flask was charged with 2-amino-5-methoxybenzoic acid (500 mg, 2.99 mmol) and acetamide (2.297 mg, 38.88 mmol) and heated at 150 °C for 29 h and then at 165 °C for additional 25 h. Afterwards, the reaction mixture was cooled down to room temperature and water was added. A dark brown precipitate was formed which was filtered, washed with water and purified by reverse phase column chromatography. **Method B:** A microwave vial (20 mL) was charged with 2-amino-5-methoxybenzoic acid (700 mg, 4.19 mmol) and acetamide (4.95 g, 83.8 mmol). The reaction mixture was irradiated at 165 °C for 12 h. The obtained solid was washed with water (50 mL x 3). It was purified by an amine column.

Off-white solid, yield (A) 14% (77 mg, 0.41 mmol); (B) 35% (280 mg, 1.47 mmol).  $^1\text{H}$  NMR (400 MHz, DMSO- $d_6$ )  $\delta$  ppm 12.15 (br. s., 1 H), 7.52 (d,  $J$ =8.8 Hz, 1 H), 7.46 (d,  $J$ =2.8 Hz, 1 H), 7.37 (dd,  $J$ =8.8, 3.0 Hz, 1 H), 3.85 (s, 3 H), 2.32 (s, 3 H).  $^{13}\text{C}$  NMR (101 MHz, DMSO- $d_6$ )  $\delta$  ppm 161.5, 157.1, 151.8, 143.4, 128.2, 123.7, 121.3, 105.7, 55.5, 21.2. UPLC-MS (ESI) (B), RT 1.11 min,  $m/z$  191.1  $[\text{M}+\text{H}]^+$  (>95%).

***N*-(3,5-dimethylphenyl)-2-(4-oxoquinazolin-3(4H)-yl)acetamide (3.64).**

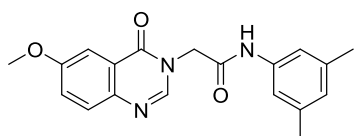
The title compound was prepared according to the general method E using quinazolin-4-ol (500 mg, 3.42 mmol), 2-bromo-*N*-(3,5-dimethylphenyl)acetamide (828 mg, 3.42 mmol) and potassium carbonate (1.419 g, 10.26 mmol) in anhydrous DMF (38 mL) and the reaction time was 3 h.

White solid; yield 95% (1.004 g, 3.266 mmol); TLC,  $R_f$  0.65 (ethyl acetate/methanol: 90/10).  $^1\text{H}$  NMR (400 MHz, DMSO- $d_6$ )  $\delta$  ppm 10.31 (s, 1 H), 8.36 (s, 1 H), 8.15 (dd,  $J$ =8.0, 1.1 Hz, 1 H), 7.83 -



7.89 (m, 1 H), 7.69 - 7.74 (m, 1 H), 7.53 - 7.61 (m, 1 H), 7.21 (s, 2 H), 6.71 (s, 1 H), 4.85 (s, 2 H), 2.22 (s, 6 H).  $^{13}\text{C}$  NMR (101 MHz, DMSO- $d_6$ )  $\delta$  ppm 165.3, 160.3, 148.6, 148.1, 138.5, 137.8, 134.5, 127.2, 127.1, 126.0, 125.1, 121.4, 116.8, 48.8, 21.1. UPLC-MS (ESI) (A), RT 1.75 min,  $m/z$  308.5  $[\text{M}+\text{H}]^+$  (>95%).

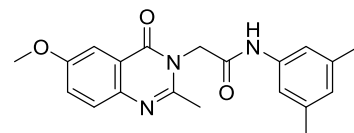
***N*-(3,5-dimethylphenyl)-2-(6-methoxy-4-oxoquinazolin-3(4H)-yl)acetamide (3.65).**



The title compound was prepared according to the general method A using 6-methoxyquinazolin-4-ol (300 mg, 1.70 mmol), 2-bromo-*N*-(3,5-dimethylphenyl) acetamide (412 mg, 1.70 mmol) and potassium carbonate (706 mg, 5.11 mmol) in anhydrous DMF (19 mL) and the reaction time was 3 h.

Light grey solid, yield 93% (533 mg, 1.58 mmol); TLC,  $R_f$  0.72 (ethyl acetate).  $^1\text{H}$  NMR (400 MHz, DMSO- $d_6$ )  $\delta$  ppm 10.29 (s, 1 H), 8.25 (s, 1 H), 7.67 (d,  $J=9.1$  Hz, 1 H), 7.51 (d,  $J=2.8$  Hz, 1 H), 7.46 (dd,  $J=8.8, 2.8$  Hz, 1 H), 7.21 (s, 2 H), 6.71 (s, 1 H), 4.84 (s, 2 H), 3.87 (s, 3 H), 2.22 (s, 6 H).  $^{13}\text{C}$  NMR (101 MHz, DMSO- $d_6$ )  $\delta$  ppm 165.3, 160.1, 158.0, 146.4, 142.6, 138.5, 137.8, 128.9, 125.1, 123.9, 122.3, 116.8, 105.9, 55.7, 48.8, 21.1. UPLC-MS (ESI) (A), RT 1.80 min,  $m/z$  338.5  $[\text{M}+\text{H}]^+$  (>95%).

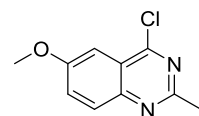
***N*-(3,5-dimethylphenyl)-2-(6-methoxy-2-methyl-4-oxoquinazolin-3(4H)-yl)acetamide (3.66).**



The title compound was prepared according to the general method E using 6-methoxy-2-methylquinazolin-4-ol (77 mg, 0.41 mmol), 2-bromo-*N*-(3,5-dimethylphenyl) acetamide (98 mg, 0.41 mmol) and potassium carbonate (168 mg, 1.22 mmol) in anhydrous DMF (4.5 mL) and the reaction time was 3 h.

White solid; yield 84% (119 mg, 0.339 mmol); TLC,  $R_f$  0.49 (ethyl acetate).  $^1\text{H}$  NMR (400 MHz, DMSO- $d_6$ )  $\delta$  ppm 10.30 (s, 1 H), 7.57 (d,  $J=8.8$  Hz, 1 H), 7.45 (d,  $J=2.8$  Hz, 1 H), 7.41 (dd,  $J=8.6, 2.9$  Hz, 1 H), 7.20 (s, 2 H), 6.71 (s, 1 H), 4.93 (s, 2 H), 3.85 (s, 3 H), 2.22 (s, 6 H).  $^{13}\text{C}$  NMR (101 MHz, DMSO- $d_6$ )  $\delta$  ppm 165.4, 161.0, 157.4, 153.0, 141.7, 138.5, 137.8, 128.3, 125.1, 124.1, 120.4, 116.9, 106.0, 55.6, 47.0, 22.7, 21.1. UPLC-MS (ESI) (A), RT 1.81 min,  $m/z$  352.5  $[\text{M}+\text{H}]^+$  (>95%).

**4-Chloro-6-methoxy-2-methylquinazoline (3.67).**

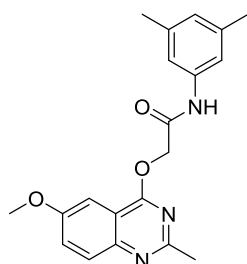


6-Methoxy-2-methylquinazolin-4-ol (233 mg, 1.23 mmol) was suspended in phosphorus oxychloride ( $\text{POCl}_3$ ) (10 mL, 108 mmol) and the reaction mixture was stirred under reflux for 2.5 days during which the suspension turned into a reddish brown solution. The mixture was allowed to cool down to room temperature and phosphorus oxychloride was evaporated under reduced pressure. Then, the residue was

partitioned between aqueous solution of sodium bicarbonate (5%, 100 mL) and ethyl acetate (100 mL). The organic layer was washed with aqueous solution of sodium bicarbonate (5%, 100 mL) and water (100 mL). Then, the organic layer was dried over sodium sulfate and evaporated under reduced pressure. The residue was purified by silica gel column chromatography.

White solid; yield 56% (142 mg, 0.681 mmol).  $^1\text{H}$  NMR (400 MHz,  $\text{DMSO-}d_6$ )  $\delta$  ppm 7.92 (d,  $J=9.1$  Hz, 1 H), 7.70 (dd,  $J=9.1, 2.8$  Hz, 1 H), 7.42 (d,  $J=2.8$  Hz, 1 H), 3.96 (s, 3 H), 2.71 (s, 3 H). UPLC-MS (ESI) (B), RT 3.88 min,  $m/z$  209  $[\text{M}+\text{H}]^+$  (>95%).

***N*-(3,5-dimethylphenyl)-2-((6-methoxy-2-methylquinazolin-4-yl)oxy)acetamide (3.68).**

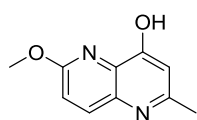


*N*-(3,5-dimethylphenyl)-2-hydroxyacetamide (60 mg, 0.34 mmol) and sodium hydride, 60% dispersion in mineral oil (27 mg, 0.67 mmol) were suspended in anhydrous tetrahydrofuran (THF) (4 mL) and left stirring at room temperature for 1 h before 4-chloro-6-methoxy-2-methylquinazoline (70 mg, 0.34 mmol) was added to the mixture. Then, the reaction mixture

was stirred at room temperature for 2.5 h. The product was purified by silica gel column chromatography and HPLC using an X-Bridge 19 column and as eluent  $\text{H}_2\text{O}/\text{ACN}$  from 60/40 to 0/100 (basic method).

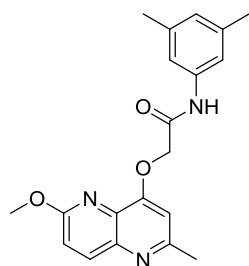
White solid; yield 14% (17 mg, 0.048 mmol); mp 180-181 °C; TLC,  $R_f$  0.40 (cyclohexane/ethyl acetate: 50/50), 0.39 (dichloromethane/methanol: 90/10).  $^1\text{H}$  NMR (400 MHz,  $\text{DMSO-}d_6$ )  $\delta$  ppm 10.10 (s, 1 H), 7.78 (d,  $J=9.1$  Hz, 1 H), 7.56 (dd,  $J=9.1, 2.8$  Hz, 1 H), 7.48 (d,  $J=2.8$  Hz, 1 H), 7.22 (s, 2 H), 6.71 (s, 1 H), 5.19 (s, 2 H), 3.92 (s, 3 H), 2.54 (s, 3 H), 2.22 (s, 6 H).  $^{13}\text{C}$  NMR (101 MHz,  $\text{DMSO-}d_6$ )  $\delta$  ppm 165.5, 164.6, 160.1, 157.2, 146.7, 138.4, 137.7, 128.4, 125.7, 125.0, 117.1, 114.3, 101.4, 64.5, 55.7, 25.7 (d,  $J=1.5$  Hz), 21.0. UPLC-MS (ESI) (B), RT 1.22 min,  $m/z$  352  $[\text{M}+\text{H}]^+$  (>95%); HRMS (ESI)  $m/z$  calcd for  $\text{C}_{20}\text{H}_{22}\text{N}_3\text{O}_3$   $[\text{M}+\text{H}]^+$ : 352.1656; found: 352.1649.

***6*-Methoxy-2-methyl-1,5-naphthyridin-4-ol (3.70).**



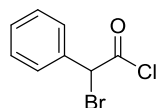
The title compound was prepared according to the general method B, using 5-amino-2-methoxypyridine (1.00 g, 8.06 mmol), ethylacetoacetate (1.02 mL, 8.06 mmol) and Dowtherm A (10 mL) and the reaction time was 3 h (130 °C) plus 1 h (250 °C).

Grey solid, yield 19% (290 mg, 1.53 mmol).  $^1\text{H}$  NMR (400 MHz,  $\text{DMSO}$ )  $\delta$  11.63 (s, 1H), 7.86 (d,  $J = 8.9$  Hz, 1H), 7.12 (d,  $J = 8.9$  Hz, 1H), 6.05 (s, 1H), 3.91 (s, 3H), 2.32 (s, 3H). UPLC-MS (A) (ESI) RT 0.29 min,  $m/z$  191.3  $[\text{M}+\text{H}]^+$  (>95%).

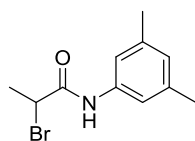
***N*-(3,5-dimethylphenyl)-2-((6-methoxy-2-methyl-1,5-naphthyridin-4-yl)oxy)acetamide (3.71).**

The title compound was prepared according to the general method A using 6-methoxy-2-methyl-1,5-naphthyridin-4-ol (265 mg, 1.39 mmol), 2-bromo-*N*-(3,5-dimethylphenyl)acetamide (337 mg, 1.39 mmol) and potassium carbonate (577 mg, 4.18 mmol) in anhydrous DMF (13 mL) and the reaction time was 18 h.

White solid; yield 72% (354 mg, 1.01 mmol); TLC,  $R_f$  0.43 (ethyl acetate).  $^1\text{H}$  NMR (400 MHz, DMSO- $d_6$ )  $\delta$  ppm 10.06 (br. s., 1 H), 8.13 (d,  $J=9.1$  Hz, 1 H), 7.24 (s, 2 H), 7.21 (d,  $J=9.1$  Hz, 1 H), 7.06 (s, 1 H), 6.73 (s, 1 H), 5.03 (s, 2 H), 4.01 (s, 3 H), 2.55 (s, 3 H), 2.23 (s, 6 H).  $^{13}\text{C}$  NMR (101 MHz, DMSO- $d_6$ )  $\delta$  ppm 165.6, 160.4, 158.6, 157.2, 141.5, 139.6, 138.2, 137.8, 132.2, 125.2, 117.1, 116.1, 106.7, 67.3, 53.4, 24.8, 21.1. UPLC-MS (ESI) (A), RT 1.54 min,  $m/z$  352.4  $[\text{M}+\text{H}]^+$  (>95%).

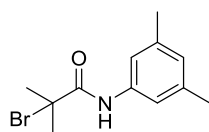
***2*-Bromo-2-phenylacetyl chloride (3.76).**

The title compound was prepared according to Dvorak *et al.*<sup>128</sup> Phenylacetylchloride (0.428 mL, 3.23 mmol), *N*-bromosuccinimide (576 mg, 3.23 mmol) and (*E*)-azobis(isobutyronitrile) (32 mg, 0.20 mmol) were taken up in carbon tetrachloride ( $\text{CCl}_4$ , 3.7 mL) and the resulting mixture was heated at 80 °C for 6 h. The reaction mixture was cooled to ambient temperature, followed by addition of *n*-heptane. The precipitate was removed by filtration and the filtrate was concentrated under reduced pressure to yield the target compound as a yellow oil. The yellow oil was used directly for the next step without further purification.

***2*-Bromo-*N*-(3,5-dimethylphenyl)propanamide (3.77).**

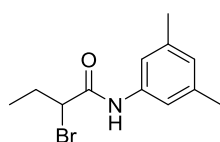
The title compound was prepared according to the general procedure D using 2-bromopropionylbromide (0.521 mL, 4.95 mmol), 3,5-xylidine (500 mg, 4.13 mmol) and triethylamine (0.690 mL, 4.95 mmol) in anhydrous DCM (5 mL) and the reaction time was 4 h.

White solid; yield 83% (882 mg, 3.44 mmol).  $^1\text{H}$  NMR (400 MHz, DMSO- $d_6$ )  $\delta$  10.15 (s, 1H), 7.22 (s, 2H), 6.73 (s, 1H), 4.68 (q,  $J = 6.7$  Hz, 1H), 2.24 (s, 6H), 1.73 (d,  $J = 6.7$  Hz, 3H). UPLC-MS (A) (ESI) RT 2.21 min,  $m/z$  256.0, 258.0 (1:1)  $[\text{M}+\text{H}]^+$  (>95%).

**2-Bromo-N-(3,5-dimethylphenyl)-2-methylpropanamide (3.78).**

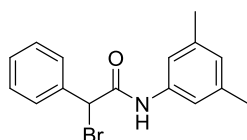
The title compound was prepared according to the general procedure D using 2-bromo-2-methylpropionylbromide (1.594 g, 6.933 mmol), 3,5-xylidine (0.720 mL, 5.78 mmol) and trimethylamine (0.966 mL, 6.93 mmol) in anhydrous DCM (5.8 mL) and the reaction time was 2 h.

Light yellow solid; yield 77% (1.200 g, 4.441 mmol).  $^1\text{H}$  NMR (400 MHz, DMSO)  $\delta$  9.61 (s, 1H), 7.28 (s, 2H), 6.74 (s, 1H), 2.24 (s, 6H), 1.98 (s, 6H). UPLC-MS (A) (ESI) RT 2.06 min,  $m/z$  270.1, 272.1 (1:1)  $[\text{M}+\text{H}]^+$  (>95%).

**2-Bromo-N-(3,5-dimethylphenyl)butanamide (3.79).**

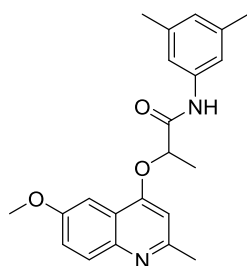
The title compound was prepared according to the general procedure D using 2-bromobutyrylbromide (0.6 mL, 5 mmol), 3,5-xylidine (500 mg, 4.13 mmol) and triethylamine (0.7 mL, 5 mmol) in anhydrous DCM (5 mL) and the reaction time was 3.5 h.

White solid; yield 100% (1.114 g, 4.123 mmol).  $^1\text{H}$  NMR (400 MHz, DMSO)  $\delta$  10.16 (s, 1H), 7.23 (s, 2H), 6.73 (s, 1H), 4.46 (t,  $J = 7.3$  Hz, 1H), 2.24 (s, 6H), 2.14 – 1.81 (m, 2H), 0.96 – 0.91 (m, 3H). UPLC-MS (A) (ESI) RT 2.43 min,  $m/z$  270.1, 272.1 (1:1)  $[\text{M}+\text{H}]^+$  (>95%).

**2-Bromo-N-(3,5-dimethylphenyl)-2-phenylacetamide (3.80).**

The title compound was prepared according to the general procedure D, using 2-bromo-2-phenylacetyl chloride **3.76**, 3,5-xylidine (0.48 mL, 3.9 mmol) and triethylamine (0.54 mL, 3.9 mmol) in anhydrous DCM (3.5 mL) and the reaction mixture was stirred overnight at room temperature. The reaction mixture was poured into water and the target compound was extracted with DCM. The organic phase was evaporated under reduce pressure and the crude product was directly used for next step without purification.

UPLC-MS (A) (ESI) RT 1.98 min,  $m/z$  318.1, 320.1 (1:1)  $[\text{M}+\text{H}]^+$ .

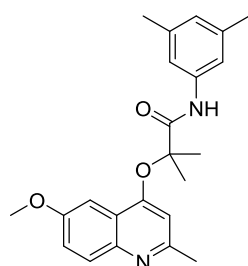
**N-(3,5-dimethylphenyl)-2-((6-methoxy-2-methylquinolin-4-yl)oxy)propanamide (3.81).**

The title compound was prepared according to the general procedure F, using 6-methoxy-2-methyl-4-quinolinol (150 mg, 0.793 mmol), sodium hydride, 60% in mineral oil (29 mg, 0.71 mmol), 2-bromo-N-(3,5-dimethylphenyl)propanamide (203 mg, 0.792 mmol) and potassium iodide

(132 mg, 0.795 mmol) in anhydrous DMF (9 mL) and the reaction mixture was stirred over weekend.

White solid; yield 49% (140 mg, 0.384 mmol); TLC,  $R_f$  0.42 (ethyl acetate).  $^1\text{H}$  NMR (400 MHz, DMSO- $d_6$ )  $\delta$  10.09 (s, 1H), 7.77 (d,  $J$  = 9.1 Hz, 1H), 7.49 (d,  $J$  = 2.9 Hz, 1H), 7.35 (dd,  $J$  = 9.1, 2.9 Hz, 1H), 7.24 (s, 2H), 6.74 (s, 1H), 6.73 (s, 1H), 5.16 (q,  $J$  = 6.5 Hz, 1H), 3.90 (s, 3H), 2.51 (s, 3H), 2.22 (s, 6H), 1.69 (d,  $J$  = 6.6 Hz, 3H).  $^{13}\text{C}$  NMR (101 MHz, DMSO- $d_6$ )  $\delta$  168.8, 158.9, 156.7, 156.2, 144.3, 138.2, 137.8, 129.5, 125.3, 121.5, 119.9, 117.5, 102.3, 100.3, 73.9, 55.4, 25.2, 21.0, 18.4. UPLC-MS (A) (ESI) RT 1.83 min,  $m/z$  365.3  $[\text{M}+\text{H}]^+$  (>95%).

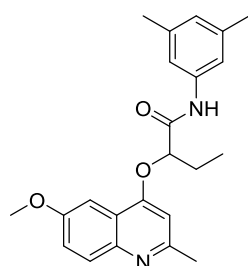
***N*-(3,5-dimethylphenyl)-2-((6-methoxy-2-methylquinolin-4-yl)oxy)-2-methylpropanamide (3.82).**



The title compound was prepared according to the general procedure F, using 6-methoxy-2-methyl-4-quinolinol (200 mg, 1.06 mmol), sodium hydride, 60% in mineral oil (63.5 mg, 1.59 mmol), 2-bromo-*N*-(3,5-dimethylphenyl)-2-methylpropanamide (286 mg, 1.06 mmol) and potassium iodide (175 mg, 1.06 mmol) in anhydrous DMF (11.5 mL) and the reaction mixture was left stirring overnight.

White solid; yield 25% (99 mg, 0.26 mmol); TLC,  $R_f$  0.49 (ethyl acetate).  $^1\text{H}$  NMR (400 MHz, DMSO- $d_6$ )  $\delta$  9.82 (s, 1H), 7.76 (d,  $J$  = 9.1 Hz, 1H), 7.51 (d,  $J$  = 2.7 Hz, 1H), 7.36 (dd,  $J$  = 9.1, 2.8 Hz, 1H), 7.21 (s, 2H), 6.72 (s, 1H), 6.54 (s, 1H), 3.91 (s, 3H), 2.47 (s, 3H), 2.21 (s, 6H), 1.74 (s, 6H).  $^{13}\text{C}$  NMR (101 MHz, DMSO- $d_6$ )  $\delta$  171.3, 156.8, 156.2, 156.2, 144.5, 138.1, 137.5, 129.5, 125.5, 121.3, 121.2, 118.5, 105.5, 100.9, 81.3, 55.3, 25.1, 24.5, 21.0. UPLC-MS (A) (ESI) RT 1.62 min,  $m/z$  379.2  $[\text{M}+\text{H}]^+$  (>95%).

***N*-(3,5-dimethylphenyl)-2-((6-methoxy-2-methylquinolin-4-yl)oxy)butanamide (3.83).**

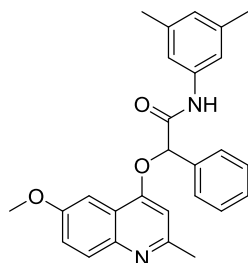


The title compound was prepared according to the general procedure F, using 6-methoxy-2-methyl-4-quinolinol (200 mg, 1.06 mmol), sodium hydride, 60% in mineral oil (30 mg, 0.76 mmol) and 2-bromo-*N*-(3,5-dimethylphenyl)butanamide (286 mg, 1.06 mmol) in anhydrous DMF (12 mL) and the reaction mixture was left stirring over weekend.

White solid; yield 15% (60 mg, 0.16 mmol); TLC,  $R_f$  0.43 (ethyl acetate).  $^1\text{H}$  NMR (400 MHz, DMSO- $d_6$ )  $\delta$  10.09 (s, 1H), 7.77 (d,  $J$  = 9.1 Hz, 1H), 7.51 (d,  $J$  = 2.9 Hz, 1H), 7.36 (dd,  $J$  = 9.1, 2.9 Hz, 1H), 7.23 (s, 2H), 6.73 (s, 1H), 6.72 (s, 1H), 4.96 (t,  $J$  = 6.3 Hz, 1H), 3.90 (s, 3H), 2.51 (s, 3H, overlaps with solvent's peak), 2.22 (s, 6H), 2.10 (tt,  $J$  = 8.6, 4.9 Hz, 2H), 1.10 (t,  $J$  = 7.4 Hz, 3H).  $^{13}\text{C}$  NMR (101 MHz, DMSO- $d_6$ )  $\delta$  168.2, 159.2, 156.7, 156.3, 144.3, 138.1, 137.8, 129.5, 125.4, 121.5, 120.0, 117.6,

102.3, 100.3, 78.8, 55.4, 25.9, 25.2, 21.0, 9.6. UPLC-MS (A) (ESI) RT 2.15 min,  $m/z$  379.3  $[M+H]^+$  (>95%).

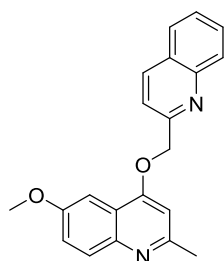
***N*-(3,5-dimethylphenyl)-2-((6-methoxy-2-methylquinolin-4-yl)oxy)-2-phenylacetamide (3.84).**



The title compound was prepared according to the general procedure F, using 2-bromo-*N*-(3,5-dimethylphenyl)-2-phenylacetamide **3.80**, 6-methoxy-2-methyl-4-quinolinol (200 mg, 2.11 mmol) and sodium hydride, 60% in mineral oil (76 mg, 1.9 mmol) in anhydrous DMF (7 mL) and the reaction mixture was left stirring overnight.

White solid; yield 14% (63 mg, 0.15 mmol); TLC,  $R_f$  0.44 (ethyl acetate).  $^1H$  NMR (400 MHz, DMSO- $d_6$ )  $\delta$  10.37 (s, 1H), 7.78 (t,  $J$  = 8.4 Hz, 3H), 7.60 (d,  $J$  = 2.9 Hz, 1H), 7.53 – 7.45 (m, 2H), 7.45 – 7.36 (m, 2H), 7.21 (s, 2H), 6.81 (s, 1H), 6.72 (s, 1H), 6.18 (s, 1H), 3.92 (s, 3H), 2.52 (s, 3H), 2.21 (s, 6H).  $^{13}C$  NMR (101 MHz, DMSO- $d_6$ )  $\delta$  166.6, 158.6, 156.7, 156.4, 144.3, 138.0, 137.9, 136.1, 129.6, 128.9, 128.8, 126.9, 125.6, 121.5, 120.0, 117.5, 102.7, 100.5, 78.8, 55.4, 25.2, 21.0. UPLC-MS (A) (ESI) RT 1.79 min,  $m/z$  427.2  $[M+H]^+$  (>95%).

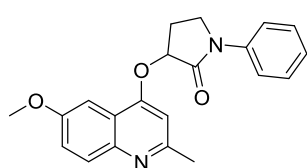
***6*-Methoxy-2-methyl-4-(quinolin-2-ylmethoxy)quinoline (3.85).**



The title compound was prepared according to the general procedure E, using 6-methoxy-2-methylquinolin-4-ol (200 mg, 1.06 mmol), 2-(chloromethyl)quinolone hydrochloride (226 mg, 1.06 mmol) and potassium carbonate (438 mg, 3.17 mmol) in anhydrous DMF (10 mL) and the reaction mixture was left stirring for 3 days.

Off-white solid; yield 81% (284 mg, 0.860 mmol); TLC,  $R_f$  0.61 (ethyl acetate/methanol: 95/5).  $^1H$  NMR (400 MHz, DMSO- $d_6$ )  $\delta$  8.46 (d,  $J$  = 8.5 Hz, 1H), 8.05 (d,  $J$  = 8.5 Hz, 1H), 8.02 (dd,  $J$  = 8.2, 1.0 Hz, 1H), 7.86 – 7.75 (m, 3H), 7.64 (ddd,  $J$  = 8.1, 6.9, 1.2 Hz, 1H), 7.50 (d,  $J$  = 2.9 Hz, 1H), 7.36 (dd,  $J$  = 9.1, 2.9 Hz, 1H), 7.03 (s, 1H), 5.65 (s, 2H), 3.89 (s, 3H), 2.53 (s, 3H).  $^{13}C$  NMR (101 MHz, DMSO- $d_6$ )  $\delta$  159.5, 157.0, 156.7, 156.4, 147.0, 144.2, 137.3, 130.0, 129.6, 128.6, 128.0, 127.3, 126.7, 121.4, 119.8, 119.4, 102.7, 99.8, 71.1, 55.4, 25.1. UPLC-MS (A) (ESI) RT 1.44 min,  $m/z$  331.4  $[M+H]^+$  (>95%).

***3*-((6-Methoxy-2-methylquinolin-4-yl)oxy)-1-phenylpyrrolidin-2-one (3.86).**

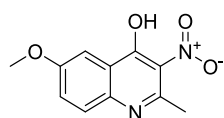


The title compound was prepared according to the general procedure F, using 6-methoxy-2-methylquinolin-4-ol (200 mg, 1.06 mmol), sodium hydride, 60% in mineral oil (76 mg, 1.9 mmol) and 3-bromo-

1-phenylpyrrolidin-2-one (257 mg, 1.06 mmol) in anhydrous DMF (10 mL) and the reaction time was 2 h.

Light brown solid; yield 20% (75 mg, 0.22 mmol); TLC,  $R_f$  0.6 (ethyl acetate/methanol: 90/10).  $^1\text{H}$  NMR (400 MHz,  $\text{DMSO-}d_6$ )  $\delta$  7.83 – 7.73 (m, 3H), 7.46 – 7.41 (m, 2H), 7.39 (d,  $J = 2.8$  Hz, 1H), 7.35 (dd,  $J = 9.1, 2.9$  Hz, 1H), 7.25 – 7.17 (m, 1H), 7.12 (s, 1H), 5.60 (t,  $J = 8.4$  Hz, 1H), 4.06 – 3.88 (m, 2H), 3.87 (s, 3H), 2.94 – 2.81 (m, 1H), 2.58 (s, 3H), 2.36 – 2.22 (m, 1H).  $^{13}\text{C}$  NMR (101 MHz,  $\text{DMSO-}d_6$ )  $\delta$  169.4, 159.0, 156.9, 156.3, 144.3, 139.1, 129.6, 128.8, 124.7, 121.6, 119.8, 119.5, 103.4, 99.7, 75.8, 55.4, 44.1, 25.4, 25.1. UPLC-MS (A) (ESI) RT 1.43 min,  $m/z$  349.4  $[\text{M}+\text{H}]^+$  (>95%).

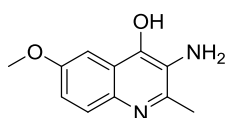
#### **6-Methoxy-2-methyl-3-nitroquinolin-4-ol (3.87).**



A suspension of 6-methoxy-2-methylquinolin-4-ol **3.4** (1.00 g, 5.29 mmol) in propionic acid (12 mL) was heated at 110 °C. Then, nitric acid (0.236 mL, 5.29 mmol) was added dropwise and the reaction mixture was heated at 110 °C for 2 h with vigorous stirring. The resulting suspension was cooled to room temperature, the solid was collected by filtration, washed with cold ethanol and dried.

Off-white solid; yield 76% (942 mg, 4.02 mmol); TLC,  $R_f$  0.4 (ethyl acetate/methanol: 90/10).  $^1\text{H}$  NMR (400 MHz,  $\text{DMSO-}d_6$ )  $\delta$  12.42 (s, 1H), 7.58 (d,  $J = 9.0$  Hz, 1H), 7.53 (d,  $J = 2.9$  Hz, 1H), 7.40 (dd,  $J = 9.0, 3.0$  Hz, 1H), 3.86 (s, 3H), 2.50 (s, 3H, overlaps with solvent's peak).  $^{13}\text{C}$  NMR (101 MHz,  $\text{DMSO-}d_6$ )  $\delta$  166.7, 156.6, 145.4, 135.0, 132.9, 126.6, 123.3, 120.4, 105.0, 55.6, 16.8. UPLC-MS (A) (ESI) RT 1.24 min,  $m/z$  234.9  $[\text{M}+\text{H}]^+$  (95%).

#### **3-Amino-6-methoxy-2-methylquinolin-4-ol (3.88).**

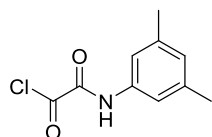


6-Methoxy-2-methyl-3-nitroquinolin-4-ol (1.612 g, 6.882 mmol) was dissolved in 2:1 mixture of THF and saturated aqueous ammonium chloride ( $\text{NH}_4\text{Cl}$ ) (60 mL). The mixture was treated with zinc (Zn) at vigorous stirring to keep the zinc dust in a suspension and to prevent it from caking on the bottom of flask. The reaction mixture was stirred at room temperature for 1 h. The reaction mixture was filtered through GF/F paper while rinsing with THF. The filtrate was evaporated under reduced pressure and the residue was purified by column chromatography reverse phase using methanol/water (50/50).

**Zinc (Zn) purification:** Zinc was purified by stirring 1 g of commercial zinc dust with 5 mL of 2% hydrochloric acid (HCl) for 1 min. The acid was removed by filtration and the zinc was washed with one 5 mL portion of 2% hydrochloric acid, three 5 mL portions of distilled water, two 5 mL portions of 95% ethanol, and finally with one 5 mL portion of absolute ether, the wash solutions being removed each time by filtration. Then, the material was quickly dried on air.

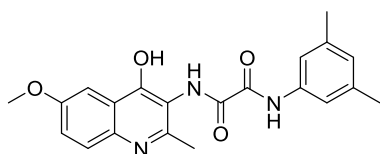
Yellow solid; yield 16% (227 mg, 1.11 mmol).  $^1\text{H}$  NMR (400 MHz,  $\text{DMSO-}d_6$ )  $\delta$  11.34 (s, 1H), 7.45 – 7.37 (m, 2H), 7.12 (dd,  $J$  = 9.1, 2.9 Hz, 1H), 4.16 (s, 2H), 3.79 (s, 3H), 2.33 (s, 3H).  $^{13}\text{C}$  NMR (101 MHz,  $\text{DMSO-}d_6$ )  $\delta$  167.7, 154.1, 132.0, 129.3, 127.7, 121.6, 120.6, 119.3, 103.0, 55.1, 15.7. UPLC-MS (A) (ESI) RT 0.39 min,  $m/z$  205.3  $[\text{M}+\text{H}]^+$  (>95%).

**2-((3,5-Dimethylphenyl)amino)-2-oxoacetyl chloride (3.90).**



The title compound was prepared according to Xu *et al.*<sup>141</sup> 3,5-Xylidine (5.14 mL, 41.3 mmol) was added dropwise to oxalyl chloride (34.9 mL, 413 mmol) at 0 °C and the resulting mixture was stirred for 1 h. The excess of oxalyl chloride was removed under vacuum. Diethyl ether was added to the residue and the solids were filtered off. The filtrate was evaporated under reduced pressure, and cyclohexane was added to the residue. After vigorous stirring for 30 min, the insoluble material was filtered, washed with *n*-pentane and dried under vacuum to give the target compound which was used directly for next step.

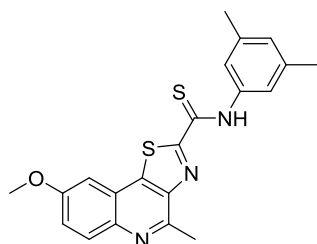
**N1-(3,5-dimethylphenyl)-N2-(4-hydroxy-6-methoxy-2-methylquinolin-3-yl)oxalamide (3.91).**



The title compound was prepared according to the procedure described by H. Kokatla *et al.*<sup>142</sup> 3-amino-6-methoxy-2-methylquinolin-4-ol **3.88** (200 mg, 0.979 mmol) was dissolved in a mixture of anhydrous DCM/DMF: 10/1 (22 mL) and stirred at room temperature for 5 min. 2-((3,5-dimethylphenyl)amino)-2-oxoacetyl chloride **3.90** (435 mg, 1.44 mmol) was added to the stirring solution at 0 °C and the reaction mixture was allowed to react for 1 h at 0 °C. Solvents were removed and the residue was purified by silica gel column chromatography.

Off-white solid; 54% (201 mg, 0.530 mmol); TLC,  $R_f$  0.33 (*n*-heptane/ethyl acetate: 50/50).  $^1\text{H}$  NMR (400 MHz,  $\text{DMSO-}d_6$ )  $\delta$  10.52 (s, 1H), 9.69 (s, 1H), 7.53 (d,  $J$  = 9.0 Hz, 1H), 7.50 – 7.46 (m, 3H), 7.31 (dd,  $J$  = 9.0, 3.0 Hz, 1H), 6.81 (s, 1H), 3.84 (s, 3H), 2.32 (s, 3H), 2.27 (s, 6H). UPLC-MS (A) (ESI) RT 1.61 min,  $m/z$  380.4  $[\text{M}+\text{H}]^+$  (>95%).

**N-(3,5-dimethylphenyl)-8-methoxy-4-methylthiazolo[4,5-c]quinoline-2-carbothioamide (3.92).**



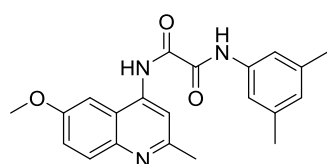
The title compound was prepared using the procedure described by H. Kokatla *et al.*<sup>142</sup> according to which *N*1-(3,5-dimethylphenyl)-*N*2-(4-hydroxy-6-methoxy-2-methylquinolin-3-yl)oxalamide **3.91** (100 mg, 0.264 mmol) was suspended in anhydrous pyridine (10 mL) and phosphorus pentasulfide (586 mg, 1.31 mmol) was added and the



reaction mixture was left stirring under reflux overnight. Pyridine was evaporated and the obtained residue was dissolved in water. The pH was adjusted ~8 using saturated aqueous solution of potassium carbonate and the target compound was extracted with ethyl acetate. It was purified by silica gel and reverse phase column chromatography.

Off-white solid; 19% (20 mg, 0.051 mmol).  $^1\text{H}$  NMR (400 MHz,  $\text{CDCl}_3$ )  $\delta$  10.82 (s, 1H), 8.06 (d,  $J$  = 9.1 Hz, 1H), 7.67 (s, 2H), 7.37 (dd,  $J$  = 9.2, 2.8 Hz, 1H), 7.25 (d,  $J$  = 2.7 Hz, 1H), 6.97 (s, 1H), 3.97 (s, 3H), 3.08 (s, 3H), 2.40 (s, 6H). UPLC-MS (A) (ESI) RT 2.54 min,  $m/z$  394.4  $[\text{M}+\text{H}]^+$  (>95%).

***N1-(3,5-dimethylphenyl)-N2-(6-methoxy-2-methylquinolin-4-yl)oxalamide (3.95).***

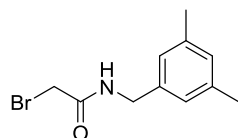


6-Methoxy-2methyl-4-quinolinamine (200 mg, 1.06 mmol) was allowed to react with sodium hydride (NaH), 60% mineral oil (85 mg, 1.3 mmol) in anhydrous DMF (10 mL) for 20 min at room temperature. Subsequently, 2-((3,5-dimethylphenyl)amino)-2-

oxoacetyl chloride **3.90** (321 mg, 1.06 mmol) was added to the mixture and left stirring overnight at room temperature. The reaction mixture was poured into water (80 mL) and the formed precipitate was filtered and washed with water (10 mL x 3). It was further purified by silica gel column chromatography.

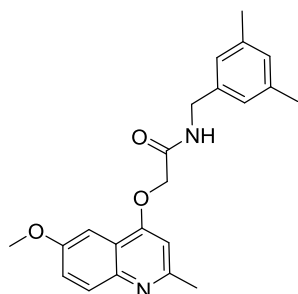
White solid; yield 12% (45 mg, 0.12 mmol); TLC,  $R_f$  0.58 (ethyl acetate).  $^1\text{H}$  NMR (400 MHz,  $\text{DMSO-}d_6$ )  $\delta$  10.94 (br. s, 1H), 10.72 (s, 1H), 7.87 (d,  $J$  = 9.1 Hz, 1H), 7.73 (s, 1H), 7.51 (s, 2H), 7.40 (dd,  $J$  = 9.1, 2.7 Hz, 1H), 7.35 (d,  $J$  = 2.7 Hz, 1H), 6.83 (s, 1H), 3.91 (s, 3H), 2.63 (s, 3H), 2.28 (s, 6H).  $^{13}\text{C}$  NMR (101 MHz,  $\text{DMSO-}d_6$ )  $\delta$  159.8, 158.2, 156.6, 155.9, 144.3, 139.4, 137.8, 137.4, 130.2, 126.3, 121.7, 121.3, 118.2, 115.4, 101.1, 55.5, 24.7, 21.1. UPLC-MS (A) (ESI) RT 1.66 min,  $m/z$  364.4  $[\text{M}+\text{H}]^+$  (>95%).

***2-Bromo-N-(3,5-dimethylbenzyl)acetamide (3.96).***



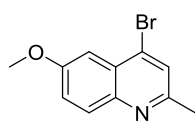
The title compound was prepared according to the general procedure D, using 2-bromoacetyl bromide (0.194 mL, 2.22 mmol), 3,5-dimethylbenzylamine (250 mg, 1.85 mmol) and triethylamine (0.309 mL, 2.22 mmol) in anhydrous DCM (1.85 mL) and the reaction time was 2 h. It was used directly for the next step without purification.

UPLC-MS (A) (ESI) RT 1.77 min,  $m/z$  256.4, 258.4 (1:1)  $[\text{M}+\text{H}]^+$ .

***N*-(3,5-dimethylbenzyl)-2-((6-methoxy-2-methylquinolin-4-yl)oxy)acetamide (3.97).**

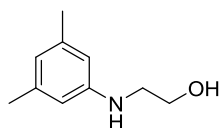
The title compound was prepared according to the general procedure E, using 2-bromo-*N*-(3,5-dimethylbenzyl)acetamide **3.96** (129 mg, 0.50 mmol), 6-methoxy-2-methyl-4-quinolinol (95 mg, 0.50 mmol) and potassium carbonate (208 mg, 1.51 mmol) in anhydrous DMF (6.5 mL) and the reaction time was 26 h.

Off-white solid; yield 64% (117 mg, 0.321 mmol); TLC,  $R_f$  0.33 (ethyl acetate), 0.83 (ethyl acetate/methanol: 90/10).  $^1\text{H}$  NMR (400 MHz,  $\text{DMSO-}d_6$ )  $\delta$  8.72 (t,  $J = 6.0$  Hz, 1H), 7.79 (d,  $J = 9.1$  Hz, 1H), 7.54 (d,  $J = 2.8$  Hz, 1H), 7.35 (dd,  $J = 9.1, 2.9$  Hz, 1H), 6.85 (s, 3H), 6.80 (s, 1H), 4.86 (s, 2H), 4.32 (d,  $J = 6.0$  Hz, 2H), 3.89 (s, 3H), 2.54 (s, 3H), 2.22 (s, 6H).  $^{13}\text{C}$  NMR (101 MHz,  $\text{DMSO-}d_6$ )  $\delta$  166.9, 159.3, 156.8, 156.2, 144.2, 139.1, 137.2, 129.5, 128.2, 124.9, 121.4, 119.7, 102.3, 100.5, 67.2, 55.4, 41.8, 25.1, 20.9. UPLC-MS (A) (ESI) RT 1.60 min,  $m/z$  365.5  $[\text{M}+\text{H}]^+$  (>95%).

***4*-Bromo-6-methoxy-2-methylquinoline (3.98).**

The title compound was prepared according to Margolis *et al.*<sup>143</sup> Phosphorous tribromide ( $\text{PBr}_3$ , 1.994 mL, 21.14 mmol) was added slowly to a suspension of 6-methoxy-4-hydroxy-2-methyl-quinoline (1.00 g, 5.29 mmol) in DMF (20 mL) at ambient temperature. The reaction mixture was stirred under nitrogen at 50 °C for 4 days. The mixture was quenched with water and stirred for 30 min. The reaction mixture was made basic by addition of potassium bicarbonate ( $\text{KHCO}_3$ ) and the formed precipitate was filtered and dried.

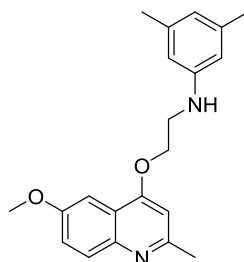
Yellow solid; yield 86% (1.141 g, 4.526 mmol).  $^1\text{H}$  NMR (400 MHz,  $\text{DMSO-}d_6$ )  $\delta$  7.89 (d,  $J = 9.1$  Hz, 1H), 7.82 (s, 1H), 7.45 (dd,  $J = 9.1, 2.8$  Hz, 1H), 7.34 (d,  $J = 2.8$  Hz, 1H), 3.93 (s, 3H), 2.60 (s, 3H).  $^{13}\text{C}$  NMR (101 MHz,  $\text{DMSO-}d_6$ )  $\delta$  157.9, 156.3, 143.8, 131.4, 130.6, 126.3, 126.0, 122.7, 104.1, 55.6, 24.0. UPLC-MS (A) (ESI) RT 1.43 min,  $m/z$  251.8, 253.8 (1:1)  $[\text{M}+\text{H}]^+$  (>95%).

***2*-((3,5-Dimethylphenyl)amino)ethanol (3.100).**

The title compound was prepared according to Zhao *et al.*<sup>129</sup> 2-Bromo ethanol (681 mg, 5.45 mmol) was added to 3,5-xylidine (1.00 g, 8.25 mmol) and the reaction mixture was heated at 90 °C for 4 h. The resulting solid was dissolved in ethyl acetate, washed with aqueous sodium hydroxide (2M), followed by brine and dried over magnesium sulfate. The solvent was removed under reduced pressure and the residue was purified through a silica gel flash column, using *n*-heptane/ethyl acetate gradient from 20-40% to yield the desired compound.

Brown liquid; yield 43% (587 mg, 3.55 mmol).  $^1\text{H}$  NMR (400 MHz,  $\text{DMSO-}d_6$ )  $\delta$  6.18 (s, 2H), 6.17 (s, 1H), 5.23 (t,  $J = 5.7$  Hz, 1H), 4.63 (t,  $J = 5.5$  Hz, 1H), 3.52 (q,  $J = 6.1$  Hz, 2H), 3.04 (q,  $J = 6.1$  Hz, 2H), 2.12 (s, 6H).  $^{13}\text{C}$  NMR (101 MHz,  $\text{DMSO-}d_6$ )  $\delta$  148.9, 137.6, 117.6, 110.0, 59.6, 45.6, 21.3. UPLC-MS (A) (ESI) RT 0.97 min,  $m/z$  166.0  $[\text{M}+\text{H}]^+$  (>95%).

***N*-2-((6-methoxy-2-methylquinolin-4-yl)oxy)ethyl)-3,5-dimethylaniline (3.101).**

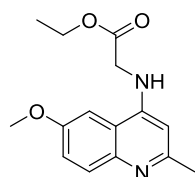


4-Bromo-6-methoxy-2-methylquinoline **3.98** (200 mg, 0.793 mmol) and 2-((3,5-dimethylphenyl)amino)ethanol **3.100** (131 mg, 0.793 mmol), tetramethylethylenediamine (TMEDA, 9 mg, 0.08 mmol), copper(I)iodide ( $\text{CuI}$ , 15 mg, 0.08 mmol) and cesium carbonate ( $\text{Cs}_2\text{CO}_3$ , 517 mg, 1.59 mmol) in anhydrous DMF (4 mL), were placed in a high pressure tube

under nitrogen atmosphere. The reaction mixture was stirred at 95 °C for 2 days, cooled down and filtered. The filtrate was evaporated and the residue was dissolved in DCM (50 mL) and washed with brine (30 mL x 3). The organic layer was dried over magnesium sulfate and evaporated under reduced pressure. The residue was purified by silica gel column chromatography.

Light yellow solid; yield 17% (45 mg, 0.13 mmol); TLC,  $R_f$  0.58 (ethyl acetate).  $^1\text{H}$  NMR (400 MHz,  $\text{DMSO-}d_6$ )  $\delta$  7.74 (d,  $J = 9.1$  Hz, 1H), 7.40 (d,  $J = 2.9$  Hz, 1H), 7.31 (dd,  $J = 9.1, 2.9$  Hz, 1H), 6.89 (s, 1H), 6.30 (s, 2H), 6.19 (s, 1H), 5.72 (t,  $J = 6.2$  Hz, 1H), 4.31 (t,  $J = 5.4$  Hz, 2H), 3.83 (s, 3H), 3.57 (q,  $J = 5.6$  Hz, 2H), 2.54 (s, 3H), 2.13 (s, 6H).  $^{13}\text{C}$  NMR (101 MHz,  $\text{DMSO-}d_6$ )  $\delta$  159.9, 157.1, 156.5, 148.5, 144.0, 137.7, 129.4, 121.2, 119.9, 117.9, 110.1, 102.0, 100.3, 67.3, 55.4, 41.8, 25.0, 21.3. UPLC-MS (A) (ESI) RT 1.63 min,  $m/z$  337.4  $[\text{M}+\text{H}]^+$  (>95%).

***Ethyl 2-((6-methoxy-2-methylquinolin-4-yl)amino)acetate (3.102).***



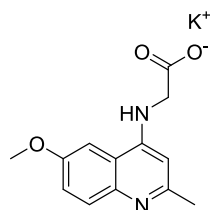
4-Bromo-6-methoxy-2-methyl quinoline **3.98** (250 mg, 0.992 mmol), glycine ethyl ester hydrochloride (277 mg, 1.98 mmol) and phenol (900 mg, 9.56 mmol) were placed in a round bottom flask and heated at 120 °C under magnetic stirring overnight. The reaction mixture was cooled at room temperature and

diluted with ethyl acetate. The formed precipitate was filtered off and washed with ethyl acetate. The target compound was purified by column chromatography using as eluent ethyl acetate/*n*-heptane gradient from 50-100%.

Off-white solid; yield 55% (150 mg, 0.547 mmol).  $^1\text{H}$  NMR (400 MHz,  $\text{DMSO-}d_6$ )  $\delta$  7.63 (d,  $J = 9.1$  Hz, 1H), 7.50 (d,  $J = 2.7$  Hz, 1H), 7.33 (t,  $J = 6.3$  Hz, 1H), 7.23 (dd,  $J = 9.1, 2.7$  Hz, 1H), 6.17 (s, 1H), 4.22 – 4.10 (m, 4H), 3.87 (s, 3H), 2.40 (s, 3H), 1.22 (t,  $J = 7.1$  Hz, 3H).  $^{13}\text{C}$  NMR (101 MHz,  $\text{DMSO-}$

*d*<sub>6</sub>)  $\delta$  170.5, 155.9, 155.5, 149.1, 143.5, 129.8, 120.3, 117.8, 100.7, 98.7, 60.5, 55.5, 44.1, 24.9, 14.2. UPLC-MS (A) (ESI) RT 1.27 min,  $m/z$  275.4 [M+H]<sup>+</sup> (>95%).

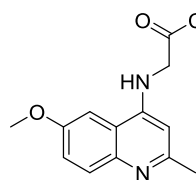
**Potassium 2-((6-methoxy-2-methylquinolin-4-yl)amino)acetate (3.103).**



In a round bottom flask, ethyl 2-((6-methoxy-2-methylquinolin-4-yl)amino)acetate **3.102** (150 mg, 0.547 mmol) was dissolved in methanol (10 mL). Potassium hydroxide (92 mg, 1.6 mmol) was added to the reaction mixture and left stirring under reflux for 1.5 h. Then, methanol was evaporated under reduced pressure. It was directly used for the next step.

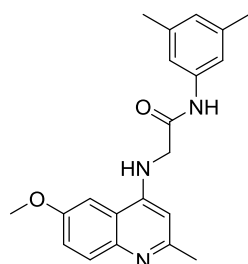
Off-white solid. <sup>1</sup>H NMR (400 MHz, MeOD)  $\delta$  7.68 (d,  $J$  = 9.2 Hz, 1H), 7.37 (d,  $J$  = 2.7 Hz, 1H), 7.24 (dd,  $J$  = 10.3, 3.8 Hz, 1H), 6.28 (s, 1H), 3.94 (s, 3H), 3.84 (s, 2H), 2.50 (s, 3H). UPLC-MS (A) (ESI) RT 0.89,  $m/z$  247.3 [M+H]<sup>+</sup> (>95%).

**2-((6-methoxy-2-methylquinolin-4-yl)amino)acetyl chloride (3.104).**



The title compound was prepared according to general procedure G using potassium 2-((6-methoxy-2-methylquinolin-4-yl)amino)acetate **3.103** (156 mg, 0.549 mmol) and thionyl chloride (0.399 mL, 5.47 mmol) in anhydrous DCM (8 mL) and the reaction time was 48 h. It was directly used for the next step.

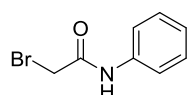
***N*-((3,5-dimethylphenyl)-2-((6-methoxy-2-methylquinolin-4-yl)amino)acetamide (3.105).**



The title compound was prepared according to the general procedure H, using 2-((6-methoxy-2-methylquinolin-4-yl)amino)acetyl chloride (145 mg, 0.548 mmol) and 3,5-xylidine (199 mg, 1.64 mmol) in anhydrous DCM (10 mL) and the reaction time was 16 h.

Off-white solid; yield 65% (125 mg, 0.358 mmol); TLC,  $R_f$  0.22 (ethyl acetate/methanol/triethylamine: 90/10/0.1). <sup>1</sup>H NMR (400 MHz, DMSO-*d*<sub>6</sub>)  $\delta$  9.96 (s, 1H), 7.64 (d,  $J$  = 9.1 Hz, 1H), 7.54 (d,  $J$  = 2.7 Hz, 1H), 7.33 (t,  $J$  = 6.0 Hz, 1H), 7.28 – 7.20 (m, 3H), 6.70 (s, 1H), 6.23 (s, 1H), 4.10 (d,  $J$  = 6.1 Hz, 2H), 3.89 (s, 3H), 2.40 (s, 3H), 2.22 (s, 6H). <sup>13</sup>C NMR (101 MHz, DMSO-*d*<sub>6</sub>)  $\delta$  168.1, 155.9, 155.5, 149.5, 143.5, 138.7, 137.7, 129.7, 124.9, 120.3, 117.9, 117.1, 100.9, 98.7, 55.6, 46.3, 25.0, 21.1. UPLC-MS (A) (ESI) RT 1.53 min,  $m/z$  350.4 [M+H]<sup>+</sup> (>95%).

**2-Bromo-*N*-phenylacetamide (3.107).**

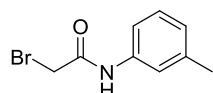


The title compound was prepared according to the general procedure D, using bromoacetic acid bromide (0.563 mL, 6.44 mmol), aniline (500 mg, 5.37 mmol)

and trimethylamine (0.898 mL, 6.44 mmol) in anhydrous DCM (6 mL) and the reaction time was 3.5 h.

Brown solid; yield 100% (1.155 g, 5.396 mmol).  $^1\text{H}$  NMR (400 MHz,  $\text{CDCl}_3$ )  $\delta$  8.16 (s, 1H), 7.57 – 7.49 (m, 2H), 7.41 – 7.31 (m, 2H), 7.23 – 7.12 (m, 1H), 4.05 (s, 2H). UPLC-MS (A) (ESI) RT 1.47 min,  $m/z$  214.0, 216.0 (1:1)  $[\text{M}+\text{H}]^+$  (>95%).

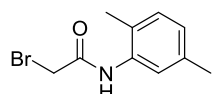
**2-Bromo-N-(*m*-tolyl)acetamide (3.108).**



The title compound was prepared according to the general procedure D, using bromo acetic acid bromide (0.489 mL, 5.60 mmol), *meta*-toluidine (500 mg, 4.67 mmol) and trimethylamine (0.780 mL, 5.60 mmol) in anhydrous DCM (5 mL) and the reaction time was 2 h.

Dark brown solid; yield 100% (1.063 g, 4.660 mmol).  $^1\text{H}$  NMR (400 MHz, DMSO)  $\delta$  10.31 (s, 1H), 7.43 (s, 1H), 7.37 (d,  $J$  = 8.6 Hz, 1H), 7.20 (t,  $J$  = 7.8 Hz, 1H), 6.90 (d,  $J$  = 7.5 Hz, 1H), 4.03 (s, 2H), 2.28 (s, 3H). UPLC-MS (A) (ESI) RT 1.67 min,  $m/z$  228.3, 230.3 (1:1)  $[\text{M}+\text{H}]^+$  (>95%).

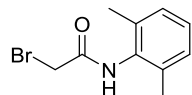
**2-Bromo-N-(2,5-dimethylphenyl)acetamide (3.109).**



The title compound was prepared according to the general procedure D, using bromo acetic acid bromide (0.865 mL, 9.90 mmol), 2,5-xylidine (1.00 g, 8.25 mmol) and triethylamine (1.38 mL, 9.90 mmol) in anhydrous DCM (8 mL) and the reaction time was 2 h.

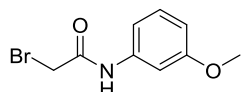
Off-white solid; yield 96% (1.919 g, 7.926 mmol).  $^1\text{H}$  NMR (400 MHz,  $\text{CDCl}_3$ )  $\delta$  8.09 (s, 1H), 7.66 (s, 1H), 7.09 (d,  $J$  = 7.7 Hz, 1H), 6.93 (d,  $J$  = 7.5 Hz, 1H), 4.07 (s, 2H), 2.33 (s, 3H), 2.26 (s, 3H). UPLC-MS (A) (ESI) RT 1.75 min,  $m/z$  242.0, 244.0 (1:1)  $[\text{M}+\text{H}]^+$  (>95%).

**2-Bromo-N-(2,6-dimethylphenyl)acetamide (3.110).**



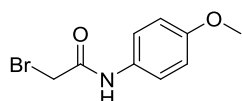
The title compound was prepared according to the general procedure D, using bromo acetic acid bromide (0.433 mL, 4.95 mmol), 2,6-xylidine (0.508 mL, 4.13 mmol) and triethylamine (0.690 mL, 4.95 mmol) in anhydrous DCM (4 mL) and the reaction mixture was stirred over the weekend.

Light brown solid; yield 45% (453 mg, 1.87 mmol).  $^1\text{H}$  NMR (400 MHz, DMSO)  $\delta$  9.71 (s, 1H), 7.12 – 7.02 (m, 3H), 4.05 (s, 2H), 2.15 (s, 6H). UPLC-MS (A) (ESI) RT 1.57 min,  $m/z$  242.4:244.4 (1:1)  $[\text{M}+\text{H}]^+$  (>95%).

**2-Bromo-N-(3-methoxyphenyl)acetamide (3.111).**

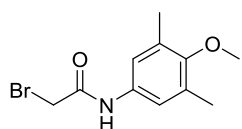
The title compound was prepared according to the general procedure D, using bromo acetic acid bromide (0.426 mL, 4.87 mmol), *m*-methoxyaniline (0.456 mL, 4.06 mmol) and triethylamine (0.679 mL, 4.87 mmol) in anhydrous DCM (4 mL) and the reaction mixture was stirred over weekend.

Dark brown solid; yield 88% (775 mg, 3.18 mmol).  $^1\text{H}$  NMR (400 MHz,  $\text{DMSO-}d_6$ ) (a mixture of amide bond rotamers)  $\delta$  ppm 9.50 - 10.88 (m, 1 H), 7.07 - 7.63 (m, 3 H), 6.48 - 6.76 (m, 1 H), 3.95 - 4.72 (m, 2 H), 3.68 - 3.83 (m, 3 H).  $^{13}\text{C}$  NMR (101 MHz,  $\text{DMSO-}d_6$ ) (major rotamer)  $\delta$  ppm 170.9, 159.4, 139.7, 129.4, 111.8, 108.8, 105.4, 61.9, 55.0. UPLC-MS (A) (ESI) RT 1.58 min,  $m/z$  244.3:246.3 (1:1)  $[\text{M}+\text{H}]^+$  (90%).

**2-Bromo-N-(4-methoxyphenyl)acetamide (3.112).**

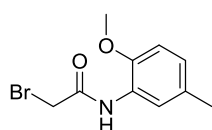
The title compound was prepared according to the general procedure D, using bromo acetic acid bromide (13.77 g, 68.22 mmol), *para*-anisidine (7.00 g, 56.8 mmol) and triethylamine (9.51 mL, 68.2 mmol) in anhydrous DCM (57.8 mL) and the reaction time was 2 h.

White solid; yield 38% (5.206 g, 21.33 mmol).  $^1\text{H}$  NMR (400 MHz,  $\text{CDCl}_3$ )  $\delta$  8.07 (br. s, 1H), 7.46 - 7.38 (m, 2H), 6.92 - 6.84 (m, 2H), 4.01 (s, 2H), 3.80 (s, 3H). UPLC-MS (A) (ESI) RT 1.43 min,  $m/z$  = 244.3:246.3 (1:1)  $[\text{M}+\text{H}]^+$  (>95%).

**2-Bromo-N-(4-methoxy-3,5-dimethylphenyl)acetamide (3.113).**

The title compound was prepared according the general procedure D, using bromo acetic acid bromide (0.173 mL, 1.98 mmol), 4-amino-2,6-dimethylanisole (250 mg, 1.65 mmol) and triethylamine (0.277 mL, 1.98 mmol) in anhydrous DCM (1.7 mL) and the reaction time was for 2 h.

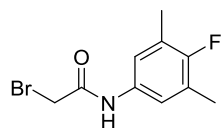
Light brown solid; yield 100% (450 mg, 1.65 mmol).  $^1\text{H}$  NMR (400 MHz,  $\text{CDCl}_3$ )  $\delta$  8.01 (s, 1H), 7.16 (s, 2H), 4.00 (s, 2H), 3.69 (s, 3H), 2.27 (s, 6H). UPLC-MS (A) (ESI) RT 1.76 min,  $m/z$  272.10, 274.1 (1:1)  $[\text{M}+\text{H}]^+$  (>95%).

**2-Bromo-N-(2-methoxy-5-methylphenyl)acetamide (3.114).**

The title compound was prepared according to the general procedure D, using bromo acetic acid bromide (0.382 mL, 4.37 mmol), 5-methyl-*o*-anisidine (500 mg, 3.64 mmol) and triethylamine (0.610 mL, 4.37 mmol) in anhydrous DCM (4 mL) and the reaction time was 2 h.

Brown solid; yield 100% (940 mg, 3.64 mmol).  $^1\text{H}$  NMR (400 MHz, DMSO)  $\delta$  9.52 (s, 1H), 7.80 (s, 1H), 6.99 – 6.84 (m, 2H), 4.18 (s, 2H), 3.80 (s, 3H), 2.22 (s, 3H). UPLC-MS (A) (ESI) RT 1.85 min,  $m/z$  258.4, 260.4 (1:1)  $[\text{M}+\text{H}]^+$  (>95%).

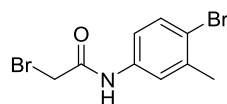
**2-Bromo-N-(4-fluoro-3,5-dimethylphenyl)acetamide (3.115).**



The title compound was prepared according to the general procedure D, using bromo acetic acid bromide (0.19 mL, 2.2 mmol), 4-fluoro-3,5-dimethylaniline (250 mg, 1.80 mmol) and triethylamine (0.30 mL, 2.2 mmol) in anhydrous DCM (1.8 mL) and the reaction mixture was stirred over weekend.

Off-white solid; yield 100% (466 mg, 1.80 mmol).  $^1\text{H}$  NMR (400 MHz,  $\text{CDCl}_3$ )  $\delta$  8.00 (s, 1H), 7.17 (d,  $J$  = 6.3 Hz, 2H), 4.01 (s, 2H), 2.25 (s, 6H). UPLC-MS (A) (ESI) RT 1.88 min,  $m/z$  260.0, 262.0 (1:1)  $[\text{M}+\text{H}]^+$  (>95%).

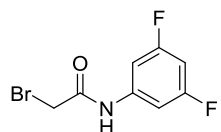
**2-Bromo-N-(4-bromo-3-methylphenyl)acetamide (3.116).**



The title compound was prepared according to the general procedure D, using bromo acetic acid bromide (0.282 mL, 3.22 mmol), 4-bromo-3-methylaniline (500 mg, 2.69 mmol) and triethylamine (0.45 mL, 3.2 mmol) in anhydrous DCM (4 mL) and the reaction mixture was stirred over weekend.

Dark brown solid; yield 100% (825 mg, 2.69 mmol).  $^1\text{H}$  NMR (400 MHz, DMSO) (major *cis/trans* amide rotamer)  $\delta$  10.50 (s, 1H), 7.72 – 7.30 (m, 3H), 4.05 (s, 2H), 2.30 (s, 3H). UPLC-MS (A) (ESI) RT 1.92 min,  $m/z$  306.3, 308.3, 310.3 (1:2:1)  $[\text{M}+\text{H}]^+$  (>95%).

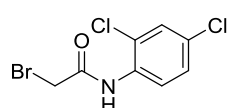
**2-Bromo-N-(3,5-difluorophenyl)acetamide (3.117).**



The title compound was prepared according to the general procedure D, using 2-bromoacetyl bromide (0.41 mL, 4.7 mmol), 3,5-difluoroaniline (500 mg, 3.87 mmol) and triethylamine (0.65 mL, 4.7 mmol) in anhydrous DCM (3.9 mL) and the reaction time was 4 h.

Brown solid; yield 91% (882 mg, 3.53 mmol).  $^1\text{H}$  NMR (400 MHz, DMSO)  $\delta$  10.76 (s, 1H), 7.36 – 7.24 (m, 2H), 6.96 (tt,  $J$  = 9.4, 2.4 Hz, 1H), 4.05 (s, 2H). UPLC-MS (A) (ESI) RT 1.81 min,  $m/z$  250.0, 252.0 (1:1)  $[\text{M}+\text{H}]^+$  (>95%).

**2-Bromo-N-(2,4-dichlorophenyl)acetamide (3.118).**

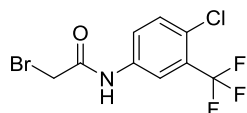


The title compound was prepared according to the general procedure D, using bromo acetic acid bromide (0.32 mL, 3.7 mmol), 2,4-dichloroaniline

(500 mg, 3.09 mmol) and triethylamine (0.52 mL, 3.7 mmol) in anhydrous DCM (3.1 mL) and the reaction time was 2 h.

Brown solid; yield 97% (846 mg, 2.99 mmol).  $^1\text{H}$  NMR (400 MHz, DMSO)  $\delta$  10.02 (s, 1H), 7.75 (d,  $J$  = 8.7 Hz, 1H), 7.69 (d,  $J$  = 2.4 Hz, 1H), 7.44 (dd,  $J$  = 8.7, 2.4 Hz, 1H), 4.17 (s, 2H). UPLC-MS (A) (ESI) RT 1.90 min,  $m/z$  282.1, 284.0, 285.9 (1:2:1)  $[\text{M}+\text{H}]^+$  (>95%).

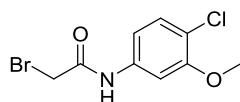
**2-Bromo-N-(4-chloro-3-(trifluoromethyl)phenyl)acetamide (3.119).**



The title compound was prepared according to the general procedure D, using bromoacetic acid bromide (0.54 mL, 6.1 mmol), 5-amino-2-chlorobenzotrifluoride (1.00 g, 5.11 mmol) and TEA (0.86 mL, 6.1 mmol) in anhydrous DCM (5 mL) and the reaction time was 3 h.

Dark brown solid; yield 99% (1.60 g, 5.05 mmol).  $^1\text{H}$  NMR (400 MHz, DMSO)  $\delta$  10.83 (s, 1H), 8.15 (d,  $J$  = 2.5 Hz, 1H), 7.83 (dd,  $J$  = 8.7, 2.4 Hz, 1H), 7.69 (d,  $J$  = 8.8 Hz, 1H), 4.07 (s, 2H).  $^{13}\text{C}$  NMR (101 MHz, DMSO)  $\delta$  171.8, 138.1, 132.0, 126.7 (q,  $^2J_{\text{C-F}}$  = 30.8 Hz), 124.5, 124.1 (q,  $^4J_{\text{C-F}}$  = 1.8 Hz), 122.8 (q,  $^1J_{\text{C-F}}$  = 273.1 Hz), 118.4 (q,  $^3J_{\text{C-F}}$  = 5.7 Hz), 61.9. UPLC-MS (A) (ESI) RT 1.92 min,  $m/z$  316.2, 318.1(1:1)  $[\text{M}+\text{H}]^+$  (>95%).

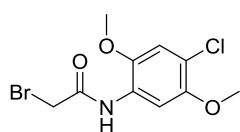
**2-Bromo-N-(4-chloro-3-methoxyphenyl)acetamide (3.120).**



The title compound was prepared according to the general procedure D, using bromoacetic acid bromide (0.665 mL, 7.61 mmol), 4-chloro-3-methoxyaniline (1.00 g, 6.35 mmol) and TEA (1.06 mL, 7.61 mmol) in anhydrous DCM (7 mL) and the reaction time was 3 h.

Grey solid; yield 100% (1.77 g, 3.34 mmol).  $^1\text{H}$  NMR (400 MHz, DMSO) (mixture of cis/trans amide rotamers, 2/1)  $\delta$  10.57 (s, 0.6H), 9.78 (s, 0.3H), 7.61 (d,  $J$  = 2.3 Hz, 0.3H), 7.48 (d,  $J$  = 2.3 Hz, 0.6H), 7.39 (dd,  $J$  = 8.7, 2.3 Hz, 0.4H), 7.35 (d,  $J$  = 8.6 Hz, 0.7H), 7.31 (d,  $J$  = 8.6 Hz, 0.4H), 7.18 (dd,  $J$  = 8.6, 2.3 Hz, 0.7H), 4.05 (s, 1.3H), 3.99 (s, 0.7H), 3.82 (s, 2H), 3.80 (s, 1H).  $^{13}\text{C}$  NMR (101 MHz, DMSO) (major cis/trans amide rotamer)  $\delta$  171.2, 154.4, 138.8, 129.6, 115.0, 112.2, 104.4, 61.9, 55.9 UPLC-MS (A) (ESI) RT 1.68 min,  $m/z$  287.1, 280.1 (1:1)  $[\text{M}+\text{H}]^+$  (>95%).

**2-Bromo-N-(4-chloro-2,5-dimethoxyphenyl)acetamide (3.121).**

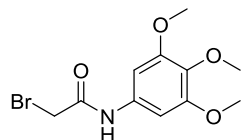


The title compound was prepared according to the general procedure D, using bromoacetic acid bromide (0.559 mL, 6.40 mmol), 2,5-dimethoxy-4-chloroaniline (1.00 g, 5.33 mmol) and TEA (0.891 mL, 6.40 mmol) in anhydrous DCM (5.5 mL) and the reaction time was 3 h.



Brown solid; yield 96% (1.57 g, 5.09 mmol).  $^1\text{H}$  NMR (400 MHz, DMSO)  $\delta$  9.71 (s, 1H), 7.94 (s, 1H), 7.17 (s, 1H), 4.22 (s, 2H), 3.82 (s, 3H), 3.76 (s, 3H).  $^{13}\text{C}$  NMR (101 MHz, DMSO) (major cis/trans amide rotamer)  $\delta$  170.4, 148.3, 142.2, 126.4, 114.6, 112.9, 104.2, 61.7, 56.7, 56.4. UPLC-MS (A) (ESI) RT 1.79 min,  $m/z$  308.2, 310.2 (1:1)  $[\text{M}+\text{H}]^+$  (>95%).

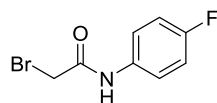
**2-Bromo-N-(3,4,5-trimethoxyphenyl)acetamide (3.122).**



The title compound was prepared according to the general procedure D, using bromoacetic acid bromide (0.572 mL, 6.55 mmol), 3,4,5-trimethoxyphenylamine (1.00 g, 5.46 mmol) and TEA (0.913 mL, 6.55 mmol) in anhydrous DCM (5.5 mL) and the reaction time was 3 h.

Brown solid; yield 97% (1.61 g, 5.30 mmol).  $^1\text{H}$  NMR (400 MHz, DMSO)  $\delta$  10.32 (s, 1H), 6.96 (s, 2H), 4.01 (s, 2H), 3.74 (s, 6H), 3.62 (s, 3H).  $^{13}\text{C}$  NMR (101 MHz, DMSO) (major cis/trans amide rotamer)  $\delta$  170.7, 152.6, 134.6, 133.4, 97.4, 61.9, 60.1, 55.7. UPLC-MS (A) (ESI) RT 1.42 min,  $m/z$  304.2, 306.2 (1:1)  $[\text{M}+\text{H}]^+$  (>95%).

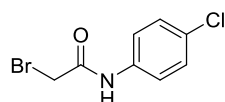
**2-Bromo-N-(4-fluorophenyl)acetamide (3.123).**



The title compound was prepared according to the general procedure D, using bromoacetic acid bromide (0.944 mL, 10.8 mmol), 4-fluoroaniline (1.00 g, 9.00 mmol) and TEA (1.505 mL, 10.80 mmol) in anhydrous DCM (9 mL) and the reaction time was 3 h.

Brown solid; yield 86% (1.79 g, 7.72 mmol).  $^1\text{H}$  NMR (400 MHz, DMSO)  $\delta$  10.43 (s, 1H), 7.65 – 7.55 (m, 2H), 7.24 – 7.11 (m, 2H), 4.02 (s, 2H).  $^{13}\text{C}$  NMR (101 MHz, DMSO) (major cis/trans amide rotamer)  $\delta$  170.8, 158.1 (d,  $^1J_{\text{CF}} = 239.8$  Hz), 134.9 (d,  $^4J_{\text{CF}} = 2.6$  Hz), 121.4 (d,  $^3J_{\text{CF}} = 8.0$  Hz), 115.1 (d,  $^2J_{\text{CF}} = 22.0$  Hz), 61.8; (minor cis/trans amide rotamer)  $\delta$  164.7, 158.3 (d,  $^1J_{\text{CF}} = 240.3$  Hz), 135.0 (d,  $^4J_{\text{CF}} = 2.6$  Hz), 121.0 (d,  $^3J_{\text{CF}} = 8.0$  Hz), 115.5 (d,  $^2J_{\text{CF}} = 22.4$  Hz), 30.3. UPLC-MS (A) (ESI) RT 1.44 min,  $m/z$  232.1, 234.1 (1:1)  $[\text{M}+\text{H}]^+$  (>95%).

**2-Bromo-N-(4-chlorophenyl)acetamide (3.124).**

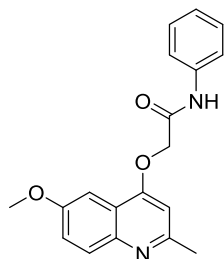


The title compound was prepared according to the general procedure D, using bromoacetic acid bromide (0.822 mL, 9.41 mmol), 4-chloroaniline (1.00 g, 7.84 mmol) and TEA (1.31 mL, 9.41 mmol) in anhydrous DCM (8 mL) and the reaction time was 2.5 h.

White solid; yield 92% (1.79 g, 7.19 mmol).  $^1\text{H}$  NMR (400 MHz, DMSO)  $\delta$  10.51 (s, 1H), 7.65 – 7.57 (m, 2H), 7.44 – 7.34 (m, 2H), 4.03 (s, 2H).  $^{13}\text{C}$  NMR (101 MHz, DMSO) (major cis/trans amide

rotamer)  $\delta$  171.1, 137.5, 128.5, 127.0, 121.2, 61.9; (minor cis/trans amide rotamer)  $\delta$  165.0, 137.6, 128.8, 127.4, 120.8, 30.3. UPLC-MS (A) (ESI) RT 1.68 min,  $m/z$  248.1, 250.1 (1:1)  $[M+H]^+$  (>95%).

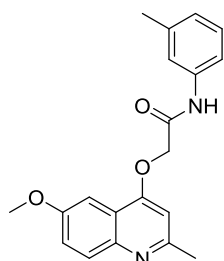
**2-((6-Methoxy-2-methylquinolin-4-yl)oxy)-N-phenylacetamide (3.125).**



The title compound was prepared according to the general procedure E, using 6-methoxy-2-methyl-4-quinolinol (150 mg, 0.792 mmol) in anhydrous DMF (5 mL) was added  $K_2CO_3$  (329 mg, 2.38 mmol) and 2-bromo-*N*-phenylacetamide (170 mg, 0.794 mmol) in anhydrous DMF (4 mL) and the reaction time was 3 d.

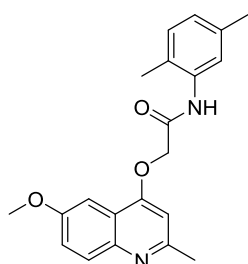
Off-white solid; yield 29% (75 mg, 0.23 mmol); mp 221-222 °C.  $^1H$  NMR (400 MHz,  $DMSO-d_6$ )  $\delta$  10.26 (s, 1H), 7.78 (d,  $J = 9.1$  Hz, 1H), 7.64 (dd,  $J = 8.5, 1.0$  Hz, 2H), 7.51 (d,  $J = 2.8$  Hz, 1H), 7.39 – 7.29 (m, 3H), 7.14 – 7.05 (m, 1H), 6.86 (s, 1H), 5.01 (s, 2H), 3.90 (s, 3H), 2.55 (s, 3H).  $^{13}C$  NMR (101 MHz,  $DMSO-d_6$ )  $\delta$  165.7, 159.5, 156.9, 156.2, 144.2, 138.4, 129.5, 128.8, 123.8, 121.6, 119.7, 119.6, 102.2, 100.1, 67.1, 55.4, 25.1. UPLC-MS (A) (ESI) RT 1.66 min,  $m/z$  323.2  $[M+H]^+$  (>95%). HRMS (ESI)  $m/z$  calcd for  $C_{19}H_{19}N_2O_3$   $[M+H]^+$ : 323.1390; found: 323.1380.

**2-((6-Methoxy-2-methylquinolin-4-yl)oxy)-N-(*m*-tolyl)acetamide (3.126).**



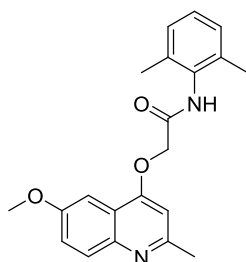
The title compound was prepared according to the general procedure E, using 6-methoxy-2-methyl-4-quinolinol (150 mg, 0.792 mmol), 2-bromo-*N*-(*m*-tolyl)acetamide (181 mg, 0.792 mmol) and  $K_2CO_3$  (329 mg, 2.38 mmol) in anhydrous DMF (9 mL) and the reaction time was 4 h.

Off-white solid; yield 58% (155 mg, 0.461 mmol); mp 142-144 °C.  $^1H$  NMR (400 MHz,  $DMSO-d_6$ )  $\delta$  10.19 (s, 1H), 7.78 (d,  $J = 9.1$  Hz, 1H), 7.57 – 7.46 (m, 2H), 7.41 (d,  $J = 8.0$  Hz, 1H), 7.35 (dd,  $J = 9.1, 2.9$  Hz, 1H), 7.21 (t,  $J = 7.8$  Hz, 1H), 6.91 (d,  $J = 7.5$  Hz, 1H), 6.84 (s, 1H), 5.00 (s, 2H), 3.89 (s, 3H), 2.54 (s, 3H), 2.28 (s, 3H).  $^{13}C$  NMR (101 MHz,  $DMSO-d_6$ )  $\delta$  165.58, 159.47, 156.85, 156.25, 144.22, 138.30, 138.02, 129.51, 128.65, 124.44, 121.59, 120.15, 119.75, 116.82, 102.19, 100.08, 67.07, 55.40, 25.10, 21.17. UPLC-MS (A) (ESI) RT 1.55 min,  $m/z$  337.2  $[M+H]^+$  (>95%). HRMS (ESI)  $m/z$  calcd for  $C_{20}H_{21}N_2O_3$   $[M+H]^+$ : 337.1547; found: 337.1533.

***N*-(2,5-dimethylphenyl)-2-((6-methoxy-2-methylquinolin-4-yl)oxy)acetamide (3.127).**

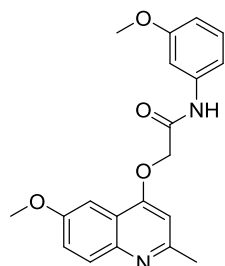
The title compound was prepared according to the general procedure E, using 6-methoxy-2-methyl-4-quinolinol (150 mg, 0.792 mmol), 2-bromo-*N*-(2,5-dimethylphenyl)acetamide (192 mg, 0.793 mmol) and  $K_2CO_3$  (329 mg, 2.38 mmol) in anhydrous DMF (9 mL) and the reaction time was 3 h.

White solid; yield 35% (97 mg, 0.28 mmol).  $^1H$  NMR (400 MHz,  $DMSO-d_6$ )  $\delta$  9.57 (s, 1H), 7.79 (d,  $J = 9.1$  Hz, 1H), 7.55 (d,  $J = 2.9$  Hz, 1H), 7.35 (dd,  $J = 9.1, 2.9$  Hz, 1H), 7.30 (s, 1H), 7.11 (d,  $J = 7.7$  Hz, 1H), 6.94 (d,  $J = 7.6$  Hz, 1H), 6.90 (s, 1H), 5.01 (s, 2H), 3.90 (s, 3H), 2.57 (s, 3H), 2.26 (s, 3H), 2.18 (s, 3H).  $^{13}C$  NMR (101 MHz,  $DMSO-d_6$ )  $\delta$  165.9, 159.5, 157.1, 156.5, 144.4, 135.5, 135.3, 130.4, 129.7, 129.0, 126.5, 125.9, 121.9, 119.9, 102.6, 100.4, 67.5, 55.6, 25.3, 20.8, 17.5. UPLC-MS (A) (ESI) RT 1.66 min,  $m/z$  351.2  $[M+H]^+$  (>95%).

***N*-(2,6-dimethylphenyl)-2-((6-methoxy-2-methylquinolin-4-yl)oxy)acetamide (3.128).**

The title compound was prepared according to the general procedure E, using 6-methoxy-2-methyl-4-quinolinol (150 mg, 0.792 mmol), 2-bromo-*N*-(2,6-dimethylphenyl)acetamide (192 mg, 0.792 mmol) and  $K_2CO_3$  (329 mg, 2.38 mmol) in anhydrous DMF (9 mL) and the reaction time was 4.5 h.

Off-white solid; yield 73% (204 mg, 0.582 mmol).  $^1H$  NMR (400 MHz,  $DMSO-d_6$ )  $\delta$  9.67 (s, 1H), 7.79 (d,  $J = 9.1$  Hz, 1H), 7.58 (d,  $J = 2.8$  Hz, 1H), 7.35 (dd,  $J = 9.1, 2.9$  Hz, 1H), 7.12 – 7.06 (m, 3H), 6.90 (s, 1H), 5.03 (s, 2H), 3.89 (s, 3H), 2.57 (s, 3H), 2.17 (s, 6H).  $^{13}C$  NMR (101 MHz,  $DMSO-d_6$ )  $\delta$  165.6, 159.3, 156.8, 156.3, 144.2, 135.4, 134.3, 129.5, 127.8, 126.8, 121.7, 119.8, 102.4, 100.4, 67.3, 55.4, 25.0, 18.1. UPLC-MS (A) (ESI) RT 1.45 min,  $m/z$  351.5  $[M+H]^+$  (>95%).

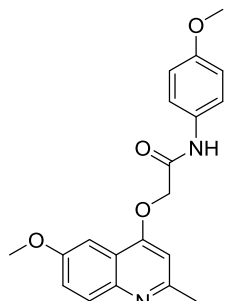
**2-((6-Methoxy-2-methylquinolin-4-yl)oxy)-*N*-(3-methoxyphenyl)acetamide (3.129).**

The title compound was prepared according to the general procedure E, using 6-methoxy-2-methyl-4-quinolinol (150 mg, 0.792 mmol), 2-bromo-*N*-(3-methoxyphenyl)acetamide (232 mg, 0.950 mmol) and  $K_2CO_3$  (329 mg, 2.38 mmol) in anhydrous DMF (9 mL) and the reaction time was 4 h.

White solid; yield 28% (77 mg, 0.22 mmol).  $^1H$  NMR (400 MHz,  $DMSO-d_6$ )  $\delta$  10.27 (s, 1H), 7.78 (d,  $J = 9.1$  Hz, 1H), 7.50 (d,  $J = 2.8$  Hz, 1H), 7.38 – 7.32 (m, 2H), 7.24 (t,  $J = 8.1$  Hz, 1H), 7.20 – 7.15 (m, 1H), 6.85 (s, 1H), 6.68 (ddd,  $J = 8.1, 2.5, 1.0$  Hz, 1H), 5.01 (s, 2H), 3.89 (s, 3H), 3.73 (s, 3H), 2.54 (s, 3H).  $^{13}C$  NMR (101 MHz,  $DMSO-d_6$ )  $\delta$  165.7, 159.5, 159.5, 156.9, 156.3, 144.2,

139.6, 129.6, 129.5, 121.6, 119.7, 111.8, 109.2, 105.4, 102.2, 100.1, 67.0, 55.4, 55.0, 25.1. UPLC-MS (A) (ESI) RT 1.48 min,  $m/z$  353.5  $[M+H]^+$  (>95%).

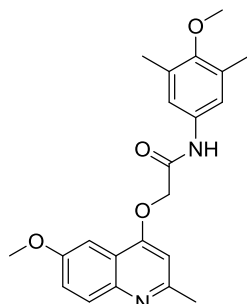
**2-((6-Methoxy-2-methylquinolin-4-yl)oxy)-N-(4-methoxyphenyl)acetamide (3.130).**



The title compound was prepared according to the general procedure E, using 6-methoxy-2-methyl-4-quinolinol (150 mg, 0.792 mmol), 2-bromo-*N*-(4-methoxyphenyl)acetamide (194 mg, 0.792 mmol) and  $K_2CO_3$  (329 mg, 2.38 mmol) in anhydrous DMF (9 mL) and the reaction time was 3 h.

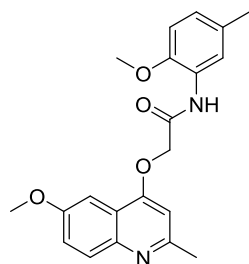
White solid; yield 85% (238 mg, 0.675 mmol); mp 205-207 °C.  $^1H$  NMR (400 MHz, MeOD)  $\delta$  7.79 (d,  $J$  = 9.2 Hz, 1H), 7.65 (d,  $J$  = 2.8 Hz, 1H), 7.55 – 7.46 (m, 2H), 7.36 (dd,  $J$  = 9.2, 2.9 Hz, 1H), 6.95 – 6.87 (m, 2H), 6.84 (s, 1H), 4.95 (s, 2H), 3.95 (s, 3H), 3.78 (s, 3H), 2.62 (s, 3H).  $^{13}C$  NMR (101 MHz, MeOD)  $\delta$  167.8, 161.9, 158.8, 158.7, 158.4, 145.2, 131.9, 129.3, 123.6, 123.5, 121.7, 115.1, 103.3, 101.4, 68.7, 56.1, 55.9, 24.8. UPLC-MS (A) (ESI) RT 1.40 min,  $m/z$  353.5  $[M+H]^+$  (>95%). HRMS (ESI)  $m/z$  calcd for  $C_{20}H_{21}N_2O_4$   $[M+H]^+$ : 353.1496; found: 353.1494.

**2-((6-Methoxy-2-methylquinolin-4-yl)oxy)-N-(4-methoxy-3,5-dimethylphenyl)acetamide (3.131).**



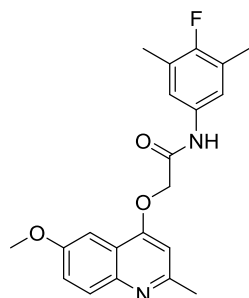
The title compound was prepared according to the general procedure E, using 6-methoxy-2-methyl-4-quinolinol (150 mg, 0.792 mmol), 2-bromo-*N*-(4-methoxy-3,5-dimethylphenyl)acetamide (237 mg, 0.871 mmol) and  $K_2CO_3$  (329 mg, 2.38 mmol) in anhydrous DMF (9 mL) and the reaction time was 3 d.

White solid; yield 60% (180 mg, 0.473 mmol); mp 202-204 °C.  $^1H$  NMR (400 MHz, DMSO- $d_6$ )  $\delta$  10.05 (s, 1H), 7.78 (d,  $J$  = 9.1 Hz, 1H), 7.50 (d,  $J$  = 2.8 Hz, 1H), 7.35 (dd,  $J$  = 9.1, 2.9 Hz, 1H), 7.28 (s, 2H), 6.83 (s, 1H), 4.97 (s, 2H), 3.89 (s, 3H), 3.61 (s, 3H), 2.54 (s, 3H), 2.19 (s, 6H).  $^{13}C$  NMR (101 MHz, DMSO- $d_6$ )  $\delta$  165.3, 159.5, 156.8, 156.2, 152.7, 144.2, 133.8, 130.4, 129.5, 121.6, 120.1, 119.8, 102.2, 100.1, 67.1, 59.4, 55.4, 25.1, 16.0. UPLC-MS (A) (ESI) RT 1.79 min,  $m/z$  381.3  $[M+H]^+$  (>95%). HRMS (ESI)  $m/z$  calcd for  $C_{22}H_{25}N_2O_4$   $[M+H]^+$ : 381.1809; found: 381.1798.

**2-((6-Methoxy-2-methylquinolin-4-yl)oxy)-N-(2-methoxy-5-methylphenyl)acetamide (3.132).**

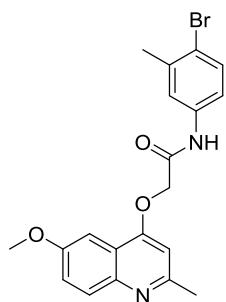
The title compound was prepared according to the general procedure E, using 6-methoxy-2-methyl-4-quinolinol (150 mg, 0.792 mmol), 2-bromo-*N*-(2-methoxy-5-methylphenyl)acetamide (205 mg, 0.792 mmol) and  $K_2CO_3$  (329 mg, 2.38 mmol) in anhydrous DMF (9 mL) and the reaction time was 24 h.

Off-white solid; yield 32% (94 mg, 0.256 mmol); mp 193-194 °C.  $^1H$  NMR (400 MHz,  $DMSO-d_6$ )  $\delta$  9.32 (s, 1H), 7.93 (s, 1H), 7.81 (d,  $J = 9.1$  Hz, 1H), 7.50 (d,  $J = 2.3$  Hz, 1H), 7.39 (dd,  $J = 9.1, 2.8$  Hz, 1H), 7.00 – 6.87 (m, 3H), 5.04 (s, 2H), 3.91 (s, 3H), 3.80 (s, 3H), 2.56 (s, 3H), 2.23 (s, 3H).  $^{13}C$  NMR (101 MHz,  $DMSO-d_6$ )  $\delta$  165.4, 158.9, 157.0, 156.4, 147.1, 144.2, 129.7, 129.3, 126.2, 124.9, 121.5, 121.3, 119.6, 111.1, 102.5, 100.1, 67.0, 55.9, 55.5, 25.1, 20.5. UPLC-MS (A) (ESI) RT 1.61 min,  $m/z$  367.3  $[M+H]^+$  (>95%). HRMS (ESI)  $m/z$  calcd for  $C_{21}H_{23}N_2O_4$   $[M+H]^+$ : 367.1652; found: 367.1653.

***N*-(4-fluoro-3,5-dimethylphenyl)-2-((6-methoxy-2-methylquinolin-4-yl)oxy)acetamide (3.133).**

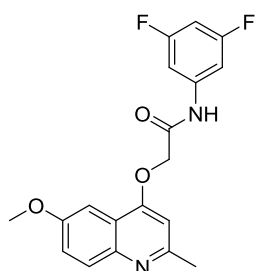
The title compound was prepared according to the general procedure E, using 6-methoxy-2-methyl-4-quinolinol (150 mg, 0.792 mmol), 2-bromo-*N*-(4-fluoro-3,5-dimethylphenyl)acetamide (247 mg, 0.950 mmol) and  $K_2CO_3$  (329 mg, 2.38 mmol) in anhydrous DMF (9 mL) and the reaction time was 3 h.

White solid; yield 68% (198 mg, 0.537 mmol); mp 207-210 °C.  $^1H$  NMR (400 MHz,  $DMSO-d_6$ )  $\delta$  10.14 (s, 1H), 7.78 (d,  $J = 9.1$  Hz, 1H), 7.50 (d,  $J = 2.8$  Hz, 1H), 7.39 – 7.31 (m, 3H), 6.84 (s, 1H), 4.98 (s, 2H), 3.89 (s, 3H), 2.54 (s, 3H), 2.19 (s, 6H).  $^{13}C$  NMR (101 MHz,  $DMSO-d_6$ )  $\delta$  165.5, 159.5, 156.9, 156.2, 155.5 (d,  $^1J_{C-F} = 238.3$  Hz), 144.2, 133.7 (d,  $^4J_{C-F} = 3.2$  Hz), 129.5, 123.9 (d,  $^2J_{C-F} = 18.8$  Hz), 121.6, 120.3 (d,  $^3J_{C-F} = 4.4$  Hz), 119.8, 102.2, 100.1, 67.0, 55.4, 25.1, 14.5 (d,  $^3J_{C-F} = 3.6$  Hz). UPLC-MS (A) (ESI) RT 1.84 min,  $m/z$  369.2  $[M+H]^+$  (>95%). HRMS (ESI)  $m/z$  calcd for  $C_{21}H_{22}N_2O_3$   $[M+H]^+$ : 369.1609; found: 369.1610.

***N*-(4-bromo-3-methylphenyl)-2-((6-methoxy-2-methylquinolin-4-yl)oxy)acetamide (3.134).**

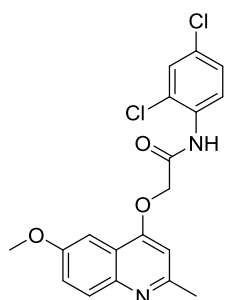
The title compound was prepared according to the general procedure E, using 6-methoxy-2-methyl-4-quinolinol (150 mg, 0.792 mmol), 2-bromo-*N*-(4-bromo-3-methylphenyl)acetamide (268 mg, 0.873 mmol) and  $K_2CO_3$  (329 mg, 2.38 mmol) in anhydrous DMF (9 mL) and the reaction time was 3 h.

Yellowish solid; yield 54% (178 mg, 0.429 mmol).  $^1H$  NMR (400 MHz,  $DMSO-d_6$ )  $\delta$  10.33 (s, 1H), 7.78 (d,  $J = 9.1$  Hz, 1H), 7.66 (d,  $J = 2.3$  Hz, 1H), 7.53 (d,  $J = 8.7$  Hz, 1H), 7.50 (d,  $J = 2.9$  Hz, 1H), 7.41 (dd,  $J = 8.7, 2.4$  Hz, 1H), 7.35 (dd,  $J = 9.1, 2.9$  Hz, 1H), 6.85 (s, 1H), 5.01 (s, 2H), 3.89 (s, 3H), 2.54 (s, 3H), 2.32 (s, 3H).  $^{13}C$  NMR (101 MHz,  $DMSO-d_6$ )  $\delta$  165.8, 159.4, 156.8, 156.2, 144.2, 137.9, 137.5, 132.3, 129.5, 121.9, 122.0, 119.7, 119.1, 117.9, 102.2, 100.1, 67.0, 55.4, 25.1, 22.7. UPLC-MS (A) (ESI) RT 1.75 min,  $m/z$  415.4, 417.4 (1:1)  $[M+H]^+$  (>95%).

***N*-(3,5-difluorophenyl)-2-((6-methoxy-2-methylquinolin-4-yl)oxy)acetamide (3.135).**

The title compound was prepared according to the general procedure E, using 6-methoxy-2-methyl-4-quinolinol (150 mg, 0.792 mmol), 2-bromo-*N*-(3,5-difluorophenyl)acetamide (218 mg, 0.872 mmol) and  $K_2CO_3$  (329 mg, 2.38 mmol) in anhydrous DMF (9 mL) and the reaction time was 1 d.

White solid; yield 53% (151 mg, 0.421 mmol); mp 175-176 °C.  $^1H$  NMR (400 MHz,  $DMSO-d_6$ )  $\delta$  10.64 (s, 1H), 7.78 (d,  $J = 9.1$  Hz, 1H), 7.50 (d,  $J = 2.9$  Hz, 1H), 7.44 – 7.31 (m, 3H), 6.97 (tt,  $J = 9.4, 2.4$  Hz, 1H), 6.86 (s, 1H), 5.04 (s, 2H), 3.89 (s, 3H), 2.55 (s, 3H).  $^{13}C$  NMR (101 MHz,  $DMSO-d_6$ )  $\delta$  166.5, 162.4 (dd,  $^1J_{CF} = 243.5$  Hz,  $^3J_{CF} = 15.3$  Hz), 159.3, 156.9, 156.3, 144.2, 140.9 (t,  $^3J_{CF} = 13.8$  Hz), 129.5, 121.6, 119.7, 102.5 (d,  $^2J_{CF} = 29.7$  Hz), 102.3, 100.1, 98.9 (t,  $^2J_{CF} = 26.0$  Hz), 66.9, 55.4, 25.1. UPLC-MS (A) (ESI) RT 1.93 min,  $m/z$  359.2  $[M+H]^+$  (>95%). HRMS (ESI)  $m/z$  calcd for  $C_{19}H_{17}F_2N_2O_3$   $[M+H]^+$ : 359.1202; found: 359.1209.

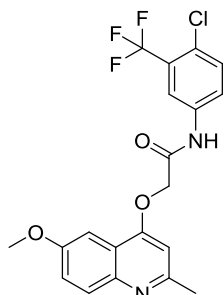
***N*-(2,4-dichlorophenyl)-2-((6-methoxy-2-methylquinolin-4-yl)oxy)acetamide (3.136).**

The title compound was prepared according to the general procedure E, using 6-methoxy-2-methyl-4-quinolinol (200 mg, 1.06 mmol), 2-bromo-*N*-(2,4-dichlorophenyl)acetamide (628 mg, 2.22 mmol) and  $K_2CO_3$  (438 mg, 3.17 mmol) in anhydrous DMF (11.5 mL) and the reaction time 2 d.

Off white solid; yield 2% (9 mg, 0.02 mmol).  $^1H$  NMR (400 MHz,  $DMSO-d_6$ )  $\delta$  9.86 (s, 1H), 7.88 (d,  $J = 8.7$  Hz, 1H), 7.79 (d,  $J = 9.1$  Hz, 1H), 7.73 (d,  $J = 2.4$  Hz, 1H), 7.54 (d,  $J = 2.8$  Hz, 1H), 7.47 (dd,  $J = 8.7, 2.4$  Hz, 1H), 7.36 (dd,  $J = 9.1, 2.9$  Hz, 1H), 6.92 (s, 1H),

5.07 (s, 2H), 3.90 (s, 3H), 2.56 (s, 3H).  $^{13}\text{C}$  NMR (101 MHz, DMSO- $d_6$ )  $\delta$  166.2, 159.0, 156.9, 156.3, 144.2, 133.3, 129.9, 129.6, 129.0, 127.8, 127.4, 126.8, 121.7, 119.6, 102.5, 100.0, 67.1, 55.4, 25.1. UPLC-MS (A) (ESI) RT 1.57 min,  $m/z$  391.1, 393.1 (1:1)  $[\text{M}+\text{H}]^+$  (>95%).

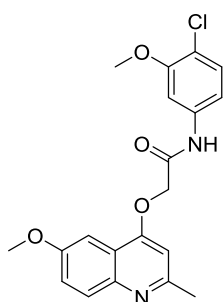
***N*-(4-chloro-3-(trifluoromethyl)phenyl)-2-((6-methoxy-2-methylquinolin-4-yl)oxy)acetamide (3.137).**



The title compound was prepared according to the general procedure E, using 2-bromo-*N*-(4-chloro-3-(trifluoromethyl)phenyl)acetamide (335 mg, 1.06 mmol), 6-methoxy-2-methylquinolin-4-ol (200 mg, 1.06 mmol) and  $\text{K}_2\text{CO}_3$  (438 mg, 3.17 mmol) in anhydrous DMF (10 mL) and the reaction time was 24 h.

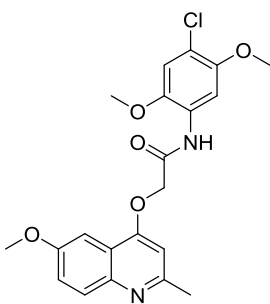
White solid; yield 43% (194 mg, 0.457 mmol).  $^1\text{H}$  NMR (400 MHz, DMSO- $d_6$ )  $\delta$  10.69 (br. s, 1H), 8.24 (d,  $J = 2.5$  Hz, 1H), 7.91 (dd,  $J = 8.8, 2.5$  Hz, 1H), 7.79 (d,  $J = 9.1$  Hz, 1H), 7.70 (d,  $J = 8.8$  Hz, 1H), 7.52 (d,  $J = 2.9$  Hz, 1H), 7.35 (dd,  $J = 11.4, 5.2$  Hz, 1H), 6.88 (s, 1H), 5.05 (s, 2H), 3.89 (s, 3H), 2.55 (s, 3H).  $^{13}\text{C}$  NMR (101 MHz, DMSO- $d_6$ )  $\delta$  166.5, 159.3, 156.9, 156.3, 144.2, 137.9, 132.2, 129.5, 126.8 (q,  $^2J_{\text{C-F}} = 30.6$  Hz), 124.49, 122.69 (q,  $^1J_{\text{C-F}} = 272.8$  Hz), 121.62, 119.70, 118.32 (m, 2C), 102.30, 100.12, 66.95, 55.40, 25.07. UPLC-MS (A) (ESI) RT 1.67 min,  $m/z$  425.4, 427.4 (3:1)  $[\text{M}+\text{H}]^+$  (>95%).

***N*-(4-chloro-3-methoxyphenyl)-2-((6-methoxy-2-methylquinolin-4-yl)oxy)acetamide (3.138).**



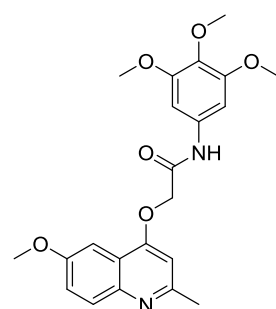
The title compound was prepared according to the general procedure E, using 2-bromo-*N*-(4-chloro-3-methoxyphenyl)acetamide (294 mg, 1.06 mmol), 6-methoxy-2-methylquinolin-4-ol (200 mg, 1.06 mmol) and  $\text{K}_2\text{CO}_3$  (438 mg, 3.17 mmol) in anhydrous DMF (10 mL) and the reaction time was 1 d.

White solid; yield 68% (278 mg, 0.719 mmol).  $^1\text{H}$  NMR (400 MHz, DMSO- $d_6$ )  $\delta$  10.38 (s, 1H), 7.78 (d,  $J = 9.2$  Hz, 1H), 7.56 (d,  $J = 2.3$  Hz, 1H), 7.51 (d,  $J = 2.9$  Hz, 1H), 7.40 – 7.31 (m, 2H), 7.22 (dd,  $J = 8.6, 2.3$  Hz, 1H), 6.86 (s, 1H), 5.02 (s, 2H), 3.90 (s, 3H), 3.82 (s, 3H), 2.55 (s, 3H).  $^{13}\text{C}$  NMR (101 MHz, DMSO- $d_6$ )  $\delta$  165.9, 159.4, 156.9, 156.3, 154.5, 144.2, 138.6, 129.8, 129.5, 121.6, 119.7, 115.4, 112.2, 104.2, 102.2, 100.1, 67.0, 55.9, 55.4, 25.1. UPLC-MS (A) (ESI) RT 1.54 min,  $m/z$  387.4, 389.4 (3:1)  $[\text{M}+\text{H}]^+$  (>95%).

***N*-(4-chloro-2,5-dimethoxyphenyl)-2-((6-methoxy-2-methylquinolin-4-yl)oxy)acetamide (3.139).**

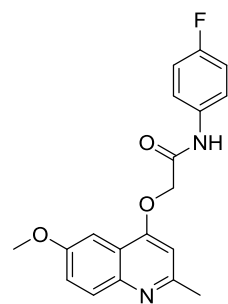
The title compound was prepared according to the general procedure E, using 2-bromo-*N*-(4-chloro-2,5-dimethoxyphenyl)acetamide (326 mg, 1.06 mmol), 6-methoxy-2-methylquinolin-4-ol (200 mg, 1.06 mmol) and  $K_2CO_3$  (438 mg, 3.17 mmol) in anhydrous DMF (10 mL) and the reaction time 4 d.

White solid; yield 27% (117 mg, 0.281 mmol).  $^1H$  NMR (400 MHz,  $DMSO-d_6$ )  $\delta$  9.49 (s, 1H), 8.04 (s, 1H), 7.81 (d,  $J = 9.1$  Hz, 1H), 7.48 (d,  $J = 2.7$  Hz, 1H), 7.39 (dd,  $J = 9.1, 2.9$  Hz, 1H), 7.21 (s, 1H), 6.93 (s, 1H), 5.08 (s, 2H), 3.91 (s, 3H), 3.83 (s, 3H), 3.77 (s, 3H), 2.56 (s, 3H).  $^{13}C$  NMR (101 MHz,  $DMSO-d_6$ )  $\delta$  165.8, 158.9, 157.0, 156.4, 148.2, 144.2, 143.2, 129.6, 126.3, 121.3, 119.6, 115.4, 113.3, 106.0, 102.4, 100.1, 66.9, 56.7, 56.4, 55.4, 25.1. UPLC-MS (A) (ESI) RT 1.56 min,  $m/z$  417.4, 419.4 (3:1)  $[M+H]^+$  (>95%).

***N*-(3,4,5-trimethoxyphenyl)-2-((6-methoxy-2-methylquinolin-4-yl)oxy)acetamide (3.140).**

The title compound was prepared according to the general procedure E, 2-bromo-*N*-(3,4,5-trimethoxyphenyl)acetamide (321 mg, 1.06 mmol), 6-methoxy-2-methylquinolin-4-ol (200 mg, 1.06 mmol) and  $K_2CO_3$  (438 mg, 3.17 mmol) in anhydrous DMF (10 mL) and the reaction time was 4 d.

Off-white solid; yield 75% (328 mg, 0.795 mmol).  $^1H$  NMR (400 MHz,  $DMSO-d_6$ )  $\delta$  10.18 (s, 1H), 7.78 (d,  $J = 9.1$  Hz, 1H), 7.51 (d,  $J = 2.8$  Hz, 1H), 7.35 (dd,  $J = 9.1, 2.9$  Hz, 1H), 7.04 (s, 2H), 6.85 (s, 1H), 4.99 (s, 2H), 3.90 (s, 3H), 3.74 (s, 6H), 3.63 (s, 3H), 2.55 (s, 3H).  $^{13}C$  NMR (101 MHz,  $DMSO-d_6$ )  $\delta$  165.5, 159.4, 156.9, 156.3, 152.8, 144.2, 134.5, 133.7, 129.5, 121.6, 119.7, 102.2, 100.1, 97.3, 67.0, 60.1, 55.7, 55.4, 25.1. UPLC-MS (A) (ESI) RT 1.36 min,  $m/z$  413.5  $[M+H]^+$  (>95%).

***N*-(4-fluorophenyl)-2-((6-methoxy-2-methylquinolin-4-yl)oxy)acetamide (3.141).**

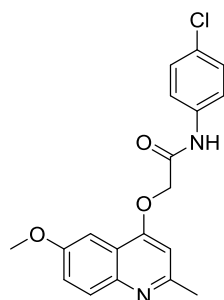
The title compound was prepared according to the general procedure E, using 6-methoxy-2-methyl-4-quinolinol (247 mg, 1.31 mmol), 2-bromo-*N*-(4-fluorophenyl)acetamide (303 mg, 1.31 mmol) and  $K_2CO_3$  (541 mg, 3.92 mmol) in anhydrous DMF (13 mL) and the reaction time was 21 h.

White solid; yield 52% (230 mg, 0.676 mmol).  $^1H$  NMR (400 MHz,  $DMSO-d_6$ )  $\delta$  10.32 (br. s, 1H), 7.78 (d,  $J = 9.1$  Hz, 1H), 7.70 – 7.62 (m, 2H), 7.52 (d,  $J = 2.8$  Hz, 1H), 7.35 (dd,  $J = 9.1, 2.9$  Hz, 1H), 7.23 – 7.14 (m, 2H), 6.86 (s, 1H), 5.00 (s, 2H), 3.89 (s, 3H),



2.55 (s, 3H).  $^{13}\text{C}$  NMR (101 MHz, DMSO- $d_6$ )  $\delta$  165.6, 159.4, 15.3 (d,  $^1J_{\text{C-F}} = 240.4$  Hz), 156.9, 156.2, 144.2, 134.7 (d,  $^4J_{\text{C-F}} = 2.5$  Hz), 129.5, 121.6, 121.6 (d,  $^3J_{\text{C-F}} = 8.1$  Hz), 119.7, 115.4 (d,  $^2J_{\text{C-F}} = 22.4$  Hz), 102.2, 100.1, 67.1, 55.4, 25.1. UPLC-MS (A) (ESI) RT 1.42 min,  $m/z$  341.4  $[\text{M}+\text{H}]^+$  (>95%).

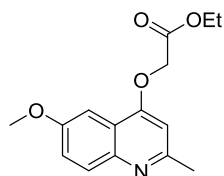
***N*-(4-chlorophenyl)-2-((6-methoxy-2-methylquinolin-4-yl)oxy)acetamide (3.142).**



The title compound was prepared according to the general procedure E, using 6-methoxy-2-methyl-4-quinolinol (250 mg, 1.32 mmol), 2-bromo-*N*-(4-chlorophenyl)acetamide (328 mg, 1.32 mmol) and  $\text{K}_2\text{CO}_3$  (548 mg, 3.96 mmol) in anhydrous DMF (12 mL) and the reaction time was 18 h.

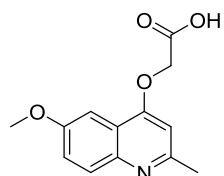
White solid; yield 75% (353 mg, 0.989 mmol); mp 224-225 °C.  $^1\text{H}$  NMR (400 MHz, DMSO- $d_6$ )  $\delta$  10.41 (br. s, 1H), 7.78 (d,  $J = 9.1$  Hz, 1H), 7.70 – 7.64 (m, 2H), 7.51 (d,  $J = 2.9$  Hz, 1H), 7.43 – 7.37 (m, 2H), 7.35 (dd,  $J = 9.1, 2.9$  Hz, 1H), 6.86 (s, 1H), 5.02 (s, 2H), 3.89 (s, 3H), 2.54 (s, 3H).  $^{13}\text{C}$  NMR (101 MHz, DMSO- $d_6$ )  $\delta$  165.9, 159.4, 156.9, 156.3, 144.2, 137.3, 129.5, 128.7, 127.3, 121.6, 121.2, 119.7, 102.2, 100.1, 67.1, 55.4, 25.1. UPLC-MS (A) (ESI) RT 1.51 min,  $m/z$  357.3, 359.3 (3:1)  $[\text{M}+\text{H}]^+$  (>95%). HRMS (ESI)  $m/z$  calcd for  $\text{C}_{19}\text{H}_{18}\text{ClN}_2\text{O}_3$   $[\text{M}+\text{H}]^+$ : 357.1000; found: 357.1001.

***Ethyl 2-((6-methoxy-2-methylquinolin-4-yl)oxy)acetate (3.143).***



The title compound was prepared according to the general procedure E, using ethyl 2-bromoacetate (1 equiv.), 6-methoxy-2-methyl-4-quinolinol (1-1.1 equiv.) and  $\text{K}_2\text{CO}_3$  (3 equiv.) in anhydrous DMF (molarity: 0.1-0.2 M) and the reaction time was 3 d. The solvent was evaporated under reduced pressure and the obtained residue was used without purification for the next step (hydrolysis of the ester bond).

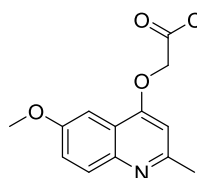
***2-((6-Methoxy-2-methylquinolin-4-yl)oxy)acetic acid (3.144).***



Ethyl 2-((6-methoxy-2-methylquinolin-4-yl)oxy)acetate **3.143** (1 equiv.) was dissolved in methanol or ethanol (molarity: 0.1-0.3 M) and potassium hydroxide (1-2 equiv.) was added to the solution. The reaction mixture was stirred under reflux for 2.5 - 24 h, and then the solvent was removed under reduced pressure. The obtained residue was dissolved in water and the pH was acidified using acetic acid ( $\text{CH}_3\text{COOH}$ ) until pH 5-6. The crystallized solid was collected by filtration, washed with water and dried to give the pure target compound.

White solid; yield (over 2 steps) 92%.  $^1\text{H}$  NMR (400 MHz,  $\text{DMSO-}d_6$ )  $\delta$  7.77 (d,  $J = 9.1$  Hz, 1H), 7.40 (d,  $J = 2.9$  Hz, 1H), 7.33 (dd,  $J = 9.1, 2.9$  Hz, 1H), 6.80 (s, 1H), 4.93 (s, 2H), 3.87 (s, 3H), 2.53 (s, 3H).  $^{13}\text{C}$  NMR (101 MHz,  $\text{DMSO-}d_6$ )  $\delta$  169.4, 159.3, 156.8, 156.3, 144.1, 129.5, 121.6, 119.7, 102.2, 99.6, 64.7, 55.4, 25.0. UPLC-MS (A) ESI RT 0.43 min,  $m/z$  248.1  $[\text{M}+\text{H}]^+$  (>95%).

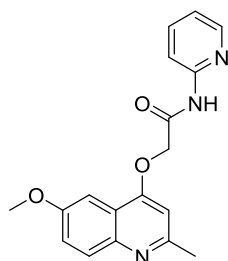
**2-((6-Methoxy-2-methylquinolin-4-yl)oxy)acetyl chloride (3.145).**



The title compound was prepared according to the general procedure G, using 2-((6-methoxy-2-methylquinolin-4-yl)oxy)acetic acid (1 equiv.) and thionyl chloride ( $\text{SOCl}_2$ , 3-45 equiv.) and the reaction time was 1-2 d.

Off-white solid; yield  $\sim 100\%$  (1.28 g, 4.80 mmol).  $^1\text{H}$  NMR (400 MHz,  $\text{DMSO-}d_6$ )  $\delta$  16.10 (s, 1H), 8.25 (d,  $J = 9.3$  Hz, 1H), 7.74 (dd,  $J = 9.3, 2.8$  Hz, 1H), 7.56 (d,  $J = 2.8$  Hz, 1H), 7.51 (s, 1H), 5.28 (s, 2H), 3.95 (s, 3H), 2.84 (s, 3H).  $^{13}\text{C}$  NMR (101 MHz,  $\text{DMSO-}d_6$ )  $\delta$  168.2, 164.9, 158.5, 155.8, 134.1, 126.1, 121.6, 120.2, 104.2, 100.9, 66.3, 56.0, 20.1.

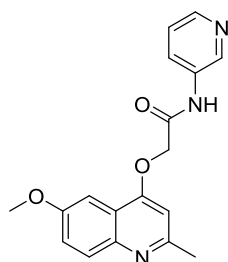
**2-((6-Methoxy-2-methylquinolin-4-yl)oxy)-N-(pyridin-2-yl)acetamide (3.146).**



The title compound was prepared according to the general procedure H, using 2-((6-methoxy-2-methylquinolin-4-yl)oxy)acetyl chloride (100 mg, 0.376 mmol), 2-aminopyridine (35 mg, 0.38 mmol) and triethylamine (0.052 mL, 0.38 mmol) in anhydrous DCM (10 mL) and the reaction time was 18 h.

Off-white solid; yield 51% (61 mg, 0.19 mmol).  $^1\text{H}$  NMR (400 MHz,  $\text{DMSO-}d_6$ )  $\delta$  ppm 10.76 (s, 1 H), 8.38 - 8.34 (m, 1 H), 8.06 (d,  $J=8.34$  Hz, 1 H), 7.86 - 7.74 (m, 2 H), 7.46 (d,  $J=3.03$  Hz, 1 H), 7.35 (dd,  $J=9.09, 2.78$  Hz, 1 H), 7.15 (ddd,  $J=7.33, 4.93, 0.88$  Hz, 1 H), 6.83 (s, 1 H), 5.12 (s, 2 H), 3.34 (s, 3 H), 2.54 (s, 3 H).  $^{13}\text{C}$  NMR (101 MHz,  $\text{DMSO-}d_6$ )  $\delta$  ppm 166.5, 159.4, 156.8, 156.3, 151.4, 148.1, 144.2, 138.4, 129.5, 121.6, 119.8, 119.7, 113.6, 102.0, 99.8, 66.6, 55.4, 25.1. UPLC-MS (C) RT 1.06 min,  $m/z$  324  $[\text{M}+\text{H}]^+$  (>95%).

**2-((6-Methoxy-2-methylquinolin-4-yl)oxy)-N-(pyridin-3-yl)acetamide (3.147).**

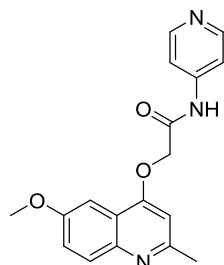


The title compound was prepared according to the general procedure H, using 2-((6-methoxy-2-methylquinolin-4-yl)oxy)acetyl chloride (100 mg, 0.376 mmol), 3-aminopyridine (35 mg, 0.38 mmol) and triethylamine (0.052 mL, 0.38 mmol) in anhydrous DCM (10 mL) and the reaction time was 18 h.

Off-white solid; yield 58% (70 mg, 0.22 mmol).  $^1\text{H}$  NMR (400 MHz,  $\text{DMSO-}d_6$ )  $\delta$  ppm 10.48 (s, 1 H), 8.80 (d,  $J=2.5$  Hz, 1 H), 8.31 (dd,  $J=4.7, 1.4$  Hz, 1 H), 8.14 - 8.03 (m, 1 H), 7.79 (d,  $J=9.1$  Hz, 1 H), 7.53 (d,  $J=2.8$  Hz, 1 H), 7.43 - 7.30 (m, 2 H), 6.88 (s, 1 H), 5.05 (s, 2 H), 3.90 (s, 3

H), 2.55 (s, 3 H).  $^{13}\text{C}$  NMR (101 MHz,  $\text{DMSO-}d_6$ )  $\delta$  ppm 166.3, 159.3, 156.8, 156.2, 144.7, 144.1, 141.3, 135.0, 129.6, 126.7, 123.7, 121.3, 119.7, 102.2, 100.1, 66.9, 55.4, 25.0. UPLC-MS (C) RT 0.97 min,  $m/z$  324  $[\text{M}+\text{H}]^+$  (>95%).

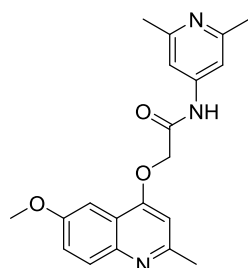
**2-((6-Methoxy-2-methylquinolin-4-yl)oxy)-N-(pyridin-4-yl)acetamide (3.148).**



The title compound was prepared according to the general procedure H, using 2-((6-methoxy-2-methylquinolin-4-yl)oxy)acetic chloride (215 mg, 0.809 mmol) and pyridin-4-amine (152 mg, 1.62 mmol) in anhydrous DCM (5 mL) and the reaction time was 7 h.

White solid; yield 31% (81 mg, 0.25 mmol).  $^1\text{H}$  NMR (400 MHz,  $\text{DMSO-}d_6$ )  $\delta$  10.66 (s, 1H), 8.46 (dd,  $J = 4.8, 1.7$  Hz, 2H), 7.78 (d,  $J = 9.1$  Hz, 1H), 7.62 (dd,  $J = 4.8, 1.7$  Hz, 2H), 7.50 (d,  $J = 2.9$  Hz, 1H), 7.35 (dd,  $J = 9.2, 2.9$  Hz, 1H), 6.86 (s, 1H), 5.07 (s, 2H), 3.89 (s, 3H), 2.54 (s, 3H).  $^{13}\text{C}$  NMR (101 MHz,  $\text{DMSO-}d_6$ )  $\delta$  166.9, 159.3, 156.9, 156.3, 150.5, 145.1, 144.2, 129.5, 121.6, 119.7, 113.5, 102.2, 100.0, 66.9, 55.4, 25.1. UPLC-MS (A) (ESI) RT 0.43 min,  $m/z$  324.1  $[\text{M}+\text{H}]^+$  (>95%).

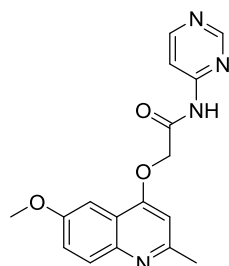
**N-(2,6-dimethylpyridin-4-yl)-2-((6-methoxy-2-methylquinolin-4-yl)oxy)acetamide (3.149).**



The title compound was prepared according to the general procedure H, using, 2-((6-methoxy-2-methylquinolin-4-yl)oxy)acetic chloride (106 mg, 0.399 mmol) and pyridin-4-amine (99 mg, 0.81 mmol) in anhydrous DCM (5.5 mL) and the reaction time was 3 d.

White solid; yield 36% (51 mg, 0.15 mmol).  $^1\text{H}$  NMR (400 MHz,  $\text{DMSO-}d_6$ )  $\delta$  10.77 (s, 1H), 7.81 (d,  $J = 9.1$  Hz, 1H), 7.49 (d,  $J = 2.8$  Hz, 1H), 7.42 – 7.34 (m, 3H), 6.89 (s, 1H), 5.11 (s, 2H), 3.89 (s, 3H), 2.56 (s, 3H), 2.42 (s, 6H).  $^{13}\text{C}$  NMR (101 MHz,  $\text{DMSO-}d_6$ )  $\delta$  167.0, 159.8, 157.1, 156.8, 156.4, 146.9, 143.6, 129.0, 122.0, 119.7, 110.2, 102.4, 100.0, 67.0, 55.4, 24.7, 23.3. UPLC-MS (A) (ESI) RT 1.01 min,  $m/z$  352.2  $[\text{M}+\text{H}]^+$  (>95%).

**2-((6-Methoxy-2-methylquinolin-4-yl)oxy)-N-(pyrimidin-4-yl)acetamide (3.150).**

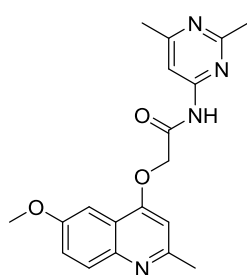


The title compound was prepared according to the general procedure H, using 2-((6-methoxy-2-methylquinolin-4-yl)oxy)acetic chloride (215 mg, 0.809 mmol) and pyrimidin-4-amine (192 mg, 2.02 mmol) in anhydrous DCM (5.5 mL) and the reaction time was 1 d.

White solid; yield 40% (105 mg, 0.324 mmol).  $^1\text{H}$  NMR (400 MHz,  $\text{DMSO-}d_6$ )  $\delta$  11.22 (s, 1H), 8.93 (d,  $J = 0.9$  Hz, 1H), 8.68 (d,  $J = 5.8$  Hz, 1H), 8.03 (dd,  $J = 5.8, 1.2$  Hz, 1H), 7.78

(d,  $J = 9.1$  Hz, 1H), 7.45 (d,  $J = 2.8$  Hz, 1H), 7.35 (dd,  $J = 9.1, 2.9$  Hz, 1H), 6.83 (s, 1H), 5.16 (s, 2H), 3.88 (s, 3H), 2.53 (s, 3H).  $^{13}\text{C}$  NMR (101 MHz, DMSO- $d_6$ )  $\delta$  167.9, 159.4, 158.5, 158.4, 157.2, 156.9, 156.3, 144.2, 129.5, 121.6, 119.7, 110.0, 102.1, 99.8, 66.6, 55.4, 25.1. UPLC-MS (A) (ESI) RT 1.36 min,  $m/z$  325.2  $[\text{M}+\text{H}]^+$  (>95%).

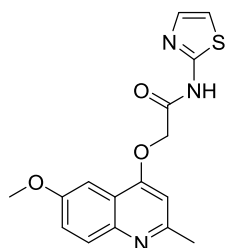
***N*-(2,6-dimethylpyrimidin-4-yl)-2-((6-methoxy-2-methylquinolin-4-yl)oxy)acetamide (3.151).**



The title compound was prepared according to the general procedure H, using 2-((6-methoxy-2-methylquinolin-4-yl)oxy)acetic chloride (215 mg, 0.809 mmol) and 4-amino-2,6-dimethylpyrimidine (199 mg, 1.62 mmol) in anhydrous DCM (6 mL) and the reaction time was 1 d.

White solid; yield 40% (115 mg, 0.326 mmol).  $^1\text{H}$  NMR (400 MHz, DMSO- $d_6$ )  $\delta$  11.06 (s, 1H), 7.78 (d,  $J = 9.1$  Hz, 1H), 7.73 (s, 1H), 7.44 (d,  $J = 2.9$  Hz, 1H), 7.35 (dd,  $J = 9.1, 2.9$  Hz, 1H), 6.80 (s, 1H), 5.12 (s, 2H), 3.88 (s, 3H), 2.53 (s, 3H), 2.50 (s, 3H, overlaps with solvent's peak) 2.37 (s, 3H).  $^{13}\text{C}$  NMR (101 MHz, DMSO- $d_6$ )  $\delta$  168.2, 167.7, 166.6, 159.4, 157.4, 156.8, 156.3, 144.2, 129.5, 121.6, 119.7, 105.6, 102.1, 99.8, 66.5, 55.4, 25.2, 25.1, 23.9. UPLC-MS (A) (ESI) RT 1.13 min,  $m/z$  353.2  $[\text{M}+\text{H}]^+$  (>95%).

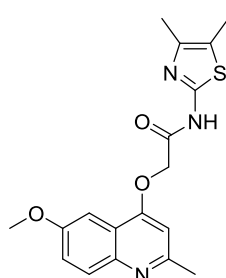
**2-((6-Methoxy-2-methylquinolin-4-yl)oxy)-*N*-(thiazol-2-yl)acetamide (3.152).**



The title compound was prepared according to the general procedure H, using 2-((6-methoxy-2-methylquinolin-4-yl)oxy)acetic chloride (215 mg, 0.809 mmol) and 2-aminothiazole (113 mg, 1.13 mmol) in anhydrous DCM (5.5 mL) and the reaction time was 3 h.

White solid; yield 59% (158 mg, 0.480 mmol).  $^1\text{H}$  NMR (400 MHz, DMSO- $d_6$ )  $\delta$  12.51 (s, 1H), 7.79 (d,  $J = 9.1$  Hz, 1H), 7.51 (d,  $J = 3.6$  Hz, 1H), 7.47 (d,  $J = 2.8$  Hz, 1H), 7.35 (dd,  $J = 9.1, 2.9$  Hz, 1H), 7.27 (d,  $J = 3.6$  Hz, 1H), 6.84 (s, 1H), 5.17 (s, 2H), 3.89 (s, 3H), 2.54 (s, 3H).  $^{13}\text{C}$  NMR (101 MHz, DMSO- $d_6$ )  $\delta$  166.0, 159.4, 157.5, 156.9, 156.3, 144.2, 137.7, 129.5, 121.7, 119.7, 113.9, 102.1, 99.9, 66.1, 55.4, 25.1. UPLC-MS (A) (ESI) RT 1.65 min,  $m/z$  330.2  $[\text{M}+\text{H}]^+$  (>95%).

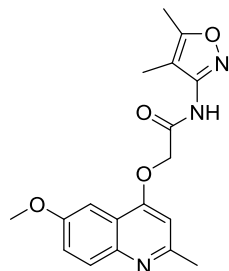
***N*-(4,5-dimethylthiazol-2-yl)-2-((6-methoxy-2-methylquinolin-4-yl)oxy)acetamide (3.153).**



The title compound was prepared according to the general procedure H, using 2-((6-methoxy-2-methylquinolin-4-yl)oxy)acetic acid (200 mg, 0.809 mmol) and 4,5-dimethyl-thiazol-2-ylamine (207 mg, 1.62 mmol) in anhydrous DCM (5.5 mL) and the reaction time was 8 h.

White solid; yield 6% (18 mg, 0.050 mmol);  $^1\text{H}$  NMR (400 MHz,  $\text{DMSO-}d_6$ )  $\delta$  12.26 (s, 1H), 7.78 (d,  $J = 9.1$  Hz, 1H), 7.47 (d,  $J = 2.9$  Hz, 1H), 7.35 (dd,  $J = 9.1, 2.9$  Hz, 1H), 6.80 (s, 1H), 5.11 (s, 2H), 3.89 (s, 3H), 2.53 (s, 3H), 2.24 (d,  $J = 0.7$  Hz, 3H), 2.17 (d,  $J = 0.7$  Hz, 3H). UPLC-MS (A) (ESI) RT 1.70 min,  $m/z$  358.2  $[\text{M}+\text{H}]^+$  (>95%).

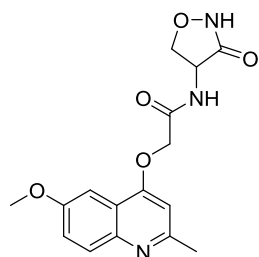
***N*-(4,5-dimethylisoxazol-3-yl)-2-((6-methoxy-2-methylquinolin-4-yl)oxy)acetamide (3.154).**



The title compound was prepared according to the general procedure H, using 2-((6-methoxy-2-methylquinolin-4-yl)oxy)acetic chloride (215 mg, 0.809 mmol) and 3-amino-4,5-dimethylisoxazole (181 mg, 1.62 mmol) in anhydrous DCM (5 mL) and the reaction time was 3 d.

White solid; yield 61% (169 mg, 0.495 mmol).  $^1\text{H}$  NMR (400 MHz,  $\text{DMSO-}d_6$ )  $\delta$  10.56 (br. s, 1H), 7.78 (d,  $J = 9.1$  Hz, 1H), 7.51 (d,  $J = 2.8$  Hz, 1H), 7.35 (dd,  $J = 9.1, 2.9$  Hz, 1H), 6.82 (s, 1H), 5.08 (s, 2H), 3.89 (s, 3H), 2.55 (s, 3H), 2.31 (s, 3H), 1.81 (s, 3H).  $^{13}\text{C}$  NMR (101 MHz,  $\text{DMSO-}d_6$ )  $\delta$  166.5, 166.2, 159.3, 157.6, 156.8, 156.3, 144.2, 129.5, 121.6, 119.7, 106.4, 102.2, 100.2, 66.7, 55.4, 25.1, 10.8, 6.8. UPLC-MS (A) (ESI) RT 1.54 min,  $m/z$  342.2  $[\text{M}+\text{H}]^+$  (>95%).

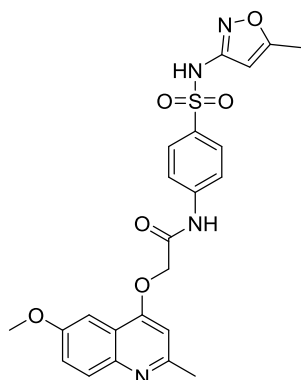
***2*-((6-Methoxy-2-methylquinolin-4-yl)oxy)-*N*-(3-oxoisoxazolidin-4-yl)acetamide (3.155).**



The title compound was prepared according to the general procedure H, using 2-((6-methoxy-2-methylquinolin-4-yl)oxy)acetyl chloride (264 mg, 1.00 mmol) and (R)-4-aminoisoxazolidin-3-one (100 mg, 0.980 mmol) in anhydrous DCM (10 mL) and the reaction time was 3 d.

Off-white solid; yield 5% (17 mg, 0.051 mmol); mp decomposition >150 °C.  $^1\text{H}$  NMR (400 MHz,  $\text{DMSO-}d_6$ )  $\delta$  ppm 8.31 (s, 1 H), 7.95 (d,  $J=4.5$  Hz, 1 H), 7.76 (d,  $J=9.0$  Hz, 1 H), 7.47 (d,  $J=3.0$  Hz, 1 H), 7.33 (dd,  $J=9.2, 2.9$  Hz, 1 H), 6.85 (s, 1 H), 4.80 (ABq,  $\Delta\delta_{\text{AB}}=0.004$ ,  $J=14.6$  Hz, 2 H), 4.30 (t,  $J=7.8$  Hz, 1 H), 4.08 - 4.17 (m, 1 H), 3.92 (s, 3 H), 3.36 - 3.39 (m, 1 H, overlaps with water peak), 2.54 (s, 3 H).  $^{13}\text{C}$  NMR (101 MHz,  $\text{DMSO-}d_6$ )  $\delta$  ppm 171.9, 166.9, 159.0, 156.9, 156.4, 144.1, 129.5, 121.7, 119.6, 102.4, 99.7, 73.0, 66.8, 55.5, 55.3, 25.0. UPLC-MS (A) (ESI) RT 0.97 min,  $m/z$  332.1  $[\text{M}+\text{H}]^+$  (>95%). HRMS (ESI)  $m/z$  calcd for  $\text{C}_{16}\text{H}_{18}\text{N}_3\text{O}_5$   $[\text{M}+\text{H}]^+$ : 332.1241; found: 332.1241.

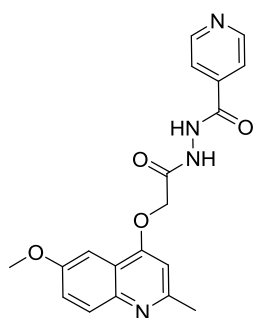
**2-((6-Methoxy-2-methylquinolin-4-yl)oxy)-N-(4-(N-(5-methylisoxazol-3-yl)sulfamoyl) phenyl) acetamide (3.156).**



The title compound was prepared according to the general procedure H, using 2-((6-methoxy-2-methylquinolin-4-yl)oxy)acetyl chloride (205 mg, 0.772 mmol), 4-amino-*N*-(5-methylisoxazol-3-yl) benzenesulfonamide (235 mg, 0.928 mmol) and TEA (0.13 mL, 0.93 mmol) in DCM (5 mL) and the reaction time was 24 h.

Off-white solid; yield 44% (165 mg, 0.342 mmol).  $^1\text{H}$  NMR (400 MHz, DMSO- $d_6$ )  $\delta$  11.38 (br. s, 1H), 10.68 (s, 1H), 7.83 (s, 4H), 7.78 (d,  $J$  = 9.1 Hz, 1H), 7.49 (d,  $J$  = 2.8 Hz, 1H), 7.35 (dd,  $J$  = 9.1, 2.9 Hz, 1H), 6.85 (s, 1H), 6.12 (s, 1H), 5.06 (s, 2H), 3.89 (s, 3H), 2.54 (s, 3H), 2.29 (s, 3H).  $^{13}\text{C}$  NMR (101 MHz, DMSO- $d_6$ )  $\delta$  170.2, 166.4, 159.4, 157.6, 156.9, 156.3, 144.1, 142.6, 133.8, 129.4, 128.1, 121.7, 119.7, 119.4, 102.2, 100.0, 95.4, 66.9, 55.4, 25.0, 12.0. UPLC-MS (A) (ESI) RT 1.40 min,  $m/z$  483.4  $[\text{M}+\text{H}]^+$  (>95%).

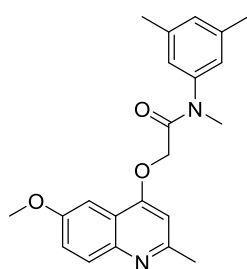
***N'*-2-((6-methoxy-2-methylquinolin-4-yl)oxy)acetyl)isonicotinohydrazide (3.157).**



The title compound was prepared according to the general procedure H, using 2-((6-methoxy-2-methylquinolin-4-yl)oxy)acetyl chloride (205 mg, 0.772 mmol), isoniazid (127 mg, 0.926 mmol) and triethylamine (94 mg, 0.93 mmol) in anhydrous DCM (5 mL) and the reaction time was 24 h.

Off-white solid; yield 19% (55 mg, 0.15 mmol).  $^1\text{H}$  NMR (400 MHz, DMSO- $d_6$ )  $\delta$  10.83 (br. s, 1H), 10.54 (s, 1H), 8.78 (dd,  $J$  = 4.4, 1.6 Hz, 2H), 7.81 – 7.75 (m, 3H), 7.57 (d,  $J$  = 2.8 Hz, 1H), 7.35 (dd,  $J$  = 9.1, 2.9 Hz, 1H), 6.94 (s, 1H), 4.99 (s, 2H), 3.90 (s, 3H), 2.58 (s, 3H).  $^{13}\text{C}$  NMR (101 MHz, DMSO- $d_6$ )  $\delta$  166.5, 164.1, 159.1, 156.9, 156.3, 150.5, 144.2, 139.3, 129.5, 121.5, 121.3, 119.7, 102.6, 100.4, 66.2, 55.5, 25.1. UPLC-MS (A) (ESI) RT 0.29 min,  $m/z$  367.4  $[\text{M}+\text{H}]^+$  (>95%).

***N*-(3,5-dimethylphenyl)-2-((6-methoxy-2-methylquinolin-4-yl)oxy)-*N*-methylacetamide (3.158).**



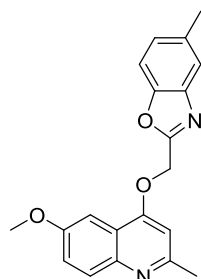
Iodomethane (MeI) (0.02 mL, 0.3 mmol) was added to a solution of *N*-(3,5-dimethylphenyl)-2-((6-methoxy-2-methylquinolin-4-yl)oxy) acetamide (100 mg, 0.285 mmol) and sodium hydride (NaH) 60% suspended in mineral oil (14 mg, 0.34 mmol) in anhydrous tetrahydrofuran (THF) (2 mL) which was maintained below 5 °C. The reaction mixture was left stirring overnight at room temperature. THF was evaporated, the obtained residue

was dissolved in water (50 mL) and the target compound was extracted with ethyl acetate (50 mL

x 3). The combined organic layers were dried over  $\text{MgSO}_4$  and evaporated under reduced pressure. The residue was purified by flash chromatography using a Merk pre-packed column (18+2 g) and eluent ethyl acetate/cyclohexane 80/20.

Yellowish solid; yield 83% (86 mg, 0.24 mmol).  $^1\text{H}$  NMR (400 MHz,  $\text{DMSO}-d_6$ )  $\delta$  ppm 7.74 (d,  $J=9.1$  Hz, 1 H), 7.31 (dd,  $J=9.1, 3.0$  Hz, 1 H), 7.22 (br. s., 1 H), 7.07 (br. s., 2 H), 7.00 (br. s., 1 H), 6.59 (br. s., 1 H), 4.79 (br. s., 2 H), 3.84 (s, 3 H), 3.19 (br. s., 3 H), 2.53 (s, 3 H), 2.25 (s, 6 H).  $^{13}\text{C}$  NMR (101 MHz,  $\text{DMSO}-d_6$ )  $\delta$  ppm 166.4 (br. s.), 159.8, 157.1, 156.6, 144.5, 142.3 (br. s.), 139.5 (br. s.), 129.8 (2 C), 124.8 (br. s.), 121.9, 120.2, 102.3 (br. s.), 100.2, 66.2, 55.8, 37.5, 25.5, 21.2. UPLC-MS (C) RT 1.23 min,  $m/z$  365  $[\text{M}+\text{H}]^+$  (>95%).

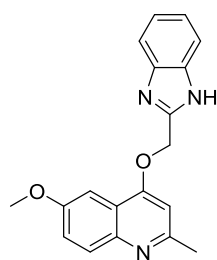
#### 2-(((6-Methoxy-2-methylquinolin-4-yl)oxy)methyl)-5-methylbenzo[d]oxazole (3.159).



The title compound was prepared according to the general procedure F, using 6-methoxy-2-methylquinolin-4-ol (50 mg, 0.26 mmol), 2-(chloromethyl)-5-methyl-1,3-benzoxazole (48 mg, 0.19 mmol) and sodium hydride (NaH, 11 mg, 0.26 mmol) in anhydrous DMF (2 mL) and the reaction time was 1 d.

White solid; yield 14% (8.5 mg, 0.025 mmol); mp 231-233 °C.  $^1\text{H}$  NMR (400 MHz,  $\text{DMSO}-d_6$ )  $\delta$  ppm 7.79 (d,  $J=9.1$  Hz, 1 H), 7.66 (d,  $J=8.3$  Hz, 1 H), 7.61 (s, 1 H), 7.39 (d,  $J=2.8$  Hz, 1 H), 7.33 - 7.38 (m, 1 H), 7.26 (dd,  $J=8.2, 1.1$  Hz, 1 H), 7.10 (s, 1 H), 5.74 (s, 2 H), 3.86 (s, 3 H), 2.55 (s, 3 H), 2.43 (s, 3 H). UPLC-MS (C) RT 1.25 min,  $m/z$  335  $[\text{M}+\text{H}]^+$  (>95%). HRMS (ESI)  $m/z$  calcd for  $\text{C}_{20}\text{H}_{19}\text{N}_2\text{O}_3$   $[\text{M}+\text{H}]^+$ : 335.1390; found: 335.1376.

#### 4-((1H-benzo[d]imidazol-2-yl)methoxy)-6-methoxy-2-methylquinoline (3.160).



The title compound was prepared according to the general procedure E, using 6-methoxy-2-methylquinolin-4-ol (100 mg, 0.529 mmol), 2-chloromethylbenzimidazole (176 mg, 1.06 mmol) and potassium carbonate ( $\text{K}_2\text{CO}_3$ , 219 mg, 1.59 mmol) in anhydrous DMF (3 mL) and the reaction time was 1 d.

Off-white solid; yield 3% (5 mg, 0.02 mmol).  $^1\text{H}$  NMR (400 MHz,  $\text{DMSO}-d_6$ )  $\delta$  ppm 12.80 (br. s, 1 H), 7.79 (d,  $J=9.1$  Hz, 1 H), 7.66 (d,  $J=7.8$  Hz, 1 H), 7.53 (d,  $J=7.1$  Hz, 1 H), 7.48 (d,  $J=2.8$  Hz, 1 H), 7.35 (dd,  $J=9.1, 3.0$  Hz, 1 H), 7.17 - 7.28 (m, 2 H), 7.12 (s, 1 H), 5.59 (s, 2 H), 3.87 (s, 3 H), 2.57 (s, 3 H). UPLC-MS (C) RT 1.05 min,  $m/z$  320  $[\text{M}+\text{H}]^+$  (>95%).

#### 3.6.4. MIC determination

**Strain and growth conditions.** *M. tuberculosis* H37Rv (ATC25618) wild-type was grown in Middlebrook 7H9-ADC broth (Difco) supplemented with 0.05% Tween 80 and on 7H10-OADC or

7H11-OADC agar (Difco) at 37 °C. Isoniazid and hygromycin were purchased from Sigma-Aldrich. Where required, hygromycin (50 µg/mL) was added to the culture medium.

The measurement of the Minimum Inhibitory Concentration (MIC) against *M. tuberculosis* H37Rv for each tested compound was performed in 96-well flat-bottom, polystyrene microtiter plates in a final volume of 200 µL. Ten two-fold drug dilutions in neat DMSO were performed. Middlebrook 7H9 (Difco) was used as medium. Isoniazid (Sigma Aldrich) was used as a positive control with two-fold dilutions of isoniazid starting at 4 µg/mL placed at row 11 of the plate layout and rifampicin (Sigma Aldrich) was used as no-growth control at concentration of 1 µM, placed at G-12 and H-12 wells. The inoculum (200 µL) was added to the entire plate. All plates were placed in a sealed box to prevent drying out of the peripheral wells and incubated at 37 °C without shaking for six days. A Resazurin solution was prepared by dissolving one tablet of resazurin (Resazurin Tablets for Milk Testing; Ref 330884Y' VWR International Ltd) in 30 mL of sterile PBS (phosphate buffered saline). Of this solution, 25 µL were added to each well. Fluorescence was measured (Spectramax M5 Molecular Devices, Excitation 530nm, Emission 590 nm) after 48 hours to determine the MIC value. Data provided were the average of 2 experimental replicates, according to the standards of the industrial partner (GSK). Furthermore, MIC-values are typically not reported with an error/SD (unlike IC<sub>50</sub> values). Standard practice is to consider that the error in the assay is on average ±1 dilution factor. In the reported work, two-fold dilution steps (1:2) are used between the assayed compound concentrations. This implies that, for example, MIC values of 2 and 4 µM should be considered equivalent.

### 3.6.5. Intracellular IC<sub>50</sub> and IC<sub>90</sub> determination

Human THP-1 (Human acute monocytic leukemia cell line, ATCC number TIB-202) macrophages differentiated with PMA (phorbol myristate acetate) was used as a model to study the intracellular stages of *M. tuberculosis*. The assay determines the effect of the compounds on mycobacteria growing inside phagocytes by determining luciferase activity per well, which is related to the number of living bacteria.

*Protocol Steps: (a) Bacterial culture and single cell suspension protocol.* A single cell suspension of *M. tuberculosis* H37Rv pATB45luc was prepared prior to infection. 25 mL of bacterial culture grown to log phase was centrifuged at 2800 g for 10 min. After removal of the supernatant, cell clumps were dispersed by vigorously shaking with sterile glass 3 mm beads (Sigma) for 2 min. Dispersed cells were then resuspended in 10 mL of Roswell Park Memorial Institute medium (RPMI medium) and left to decant for 5 min at room temperature. Cells were then centrifuged at 400 g for 5 min. Supernatant was collected and its optical density at 600 nm (OD<sub>600</sub>) was measured. OD



mL<sup>-1</sup> was converted to colony-forming unit (CFU) mL<sup>-1</sup> considering that 0.125 OD is equal to 10<sup>7</sup> CFU mL<sup>-1</sup>.

(b) *THP-1 cell preparation and infection with M. tuberculosis.* THP-1 cells were maintained in suspension with RPMI-1640 media (Sigma) containing 10% fetal bovine serum (Gibco), 1 mM of Pyruvate (Sigma), 2 mM of L-Glutamine (Sigma), and incubated at 37 °C with 5% CO<sub>2</sub>. THP-1 cells were routinely subcultured every 3 days at a cell density of 10<sup>5</sup> cells/mL. THP-1 cells were simultaneously differentiated with phorbol myristate acetate (PMA, 40 ng mL<sup>-1</sup>, Sigma) and infected with a single cell suspension of *M. tuberculosis* H37Rv-pATB45luc in a roller bottle at a MOI of 1:1. Cells were put in a roller bottle apparatus for 4 hours at 37 °C at 1.5 rpm. After this step of incubation, infected cells were washed four times by centrifugation at 400 g for 5 min and resuspended in fresh RPMI medium to remove extracellular bacilli. In the last wash, infected cells were resuspended in RPMI medium supplemented with 10% fetal bovine serum (Gibco), 2 mM L-glutamine and pyruvate at a concentration of 2 x 10<sup>5</sup> cells/mL. 50 µl of this cell suspension (typically 10000 cells per well) were dispensed into the wells of 384-well plates (white, flat bottom, Greiner).

(c) *Incubation of infected THP-1 cells with tested compounds.* Prior to addition of the infected cell suspension, the compounds (250 nL/well) were dispensed into the plates with an Echo liquid handler. The maximum DMSO concentration is 0.5%. Plates were allowed to incubate at 37 °C at 80% relative humidity for 4 days. Luciferase activity, proportional to bacterial load, was determined by using BrightGlo™ Luciferase Assay System (Promega, Madison, WI) according to the manufacturer's protocol. Resultant luminescence was measured in an Envision Multilabel Plate Reader (PerkinElmer) using the 384-plate Ultra Sensitive luminescence mode, with a measurement time of 200 ms per well. Results were processed by using an Excel spreadsheet and Grafit software. IC<sub>50</sub> and IC<sub>90</sub> values were calculated from the dose-response curves by non-linear regression analysis.

### 3.6.6. HepG2 cytotoxicity assay

HepG2 cells were cultured using Eagle's Minimum Essential Medium (MEM) supplemented with 10% heat-inactivated fetal bovine serum (FBS), 1% Non-Essential Amino Acid (NEAA) supplement and 1% penicillin/streptomycin. Prior to addition of the cell suspension, 250 nL of test compounds per well were pre-dispensed in tissue culture treated black clear-bottomed 384 well plates (Greiner, cat.# 781091) with an Echo 555 instrument. After that, 25 µL of HepG2 (ATCC HB-8065) cells (~3000 cells/well) grown to confluency in Eagle's MEM supplemented with 10% heat-

inactivated FBS, 1% NEAA and 1% Pencillin/Streptomycin were added to each well with the reagent dispenser. Plates were allowed to incubate at 37 °C with 20% O<sub>2</sub> and 5% CO<sub>2</sub> for 48 h.

After the incubation period (48 h), the plates were equilibrated to room temperature before proceeding to develop the luminescent signal. ATP levels measured with CellTiter Glo kit (Promega) were used as cell viability read-out. 25 µL of CellTiter Glo substrate dissolved in the buffer was added to each well. Plates were incubated at room temperature for 10 minutes for stabilization of luminescence signal and read on View Lux with excitation and emission filters of 613 and 655 nm, respectively.

### **3.6.7. Artificial membrane permeability**

The artificial phospholipid membrane technique was similar to the widely used Caco-2 cell monolayer permeation technique. In short, egg phosphatidyl choline (1.8%) and cholesterol (1%) were dissolved in *n*-decane. A small amount of the volatile mixture was applied to the bottom of the microfiltration filter inserts. Phosphate buffer (0.05 M, pH 7.05) was quickly added to the donors and receivers, and the lipids were allowed to form self-assembled lipid bilayers across the small holes in the filter. Permeation experiment was initiated by spiking the compounds of interest to the donor sides, and the experiment was stopped at a pre-determined elapsed time. The samples were withdrawn and transferred to appropriate vials for analysis by HPLC with UV detection.

### **3.6.8. Kinetic aqueous solubility (Chemi-Luminescent Nitrogen Detection, CLND)**

5 µL of 10 mM DMSO stock solution diluted to 100 µL with pH 7.4 phosphate buffered saline, equilibrated for 1 hour at room temperature, filtered through Millipore Multiscreen HTS-PCF filter plates (MSSL BPC). The filtrate was quantified by suitably calibrated flow injection Chemi-Luminescent Nitrogen Detection. The standard error of the CLND solubility determination is ±30 µM, the upper limit of the solubility is 500 µM when working from 10 mM DMSO stock solution.

### **3.6.9. Hydrophobicity (chromlogD) assay**

The chromatographic hydrophobicity index (CHI) values were measured using a reversed phase HPLC column (50 × 2 mm, 3 µm, Gemini NX C18, Phenomenex, UK) with fast acetonitrile gradient at starting mobile phase of pH = 7.4 as described.<sup>3</sup> CHI values were derived directly from the gradient retention time by using a calibration line obtained for standard compounds. The CHI value approximates to the volume % organic concentration when the compound eluted. CHI was

linearly transformed into ChromlogD by least-square fitting of experimental CHI values to calculated clogP values using the following formula:

$$\text{ChromlogD} = 0.0857 \times \text{CHI} - 2.0$$

The average error of the assay was  $\pm 3$  CHI unit or  $\pm 0.25$  ChromlogD.

### 3.6.10. Microsomal fraction stability experimental procedure

Pooled murine liver microsomes were purchased from Xenotech. Microsomes (final protein concentration 0.5 mg/mL),  $\text{MgCl}_2$  (final concentration 5 mM) and test compound (final substrate concentration 0.5  $\mu\text{M}$ ; final DMSO concentration 0.5 %) in 0.1 M phosphate buffer pH 7.4 were pre-incubated at 37 °C prior to the addition of NADPH (final concentration 1 mM) to initiate the reaction. The final incubation volume was 600  $\mu\text{L}$ . All incubations were performed singularly for each test compound. Each compound was incubated for 30 minutes and samples (90  $\mu\text{L}$ ) of incubate were taken at 0, 5, 10, 20 and 30 minutes. The reactions were stopped by the addition of sample to 200  $\mu\text{L}$  of acetonitrile:methanol (3:1) containing an internal standard. The terminated samples were centrifuged at 3700 rpm for 15 minutes at 4 °C to precipitate the protein. Quantitative analysis: following protein precipitation, the samples were analyzed using specific LC-MS/MS conditions. Data analysis: from a plot of  $\ln$  peak area ratio (compound peak area/internal standard peak area) against time, the gradient of the line was determined. Subsequently, half-life and intrinsic clearance were calculated using the equations below:

$$\text{Elimination rate constant (k)} = (-\text{gradient})$$

$$\text{Half life (t}_{1/2}\text{)}(\text{min}) = \frac{0.693}{k}$$

$$\text{Intrinsic Clearance (Cl}_{\text{int}}\text{)} (\text{mL}/\text{min}/\text{g}) =$$

$$\frac{0.693}{t_{1/2}} \times \frac{\text{mL of incubation}}{(\text{mg microsomal protein})} \times \frac{(\text{mg microsomal protein})}{(\text{g liver})}$$

The human biological samples were sourced ethically and their research use was in accord with the terms of the informed consents.

### 3.6.11. Blood stability assay

The stability of each compound was assessed in CD1 murine whole blood collected on the day of the experiment in EDTA tubes. Typically 1 mL of blood was spiked with 2  $\mu\text{L}$  of a 0.5 mM of each test compound solution to produce a 1  $\mu\text{M}$  incubation.

Three separate 300  $\mu\text{L}$  aliquots were then taken from each tube and incubated at 37 °C. At each time point (0, 5, 10, 20, 30, 60, 120, (240) min), 50  $\mu\text{L}$  of blood were collected from each sample over 50  $\mu\text{L}$  of MilliQ water. Samples were extracted by protein precipitation with 350  $\mu\text{L}$  of 0.1% AcOH acetonitrile methanol 3-1 (v:v) containing 1  $\mu\text{M}$  internal standard and centrifuged for 10 min. Supernatants were collected prior the injection onto an LC-MS/MS system. Analyte/Internal standard peak area ratios were referenced to the zero time-point samples as 100% in order to determine the percentage of compound remaining for each time-point. Ln plots of the % remaining for each compound were used to determine the half-life for the blood incubations.

#### **3.6.12. hERG assay**

The hERG activity was measured using medium-throughput electrophysiology (IonWorks™ HT).<sup>139,140,144</sup> These assays were performed at the PTS (Platform Technology Science) Department in GSK Stevenage.

# Chapter 4

---

*DprE1 inhibitors: Aims and Objectives*



## 4. DprE1 inhibitors: aims and objectives

### 4.1. DprE<sub>1</sub> as drug target

The major cell wall polysaccharide of mycobacteria is a branched-chain arabinogalactan in which arabinan chains, which are composed exclusively of D-arabinofuranose residues, are attached to galactofuranose residues.<sup>145</sup> Decaprenylphosphoryl-β-D-arabinose (DPA) is the only known donor of arabinose residues in bacteria for the synthesis of the essential cell wall components, arabinogalactan and lipoarabinomannan.<sup>146</sup> *M. tuberculosis* DprE1 (Figure 4.1) catalyzes the flavin adenine dinucleotide (FAD) dependent oxidation of decaprenylphosphoryl-β-D-ribose (DPR) to decaprenylphosphoryl-β-D-2'-keto-erythro-pentafuranose (DPX). DPX is subsequently reduced to DPA by the reduced pyridine nucleotide dependent enzyme, DprE2.<sup>147</sup>

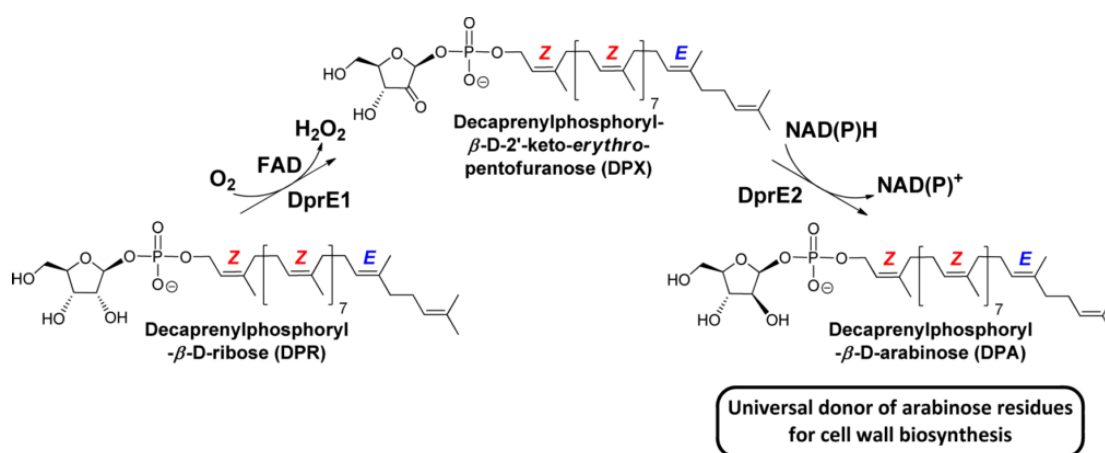


**Figure 4.1. Reactions catalysed by DprE<sub>1</sub> and DprE<sub>2</sub>. Conversion of DPR to DPA involves oxidation and subsequent reduction of the C2' hydroxyl via a keto-intermediate (DPX).<sup>147</sup>**

Using gene knockout and knock-down technologies, Kolly *et al.* have genetically validated DprE1 as a drug target. Downregulation or depletion of DprE1 resulted in swelling of the bacteria, cell wall damage and lysis as observed at the single cell level, by real time microscopy and electron microscopy.<sup>148</sup> Inhibition of the DprE<sub>1</sub> enzyme interrupts the essential cell wall biosynthesis leading to mycobacteria death.

DprE<sub>1</sub> is localized in the periplasmic space of the mycobacterial cell wall, which makes it more accessible to drugs and could be a critical factor contributing to its vulnerability.<sup>149</sup> Due to its localization, drugs targeting DprE<sub>1</sub> might escape the action of efflux pumps, and potential cytoplasmic trapping or inactivation mechanisms that might confer intrinsic resistance.

DprE<sub>1</sub> has been shown to be the target of the mechanism-based suicide inhibitor class of nitroaromatic compounds, including BTZ043, which covalently bind to the active site, thereby

quantitatively and irreversibly inactivating DprE<sub>1</sub>, demonstrating nanomolar potency against both drug-susceptible and multidrug-resistant strains of the tubercle bacillus.<sup>150,151</sup> Several reversible inhibitors of DprE1 such as TCA1,<sup>152</sup> azaindoles,<sup>153,154</sup> 4-aminoquinolones<sup>155</sup> and pyrazolopyridones<sup>156</sup> (shown in Figure 4.2) have also been identified recently suggesting that *M. tuberculosis* DprE<sub>1</sub> is a highly tractable target.

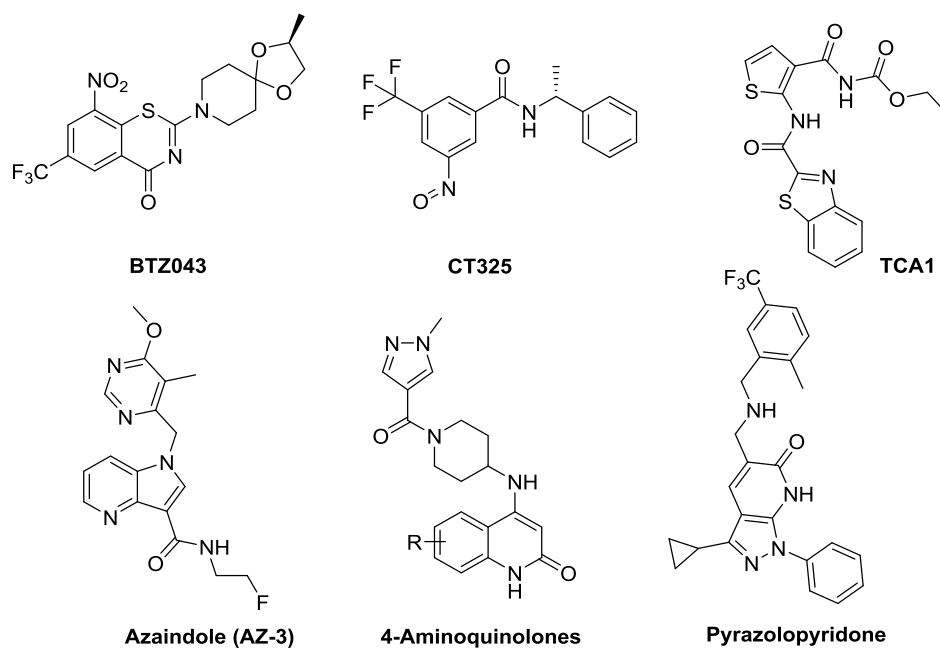


**Figure 4.2. Known DprE<sub>1</sub> inhibitors.**

The enzyme consists of an FAD binding and a substrate binding domain, with the flavin moiety of FAD positioned at the interface between the two domains. The substrate binding domain includes two disordered loop regions that leave the active site open and accessible for inhibitors.<sup>152</sup> Structures of complexes with the BTZ-derived nitroso derivative CT325 (Figure 4.2) reveal the mode of inhibitor binding, which includes a covalent link.<sup>150</sup> On the other hand, the reversible inhibitor TCA1 binds in the central cavity of the enzyme (Figure 4.3) where noncovalent interactions between TCA1 and the enzyme are dominated by hydrophobic and van der Waals interactions.<sup>152</sup> Flavin contributes a large fraction of the total contact surface, while polar contacts are sparse. Superimposition of the structures of DprE1 bound to the BTZ analog (CT325) and TCA1 showed that the binding sites of these two inhibitors overlap significantly.<sup>152</sup>



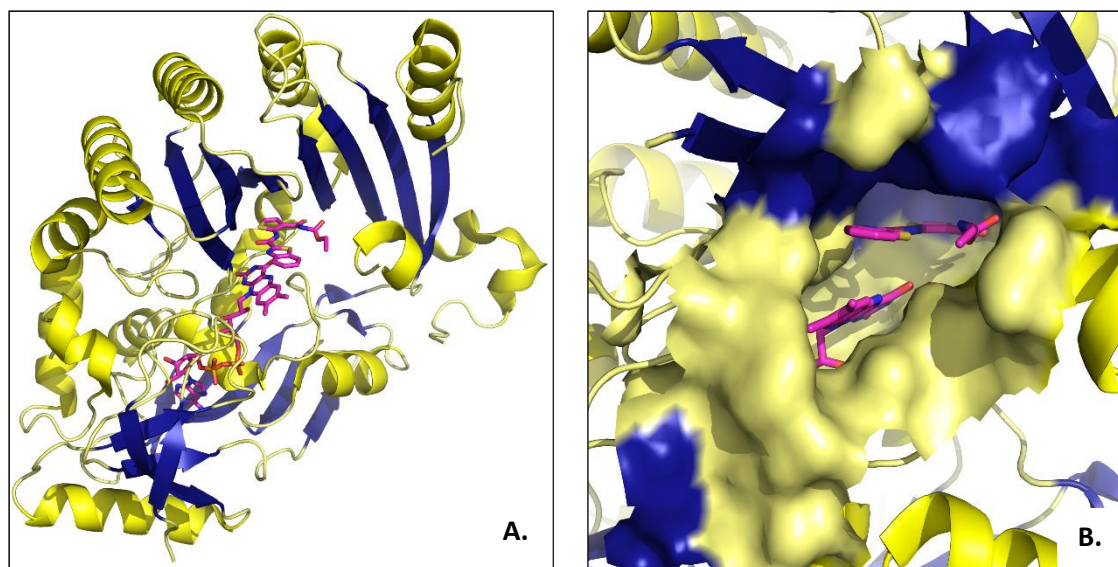


**Figure 4.3. Three-dimensional (3D) structure of DprE1. A. Ribbon diagram of the crystal structure of DprE1 in complex with TCA1 (PDB:4KW5). B. Close-up view of the DprE1-TCA1 active site structure showing inhibitor binding in more detail. Images were prepared using MOE.**

The vulnerability of DprE<sub>1</sub> and the remarkable potency of the best inhibitors make this enzyme a promising drug target for the discovery of new drugs to combat TB. Therefore, in recent years DprE1 has been one of the hottest targets, with five inhibitors belonging to different chemical classes having been published and others are under investigation. Taking into account the extensive research that has been made in drugs targeting *M. tuberculosis* DprE1, it is likely that at least one of these drugs could enter clinical trials, which would greatly increase the chances of survival of patients affected from MDR-TB.<sup>157</sup>

## 4.2.Aims and objectives

In continuation of our research efforts on novel antimycobacterial compounds, a second project was initiated related with DprE1 inhibitors. Under the OpenMedChem project, we were working in a team of three medicinal chemists (Eleni Pitta, Maciej Rogacki and Olga Balabon).

During the DprE1 high-throughput screening (HTS) campaign performed by GSK, approximately 1.8 million compounds were evaluated using a fluorescence-based biochemical assay. This assay is a redox cycling enzyme assay that uses farnesylphosphoryl- $\beta$ -D-ribose (FPR) and resazurin as substrates and generates farnesylphosphoryl- $\beta$ -D-2'-keto-erythro-pentafuranose (FPX) and resorufin as products. Oxidation of FPR to FPX by DprE1 results in the formation of a two-electron reduced flavin intermediate (FADH<sub>2</sub>). To complete the catalytic cycle, the FADH<sub>2</sub> has to be reoxidized to FAD that is accomplished by resazurin, which upon reduction generates the highly fluorescent product resorufin (Figure 4.4).<sup>147</sup>

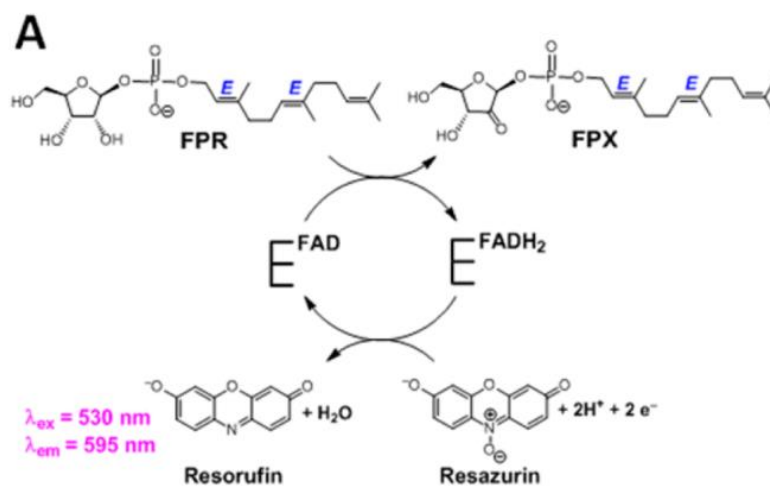


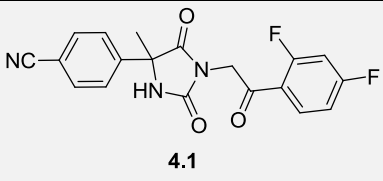
**Figure 4.4. Redox cycling enzymatic assay principle for DprE1. As FPR is oxidized to FPX, resazurin is reduced to resorufin and can be monitored by an increase in fluorescence intensity at 595 nm. E-FAD and E-FADH<sub>2</sub> denote oxidized enzyme and two-electron reduced enzyme, respectively.**

After triaging the hits, 3986 compounds were progressed to dose-response analysis allowing pIC<sub>50</sub> estimation and ranking of hits based on potency and ligand efficiency. An orthogonal mass spectrometry-based assay (the RapidFire™ assay) was then used to reconfirm (or dismiss) the potency data from the primary assay. Mass spectrometry offers an attractive alternative to fluorescent assays for screening, because it can be monitored directly based on mass without the risk of fluorescence interference.<sup>158,159</sup>

Once the DprE1 inhibitory activity was confirmed using both methods, the obtained hits were clustered and profiled (physicochemical/*in vitro* properties). The criteria used during this process were the DprE1 potency - pIC<sub>50</sub> to be ≥5 (desirable ≥6), the cellular potency - MIC to be ≤50 μM (desirable ≤10 μM), and HepG2 IC<sub>50</sub> to be >100 or the ratio HepG2 IC<sub>50</sub>/MIC to be >10. Also, lipophilicity (chromlogD) to be ≤5. An analogue search was performed and the obtained analogues were evaluated for DprE1 inhibitory activity and an indication of SAR. The possible risks were identified and the synthetic feasibility was determined. Taking into account the above mentioned parameters, the clusters were prioritized.

One of the more promising clusters was represented by the hydantoin derivative **4.1** (shown in Table 4.1) which appeared especially promising due to its significant DprE1 inhibition (pIC<sub>50</sub> = 7) and cellular activity with a MIC value of 8.3 μM (Table 4.1). This compound contained a hydantoin core alkylated at N-3 with a disubstituted phenyloxyethyl group and at position 5 possesses two substituents, a 4-cyanophenyl and a methyl group.

Table 4.1. *In vitro* profile and physicochemical properties

Compound		Racemic mixture	( <i>R</i> )-enantiomer	( <i>S</i> )-enantiomer
	4.1			
<b>Activity</b>	Molecular weight	369	369	369
	DprE1 pIC <sub>50</sub>	7.0	7.2	4.2
	MIC (μM) <sup>[a]</sup>	8.3	6.7	>125
<b>Physicochemical properties</b>	Intracellular IC <sub>90</sub> (μM) <sup>[b]</sup>	4.0	1.3	>50
	Permeability (nm/sec) <sup>[c]</sup>	515	493	507
	Solubility (μM) <sup>[d]</sup>	202	355	344
<b>Toxicity</b>	ChromlogD <sup>[e]</sup>	4.54	4.51	4.51
	Cytotoxicity IC <sub>50</sub> (μM) <sup>[f]</sup>	>100	>100	>100
	Cardiotoxicity hERG IC <sub>50</sub> (μM)	25	13	32
<b>Metabolic stability<sup>[g]</sup></b>	Cl <sub>int</sub> (mouse) (mL/min.g tissue)	4.39	2.61	5.08
	Cl <sub>int</sub> (human) (mL/min.g tissue)	0.56	0.56	0.72

<sup>a</sup>MIC against *M. tuberculosis* (H37Rv); <sup>b</sup>IC<sub>90</sub> against infected Human THP-1 macrophages with *M. tuberculosis* (H37Rv). <sup>c</sup>artificial membrane permeability (AMP); <sup>d</sup>*in vitro* profiling for kinetic aqueous solubility (CLND, chemiluminescent nitrogen detection); <sup>e</sup> chromlogD values at pH = 7.4; <sup>f</sup>HepG2, human caucasian hepatocyte carcinoma; <sup>g</sup>*in vitro* microsomal fraction stability (mouse and human) results, imidazolam was used as control with Cl<sub>int</sub> = 27.5 ±0.4 and 6.4 mL min<sup>-1</sup>g<sup>-1</sup> in mouse and human, respectively.

In addition to the promising pharmacological profile, **4.1** possessed a good physicochemical profile for a hit-compound, with good solubility, artificial membrane permeability and lipophilicity (chromlogD) (Table 4.1). Regarding the cytotoxicity data, the hit compound showed no measurable toxicity at the HepG2 assay (IC<sub>50</sub> >100 μM). Also, the hit compound presented a moderate to good *in vitro* clearance in mouse (4.4 mL/min.g tissue) and in human (0.56 mL/min.g tissue) liver microsomes. An analogue search revealed eleven analogues with DprE<sub>1</sub> pIC<sub>50</sub> >4.

Enantiomeric separation showed that only the (*R*)-enantiomer is active while the (*S*)-enantiomer is completely inactive.

Lastly, hit **4.1** was tested in a series of assays designed to measure the effect of test compounds on transporters, receptor sites, ion channels, and other enzymes associated with toxic and adverse events – such as hERG, GABA and the PXR receptors. The results from this panel raised no flags against the enzymes included in the panel, with the exception of the hERG and GABA-A receptors. Further investigation about hERG inhibition as an indicator of possible cardiotoxicity revealed a hERG flag with an IC<sub>50</sub> value at 25 μM. Unfortunately, the (*R*)-enantiomer which is the

most active was also characterized by higher hERG-inhibition potency ( $IC_{50}$  13  $\mu$ M) than the inactive (*S*)-enantiomer ( $IC_{50}$  32  $\mu$ M). The activity against the GABA-A receptor was a concern but the compound was only very weakly active, therefore further investigation was postponed for later stages of the series development.

Summarizing, compound **4.1** had a satisfactory hit-profile. However, further optimization was necessary to produce a high quality lead. Therefore, Hit-to-Lead (H2L) optimization was the main objective of this work dealing with hydantoin-derived DprE1 inhibitors. At the same time, the analogues that were prepared as part of these H2L endeavors generated a significant amount of SAR information for this class of molecules.

Specific aspects of the H2L program are discussed below:

#### **4.2.1. Improvement of safety and metabolic stability**

There were three structural elements of hit compound **4.1** that were considered potentially problematic for safety and metabolic stability: (1) the hydantoin (imidazolidine-2,4-dione) core, (2) the carbonitrile group and (3) the benzylic keto function.

The first moiety selected for replacement was the hydantoin function. Importantly, several hydantoin-containing drugs, mainly used as anticonvulsants, have been linked to the fetal hydantoin syndrome which includes congenital malformations in the offspring of epileptic mothers.<sup>160,161,162</sup> Additionally, it has been found that many hydantoins bind to voltage-gate sodium channels, leading to potential cardiotoxicity.<sup>163</sup> Moreover, for the preparation of the hydantoin core, potassium cyanide is used. Especially in large scale synthesis, unreacted cyanide salt could remain as an impurity, potentially leading to significant safety issues. All these concerns justified replacing the hydantoin with another, structurally related ring system.

In addition, aliphatic and aromatic carbonitriles have been reported to react covalently with cysteines present in proteins, to form thiazoline derivatives.<sup>164</sup> This reactivity could lead to organ toxicity or idiosyncratic reactions.<sup>165</sup> Although several carbonitrile-containing drugs are currently used clinically, a decrease of risks related to nonspecific covalent binding could be obtained by removing the carbonitrile. This is certainly important in the framework of Tb-therapy that generally involves long-term pharmacological treatment.

Lastly, the methylene linker between the hydantoin ring and the keto group was highly activated potentially making it susceptible to oxidative metabolization. Moreover, the electrophilic benzylic keto group was considered a possible metabolic liability of the molecule which could possibly lead to the corresponding secondary alcohol after reduction.<sup>166</sup> Therefore, a linker exploration was

planned in order to evaluate the significance of the ketone and the possibility to omit or replace it with other groups. Moreover, the possible metabolite of the hit compound **4.1** possessing a secondary alcohol instead of the keto group was prepared and evaluated.

#### 4.2.2. Enhancement of potency and affinity

Along with addressing potential safety and metabolic issues, an increase of anti-tubercular potency and the DprE<sub>1</sub> affinity was also pursued. In order to progress a compound to a Lead Optimization program, an MIC value <1 μM and a pIC<sub>50</sub> value >7 were considered important.

In this framework, the carbonitrile group deserves additional mentioning. The analogue of **4.1** lacking a carbonitrile, was already present among the evaluated compounds and had been found to possess significantly lower target activity (pIC<sub>50</sub>=4.4) and no cellular potency against *M. tuberculosis* (MIC >80 μM). Whether this is related to the functional group's potential for covalent binding was unclear at the onset of our investigations. Nonetheless, the finding indicates that exploring the left-side aryl ring's substitution pattern would be a critical element of any H2L study undertaken for **4.1**. In addition, exploration of the phenyl group at the right-hand side of the molecule was also considered a chance for improving activity. A second round of optimization dealing with this side of the molecule was planned once an appropriate replacement for the carbonitrile was found.

#### 4.2.3. Improvement of physicochemical properties

Although most of the physicochemical parameters of hit **4.1** were well within acceptable ranges for a hit compound, further improvement was desired for a derived lead. Reduction of the chromlogD value below 4 is highly desirable in drug discovery programs because it can reduce non-specific binding. Furthermore, it can be expected to slow down intrinsic clearance and increase solubility. A balance between hydro- and lipophilicity should nonetheless be respected, since very low values can lead to low permeability and low bioavailability.<sup>167,101</sup>

#### 4.2.4. *In vivo* proof of concept

The ultimate goal of this H2L program was to achieve *in vivo* proof of concept. Therefore, the best compound(s) would be evaluated in a murine model of *M. tuberculosis* infection that uses CFU reduction, compound bioavailability and eventual toxicity as decisive read-outs. The *in vivo* efficacy is one of the most important requirements in order to progress a compound to Lead Optimization.



# Chapter 5

---

*DprE1 Inhibitors*





## 5. DprE<sub>1</sub> inhibitors

### 5.1.Design

Prompted by the promising results regarding the hit compound **4.1**, we decided to initiate medicinal chemistry efforts around this novel class of DprE1 inhibitors. Therefore, we divided the structure of the initial hit into four parts as shown in Figure 5.1., namely the left-hand side aryl, hydantoin core, linker and right-hand side aryl. Taking into account the structural concerns mentioned earlier together with a SAR exploration, initial efforts focused around the linker, hydantoin core and left-hand side aryl.

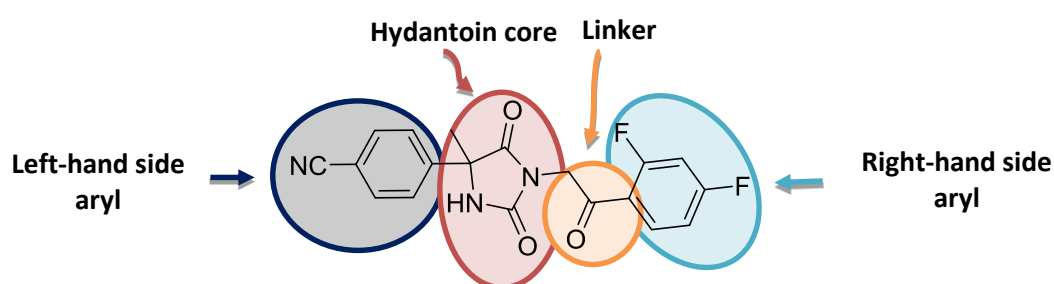
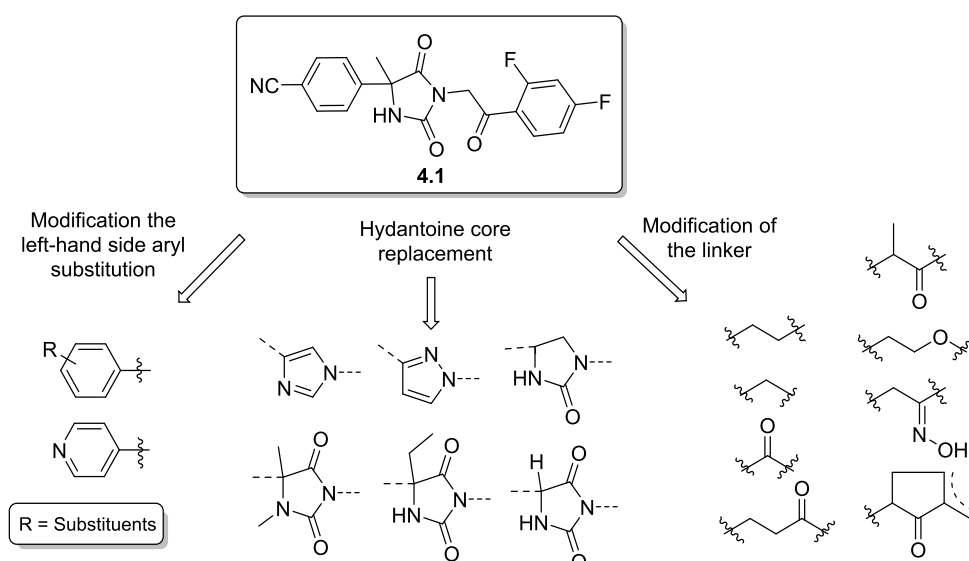


Figure 5.1. Initial hit **4.1** and structure division.

As shown in Scheme 5.1, the design of new compounds included:

- Modifications of the linker.** Removal of the keto group, elongation or shortening of the linker, substitution of the methylene bridge, an ether, an oxime, a 5-membered ring closure.
- Hydantoin core replacements.** Replacement by 5-membered aromatic or non-aromatic rings, methylation, elongation or removal of the methyl group at position 5.
- Left-hand side modifications.** Different substituents, heterocycles.



Scheme 5.1. Design of new compounds.

## 5.2. First round of Hit-to-Lead optimization

Due to internal availability of intermediate **5.1** (Figure 5.2), it was decided that for the initial round of optimization this fragment could be used as a surrogate for the corresponding, carbonitrile containing portion of hit **4.1**. To verify the validity of this approach, *para*-methoxy-based compounds **5.2** and **5.3**, present in GSK library, were evaluated as antimycobacterials and DprE1 inhibitors. Although they did not achieve the same whole cell potency as **4.1**, they exhibited sufficient DprE<sub>1</sub> inhibitory enzymatic potency (pIC<sub>50</sub> 5.7-6.8) for early comparative purposes. Therefore, intermediate **5.1** was considered suitable to be used in compounds with linker and hydantoin core modifications.

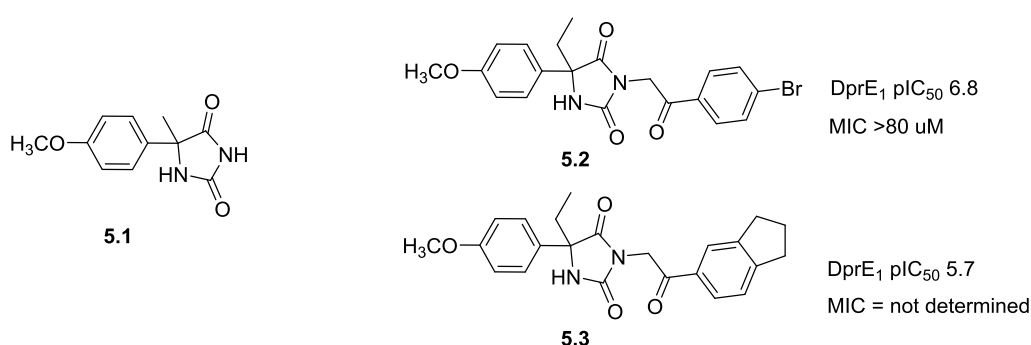


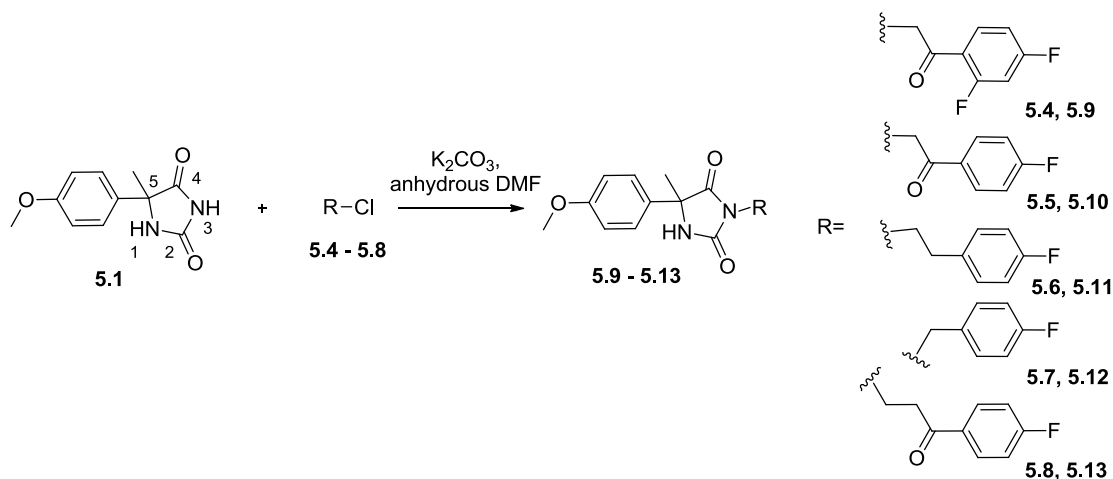
**Figure 5.2.** Available intermediate **5.1** and GSK library compounds **5.2** and **5.3**.

A total of around 120 novel inhibitors were synthesized for this first round of optimization within the OpenMedChem project, while in the present thesis, around 40 analogues are described. The target compounds were clustered according to the modification type they contained, relative to reference compound **4.1**.

### 5.2.1. Chemistry

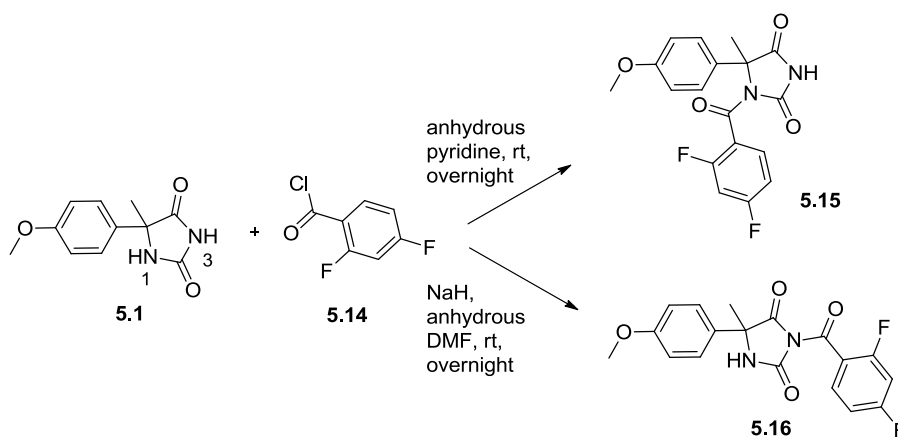
#### 5.2.1.1. Linker modification

For the exploration of the linker, analogues with different linker lengths (shorter or longer) were prepared and the linker keto group was removed or replaced. For the first group of compounds, the 4-fluoro reagent was used due to commercial availability instead of the 2,4-difluoro which was not available. Therefore, compound **5.10** was synthesized in order to be used for direct comparisons. As shown in Scheme 5.2, alkylation of hydantoin **5.1** using different halides **5.4-5.8** in the presence of potassium carbonate (K<sub>2</sub>CO<sub>3</sub>) resulted in final compounds **5.9-5.13**. Under these conditions, alkylation occurred selectively at the *N*(3) position (unambiguous structural identification was carried out as described in the next section, *Structure Elucidation*).



**Scheme 5.2. Synthesis of compounds 5.9-5.13 with a modified linker.**

On the other hand, acylation of **5.1** with acyl chloride **5.14** in the presence of anhydrous pyridine led to compound **5.15** which was acylated at *N*(1) (structural identification was carried out as described in the next section, *Structure Elucidation*), as shown in Scheme 5.3. In order to prepare the target compound **5.16**, hydantoin **5.1** was first treated with sodium hydride (NaH) and followed by addition of acyl chloride **5.14**. However, the obtained product **5.16** was unstable and hydrolysis was observed in acidic aqueous media.

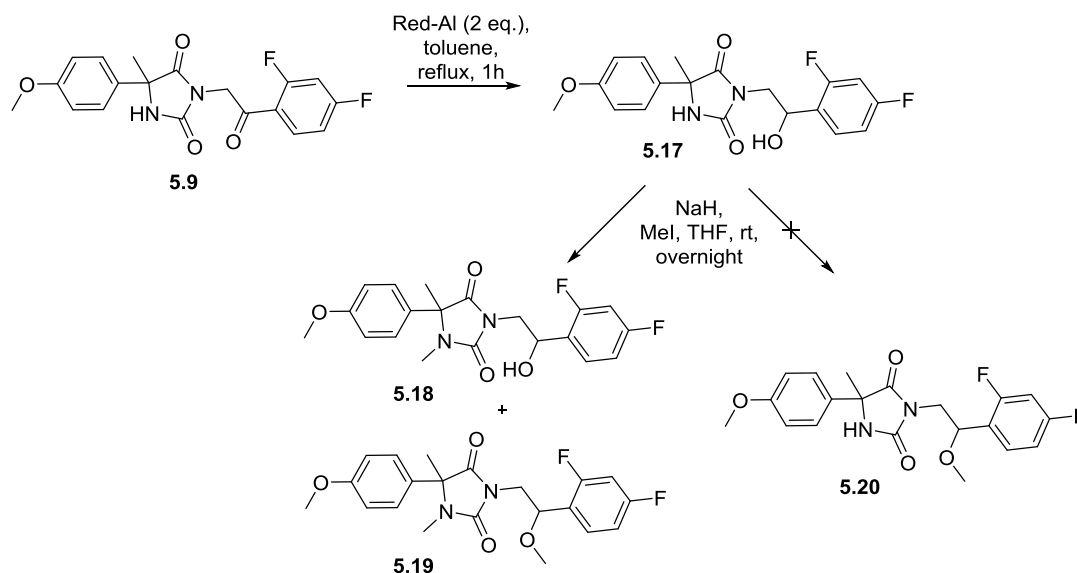


**Scheme 5.3. Synthesis of acylated analogues 5.15 and 5.16.**

The regioselectivity observed under these first acylation conditions could be justified due to the expected instability of the *N*(3)-acylated compound which would have three carbonyl groups attached on the same nitrogen atom. However, when sodium hydride which is a strong base was used, the most acidic proton *H*(3) was deprotonated and acylation was forced to occur at position 3.

Reduction of compound **5.9** using Red-Al in toluene and heating under reflux for 1 h gave the desired mono-reduced alcohol **5.17**. Compound **5.17** could be a possible metabolite of **5.9**, making

its potential bioactivity particularly interesting<sup>168</sup> Subsequently, methylation of compound **5.17** targeting compound **5.20** did not furnish the desired compound. Instead, it provided the mono-*N*-methylated compound **5.18** (structural identification was carried out as described in the next section, *Structure Elucidation*) with the methyl group attached on the hydantoin *N*(1) atom and the dimethylated compound **5.19** (Scheme 5.4).



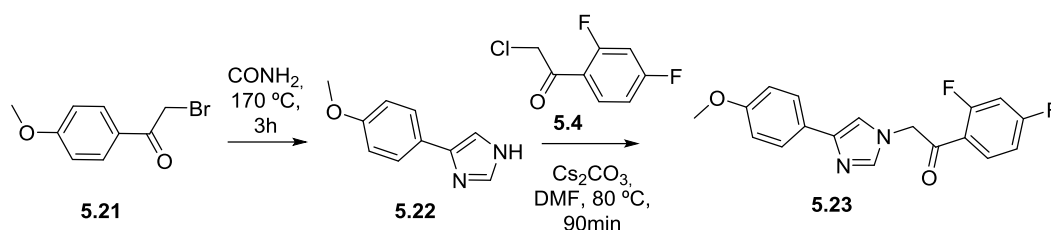
**Scheme 5.4.** Synthesis of the alcohol **5.14** and attempts for *O*-methylation.

Since the originally desired methyl ether **5.20** was not considered crucial for the exploration and development of the series, no further attempts to synthesize this analogue were made.

#### 5.2.1.2. Hydantoin core replacements

To replace the hydantoin core, two compounds were prepared containing an aromatic ring (imidazole) or a non-aromatic ring (imidazolidin-2-one).

Formation of the imidazole ring by a Hantzsch reaction starting from **5.21** and subsequent alkylation of the obtained intermediate **5.22** with 2-chloro-2',4'-difluoroacetophenone **5.4** under basic conditions delivered compound **5.23** (Scheme 5.5). Alkylation occurred at the desired position 1 (unambiguous structural identification was carried out as described in the next section, *Structure Elucidation*).

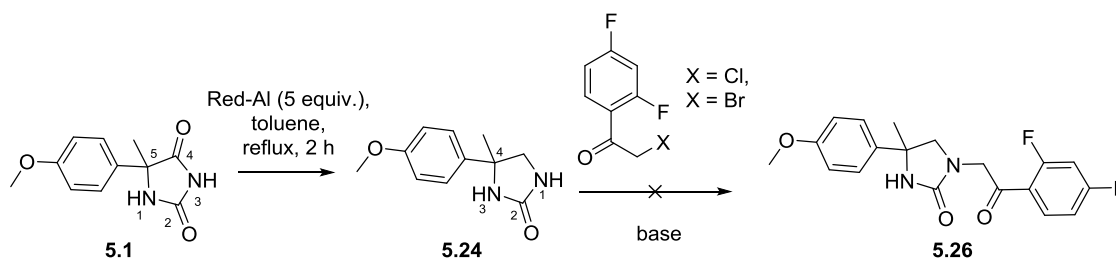


**Scheme 5.5. Replacement of the hydantoin core with imidazole.**

On the contrary, the synthesis of the imidazolidin-2-one analogue (**5.26**) was more challenging and required three different synthetic approaches in order to obtain the desired compound.

#### Approach A: Reduction of the hydantoin core followed by alkylation

Reduction of the hydantoin core prior to alkylation was considered preferable, since it avoids problems related to potential linker incompatibility with the reductant. Therefore, compound **5.1** was subjected to Red-Al reduction in refluxing toluene to yield imidazolidin-2-one derivative **5.24**. The position of carbonyl reduction (at carbon atom 4) was in accordance with the literature<sup>169</sup> and confirmed by <sup>13</sup>C-NMR spectra. However, all alkylation attempts on the latter intermediate failed due to degradation or self-reaction of 2-chloro-2',4'-difluoroacetophenone **5.4** during long reaction times under basic conditions (Scheme 5.6).



**Scheme 5.6. Synthetic approach A to obtain the imidazolidin-2-one analogue 5.26.**

An overview of the alkylation conditions evaluated, is given in Table 5.1.

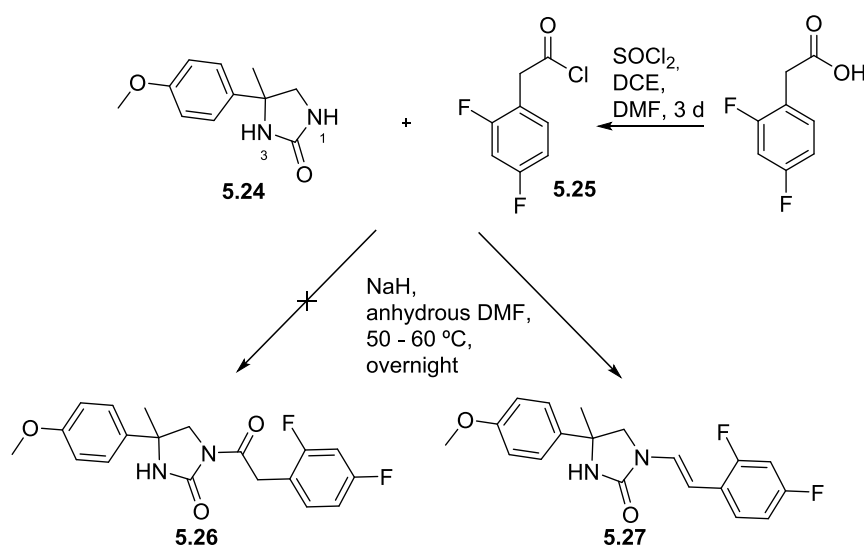
**Table 5.1. Experimental conditions tested for the alkylation of the imidazolidin-2-one core 5.24.**

	Reactants and relative amounts (Mol. Equiv.)			Solvent	Reaction time	Temperature
	5.24	Alkyl halide	Base			
<b>1</b>	1	R-Cl, 1.1	K <sub>2</sub> CO <sub>3</sub> , 1.1	anhyd. DMF	3 h	r.t. <sup>[a]</sup>
<b>2</b>	1	R-Cl, 1	K <sub>2</sub> CO <sub>3</sub> , 1.1	anhyd. DMF	20 h	r.t. <sup>[a]</sup>
<b>3</b>	1	R-Cl, 1	K <sub>2</sub> CO <sub>3</sub> , 1.2	anhyd. acetone	4 d	r.t. <sup>[a]</sup>
<b>4</b>	1	R-Cl, 2	Cs <sub>2</sub> CO <sub>3</sub> , 1.2	DMF	2.5 h	80 °C

<b>5</b>	1	R-Cl, 2	Cs <sub>2</sub> CO <sub>3</sub> , 1.2	DMSO	18 h	80 °C
<b>6</b>	1	R-Cl, 1	NaH, 1.2	anhyd. acetone	4 d	r.t. <sup>[a]</sup>
<b>7</b>	1	R-Cl, 1	NaH, 1.2	anhyd. DMF	40 h	r.t. <sup>[a]</sup>
<b>8</b>	1	R-Cl, 2	NaH, 10	anhyd. DMSO	18 h	r.t. <sup>[a]</sup>
<b>9</b>	1	R-Br, 1.5	NaH, 10	anhyd. DMSO	18 h	r.t. <sup>[a]</sup>
<b>10</b>	1	R-Cl, 2 KI, 0.1	NaH, 1.3	anhyd. THF	4 h	70 °C

<sup>a</sup>r.t. = room temperature.

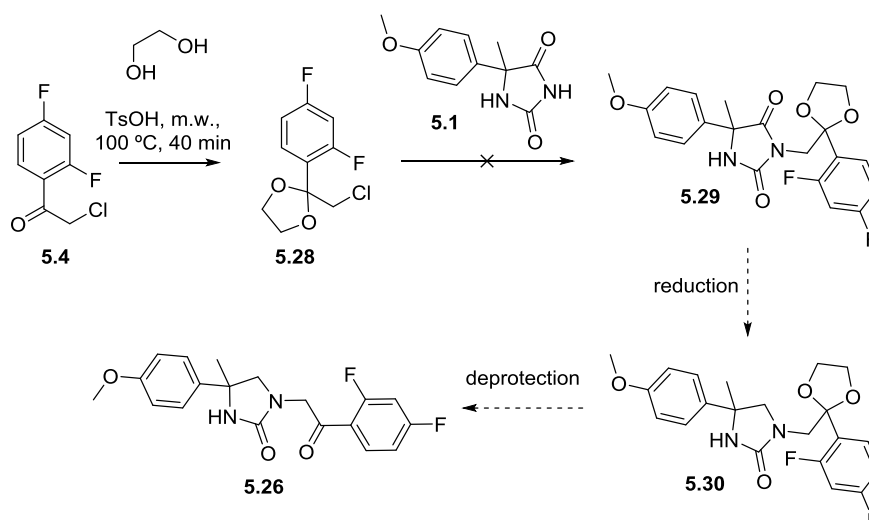
Next, acylation of the imidazolidin-2-one core was attempted as shown in Scheme 5.7. The acyl chloride **5.25** was obtained from the corresponding carboxylic acid using thionyl chloride (SOCl<sub>2</sub>). Subsequent acylation of intermediate **5.24** delivered the non-expected enamine **5.27** (assignment details in the following section *Structure elucidation*) in very low yield instead of the expected **5.26** compound. The obtained side product **5.27** was considered relevant to the series and therefore submitted to biological evaluation.



**Scheme 5.7. Acylation of the imidazolidin-2-one core 5.24.**

### Approach B: Protection of the linker keto group before reduction

Since alkylation of the imidazolin-2-one core failed, an alternative strategy was investigated that involved reduction of the hydantoin core after introduction of the *N*-substituent. To circumvent reduction chemoselectivity issues, the keto group of the linker had to be protected first (Scheme 5.8).



**Scheme 5.8. Synthetic approach B to obtain the imidazolidine-2-one analogue 5.26.**

For protection of the linker keto group, transformation to the corresponding acetal (**5.28**) was chosen. Reaction conditions evaluated during the optimization of this reaction are presented in Table 5.2. As can be seen, the first reaction using trimethylchlorosilane ( $\text{Me}_3\text{SiCl}$ ) at room temperature did not give the desired product. However, a second method using a catalytic amount of toluene sulfonic acid (TsOH) and microwave irradiation for 40 min at 100 °C gave the target compound with modest yield (35%). To increase the yield, addition of drying agents was tested as water was produced during the reaction. However, molecular sieves were found not to significantly influence the outcome of the reaction, while addition of sodium sulfate ( $\text{Na}_2\text{SO}_4$ ) to the reaction mixture completely inhibited acetal formation.

**Table 5.2. Experimental conditions tested for the protection of the keto group (5.4).**

	Reactants and relative amounts (Mol. Equiv.)			Drying agent	Time	Temperature, method	Yield (%)
	5.4	Ethylene glycol	Catalyst				
1	1	136	$\text{Me}_3\text{SiCl}$ , 0.5	molecular sieves	18 h	r.t. <sup>[a]</sup>	0
2	1	15	TsOH, 0.015	-	10 m	200 °C, m.w. <sup>[b]</sup>	n.i. <sup>[c]</sup>
3	1	34	TsOH, 0.015	-	40 m	100 °C, m.w. <sup>[b]</sup>	35
4	1	15	TsOH, 0.015	molecular sieves	1 h	100 °C, m.w. <sup>[b]</sup>	34
5	1	15	TsOH, 0.015	$\text{Na}_2\text{SO}_4$	1 h	100 °C, m.w. <sup>[b]</sup>	0

<sup>a</sup>r.t. = room temperature; <sup>b</sup>m.w. = microwave irradiation; <sup>c</sup>n.i. = not isolated.

The next step involved alkylation of the hydantoin core with the obtained  $\alpha$ -chloro acetal **5.28**. All tested conditions which are reported in Table 5.3, failed to deliver the desired compound **5.29**.

**Table 5.3. Experimental conditions tested for the coupling of acetal 5.28 with the hydantoin core 5.1.**

	Reactants and relative amounts (Mol. Equiv.)				Solvent	Time	Temperature	Yield (%)
	5.1	5.28	Base	Alkali metal iodide				
<b>1</b>	1	1	K <sub>2</sub> CO <sub>3</sub> , 1.2	-	anhyd. DMF	23 h	r.t. <sup>[a]</sup>	0
<b>2</b>	1	1	K <sub>2</sub> CO <sub>3</sub> , 3.2	NaI, 0.1	anhyd. DMF	O/N <sup>[b]</sup>	60 °C	0
<b>3</b>	1	1.1	NaH, 1.2	-	anhyd. DMF	O/N <sup>[b]</sup>	r.t. <sup>[a]</sup>	0
<b>4</b>	1	1.1	NaH, 1.2	KI, 0.1	anhyd. DMF	O/W <sup>[c]</sup>	60 °C	0
<b>5</b>	1	2	NaH, 1.3	KI, 0.1	anhyd. THF	4 h	70 °C	0

<sup>a</sup>r.t. = room temperature; <sup>b</sup>O/N = overnight; <sup>c</sup>O/W = over weekend.

A mild (K<sub>2</sub>CO<sub>3</sub>) and a stronger base (NaH) were used to promote the reaction without success though. Addition of alkali metal iodides such as NaI or KI (Finkelstein reaction), with the purpose to replace chlorine by iodine and therefore to increase the reactivity of intermediate **5.28**, also failed to give the desired product. Steric hindrance and electronics of the ketal which are highly unfavourable could be possible explanations for the very low reactivity observed.

### Approach C: Alkylation followed by reduction and mild oxidation

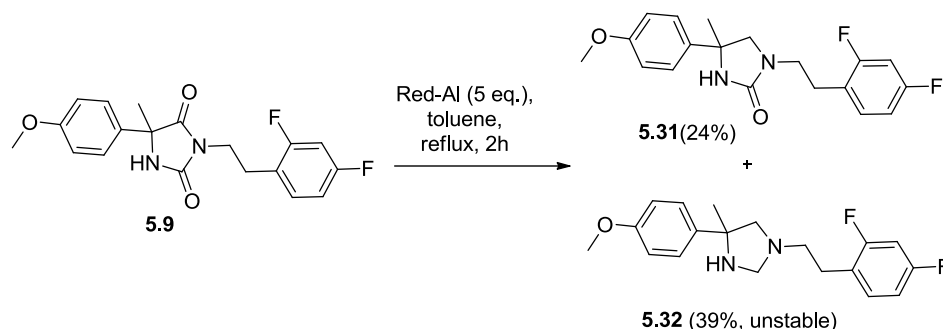
The third approach included the simultaneous reduction of the keto group and the hydantoin's 4-oxo function in **5.9** to the corresponding secondary alcohol and imidazolidin-2-one core. Afterwards, selective re-oxidation of the alcohol was expected to lead to target compound **5.26**.

As shown in Schemes 5.4 and 5.6, Red-Al had already been used successfully for either reducing the keto-group or the 4-oxo function in intermediates containing one of both functionalities. For the keto group, 2 equivalents of Red-Al in toluene under reflux for 1 hour were used (Scheme 5.4). For the oxo-function, 5 equivalents of Red-Al in toluene under reflux for 2 hours delivered the corresponding 4-methylene analogue (Scheme 5.6).

In order to evaluate reaction conditions for the reduction of the oxo-group in *N*-substituted hydantoin derivatives, **5.9** was used as a test compound (Scheme 5.9). The same conditions (Red-Al (5 equiv.), reflux, 2 h) as used previously for the reduction of **5.1** to **5.24** were applied. The

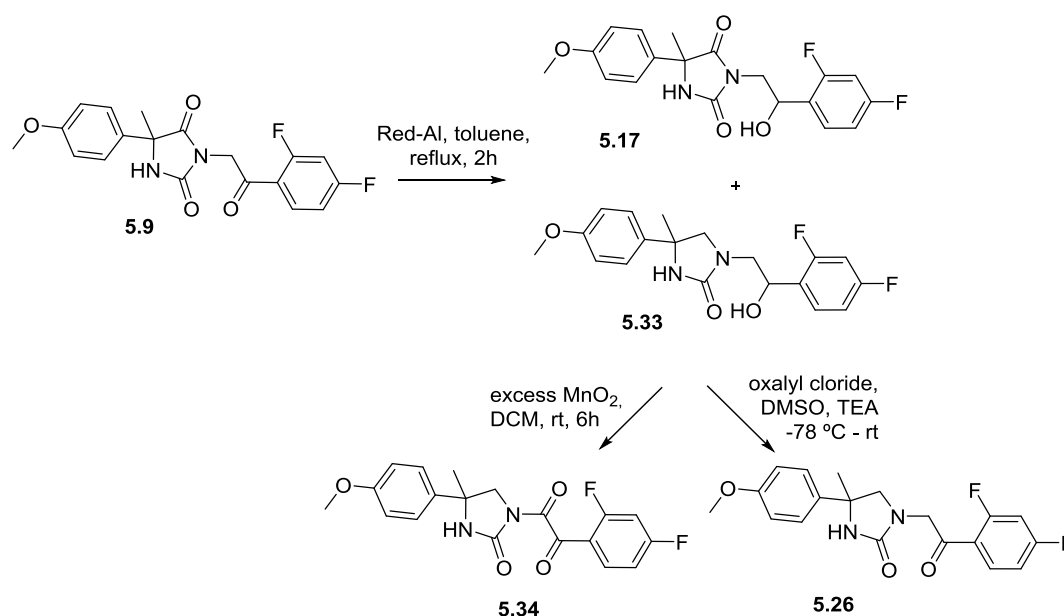


mono- (**5.31**) and doubly reduced (**5.32**) analogues were obtained. The latter, an unstable imidazolidine derivative was the major product of the transformation.



**Scheme 5.9. Validation of the reduction method.**

Therefore, for the reduction of compound **5.9** (a precursor to target product **5.26**), only 2 equivalents of Red-Al and 2 hours of reflux were applied. As expected, the linker keto group was converted to the corresponding secondary alcohol while the hydantoin core was converted to the imidazolidin-2-one to give the desired compound **5.33** together with a small amount of the mono reduced compound **5.17** (Scheme 5.10, unambiguous structural identification was carried out as described in the next section, *Structure Elucidation*).



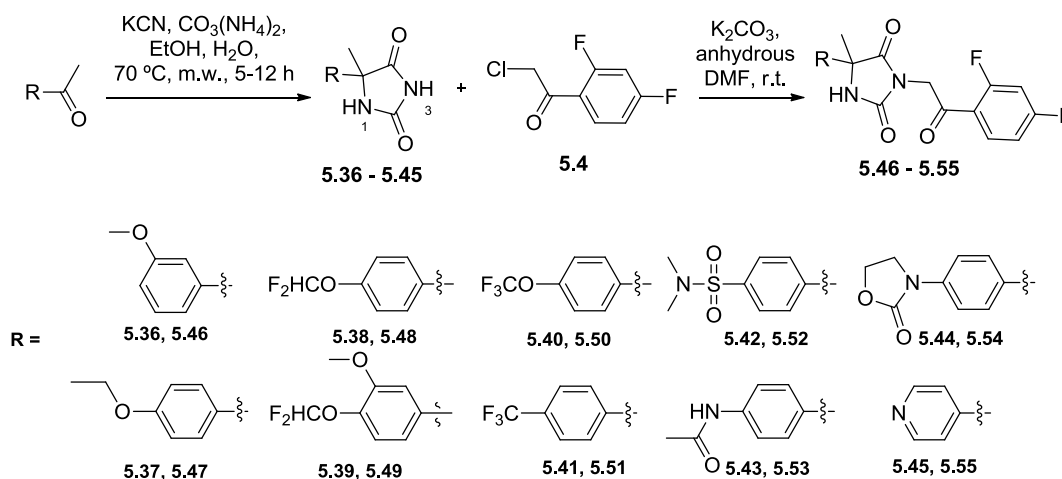
**Scheme 5.10. Synthetic approach C to obtain the imidazolidine-2-one analogue 5.26.**

For the subsequent re-oxidation of the alcohol group in **5.33**, two methods were tested. Firstly, manganese dioxide ( $\text{MnO}_2$ ) was used. However, the reaction was not very clean and only traces of the desired product were formed together with the undesired dicarbonyl compound **5.34**. The second method tested was the classical Swern oxidation using oxalyl chloride, dimethyl sulfoxide

(DMSO) and an organic base such as triethylamine (TEA) at  $-78\text{ }^{\circ}\text{C}$  to ambient temperature. This reaction worked well, resulting in the desired product **5.26** (Scheme 5.11).

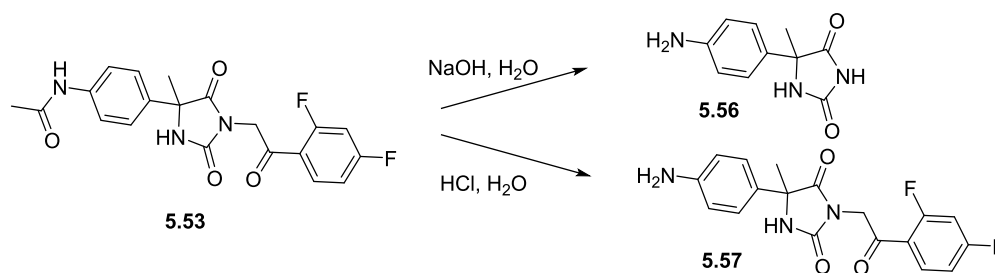
### 5.2.1.3. Carbonitrile replacement

The hydantoin ring system has been synthesized in the literature in a variety of ways using amino acids, ketones/aldehydes or unsubstituted hydantoins as starting materials.<sup>170,171,172,173,174</sup> The Bucherer–Bergs synthesis is the most common procedure using the corresponding phenyl keto as starting material. We synthesized our hydantoins using microwave irradiation according to a published procedure by Safari *et al.* with some improvements.<sup>175</sup> More specifically, the suitable *para*-substituted phenyl ethanone reacted with potassium cyanide (KCN) and ammonium carbonate ( $(\text{NH}_4)_2\text{CO}_3$ ) under microwave irradiation for 6 to 12 hours. Subsequently, alkylation of the obtained intermediates **5.36-5.45** with 2-chloro-2',4'-difluoroacetophenone **5.4** in the presence of potassium carbonate ( $\text{K}_2\text{CO}_3$ ) resulted in final compounds (**5.46 - 5.55**) in good yields (Scheme 5.11). The  $^1\text{H-NMR}$  peaks representing hydantoin NH were found between 8.83-9.21 ppm suggesting that the alkylation had occurred on the desired *N*(3) position of **5.36-5.45** hydantoins. Shifting the methoxy group from 4- to 3-position gave regioisomer **5.46** of reference compound **5.9**. Replacement of the 4-methoxy substituent with ethoxy or fluoro containing substituents gave compounds **5.47-5.51**. Inserting more hydrophilic substituents such as dimethyl sulfonamide, acetamide, oxazolidin-2-one or a pyridine ring resulted in compounds **5.52-5.55**.



**Scheme 5.11. Synthesis of the final compounds with left-hand side modifications.**

As shown in Scheme 5.12, compound **5.53** was also subjected hydrolysis under basic and acidic conditions. Only the acidic conditions delivered the desired compound **5.57**, while basic hydrolysis led to the fragment **5.56**.



Scheme 5.12. Acidic and basic hydrolysis of compound 5.53.

#### 5.2.1.4. Structure elucidation

For structural elucidations, NMR methods were used as described in Chapter 3. 2D HSQC and HMBC spectra for compound **5.9** allowed full assignment of <sup>1</sup>H- and <sup>13</sup>C-NMR peaks, specifying the alkylation position.

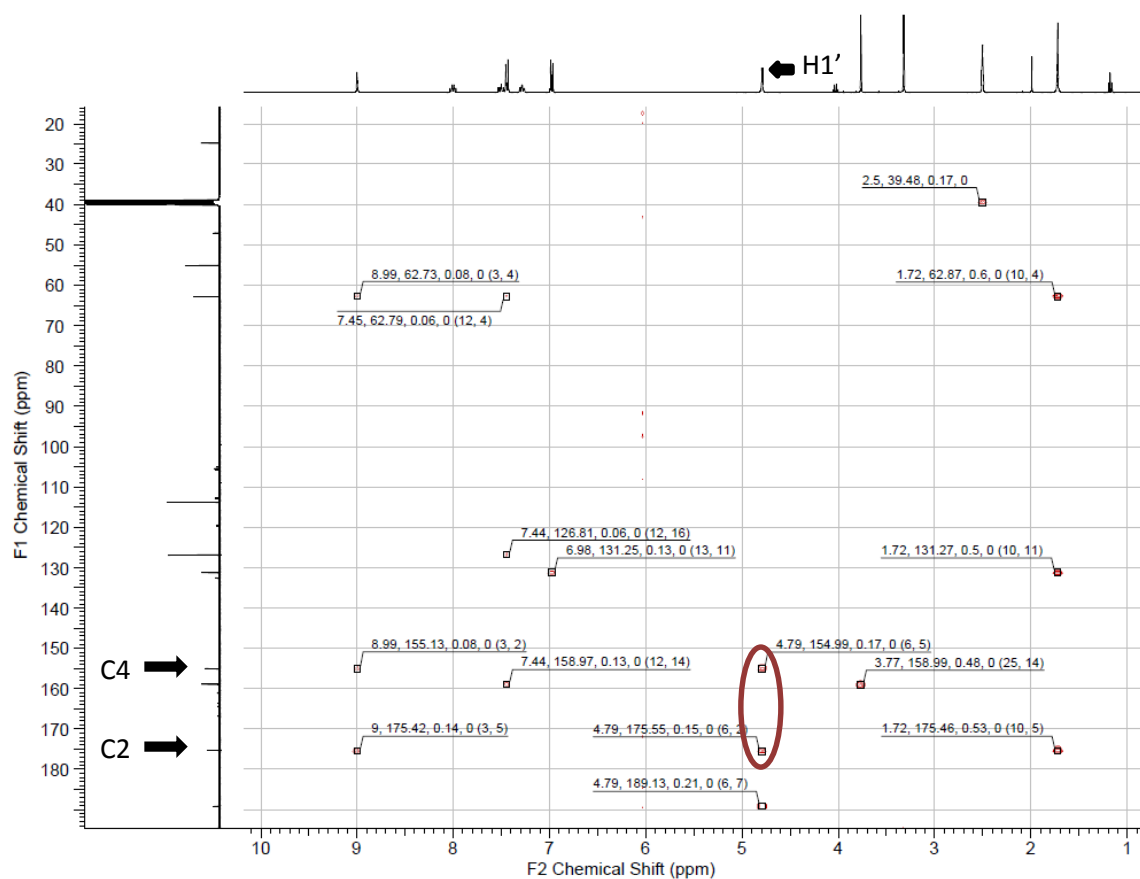
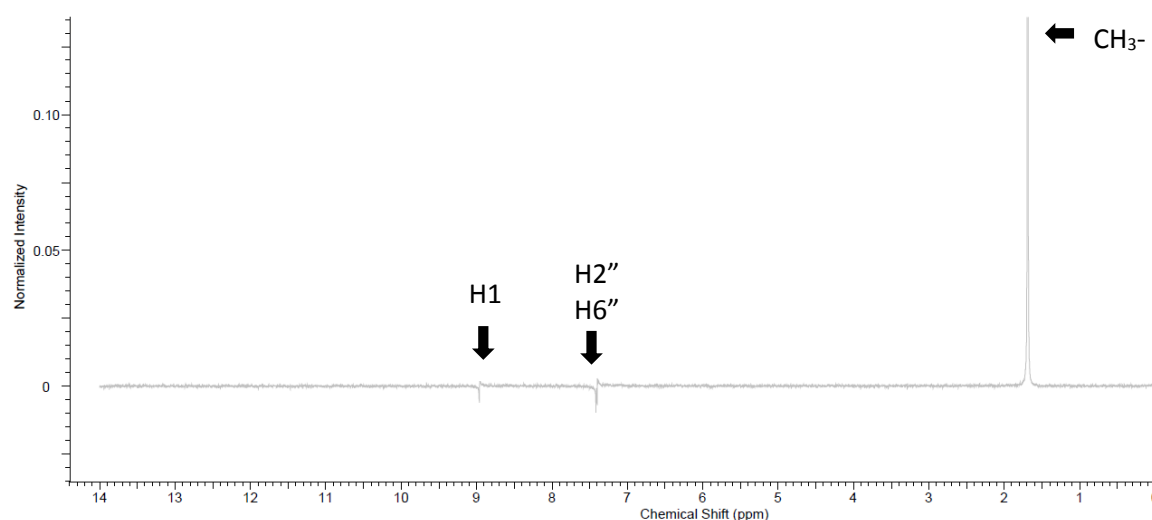


Figure 5.3. HMBC correlations for compound 5.9.

More specifically, the HMBC spectrum of compound **5.9** demonstrated crosspeaks within H1'/C2 and H1'/C4, which were consistent with alkylation on the nitrogen atom at position 3. It is worth

noticing that the correlation of H1' with C4 of the carbonyl group and absence of H1'/C5 crosspeak excluded the possibility of alkylation on nitrogen atom at position 1.

Furthermore, 1D NOE experiments were performed to confirm our findings from the previous method. The presence of H1 peak at 9.00 ppm and H2'', H6'' peaks at 7.41-7.46 ppm in the NOE spectrum of **5.9** upon irradiation of the methyl group at position 5 of the hydantoin core at 1.72 ppm, indicated that it was in proximity of those protons (Figure 5.4). This is consistent with the *N*(3)-alkylated analogue.



**Figure 5.4.** NOE spectrum of compound **5.9** upon irradiation of methyl group (-CH<sub>3</sub>).

Graphical representation of relevant HMBC correlations for compound **5.9** is shown in Figure 5.5(A), while relevant NOE correlations are represented in Figure 5.5(B). Moreover, direct comparison of the <sup>1</sup>H-NMR chemical shifts of compound **5.9** and intermediate **5.1** allowed the assignment of the peaks representing the amide protons (NH) for intermediate **5.1**, as shown in Figure 5.5(C).

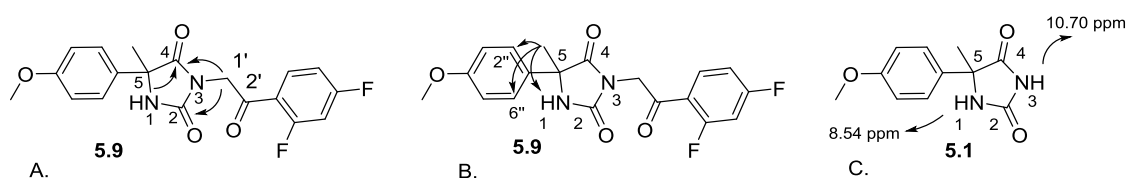


**Figure 5.5.** (A) Key HMBC correlations for structure determination of compound **5.9**; (B) Key NOE correlations for compound **5.9**; (C) Assignment of <sup>1</sup>H-NMR shifts for amide protons of intermediate **5.1**.

The amide proton at position 3 possessed a chemical shift of 10.70 ppm which means that it is more deshielded than the amide proton at position 1 with a chemical shift at 8.54 ppm. There is

a general tendency for the more acidic OH and NH protons to move further downfield.<sup>176</sup> According to this, proton H3 is expected to be more acidic than proton H1. As expected, the more acidic proton at *N*(3) is deprotonated first in the presence of potassium carbonate and therefore alkylation occurred at this position. Acidity could be a possible reason for the regioselectivity observed, along with the fact that *N*(3) was sterically less hindered than *N*(1).

Based on these conclusions, for compounds **5.10-5.13**, <sup>1</sup>H-NMR shifts of the peaks representing hydantoin amide protons (NH) were used as fast primary screening for structure determination, followed by full assignment using HSQC and HMBC spectra for verification purposes. For compound **5.15**, <sup>1</sup>H-NMR peak of the amide proton (NH) at 12.04 ppm indicated acylation at position *N*(1) instead of the desired *N*(3), while for compound **5.16** <sup>1</sup>H-NMR peak of the amide proton (NH) at 9.47 ppm indicated acylation at the desired position *N*(3).

As mentioned above, <sup>1</sup>H-NMR and <sup>13</sup>C-NMR chemical shifts for compound **5.9** were fully assigned using HSQC and HMBC spectra. Direct comparison of <sup>13</sup>C-NMR shifts corresponding to carbonyl groups allowed identification of the reduction position for compound **5.17**.

The methylation position of compound **5.18** was primarily determined by comparison of <sup>1</sup>H-NMR spectra of compounds **5.9**, **5.17** and **5.18**. This was further proven by HSQC and HMBC spectra that showed strong correlations of the newly inserted methyl group with the hydantoin quaternary carbon C(5) and the closest carbonyl C(2), as shown in Figure 5.6.

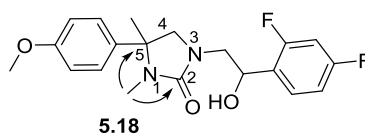


**Figure 5.6.** Key NOE correlations for structure determination of compound **5.18**.

Full assignment using 2D HSQC and HMBC spectra, together with a 1D NOE experiment, confirmed the alkylation position of the obtained product **5.23** (Figure 5.7). More specifically, HMBC spectrum showed crosspeaks between linker's protons H1' and imidazole C2 and C5, suggesting that the alkylation occurred on the desired position *N*(1) of the imidazole ring. Moreover, NOE experiments showed correlation with both imidazole protons upon irradiation of linker C1', which verifies our previous findings.

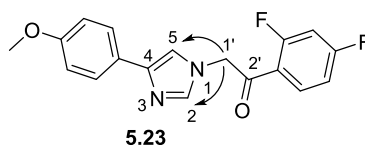


**Figure 5.7.** Key HMBC and NOE correlations for structure determination of compound **5.23**

For compound **5.27**, the obtained  $m/z$  was indicative of the dehydrated product instead of the desired one **5.26**. The alkylation position for compound **5.27** was determined using 1D NOE experiment, which upon irradiation of the linker proton  $H(1')$  displayed correlations with the methylene protons of the imidazolidin-2-one ring  $H(5)$  and linker proton  $H(2')$  (proven by COSY) (Figure 5.8). These findings indicated that alkylation occurred on the desired position  $N(1)$ . Moreover, absence of correlation with the methyl group was in accordance with the  $N(1)$ -alkylation. The coupling constant (14.9 Hz) of the double bond protons was indicative of *E* (trans) geometric isomerism.

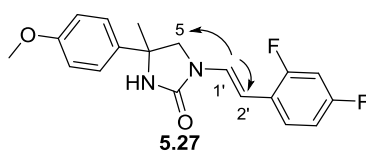


**Figure 5.8.** Key NOE correlations for structure determination for compound **5.27**.

Structure determination for compounds **5.26**, **5.31**, **5.33** and **5.34** was based on direct comparison with the previously assigned carbonyls in  $^{13}\text{C}$ -NMR spectrum of **5.9**.

## 5.2.2. Results and discussion

All synthesized compounds were evaluated for their ability to inhibit the growth of *M. tuberculosis* ( $H_{37}\text{Rv}$  strain) and for cytotoxicity in HepG2 cells. In addition, three physicochemical properties were measured: artificial membrane permeability, kinetic aqueous solubility (using chemiluminescent nitrogen detection, CLND) and ChromLogD.<sup>132,167</sup> Compound **5.9** was used as a reference and in most cases direct comparisons were performed.

### 5.2.2.1. Linker modification

Table 5.4 presents the results for the reference compounds **4.1**, **5.9-5.10** and the first set of compounds possessing variations on the linker (**5.11-5.13**, **5.17**). Unexpected by-products **5.15**, **5.18** and **5.19** were also evaluated.

Table 5.4. Biological and physicochemical profile for compounds with linker modifications.

	Structure	DprE <sub>1</sub> pIC <sub>50</sub>	Mtb MIC ( $\mu\text{M}$ ) <sup>[a]</sup>	TOX <sub>50</sub> ( $\mu\text{M}$ ) <sup>[b]</sup>	AMP (nm/sec) <sup>[c]</sup>	Solubility ( $\mu\text{M}$ ) <sup>[d]</sup>	Chrom logD <sup>[e]</sup>
4.1		7	8.3	>100	515	202	4.54
5.9		6.7	40	>100	590	358	4.78
5.10		6.0	62	>100	570	260	4.53
5.11		<4.0	>125	>100	620	327	4.84
5.12		<4.0	>125	>100	530	≥381	4.72
5.13		4.4	>125	>100	750	≥409	4.60
5.15		<4.0	>40	>100	170	≥484	3.43
5.17		4.2	>80	>100	610	287	3.96
5.18		4.3	>80	>100	760	≥445	4.53
5.19		<4.5	>80	>100	740	≥392	5.79

<sup>a</sup>MIC against *M. tuberculosis* (H37Rv), isoniazid was used as reference with MIC = 1.8  $\mu\text{M}$ ; <sup>b</sup>HepG2, human caucasian hepatocyte carcinoma; <sup>c</sup>artificial membrane permeability; <sup>d</sup>*in vitro* profiling for kinetic aqueous solubility (CLND, chemiluminescent nitrogen detection); <sup>e</sup>chromlogD values at pH = 7.4.

The obtained results showed that all modifications of the linker led to inactive compounds, and that the length of the linker together with the presence of the keto group appeared to be essential for the activity.

Other linker modifications performed by other researchers working in the OMC/DprE1 team at GSK included a methyl group on the methylene (**5.58**), a 5-membered ring closure (**5.59**) and replacement of the carbonyl group by an ether (**5.60**) or oxime (**5.61**) (Figure 5.9). Biological evaluation of these compounds resulted in mostly inactive compounds.

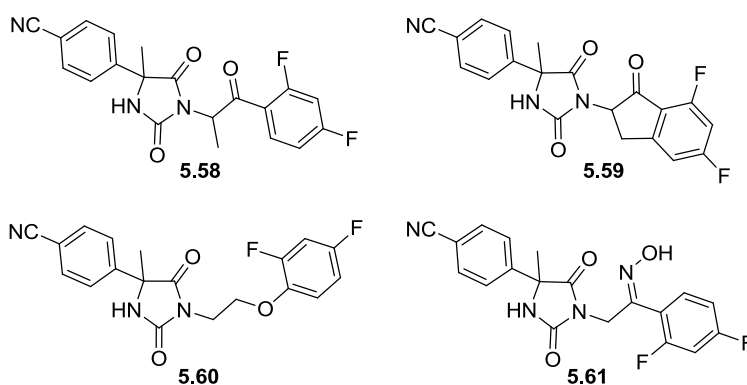


Figure 5.9. Other linker modifications.

### 5.2.2.2. Hydantoin modification

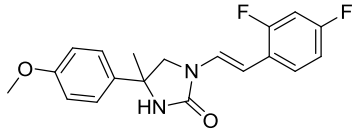
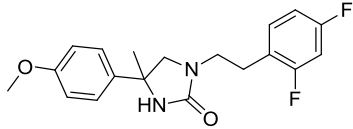
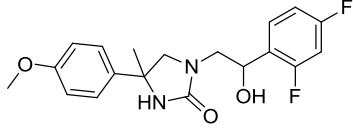
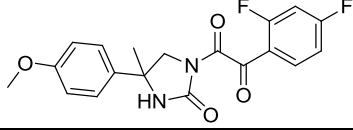
Table 5.5 presents the results for the second set of compounds, possessing modifications at the hydantoin core.

Modification types in this part of the hit molecule included the replacement of the hydantoin with an imidazolidin-2-one ring or imidazole ring. During the preparation of compound **5.26**, compounds **5.27**, **5.31**, **5.33** and **5.34** were obtained either as intermediates or as side products and they were also allowed to enter the biological evaluation.

Table 5.5. Biological and physicochemical profile for compounds with core modifications.

Structure	DprE <sub>1</sub> pIC <sub>50</sub>	Mtb MIC ( $\mu$ M) <sup>[a]</sup>	TOX <sub>50</sub> ( $\mu$ M) <sup>[b]</sup>	AMP (nm/sec) <sup>[c]</sup>	Solubility ( $\mu$ M) <sup>[d]</sup>	Chrom logD <sup>[e]</sup>
	<4.0	>125	>100	360	352	4.68
	E <sub>1</sub> <sup>[f]</sup>	<4.0	>80	>100	610	88
	E <sub>2</sub> <sup>[g]</sup>	4.5	>80	>100	580	177



	4.5	>40	>100	n.d. <sup>[h]</sup>	n.d. <sup>[h]</sup>	n.d. <sup>[h]</sup>
	<4.0	>125	>100	590	≥430	5.18
	<4.0	>80	>100	540	119	4.17
	4.2	n.d. <sup>[h]</sup>	n.d. <sup>[h]</sup>	n.d. <sup>[h]</sup>	n.d. <sup>[h]</sup>	n.d. <sup>[h]</sup>

<sup>a</sup>MIC against *M. tuberculosis* (H37Rv), isoniazid was used as reference with MIC = 1.8 μM; <sup>b</sup>HepG2, human caucasian hepatocyte carcinoma; <sup>c</sup>artificial membrane permeability; <sup>d</sup>*in vitro* profiling for kinetic aqueous solubility (CLND, chemiluminescent nitrogen detection); <sup>e</sup>chromlogD values at pH = 7.4; <sup>f</sup>E<sub>1</sub> = enantiomer 1; <sup>g</sup>E<sub>2</sub> = enantiomer 2; <sup>h</sup>n.d.= not determined.

Replacement of the hydantoin ring with an aromatic 5-membered ring (imidazole) led to the inactive compound **5.23**. A possible explanation could be that a non-planar arrangement of substituents or keto groups play a crucial role for activity. Also, removal of the hydantoin 4-oxo function, gave the inactive compound **5.26**. All the other compounds obtained as side-products or intermediates (**5.27**, **5.31**, **5.33** and **5.34**) lost their potency too.

Complementary modifications performed by other researchers working in the DprE1-team at GSK consisted of introducing another aromatic ring, pyrazole (**5.62**), methylation of the hydantoin ring (**5.63**), elongation of the methyl group to ethyl (**5.64**) or removal of the methyl group (**5.65**) (Figure 5.10). Only elongation of the methyl group with an ethyl group (**5.64**) increased the enzymatic inhibitory potency in comparison with the hit compound **4.1**. The other three modifications led to practically inactive compounds (**5.62**, **5.63** and **5.65**).

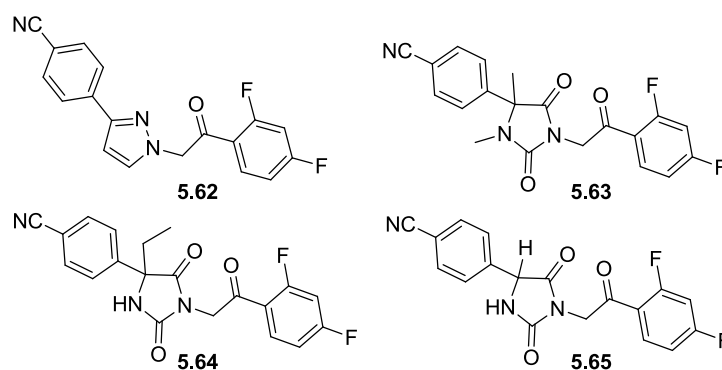
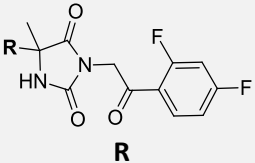
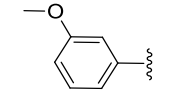
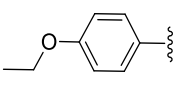
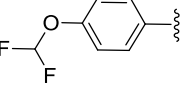
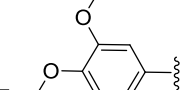
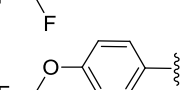
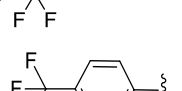
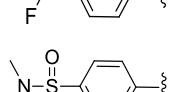


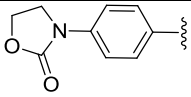
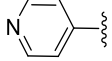
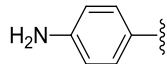
Figure 5.10. Other core modifications.

### 5.2.2.3. Carbonitrile replacement

Bioisosteric replacement of a functional group is an established method in drug discovery for compound optimization. It is defined as “the replacement of a functionality by groups or molecules, which have chemical and physical similarities producing broadly similar biological properties but may not necessarily have a strict atom-for-atom replacement”.<sup>177</sup> Moreover, the role of fluorine in drug design and development has expanded rapidly during the past decades, as introduction of this element into a molecule can productively influence pK<sub>a</sub>, intrinsic potency, membrane permeability, metabolic pathways and pharmacokinetic properties.<sup>178</sup> Keeping these concepts in mind, a set of compounds possessing alternative groups for the carbonitrile or inserted fluorine atoms was designed and synthesized for this study and the obtained data are shown in Table 5.6 and 5.7.

**Table 5.6. Biological and physicochemical profile for compounds with carbonitrile replacements.**

Structure	DprE1 pIC <sub>50</sub>	Mtb MIC ( $\mu$ M) <sup>[a]</sup>	TOX <sub>50</sub> ( $\mu$ M) <sup>[b]</sup>	AMP (nm/sec) <sup>[c]</sup>	Solubility ( $\mu$ M) <sup>[d]</sup>	Chrom logD <sup>[e]</sup>
 R	<4.0	>80	>100	510	285	4.96
	7.0	20	>100	650	167	5.43
	7.4	10	>100	500	85	5.36
	6.9	80	>100	400	106	5.50
	7.3	35	>100	230	4	6.05
	6.9	20	>100	320	43	6.01
	5.7	80	>100	360	224	4.60
	5.6	40	>100	110	≥489	3.28

<b>5.54</b>		6.6	5.6	>100	190	359	3.94
<b>5.55</b>		4.4	>125	>100	390	≥462	3.04
<b>5.57</b>		4.1	>80	>100	260	≥436	3.38

<sup>a</sup>MIC against *M. tuberculosis* (H37Rv), isoniazid was used as reference with MIC = 1.8 μM; <sup>b</sup>HepG2, human caucasian hepatocyte carcinoma; <sup>c</sup>artificial membrane permeability; <sup>d</sup>*in vitro* profiling for kinetic aqueous solubility (CLND, chemiluminescent nitrogen detection); <sup>e</sup>chromlogD values at pH = 7.4.

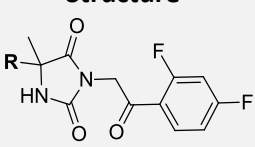
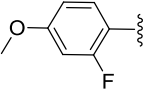
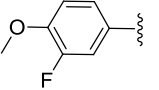
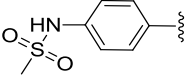
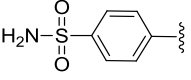
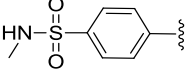
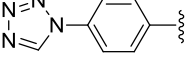
Shifting the methoxy group from position 4 to 3 (compound **5.46**) led to complete loss of potency ( $pIC_{50} < 4$ , MIC >80 μM). Conversely, elongation of the methoxy group to ethoxy group (**5.47**) seemed to be favourable and resulted in enhancement of enzymatic potency ( $pIC_{50} = 7.0$ ) and cellular potency (MIC = 20 μM) in comparison with the reference compound **5.9**. Replacement of the ethoxy group with a 2,2-difluoroethoxy group gave compound **5.48** which exhibited even higher enzymatic potency, leading to a very potent DprE1 inhibitor with  $pIC_{50}$  value of 7.4 accompanied by improvement in cellular potency (MIC = 10 μM). Unfortunately, this compound exhibited lower solubility (CLND = 85 μM). In an attempt to increase the solubility of **5.48**, compound **5.49** that possessed an additional 3-methoxy group was prepared. Although there was a small improvement in solubility, it did not preserve potency. Furthermore, compound **5.50** with a 4-trifluoromethoxy group led to a further decrease of solubility (CLND = 4 μM), although the enzymatic potency was also very high ( $pIC_{50} = 7.3$ ) and the cellular activity (MIC = 35 μM) similar to the reference compound **5.9**. Also, compound **5.51** possessing a 4-trifluoromethyl group showed slight improvement of enzymatic potency ( $pIC_{50} = 6.9$ ) and MIC value (20 μM) in comparison with reference **5.9**.

Due to the low solubility and relatively high chromlogD values, several more hydrophilic groups were also inserted at position 4. Insertion of a dimethyl sulfonamide group led to a poorly active compound (**5.52**,  $pIC_{50} = 5.7$ , MIC = 80 μM). The acetamide **5.53** exhibited a similar DprE1 inhibitory activity ( $pIC_{50} = 5.6$ ) accompanied by doubling of cellular activity (MIC = 40 μM). In an attempt to introduce a 5-membered ring, oxazolidin-2-one was selected and the obtained compound **5.54** showed moderate enzymatic inhibitory activity ( $pIC_{50} = 6.6$ ) and surprisingly good cellular activity (MIC = 5.6 μM), better than reference **5.9**. Also, a pyridine analogue was prepared as an alternative for the nitrile group. Although it is not a typical isosteric replacement, the nitrogen of the pyridine could form a hydrogen bond with a water molecule and therefore preserve the same interaction as the nitrile group.<sup>177</sup> Biological evaluation revealed that the pyridine analogue **5.55** completely lost the inhibitory activity ( $pIC_{50} = 4.4$ ). After hydrolysis of the

acetamide **5.53**, the inactive aniline derivative **5.57** was obtained ( $pIC_{50} = 4.1$ ). Despite the potential toxicity risks of introducing an aniline, we were interested in this compound as it could appear as a metabolite of the particularly active sulfonamide **5.69** (discussed later). In the cytotoxicity test, compound **5.69** appeared to be non-cytotoxic ( $TOX_{50} > 100 \mu M$ ).

Further relevant replacements of the carbonitrile group performed by other researchers working in the OMC-DprE<sub>1</sub> team at GSK are presented in Table 5.7.

**Table 5.7. Biological and physicochemical profile for compounds with other carbonitrile replacements.**

Structure	DprE1 $pIC_{50}$	<i>Mtb</i> MIC ( $\mu M$ ) <sup>[a]</sup>	$TOX_{50}$ ( $\mu M$ ) <sup>[b]</sup>	AMP (nm/sec) <sup>[c]</sup>	Solubility ( $\mu M$ ) <sup>[d]</sup>	Chrom logD <sup>[e]</sup>
						
	6.5	58	>100	650	186	5.05
	5.7	>80	>100	680	147	4.84
	7.0	2.5	>100	110	≥487	3.57
	7.3	0.9	>100	<6.5	≥486	3.19
	6.2	20	>100	110	≥478	3.88
	7.3	3.1	>100	310	379	3.78
<sup>a</sup> MIC against <i>M. tuberculosis</i> (H37Rv), isoniazid was used as reference with MIC = 1.8 $\mu M$ ; <sup>b</sup> HepG2, human caucasian hepatocyte carcinoma; <sup>c</sup> artificial membrane permeability; <sup>d</sup> <i>in vitro</i> profiling for kinetic aqueous solubility (CLND, chemiluminescent nitrogen detection); <sup>e</sup> chromlogD values at pH = 7.4.						

Compounds **5.66** and **5.67** containing fluorine atoms at positions 2 and 3 of the phenyl ring were specifically designed in an attempt to influence electron density of the aromatic ring aiming at a more favourable interactions. Addition of fluorine at position 2 gave compound **5.66** of the reference compound **5.9** had only a minor effect on enzymatic potency ( $pIC_{50} = 6.5$ ), while introduction of a fluorine at position 3 gave compound **5.67** which led to reduction of the enzymatic potency ( $pIC_{50} = 5.7$ ).

A significant number of sulfonamide compounds were also prepared and some selected compounds **5.68-5.70** are shown in Table 5.7. Sulfonamide derivative **5.68** exhibited good enzymatic inhibitory activity ( $pIC_{50} = 7$ ) and very good MIC value of  $2.5 \mu\text{M}$ . Subsequently, the retro sulfonamide **5.69** was prepared exhibiting excellent enzymatic ( $pIC_{50} = 7.3$ ) and cellular activity with a MIC value of  $0.9 \mu\text{M}$ . It was observed that compound **5.69** displayed very low artificial membrane permeability ( $\text{AMP} < 6.5 \mu\text{M}$ ), nevertheless it showed satisfactory bioavailability (see at *Therapeutic Efficacy* section). Furthermore, the sulfonamide **5.69** was mono- or doubly methylated but the resulting compounds (**5.70**, **5.52**) lost their potency. Lastly, tetrazole derivative **5.71**, exhibited high enzymatic potency ( $pIC_{50} = 7.3$ ) with very good cellular potency with MIC value of  $3 \mu\text{M}$ .

Within these results, some disconnection between enzymatic and cellular potencies could be observed. For example, compounds **5.48** and **5.69** that possessed very high enzymatic inhibitory activity ( $pIC_{50} = 7.4$  and  $7.3$ , respectively), did not exhibit the same cellular potency (MIC =  $10$  and  $0.9 \mu\text{M}$ , respectively). Similarly, compounds **5.47** and **5.68** shared comparable, potent DprE1 inhibitory activity ( $pIC_{50} = 7$ ) but the measured cellular potencies were found to be  $20$  and  $2.5 \mu\text{M}$ , respectively. The same mismatch was observed between the reference compound **5.9** and compound **5.54** ( $pIC_{50} = 6.7$  and  $6.6$ , respectively and MIC =  $40$  and  $5.6 \mu\text{M}$ , respectively).

In Figure 5.11, antimycobacterial potencies (MIC values) have been plotted against either their corresponding DprE1 inhibitory activities ( $pIC_{50}$ ), or their lipophilicities ( $\text{chromlogD}$ ). In both cases, no statistically significant correlation ( $R^2 < 0.5$ ) was present between the compared variables.

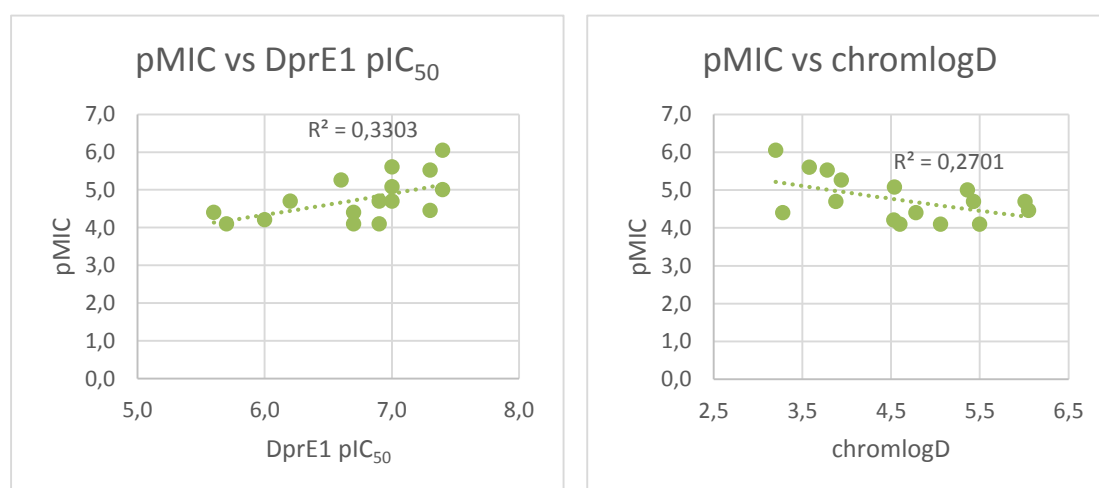


**Figure 5.11. Representation of pMIC vs DprE<sub>1</sub> pIC<sub>50</sub> and pMIC vs chromlogD (data sets used: compounds from tables 5.4 - 5.7 which showed a measurable MIC value ( $\leq 80 \mu\text{M}$ )).**

However, for each of the aforementioned inhibitor pairs (having comparable enzymatic potencies but differing cellular activities), a significant difference in lipophilicity was observed. Notably, in all pairs, the less lipophilic compounds (chromlogD values ranging from 3 to 4), showed better MIC values than compounds of higher lipophilicity (chromlogD values ranging from 4.5 to 5.5). As apparent, lipophilicity is an extremely important quantity to control during optimization. And our results seem to indicate that a lipophilicity-normalized representation of enzymatic potency could be a better predictor of cellular potency.

Among several lipophilicity metrics, lipophilic ligand efficiency (LLE) explicitly considers the balance of lipophilicity with potency and can be very useful in comparing HTS hits or during lead optimization.<sup>179</sup> LLE, introduced by Leeson and Springthorpe, is defined as the difference of log P (or log D) and the negative logarithm of a potency measure (pKd, pKi, or pXC<sub>50</sub>).<sup>180</sup>

$$\text{LLE} = \text{pIC}_{50} (\text{or pKi}) - \text{clogP} \text{ or } (\text{logD or clogD})$$

In other words, LLE describes the contribution of lipophilicity to potency.<sup>181</sup> Therefore, LLE was considered a suitable parameter for our H2L program and cellular activity was plotted against LLE for all compounds with MIC  $\leq 80 \mu\text{M}$ , as shown in Figure 5.12. The obtained graph gave a more satisfactory trend with  $R^2 = 0.7868$ .

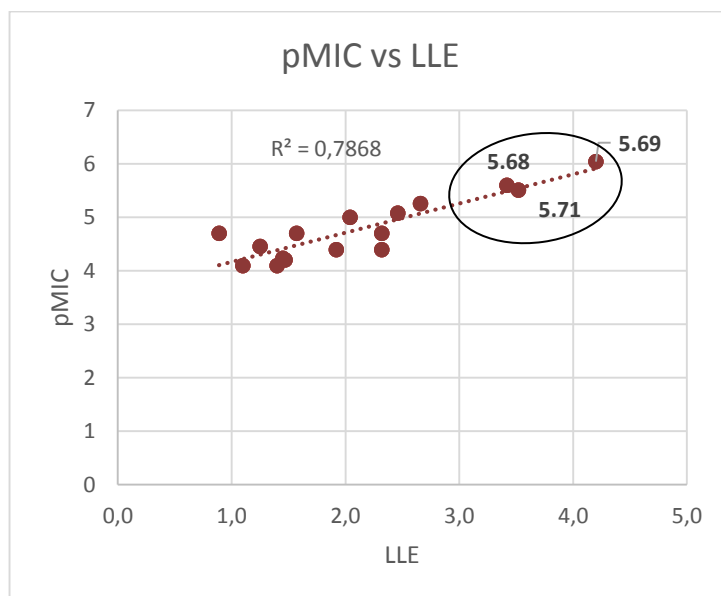


**Figure 5.12. Representation of pMIC vs LLE (data set used: compounds from tables 5.4 - 5.7 which showed a measurable MIC value ( $\leq 80 \mu\text{M}$ )).**

As apparent from this plot, the best compounds in the series had LLE value  $>3$ . In conclusion, it seems that not only high enzymatic inhibitory activity is required to obtain a good MIC value, but

also a sufficiently low chromlogD is necessary. Therefore, LLE would be an interesting parameter to monitor during the design of future compounds.

### 5.2.3. Conclusion of the first round of Hit-to-Lead optimization

In our attempts to meet the previously mentioned goals, a range of compounds were synthesized as part of the first round of Hit-to-Lead optimization.

Linker and core modifications performed so far did not provide any improvement in comparison with the reference compounds. On the other hand, more potent compounds were obtained from the replacement of the nitrile group by sulfonamides, difluoromethoxy group, tetrazole and oxazolidin-2-one ring. Compounds **5.48**, **5.69** and **5.71** shown in Figure 5.13 possessed the highest enzymatic inhibitory activity ( $pIC_{50}$  7.4 and 7.3 respectively) so far. However, only compound **5.69** achieved a sub-micromolar MIC value of 0.9  $\mu$ M, while compound **5.48** displayed a moderate MIC of 10  $\mu$ M and compound **5.71** a good MIC of 3  $\mu$ M. On the other hand, although compound **5.54** possessed a moderate enzymatic inhibitory activity ( $pIC_{50}$  = 6.6), it gave a good MIC value of 5.6  $\mu$ M.

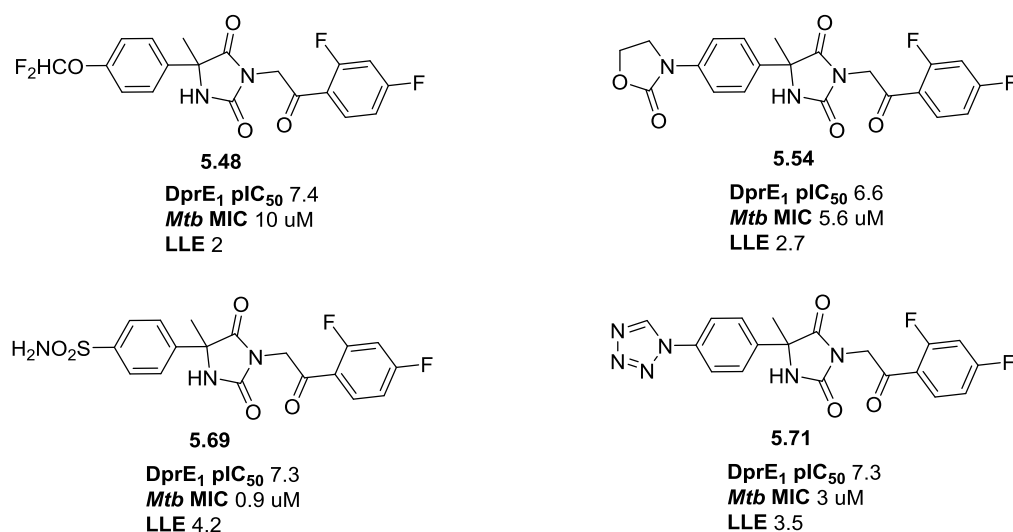


**Figure 5.13. Compounds with the best DprE<sub>1</sub> inhibitory activity.**

Furthermore, LLE was calculated and found to correlate nicely with cellular potency. All compounds depicted in Figure 5.13 were chosen for further exploration. In this thesis, only the optimization of **5.48** will be covered, while the other compounds were followed by other team members. This compound showed a LLE value of 2. Thus, increasing this value, by decreasing the overall lipophilicity and/or increasing affinity, was considered an important goal during the second

round of optimization that focused on the right-hand side of the molecule. Introduction of hydrophilic groups was considered a straightforward way of reaching this goal.

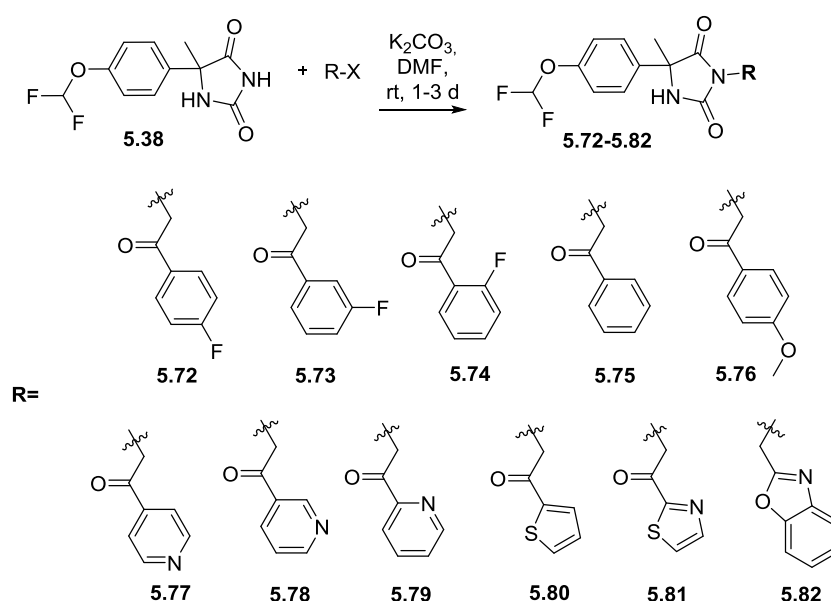
### 5.3. Second round of Hit-to-Lead optimization

The first compounds of this section contained differently substituted right-hand side phenyl rings and provided SAR information in the chemical space immediately surrounding the reference **5.48**. Additionally, a number of analogues containing 6- or 5-membered heterocycles were prepared. Both subsets were supplemented with several commercially available analogues of reference **5.48** with non-aromatic, aliphatic or bicyclic phenyl replacements that were also considered to be within the scope of this exploration.

#### 5.3.1. Chemistry

An important goal of the first subset of compounds (characterized by different phenyl substitutions), was to quantify the influence of fluorination on lipophilicity. Therefore, compounds with monofluoro- or non-fluorinated phenyl rings were prepared. Moreover, a methoxy group was inserted replacing fluorines. Our second subset of compounds consisted of 6- and 5-membered heterocycles such as pyridine, thiophene, pyrrole and thiazole which were expected to further reduce the chromlogD values.

As shown in Scheme 5.13, final compounds **5.72-5.82** were obtained by alkylation of the hydantoin core **5.38** with the appropriate  $\alpha$ -halo keto aryls (R-X) in the presence of potassium carbonate ( $K_2CO_3$ ) in DMF.



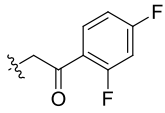
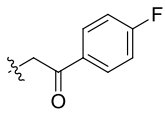
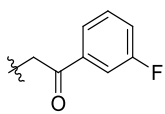
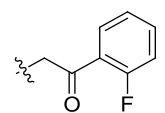
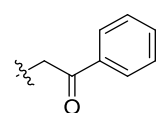
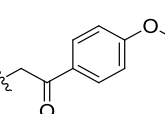
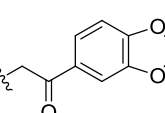
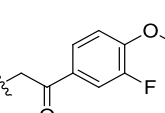
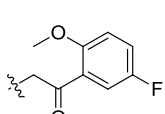
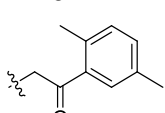
**Scheme 5.13. Synthesis of the compounds with modifications at the right-hand side part of the molecule.**

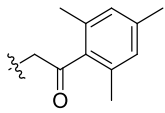


### 5.3.2. Results and discussion

In addition to the synthesized molecules **5.72-5.82**, commercially available compounds or analogues present in the GSK database (marked with *f*) were also tested and the obtained results are shown in Table 5.8.

**Table 5.8. Biological and physicochemical profile for compounds with modifications to the right-hand side phenyl group.**

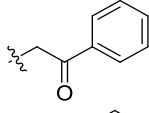
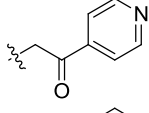
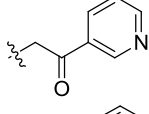
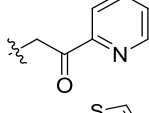
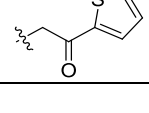
	Structure	DprE1 pIC <sub>50</sub>	<i>Mtb</i> MIC ( $\mu$ M) <sup>[a]</sup>	TOX <sub>50</sub> ( $\mu$ M) <sup>[b]</sup>	AMP (nm/sec) <sup>[c]</sup>	Solubility ( $\mu$ M) <sup>[d]</sup>	Chrom logD <sup>[e]</sup>
Ref. <b>5.48</b>		7.4	10	>100	500	85	5.36
<b>5.72</b>		7.2	15	>100	540	98	5.08
<b>5.73</b>		6.4	20	>100	480	144	5.13
<b>5.74</b>		7.3	20	>100	560	141	5.23
<b>5.75</b>		7.2	30	>100	520	180	4.97
<b>5.76</b>		6.2	80	>100	490	104	4.92
<b>5.83</b> <sup>[f]</sup>		6.6	>80	>100	500	80	4.90
<b>5.84</b> <sup>[f]</sup>		6.4	80	>100	450	105	5.03
<b>5.85</b> <sup>[f]</sup>		5.4	>80	>100	400	183	5.42
<b>5.86</b> <sup>[f]</sup>		7	80	63	310	69	5.97

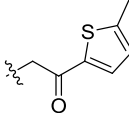
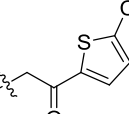
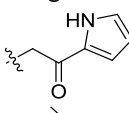
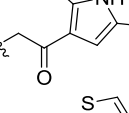
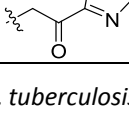
<b>5.87<sup>[f]</sup></b>		5	>80	50	140	18	6.48
<sup>a</sup> MIC against <i>M. tuberculosis</i> (H37Rv), isoniazid was used as reference with MIC = 1.8 μM; <sup>b</sup> HepG2, human caucasian hepatocyte carcinoma; <sup>c</sup> artificial membrane permeability; <sup>d</sup> <i>in vitro</i> profiling for kinetic aqueous solubility (CLND, chemiluminescent nitrogen detection); <sup>e</sup> chromlogD values at pH = 7.4; <sup>f</sup> commercially available.							

Removal of one fluorine atom and positional scanning with the remaining fluorine, or removal of both fluorines resulted in a small drop of the DprE<sub>1</sub> inhibitory activity (pIC<sub>50</sub> 7.2-7.3). This was accompanied by a small decrease of the chromlogD values, from 5.36 (reference **5.48**) to 4.97-5.23 (compounds **5.72-5.74**). The overall hydrophilicity improvement together with the small drop of enzymatic potency did not lead to the desired LLE (>3) and the cellular activity obtained was moderate (15-30 μM). Moreover, more hydrophilic substituents such as a methoxy group and dioxole or their combination with fluorine led to a significant drop in both enzymatic and mycobacterial potency.

The biological data and physicochemical properties for the second subset of compounds consisted of 6- and 5-membered heterocycles are presented in Table 5.9. Compound **5.75** possessing a non-substituted phenyl is shown again in this table, since it serves as a useful reference for assessing the impact of heterocycle-for-phenyl replacement.

**Table 5.9. Biological and physicochemical profile for compounds with heterocyclic modifications.**

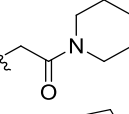
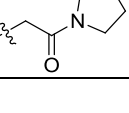
	<b>Structure</b>	<b>DprE1 pIC<sub>50</sub></b>	<b><i>Mtb</i> MIC (μM)<sup>[a]</sup></b>	<b>TOX<sub>50</sub> (μM)<sup>[b]</sup></b>	<b>AMP (nm/sec)<sup>[c]</sup></b>	<b>Solubility (μM)<sup>[d]</sup></b>	<b>Chrom logD<sup>[e]</sup></b>
<b>5.75</b>		7.2	30	100	520	180	4.97
<b>5.77</b>		6.3	30	>100	320	≥328	3.52
<b>5.78</b>		5.7	80	>100	240	≥503	3.54
<b>5.79</b>		6.7	15	>100	550	≥497	4.35
<b>5.80</b>		6.8	20	>100	500	356	4.59

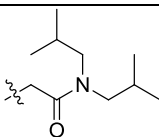
5.88 <sup>[f]</sup>		7.0	80	>100	600	132	5.06
5.89 <sup>[f]</sup>		7.2	20	>100	330	97	5.49
5.90 <sup>[f]</sup>		4.3	>80	>100	390	≥456	3.91
5.91 <sup>[f]</sup>		4.4	>80	>100	380	≥455	4.12
5.81		6.7	20	>100	510	≥409	4.45
<p><sup>a</sup>MIC against <i>M. tuberculosis</i> (H37Rv), isoniazid was used as reference with MIC = 1.8 μM; <sup>b</sup>HepG2, human caucasian hepatocyte carcinoma; <sup>c</sup>artificial membrane permeability; <sup>d</sup><i>in vitro</i> profiling for kinetic aqueous solubility (CLND, chemiluminescent nitrogen detection); <sup>e</sup>chromlogD values at pH = 7.4; <sup>f</sup>commercially available.</p>							

The obtained results showed that replacement of the phenyl ring with a heterocycle generally leads to decreased chromlogD values. However, enzymatic inhibitory activity was found to be negatively affected too. Obtained MIC values are grossly comparable to those of the phenyl-based subset (MIC 15-20). This is in overall accordance with our hypothesis that the MIC values correlate with the LLE values: with both lower enzymatic potencies and lower chromlogD values, the LLE ratios remain similar, and so do the MIC values.

The data for the next small subset of compounds consisting of non-aromatic cyclic or aliphatic chains instead of phenyl ring are shown in Table 5.10. The obtained results indicated that non-aromatic substitution diminished the activity.

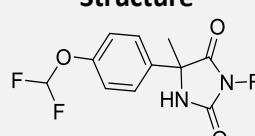
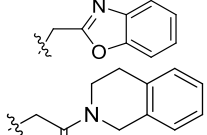
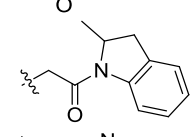
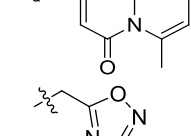
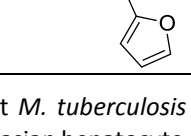
**Table 5.10. Biological and physicochemical profile for compounds with aliphatic modifications.**

Structure	DprE1 pIC <sub>50</sub>	<i>Mtb</i> MIC (μM) <sup>[a]</sup>	TOX <sub>50</sub> (μM) <sup>[b]</sup>	AMP (nm/sec) <sup>[c]</sup>	Solubility (μM) <sup>[d]</sup>	Chrom logD <sup>[e]</sup>
	5.3	80	>100	210	≥472	4.03
	4.6	>80	>100	120	≥467	3.37

5.94 <sup>[f]</sup>		4.9	>80	>100	640	313	6.05
<sup>a</sup> MIC against <i>M. tuberculosis</i> (H37Rv), isoniazid was used as reference with MIC = 1.8 μM; <sup>b</sup> HepG2, human caucasian hepatocyte carcinoma; <sup>c</sup> artificial membrane permeability; <sup>d</sup> <i>in vitro</i> profiling for kinetic aqueous solubility (CLND, chemiluminescent nitrogen detection); <sup>e</sup> chromlogD values at pH = 7.4; <sup>f</sup> commercially available.							

Lastly, a small set of compounds including bicyclic systems was evaluated (Table 5.11). In general, all the obtained compounds showed lower DprE<sub>1</sub> potency and no significant MIC. However, it is worth noting that compound **5.82** which possesses a benzoxazole system (with the oxazole part replacing the keto function) preserved some inhibitory activity (pIC<sub>50</sub> = 6.3). This analogue represents the first example of a ketone modification that is not completely detrimental to enzymatic potency. These data point out that further exploration of chemical space around the benzoxazole system could yield SAR insights leading to the identification of even more promising replacements for the keto function.

**Table 5.11. Biological and physicochemical profile for compounds with bicyclic systems.**

Structure	DprE1 pIC <sub>50</sub>	<i>Mtb</i> MIC (μM) <sup>[a]</sup>	TOX <sub>50</sub> (μM) <sup>[b]</sup>	AMP (nm/sec) <sup>[c]</sup>	Solubility (μM) <sup>[d]</sup>	Chrom logD <sup>[e]</sup>
	6.3	80	>100	490	140	5.00
	6.0	>80	>100	480	34	4.90
	5.9	80	63	520	114	5.37
	5.7	80	>100	540	336	3.83
	5.3	>80	>100	440	212	4.77
<sup>a</sup> MIC against <i>M. tuberculosis</i> (H37Rv), isoniazid was used as reference with MIC = 1.8 μM; <sup>b</sup> HepG2, human caucasian hepatocyte carcinoma; <sup>c</sup> artificial membrane permeability; <sup>d</sup> <i>in vitro</i> profiling for kinetic aqueous solubility (CLND, chemiluminescent nitrogen detection); <sup>e</sup> chromlogD values at pH = 7.4; <sup>f</sup> commercially available.						

In Figure 5.14, antimycobacterial potencies (pMIC values) of compounds which showed a measurable MIC value ( $\leq 80 \mu\text{M}$ ) during the second round of optimization have been plotted against their LLE values.

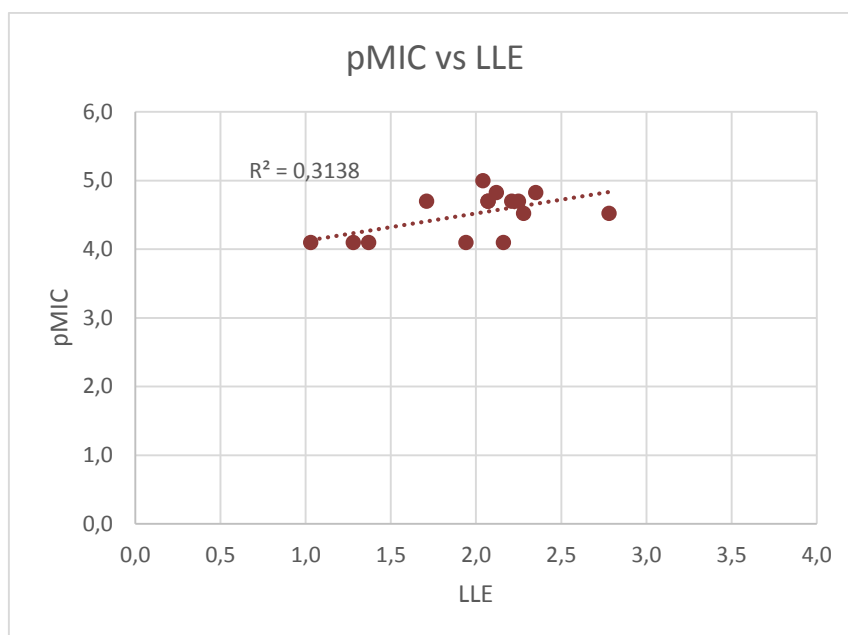


**Figure 5.14. Representation of the pMIC versus LLE (data set used: compounds from table 5.8-5.11 which showed a measurable MIC value ( $\leq 80 \mu\text{M}$ )).**

As shown in Figure 5.14, none of the compounds offered an LLE value greater than 3. In the cases where some improvement of the chromlogD was achieved, a simultaneous reduction of the enzymatic affinity was observed.

### 5.3.3. Conclusions for the second round of Hit-to-Lead optimization

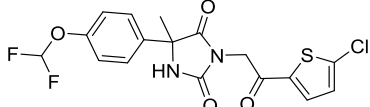
As previously discussed, the aim of this second round of H2L optimization was to reduce the lipophilicity of compound **5.48** maintaining the enzymatic potency, in an attempt to improve LLE values. The latter was found during the first round of optimization to correlate better with antimycobacterial potency (MIC). However, all the efforts so far did not result in reaching values  $>3$ . In the cases where some improvement of the chromlogD was achieved, a simultaneous reduction of the enzymatic affinity was observed. All the compounds were found in the region where  $\text{LLE} < 3$ . Further work is necessary in order to explore other parts of the molecule where hydrophilic groups can be introduced without affecting enzymatic potency.

### 5.4. Intracellular *M. tuberculosis* activity

As shown in Table 5.12, a number of selected compounds were tested for their intracellular activity. This assay determines the effect of the compounds on mycobacteria growing inside human macrophages. Activity in this assay is considered highly desirable as many of the bacteria during an active *M. tuberculosis* infection are found intracellularly in phagocytotic cell types.

**Table 5.12. MIC and intracellular IC<sub>50</sub>, IC<sub>90</sub> values for selected compounds.**

Compd	Structure	MIC (μM)	Intracellular	
			IC <sub>50</sub> (μM) <sup>[a]</sup>	IC <sub>90</sub> (μM) <sup>[a]</sup>
4.1		8.3	1	4.0
4.1 R-enant.		6.7	0.4	1.3
5.48		10	1.3	Max percent inhibition 88
5.54		5.6	1.3	19.95
5.68		2.5	2.0	31.62
5.69		0.9	0.3	Max percent inhibition 86
5.71		3.1	0.2	Max percent inhibition 84
5.79		15	1.6	5.01
5.86		80	6.3	25

5.89		20	5	7.94
<sup>a</sup> IC <sub>50</sub> and IC <sub>90</sub> against infected Human THP-1 macrophages with <i>M. tuberculosis</i> (H37Rv).				

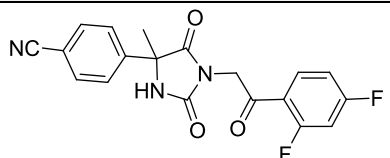
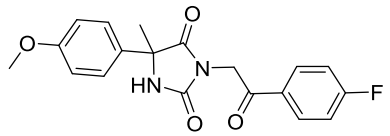
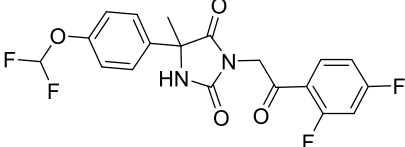
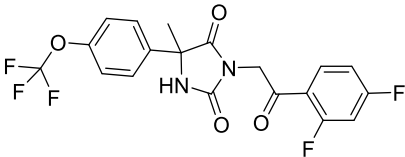
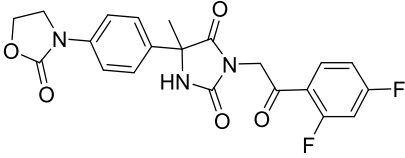
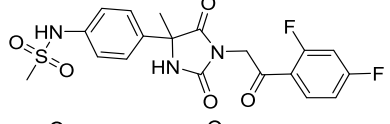
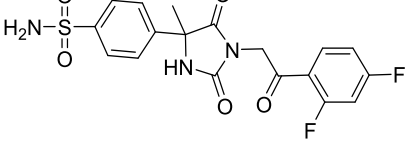
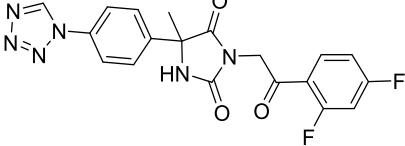
According to the data, the hit compound **4.1** exhibited a very good intracellular IC<sub>90</sub> value of 4 μM, while its active enantiomer (*R*-) showed an improvement with an IC<sub>90</sub> value of 1.26 μM. On the other hand, compounds **5.48**, **5.69** and **5.71** did not reach 90% inhibition at 50 μM (IC<sub>90</sub> >50 μM) in the intracellular assay, although their IC<sub>50</sub> values were excellent (IC<sub>50</sub> 1.3, 0.3, 0.2 μM, respectively). Compounds **5.79** and **5.89** showed good activity with IC<sub>90</sub> values 5.01 and 7.94 μM, respectively, while the rest of the tested compounds (**5.54**, **5.68** and **5.86**) exhibited moderate IC<sub>90</sub> values (19.95-31.62 μM).

Direct comparison of the intracellular values (IC<sub>90</sub>) with the “extracellular” values (MIC) is not reliable, since they depend on different readouts and are calculated differently. Nevertheless, a qualitative comparison between them could give some useful information on their properties for macrophage penetration of the tested compounds. Compounds **5.54** and **5.68** exhibited moderate intracellular IC<sub>90</sub> values and are less potent in macrophages than the “extracellular” MIC values would suggest. This could be due to poor permeability of the compounds through the cell membrane, to bacterial efflux pumps activated by the macrophage or to inactivation of the compounds by host cell-derived metabolites such as reactive species.<sup>137</sup> On the other hand, compounds **4.1**, **5.79**, **5.86** and **5.89** possessing heterocycles on the right-hand part of the molecule exhibited better intracellular IC<sub>90</sub> values than “extracellular” MIC values indicating that these compounds might be targeting pathways, either in the bacteria or in the macrophage, that are essential during infection but not for *in vitro* growth.<sup>138</sup> Accumulation inside the macrophage vacuoles might be another reason for the observed increase in potency.

### 5.5. Metabolic stability

Selected compounds were tested for their *in vitro* metabolic stability using murine and human microsomes and the obtained results are presented at Table 5.13.

Table 5.13. Microsomal stability of selected compounds.

Compd	Structure	Cl <sub>int</sub> (mL/min/g)	
		Mouse	Human
4.1		4.39	0.56
5.10		0.75	1.65
5.48		1.78	<0.40
5.50		1.59	<0.40
5.54		3.54	<0.40
5.68		3.29	0.47
5.69		2.67	<0.40
5.71		2.44	<0.40

The data indicated that all tested compounds were very stable with the majority of them exhibiting intrinsic clearance values <3 mL/min/g using murine microsomes and <0.6 mL/min/g using human microsomes.

### 5.6. Cardiotoxicity (hERG binding assay)

A number of selected compound were tested for hERG liabilities and the results are shown in Table 5.14.



Table 5.14. hERG binding values of selected compounds.

Compd	Structure	hERG IC <sub>50</sub> (μM) IonWorks
4.1		25
5.9		>50
5.10		>50
5.48		5
5.54		>50
5.68		40
5.69		>50
5.71		6
5.79		13
5.89		8

The obtained results indicated that *para*-substitution plays an important role for hERG reactivity. More specifically, compounds **5.9** and **5.10** which possess a methoxy group, compound **5.54** with an oxazolidinone cycle and compound **5.69** with a sulphonamide group did exhibit any hERG reactivity. On the other hand, the initial hit compound **4.1** with a carbonitrile group, compounds **5.48**, **5.79** and **5.89** that have a difluoromethoxy group and compounds **5.68** and **5.71** with methylsulfonamide and tetrazole groups respectively, displayed hERG liabilities.

### 5.7. General antimicrobial activity profile

To understand the antimicrobial spectrum of the series, minimum inhibitory concentrations (MICs) of the primary hit **4.1** and three selected compounds (**5.54**, **5.68** and **5.69**) were measured against a panel of primary isolates comprising medically important Gram-positive as well as Gram-negative pathogens and the obtained results are shown in Table 5.15.

**Table 5.15. Minimum inhibitory concentrations (MICs) against a panel of Gram-positive as well as Gram-negative pathogens.**

Species Strain	Compd	4.1	5.54	5.68	5.69	Ceftazidime
	MIC ( $\mu\text{M}$ )					
<i>A.baumannii</i> 1484749	>128	>128	>128	>128	>128	>16
<i>A.baumannii</i> BM4454	>128	>128	>128	>128	>128	4
<i>A.baumannii</i> BM4652 (efflux mutant)	>128	>128	>128	>128	>128	1
<i>A.baumannii</i> ATCC 19606-1 LpxC-	>128	>128	>128	>128	>128	0.25
<i>E.coli</i> 1162222	>128	>128	>128	>128	>128	1
<i>E.coli</i> 7623	>128	>128	>128	>128	>128	0.125
<i>E.coli</i> 7623 TolC-	>128	>128	>128	>128	>128	0.25
<i>E.coli</i> Top 10 TolC- Parent	n.d.	>128	>128	>128	>128	0.25
<i>E.cloacae</i> X4422	>128	>128	>128	>128	>128	0.5
<i>H.influenzae</i> H128	>128	>128	128	>128	>128	0,03
<i>H.influenzae</i> H128 Acr A-	>128	128	128	128	128	0.03
<i>K.pneumoniae</i> 1511191	>128	>128	>128	>128	>128	4
<i>K.pneumoniae</i> 1161486	>128	>128	>128	>128	>128	0.25
<i>K.pneumoniae</i> 1161486a	>128	>128	>128	>128	>128	0.125
<i>P.aeruginosa</i> 394303	>128	>128	>128	>128	>128	4
<i>P.aeruginosa</i> PAO1 (MV)	>128	>128	>128	>128	>128	1

<i>P.aeruginosa</i> PAO322	>128	>128	>128	>128	0.5
<i>S.aureus</i> WCUH29	>128	>128	>128	>128	>16
<i>S.pneumoniae</i> ERY2	>128	>128	>128	>128	0.125
<i>S.pyogenes</i> 1308007P	>128	>128	>128	>128	0.125

All tested compounds lacked any appreciable antibacterial activity (MIC  $\geq$  128  $\mu$ M) suggesting the target to be specific for mycobacteria. This is a desirable characteristic as they are not accompanied by the side effects of the broad spectrum antibiotics.

## 5.8.Mode of action

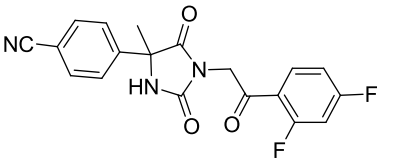
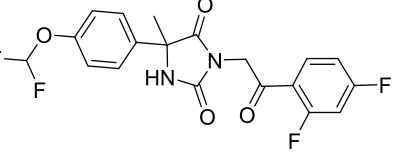
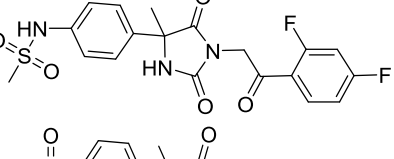
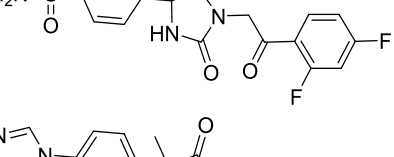
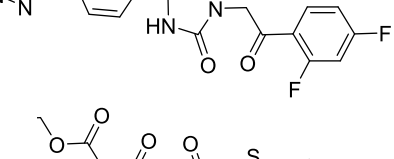
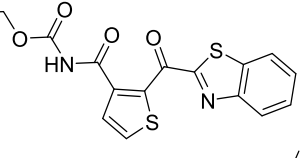
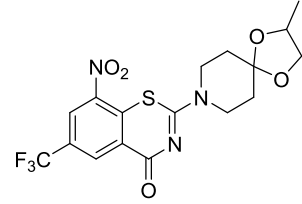
### 5.8.1. Evaluation against *M. tuberculosis* DprE1 overexpressor strain

Overexpression of a target is a clinically observed mechanism of bacterial resistance to antibiotics.<sup>182,183</sup> In this case, antibiotic inhibition of an essential cellular process is overcome because the target is overexpressed and exists in excess to the local inhibitor concentration. Target overexpression can occur through point mutations in gene promoters resulting in increased transcription and translation.<sup>25</sup> For example, mutation in the promoter of the *M. tuberculosis* inhA gene is a mechanism of clinical resistance to isoniazid and ethionamide, key drugs used to treat TB.<sup>182,184</sup>

Overexpression of proteins in the laboratory can be achieved using plasmids that overexpress these genes.<sup>185</sup> This strategy has been successfully applied to indicate possible drug targets by MIC shift. Therefore, shifts in MIC values caused by target overexpression, can provide a simple measure of target engagement at cellular level, which is extremely valuable information for drug discovery programs.<sup>186</sup>

During our project, this approach was used to validate DprE1 as the target enzyme of this series. MIC values of the initial hit compound **4.1** together with a number of selected compounds (**5.48**, **5.68**, **5.69** and **5.71**) were determined against the wild type of *M. Tuberculosis* (WT), *M. tuberculosis* transformed with pMV261 (empty vector, EV) and against *M. tuberculosis* transformed with pMV261:dprE1 (overexpressor, OE). The obtained data are shown in Table 5.16. Shifts in the MIC values when *M. tuberculosis* DprE1 was overexpressed were calculated.

**Table 5.16.** MIC values using wild type of *M. tuberculosis* H37Rv, *M. tuberculosis* transformed with pMV261 (empty vector) and *M. tuberculosis* transformed with pMV261:dprE1 (overexpressor). Ratio of MIC values for *M. tuberculosis* transformed with pMV261:dprE1 to that for *M. tuberculosis* wild type or transformed with pMV261.

Compd	Structure	MIC ( $\mu$ M) WT <sup>[a]</sup>	MIC ( $\mu$ M) EV <sup>[b]</sup>	MIC ( $\mu$ M) OE <sup>[c]</sup>	MIC <sub>OE</sub> /MIC <sub>WT</sub> <sup>[d]</sup>	MIC <sub>OE</sub> /MIC <sub>EV</sub> <sup>[e]</sup>
4.1		7.8	n.d. <sup>[f]</sup>	125	16	n.d. <sup>[f]</sup>
5.48		15	20 <sup>[g]</sup>	>80	>5.3	>4
5.68		10 <sup>[g]</sup>	5	>80	>8.0	>16
5.69		2.5	2.5	>80	>32	>32
5.71		2.5	2.5	>80	>32	>32
TCA-1		1.56	1.56	100	64	64
BTZ-043		0.0156	0.0156	>1	64	>64

<sup>a</sup>WT = wild type, MIC values for *M. tuberculosis* H37Rv, isoniazid was used as reference with MIC = 1.8  $\mu$ M; <sup>b</sup>EV = empty vector, MIC values are for *M. tuberculosis* transformed with pMV261; <sup>c</sup>OE = overexpressor, MIC values are for *M. tuberculosis* transformed with pMV261:dprE1; <sup>d</sup>Ratio of MIC values for *M. tuberculosis* transformed with pMV261:dprE1 to that for wild type *M. tuberculosis*; <sup>e</sup>Ratio of MIC values for *M. tuberculosis* transformed with pMV261:dprE1 to that for *M. tuberculosis* transformed with pMV261; <sup>f</sup>n.d. = not determined; <sup>g</sup>the inhibition profile was not very clear at high concentration of the compound.

Screening of the selected compounds showed that overexpression of DprE1 enzyme in *M. tuberculosis* conferred resistance to all tested compounds compared to the empty vector or wild

type. In detail, they showed greater than 4-fold shifts in the MIC values when DprE1 was overexpressed. The MIC modulation is in agreement with the proposed target of the series.

### 5.8.2. Evaluation against *M. tuberculosis* DprE1 mutant strains

To provide a further genetic link to the mechanism of action, the primary hit compound **4.1** was tested against three in-house *M. tuberculosis* DprE<sub>1</sub> resistant mutants (E221Q, G248S and Y314H) generated using recombineering technique and three spontaneous resistant mutants (L368P, G17C and C387S) provided by S. Cole's group.

**Table 5.17. MIC of the primary hit 4.1 against a panel of *M. tuberculosis* DprE<sub>1</sub> spontaneous resistant mutants.**

Compd	MIC <sub>mutant</sub> /MIC <sub>H37Rv</sub> Ratio					
	E221Q	G248S	Y314H	L368P	G17C	C387S
<b>4.1</b>	16	> 16	16	2	1	<1
<b>TCA-1</b>	≥4	≥2	≥24	≥4	≥1	≥2
<b>AZ-3</b>	16	>63	>63	4	2	1
<b>BTZ-043</b>	4	1	1	1	1	64

As shown in Table 5.17, compound **4.1** showed cross resistance with E221Q, G248S and Y314H strains, sharing a similar profile with **AZ-3**, another DprE1 inhibitor.

Together, the inhibition of purified DprE1 enzyme using a fluorescence-based assay, the MIC modulation against isolated resistant mutants to other classes of DprE1 inhibitors and the MIC modulation observed in the overexpression strain strongly support the assignment of DprE1 as the driver of antimycobacterial activity for these compounds.

### 5.8.3. Time course curves

Once we validated DprE1 as target of the series, time course curves for the hit compound **4.1** and compound **5.9** were plotted in order to better understand the inhibition mode (covalent or noncovalent). Since these compounds possess potentially reactive hydantoin, cyano and keto groups (for hit compound **4.1**), there was a possibility of covalent bond formation with an enzyme nucleophile. Therefore, they were tested using the resazurin reduction assay to determine if there is any evidence of time-dependent inhibition which would suggest covalent bond formation.

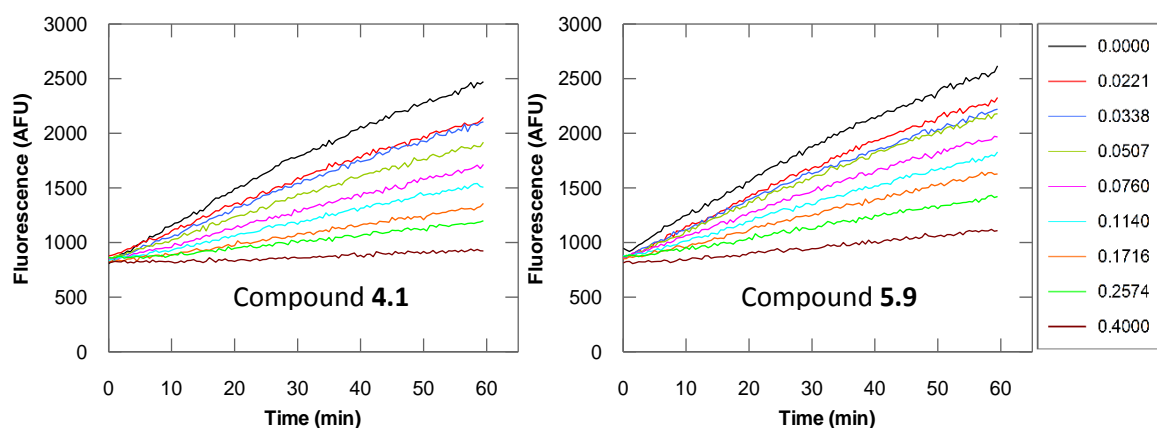


**Figure 5.15. Time courses for compounds 4.1 and 5.9, illustrating reaction linearity for up to 60 min and inhibition of enzyme activity by the tested compounds.**

Figure 5.15 illustrating reaction linearity for up to 60 min and inhibition of enzyme activity in the presence of increasing concentrations of **4.1** and **5.9**. Both compounds behaved like normal reversible inhibitors, and there was no evidence of time-dependent inhibition.

### 5.9. Therapeutic efficacy

The two most potent derivatives obtained so far (**5.69** and **5.71**) were selected for *in vivo* studies in an acute murine model of intratracheal infection. The therapeutic efficacy against *M. tuberculosis* (H37Rv) was determined using an acute infection model in C57BL/6J mice.<sup>187</sup> Mice were intratracheally infected with *M. tuberculosis* (H37Rv strain). Compounds were administered for four consecutive days starting five days after the infection and moxifloxacin was used as an interassay control. Blood samples were obtained at different time points from infected mice to measure the levels of the tested compounds and lungs were harvested on day 9, 24 hours after the last administration. The blood exposure levels and the differences in the lung microorganism burden ( $\log_{10}$ CFUs/lungs) obtained in the treated mice with respect to untreated controls (day 9 after infection) are shown in Table 5.18 and Figure 5.16. No adverse clinical signs were observed in any animal.

**Table 5.18. Blood exposure levels and  $\log_{10}$ CFU for tested compounds.**

Compound	Dose (mg/Kg) (u.i.d. p.o.) <sup>a</sup>	Blood exposure		Difference to untreated mice ( $\log_{10}$ CFU)
		C <sub>max</sub> (ng/mL)	AUC (h*ng/mL)	
Moxifloxacin	100			4.1 ± 0.3
<b>5.69</b>	200	6380	31400 (24h)	0.5 ± 0.1
<b>5.71</b>	170	1870	6738 (6 h)	0.2 ± 0.1

<sup>a</sup>u.i.d. = once per day; p.o. = per os, oral.

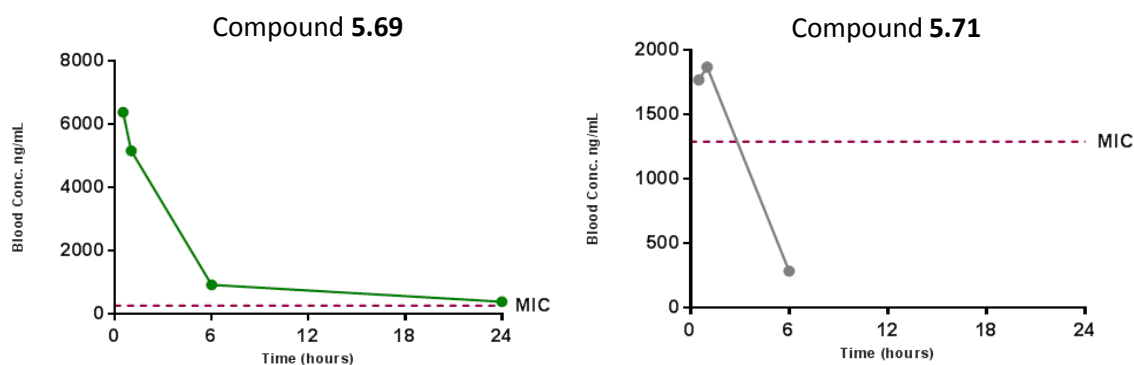


**Figure 5.16. Representation of blood exposure vs time (h) for tested compounds.**

Compound **5.69** demonstrated the best blood exposure with a  $C_{max}$  value of 6380 ng/mL and an AUC value of 31.400 h\*ng/mL. Moreover, the same compound showed the highest reduction of logCFU units (0.5). Although this value reflects limited *in vivo* activity compared to reference moxifloxacin, it demonstrates that the hydantoin series is capable of reaching the lungs of the mice to achieve a statistically significant bacterial load reduction. Compound **5.71** showed low exposure levels and a reduction of only 0.2 logCFU in comparison with the untreated mice which is not statistically significant.

## 5.10. Conclusion

During an HTS campaign performed by GSK, hydantoin **4.1** was identified as a potent DprE<sub>1</sub> inhibitor ( $pIC_{50} = 7$ ) with significant cellular potency (MIC = 8.3  $\mu$ M) against *M. tuberculosis*. The compound was subjected to Hit-to-Lead optimization.

During the first round of optimization, three types of modifications around the initial hit were performed including linker, core and carbonitrile replacements. The best compounds obtained possessed modifications of the carbonitrile substituent and exhibited potent enzymatic inhibitory activities accompanied by very good cellular activities. A correlation between cellular potency (MIC) and LLE was found, with the best compounds possessing a value >3. More specifically, compound **5.69** showed the best MIC value (0.9  $\mu$ M) and excellent enzymatic inhibitory activity ( $pIC_{50} = 7.3$ ). However, the slightly more potent DprE<sub>1</sub> inhibitor **5.48** ( $pIC_{50} = 7.4$ ) displayed a significantly lower potency (MIC 10  $\mu$ M). This mismatch is tentatively explained by the high lipophilicity of the molecule (**5.48**), translating into a lower LLE value of 2.

Based upon these results, a second round of optimization was initiated around compound **5.48**. A number of compounds containing variations of the right-hand side of the molecule were synthesized or purchased with the aim to reduce lipophilicity. Unfortunately, all attempts to

reduce the chromlogD values of **5.48** led to a drop of the enzymatic inhibitory activity too. As a result, no compounds were identified with LLE values exceeding 3, and MIC values of these molecules were moderate ( $>10 \mu\text{M}$ ). Possibly, these data indicate that right-hand side aryl lies in a lipophilic cavity and therefore any attempt to increase hydrophilicity of this part of the molecule led to reduced affinity in the active center.

Additionally, a number of selected compounds were tested for intracellular *in vitro* anti-tubercular activity against infected murine macrophages, *in vitro* microsomal stability and hERG inhibition. The obtained results indicated that almost all of them possessed excellent intramacrophage activity with submicromolar values. At the microsomal stability assay, all tested compounds were very stable with intrinsic clearance values within the desired range. On the other hand, hERG reactivity was an issue for some of the tested compounds and reactivity was mainly driven by *para*-phenyl substituent.

Three compounds were evaluated against a panel of Gram-positive and Gram-negative pathogens without any significant activity, showing that the hydantoins series is very specific against mycobacteria.

To confirm the mode of action of this series, selected compounds were evaluated against the overexpressor strain where the MIC modulation confirmed our target. Moreover, the hit compound was evaluated against a number of DprE1 mutant strains. The hit compound showed a similar profile as AZ-3 another DprE1 inhibitor. Lastly, time curves revealed that the tested compounds are reversible inhibitors of the enzyme.

The three most potent compounds in terms of cellular activity in this project were selected for *in vivo* studies, and one (**5.69**) achieved high blood exposure levels and demonstrated a statistically significant reduction of 0.5 logCFU compared with the untreated mice.

In conclusion, a novel class of hydantoin inhibitors of DprE1 was identified by HTS. Subsequent medicinal chemistry efforts followed, delivering a very potent DprE1 inhibitor (**5.69**,  $\text{pIC}_{50} = 7.3$ ) with significant cellular potency against *M. tuberculosis* H37Rv (MIC =  $0.9 \mu\text{M}$ ) and acceptable physicochemical properties. Importantly, this compound also demonstrated *in vivo* efficacy in infected mice.

### 5.11. Experimental section

All specifications with respect to reagents, solvents, analytical and structure elucidation techniques and apparatuses are identical to the corresponding details mentioned in the



Experimental section of Chapter 3 (Part 3.6). The microwave apparatus used was a Biotage Initiator instrument.

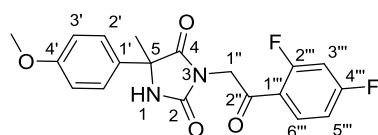
### 5.11.1. General methods

**General method A. Alkylation of the hydantoin core.** A mixture of the appropriate 2,4-imidazolidinedione (1 equiv.), the appropriate 2-halo-acetophenone (1-2.5 equiv.) and potassium carbonate ( $K_2CO_3$ ) (1-1.2 equiv.) were suspended in DMF or acetone (Molarity: 0.06-0.3 M) at room temperature and the reaction mixture was stirred for 1-3 d at room temperature. The solvent was evaporated under reduced pressure and the residue was dissolved in EtOAc (50 mL) and the organic layer was washed with ammonium chloride ( $NH_4Cl$ ) (50 mL), brine (NaCl) (50 mL) and water ( $H_2O$ ) (50 mL). The organic phase was dried over  $MgSO_4$  and evaporated until dryness under reduced pressure. The obtained residue was purified by silica gel column chromatography using as eluent cyclohexane/EtOAc or HPLC using as eluent ACN/ $H_2O$ .

**General Method B. Synthesis of hydantoin core.** For the synthesis of the intermediates that contain a hydantoin core a Bucherer–Bergs protocol was employed. The appropriate ketone (1 equiv.), ammonium carbonate ( $(NH_4)_2CO_3$ ) (9 equiv.) and potassium cyanide (KCN) (1.3-2 equiv.) were dissolved in a mixture of ethanol and water (1:1) and microwave irradiated continuously at 70 °C for 5-12 h. Subsequently, the reaction mixture was cooled down, acidified with HCl (6M) and the pH was adjusted to approximately 7 with aqueous solution of sodium carbonate (10%). In case of precipitation, the obtained solid was filtered and washed with water. Otherwise, the volatiles of the reaction mixture were evaporated under reduced pressure, the residue was dissolved in water and the target compound was extracted with ethyl acetate. If necessary, the desired intermediates were purified using silica gel column chromatography usually using as eluent a cyclohexane/ethyl acetate gradient from 100/0 to 50/50.

### 5.11.2. Chemistry

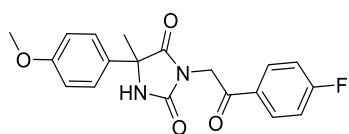
#### **3-(2-(2,4-Difluorophenyl)-2-oxoethyl)-5-(4-methoxyphenyl)-5-methylimidazolidine-2,4-dione (5.9).**



The title compound was prepared according to the general method A, using 5-(4-methoxyphenyl)-5-methyl-2,4-imidazolidinedione (100 mg, 0.454 mmol or 300 mg, 1.36 mmol or 500 mg, 2.27 mmol), 2-chloro-2',4'-difluoroacetophenone (95 mg, 0.50 mmol or 650 mg, 3.41 mmol or 1.08 g, 5.68 mmol) and  $K_2CO_3$  (63 mg, 0.45 mmol or 226 mg, 1.63 mmol or 377 mg, 2.71 mmol) in acetone (7-7.5 mL) and the reaction time was 24-48 h.

Glassy solid; yield 25% (45 mg, 0.11 mmol) or 43% (220 mg, 0.588 mmol) or 25% (215 mg, 0.574 mmol); TLC,  $R_f$  0.52 (cyclohexane/ethyl acetate: 50/50).  $^1\text{H}$  NMR (400 MHz,  $\text{DMSO-}d_6$ )  $\delta$  ppm 9.00 (s, 1 H (N1)), 8.00 (td,  $J=8.6, 6.8$  Hz, 1 H (5''' or 6''')), 7.50 (ddd,  $J=11.6, 9.3, 2.4$  Hz, 1 H (3''')), 7.41 - 7.46 (m, 2 H (2')), 7.28 (td,  $J=8.5, 2.3$  Hz, 1 H (5''' or 6''')), 6.90 - 7.03 (m, 2 H (3')), 4.79 (d,  $J=2.5$  Hz, 2 H (1'')), 3.76 (s, 3 H, -OMe), 1.72 (s, 3 H, -Me).  $^{13}\text{C}$  NMR (101 MHz,  $\text{DMSO-}d_6$ )  $\delta$  ppm 189.2 (d,  $^3J_{\text{CF}}=5.1$  Hz, C(2'')=O), 175.4 (C(4)=O), 165.7 (dd,  $^1J_{\text{CF}}=255.4$  Hz,  $^3J_{\text{CF}}=13.2$  Hz, C-F), 162.4 (dd,  $^1J_{\text{CF}}=256.9$  Hz,  $^3J_{\text{CF}}=13.9$  Hz, C-F), 159.0 (C4'), 155.0 (C(2)=O), 132.6 (dd,  $^3J_{\text{CF}}=11.0$  Hz,  $^3J_{\text{CF}}=4.4$  Hz, 5''' or 6'''), 131.3 (C1'), 126.9 (C2'), 119.5 (dd,  $^2J_{\text{CF}}=13.2$  Hz,  $^4J_{\text{CF}}=3.7$  Hz, C1'''), 113.8 (C3'), 112.8 (dd,  $^2J_{\text{CF}}=22.0$  Hz,  $^4J_{\text{CF}}=3.7$  Hz, 5''' or 6'''), 105.4 (t,  $^2J_{\text{CF}}=27.1$  Hz, C3'''), 62.9 (C5), 55.2(-OMe), 47.1 (d,  $^4J_{\text{CF}}=10.3$  Hz, C1''), 24.8 (-CH<sub>3</sub>). UPLC-MS (C) RT 1.16 min,  $m/z$  375 [M+H]<sup>+</sup> (>95%). HRMS (ESI)  $m/z$  calcd for C<sub>19</sub>H<sub>17</sub>F<sub>2</sub>N<sub>2</sub>O<sub>4</sub> [M+H]<sup>+</sup>: 375.1151; found: 375.1139.

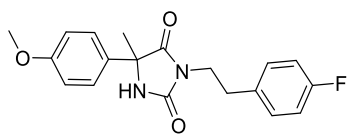
**3-(2-(4-Fluorophenyl)-2-oxoethyl)-5-(4-methoxyphenyl)-5-methylimidazolidine-2,4-dione (5.10).**



The title compound was prepared according to the general method A, using 5-(4-methoxyphenyl)-5-methylimidazolidine-2,4-dione (100 mg, 0.454 mmol), 2-chloro-4'-fluoroacetophenone (78 mg, 0.45 mmol) and K<sub>2</sub>CO<sub>3</sub> (75 mg, 0.54 mmol) in DMF (3 mL) and the reaction time was 1 d.

White solid; yield 69% (112 mg, 0.314 mmol); TLC,  $R_f$  0.48 (cyclohexane/ethyl acetate: 50/50).  $^1\text{H}$  NMR (400 MHz,  $\text{DMSO-}d_6$ )  $\delta$  ppm 8.99 (s, 1 H), 8.07 - 8.19 (m, 2 H), 7.35 - 7.51 (m, 4 H), 6.94 - 7.03 (m, 2 H), 4.96 (s, 2 H), 3.76 (s, 3 H), 1.73 (s, 3 H).  $^{13}\text{C}$  NMR (101 MHz,  $\text{DMSO-}d_6$ )  $\delta$  ppm 191.0, 175.6, 165.5 (d,  $^1J_{\text{CF}}=251.0$  Hz), 159.0, 155.2, 131.3, 131.2, 130.8 (d,  $^4J_{\text{CF}}=2.2$  Hz), 126.9, 116.1 (d,  $^3J_{\text{CF}}=22.7$  Hz), 113.8, 62.9, 55.2, 44.4, 24.8. UPLC-MS (C) RT 1.14 min,  $m/z$  357 [M+H]<sup>+</sup> (>95%)

**3-(4-Fluorophenethyl)-5-(4-methoxyphenyl)-5-methylimidazolidine-2,4-dione (5.11).**

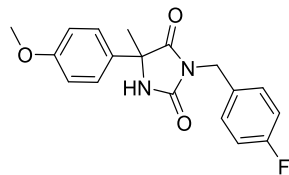


The title compound was prepared according to the general method A, using 5-(4-methoxyphenyl)-5-methylimidazolidine-2,4-dione (200 mg, 0.908 mmol), 4-fluoro-phenethyl bromide (184 mg, 0.906 mmol) and K<sub>2</sub>CO<sub>3</sub> (151 mg, 1.09 mmol) in anhydrous DMF (3 mL) and the reaction time was 3 d.

White solid; yield 78% (242 mg, 0.707 mmol); TLC,  $R_f$  0.49 (cyclohexane/ethyl acetate: 50/50).  $^1\text{H}$  NMR (400 MHz,  $\text{DMSO-}d_6$ )  $\delta$  ppm 8.76 (s, 1 H), 7.18 - 7.27 (m, 2 H), 7.06 - 7.16 (m, 2 H), 6.96 - 7.06 (m, 2 H), 6.85 - 6.95 (m, 2 H), 3.74 (s, 3 H), 3.52 - 3.66 (m, 2 H), 2.83 (t,  $J=6.8$  Hz, 2 H), 1.53 (s, 3 H).  $^{13}\text{C}$  NMR (101 MHz,  $\text{DMSO-}d_6$ )  $\delta$  ppm 175.3, 160.9 (d,  $^1J_{\text{CF}}=242.2$  Hz), 158.8, 155.4, 134.0 (d,  $^4J_{\text{CF}}=2.9$

Hz), 131.4, 130.6 (d,  $^3J_{CF}=8.1$  Hz), 126.6, 114.9 (d,  $^2J_{CF}=21.2$  Hz), 113.7, 62.1, 55.1, 38.8, 32.0, 24.7. UPLC-MS (C) RT 1.17,  $m/z$  341 [M-H]<sup>-</sup> (>95%).

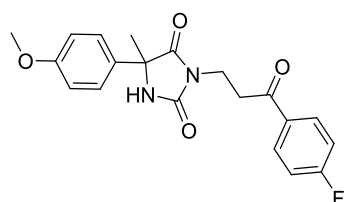
**3-(4-Fluorobenzyl)-5-(4-methoxyphenyl)-5-methylimidazolidine-2,4-dione (5.12).**



The title compound was prepared according to the general method A, using 5-(4-methoxyphenyl)-5-methylimidazolidine-2,4-dione (100 mg, 0.454 mmol), 4-fluorobenzyl bromide (86 mg, 0.45 mmol) and K<sub>2</sub>CO<sub>3</sub> (75 mg, 0.55 mmol) in DMF (3 mL) and the reaction time was 1 d.

White solid; yield 79% (118 mg, 0.359 mmol); TLC, R<sub>f</sub> 0.58 (cyclohexane/ethyl acetate: 50/50). <sup>1</sup>H NMR (400 MHz, DMSO-d<sub>6</sub>) δ ppm 8.97 (s, 1 H), 7.31 - 7.41 (m, 2H), 7.20 - 7.30 (m, 2 H), 7.10 - 7.19 (m, 2 H), 6.88 - 6.98 (m, 2 H), 4.52 (s, 2 H), 3.74 (s, 3 H), 1.65 (s, 3 H). <sup>13</sup>C NMR (101 MHz, DMSO-d<sub>6</sub>) δ ppm 175.3, 161.4 (d,  $^1J_{CF}=243.0$  Hz), 158.9, 155.3, 132.9 (d,  $^4J_{CF}=2.9$  Hz), 131.3, 129.4 (d,  $^3J_{CF}=8.8$  Hz), 126.6, 115.3 (d,  $^2J_{CF}=21.2$  Hz), 113.9, 62.5, 55.1, 40.5, 25.0. UPLC-MS (C) RT 1.16 min,  $m/z$  327 [M-H]<sup>-</sup> (>95%)

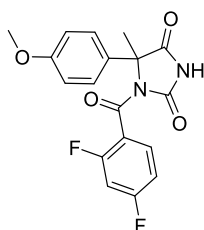
**3-(3-(4-Fluorophenyl)-3-oxopropyl)-5-(4-methoxyphenyl)-5-methylimidazolidine-2,4-dione (5.13).**



The title compound was prepared according to the general method A, using 5-(4-methoxyphenyl)-5-methylimidazolidine-2,4-dione (100 mg, 0.454 mmol), 3-chloro-4'-fluoropropiophenone (85 mg, 0.45 mmol) and K<sub>2</sub>CO<sub>3</sub> (75 mg, 0.55 mmol) in DMF (3 mL) and the reaction time was 1 d.

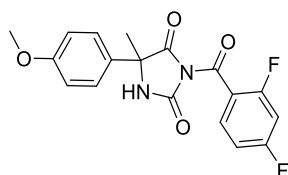
White solid; yield 25% (42 mg, 0.11 mmol); TLC, R<sub>f</sub> 0.38 (cyclohexane/ethyl acetate: 50/50). <sup>1</sup>H NMR (400 MHz, DMSO-d<sub>6</sub>) δ ppm 8.84 (s, 1 H), 7.94 - 8.04 (m, 2 H), 7.28 - 7.40 (m, 4 H), 6.89 - 6.96 (m, 2 H), 3.74 (s, 3 H), 3.71 (t,  $J=7.1$  Hz, 2 H), 3.30\* (t,  $J=7.1$  Hz, 2 H), 1.62 (s, 3 H). <sup>13</sup>C NMR (151 MHz, DMSO-d<sub>6</sub>) δ ppm 196.5, 175.3, 165.1 (d,  $^1J_{CF}=252.3$  Hz), 158.8, 155.3, 132.9 (d,  $^4J_{CF}=2.9$  Hz), 131.4, 131.0 (d,  $^3J_{CF}=9.7$  Hz), 126.7, 115.7 (d,  $^2J_{CF}=22.2$  Hz), 113.8, 62.2, 55.1, 36.0, 33.8, 24.8. UPLC-MS (C) RT 1.14 min,  $m/z$  371 [M+H]<sup>+</sup> (>95%).

\*The triple peak at 3.30 ppm was partially covered by water peak at 3.33 ppm.

**1-(2,4-Difluorobenzoyl)-5-(4-methoxyphenyl)-5-methylimidazolidine-2,4-dione (5.15).**

5-(4-methoxyphenyl)-5-methyl-2,4-imidazolidinedione (100 mg, 0.454 mmol) was dissolved in anhydrous pyridine (1 mL) and 2,4-difluorobenzoyl chloride (80 mg, 0.45 mmol) was added dropwise to the mixture under nitrogen atmosphere. The reaction mixture was left stirring at room temperature overnight. Then, the solvent was removed under reduced pressure and the obtained residue was dissolved in ethyl acetate (10 mL). It was passed through a 2-cm thick pad of silica gel which was subsequently washed with ethyl acetate (5 mL x 2). The combined organics were concentrated by rotary evaporation to provide the crude product which was purified by silica gel column chromatography using a Merck pre-packed column (9+1 g) and as eluent cyclohexane/ethyl acetate (80/20). Subsequently, the organic phase was washed with saturated aqueous solution of sodium bicarbonate ( $\text{NaHCO}_3$ ) (40 mL x 3) and water (40 mL), dried over magnesium sulfate ( $\text{MgSO}_4$ ) and evaporated under reduced pressure to give 1-(2,4-difluorobenzoyl)-5-(4-methoxyphenyl)-5-methylimidazolidine-2,4-dione.

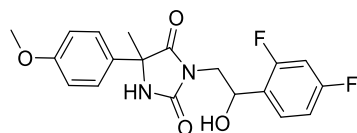
Off-white solid; yield 63% (103 mg, 0.286 mmol); TLC,  $R_f$  0.63 (ethyl acetate/cyclohexane: 50/50).  $^1\text{H}$  NMR (400 MHz,  $\text{DMSO}-d_6$ )  $\delta$  ppm 12.04 (br. s., 1 H), 7.59 (td,  $J=8.3, 6.4$  Hz, 1 H), 7.30 - 7.40 (m, 3 H), 7.17 (td,  $J=8.5, 2.3$  Hz, 1 H), 6.93 - 7.02 (m, 2 H), 3.76 (s, 3 H), 2.05 (s, 3 H).  $^{13}\text{C}$  NMR (101 MHz,  $\text{DMSO}-d_6$ )  $\delta$  ppm 174.8, 163.5 (dd,  $^1J_{\text{C-F}}=250.3$  Hz,  $^3J_{\text{C-F}}=12.4$  Hz), 161.7, 159.0, 159.1 (dd,  $^1J_{\text{C-F}}=250.3$  Hz,  $^3J_{\text{C-F}}=13.2$  Hz), 153.7, 130.9 (dd,  $^3J_{\text{C-F}}=10.2$  Hz,  $^3J_{\text{C-F}}=4.4$  Hz), 129.0, 126.7, 121.3 (dd,  $^2J_{\text{C-F}}=15.7$  Hz,  $^4J_{\text{C-F}}=4.0$  Hz), 114.0, 111.7 (dd,  $^2J_{\text{C-F}}=22.0$  Hz,  $^4J_{\text{C-F}}=3.7$  Hz), 104.0 (t,  $^2J_{\text{C-F}}=26.3$  Hz), 68.1, 55.2, 20.3. UPLC-MS (C) RT 1.06 min,  $m/z$  361  $[\text{M}+\text{H}]^+$  (>95%).

**3-(2,4-Difluorobenzoyl)-5-(4-methoxyphenyl)-5-methylimidazolidine-2,4-dione (5.16).**

5-(4-methoxyphenyl)-5-methyl-2,4-imidazolidinedione (100 mg, 0.454 mmol) and sodium hydride, 60% dispersion in mineral oil ( $\text{NaH}$ , 22mg, 0.92 mmol) were dissolved in anhydrous DMF (1 mL) and the mixture was stirred at room temperature for 15 min. Subsequently, 2,4-difluorobenzoyl chloride (0.056  $\mu\text{L}$ , 0.45 mmol) was added to the mixture under nitrogen atmosphere and stirred at room temperature overnight. Then, the reaction mixture was poured into water (40 mL) and the target compound was extracted with ethyl acetate (50 mL x 3). The combined organics layers were evaporated by rotary evaporation to provide the crude product. Attempts to purify it by silica gel column chromatography or HPLC failed. Partial hydrolysis was observed during the HPLC purification.

TLC,  $R_f$  0.48 (EtOAc/cyclohexane: 50/50).  $^1\text{H}$  NMR (400 MHz,  $\text{DMSO-}d_6$ )  $\delta$  ppm 9.47 (s, 1 H), 7.84 (td,  $J=8.5, 6.4$  Hz, 1 H), 7.40 - 7.49 (m, 3 H), 7.27 (td,  $J=8.5, 2.0$  Hz, 1 H), 6.97 - 7.04 (m, 2 H), 3.74 - 3.80 (m, 3 H), 1.77 (s, 3 H). UPLC-MS (C) RT 3.00 min,  $m/z$  361  $[\text{M}+\text{H}]^+$  (90%).

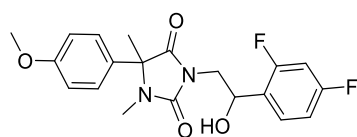
**3-(2-(2,4-Difluorophenyl)-2-hydroxyethyl)-5-(4-methoxyphenyl)-5-methylimidazolidine-2,4-dione (5.17).**



3-(2-(2,4-difluorophenyl)-2-oxoethyl)-5-(4-methoxyphenyl)-5-methylimidazolidine-2,4-dione **5.9** (100 mg, 0.267 mmol) was dissolved in anhydrous toluene (50 mL) and sodium bis(2-methoxyethoxy)aluminum hydride solution (Red-Al) (0.16 mL, 0.53 mmol) was added to the solution under nitrogen atmosphere. The reaction mixture was heated until 120 °C for 1 h using an oil bath. Then, the reaction mixture was cooled down and quenched by careful addition of aqueous NaOH (2N, 2 mL) followed by addition of ethyl acetate (20 mL) and water (70 mL). The resulting biphasic system was separated and the organic layer was further washed with water (50 mL x 2) to get rid of the produced 2-methoxyethanol. The organic layer was evaporated under reduced pressure to provide the crude product which was separated by silica gel column chromatography using a pre-packed Merck column (18+2 g) and as eluent cyclohexane/EtOAc gradient from 100/0 to 50/50 to give 3-(2-(2,4-difluorophenyl)-2-hydroxyethyl)-5-(4-methoxyphenyl)-5-methylimidazolidine-2,4-dione.

Glassy colorless solid; yield 50% (50 mg, 0.13 mmol); TLC,  $R_f$  0.77 (ethyl acetate).  $^1\text{H}$  NMR (400 MHz,  $\text{DMSO-}d_6$ )  $\delta$  ppm 8.76 (d,  $J=5.6$  Hz, 1 H), 7.40 - 7.52 (m, 1 H), 7.21 - 7.33 (m, 2 H), 6.95 - 7.17 (m, 2 H), 6.84 - 6.94 (m, 2 H), 5.71 - 5.78 (m, 1 H), 5.09 (q,  $J=6.5$  Hz, 1 H), 3.75 (d,  $J=0.8$  Hz, 3 H), 3.45 - 3.63 (m, 2 H), 1.55 (d,  $J=14.1$  Hz, 3 H).  $^{13}\text{C}$  NMR (101 MHz,  $\text{DMSO-}d_6$ ) (mixture of diastereoisomers)  $\delta$  ppm 175.3, 175.2, 160.1 - 162.9 (m), 158.8, 158.8 (s), 157.9 - 160.7 (m), 155.4, 155.4, 131.5, 131.4, 129.2 - 129.7 (m), 126.7, 126.6, 125.4 - 125.9 (m), 113.7, 113.6, 111.1 - 111.6 (m), 103.1 (m), 62.8, 62.7, 62.2, 62.2, 55.1, 43.9, 43.8, 24.8. UPLC-MS (C) RT 1.09-1.10 min,  $m/z$  375  $[\text{M}+\text{H}]^+$  (>95%).

**3-(2-(2,4-Difluorophenyl)-2-hydroxyethyl)-5-(4-methoxyphenyl)-1,5-dimethylimidazolidine-2,4-dione (5.18).**

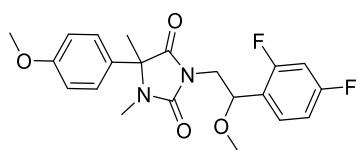


A solution of 3-(2-(2,4-difluorophenyl)-2-hydroxyethyl)-5-(4-methoxyphenyl)-5-methylimidazolidine-2,4-dione (47 mg, 0.13 mmol) and sodium hydride, 60% dispersion in mineral oil (NaH, 5.5 mg, 0.14 mmol) in anhydrous tetrahydrofuran (THF, 5 mL) was stirred for 1 h at room temperature. Then, iodomethane (MeI, 17  $\mu\text{L}$ , 0.27 mmol) was added to the solution and the

reaction mixture was left stirring for 2 days at room temperature. THF was evaporated and the residue was purified by HPLC using an X-Bridge 19 column and as eluent ACN/H<sub>2</sub>O (+0.1% NH<sub>4</sub>HCO<sub>3</sub>) from 40/60 until 100/0. The separation gave the *N*-methylated product (**5.18**) and the dimethylated product (**5.19**).

Colorless glassy solid; yield 40% (20 mg, 0.051 mmol); TLC, R<sub>f</sub> 0.36 (cyclohexane/ethyl acetate: 50/50). <sup>1</sup>H NMR (400 MHz, DMSO-*d*<sub>6</sub>) δ ppm 7.44 - 7.57 (m, 1 H), 7.00 - 7.21 (m, 4 H), 6.89 - 6.97 (m, 2 H), 5.78 (t, *J*=4.8 Hz, 1 H), 5.10 - 5.18 (m, 1 H), 3.76 (d, *J*=0.8 Hz, 3 H), 3.49 - 3.70 (m, 2 H), 2.63 (d, *J*=1.8 Hz, 3 H), 1.64 (d, *J*=14.7 Hz, 3 H). <sup>13</sup>C NMR (101 MHz, DMSO-*d*<sub>6</sub>) (mixture of diastereoisomers) δ ppm 174.5, 174.5, 160.1 - 162.9 (m), 159.2, 159.1, 158.0 - 160.7 (m), 155.0, 155.0, 129.3 - 129.7 (m), 128.4, 128.3, 127.5, 127.3, 125.4 - 125.9 (m), 114.1, 111.5 (dd, <sup>2</sup>*J*<sub>CF</sub>=21.2 Hz, <sup>4</sup>*J*<sub>CF</sub>=2.9 Hz), 103.4 (t, <sup>2</sup>*J*<sub>CF</sub>=26.3 Hz), 65.6, 65.5, 62.8 (d, <sup>3</sup>*J*<sub>CF</sub>=8.1 Hz), 55.2, 44.2 (d, <sup>4</sup>*J*<sub>CF</sub>=8.1 Hz), 24.8, 24.8, 19.4. UPLC-MS (C) RT 1.23 min, *m/z* 391[M+H]<sup>+</sup> (>95%).

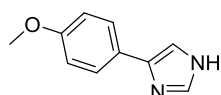
**3-(2-(2,4-Difluorophenyl)-2-methoxyethyl)-5-(4-methoxyphenyl)-1,5-dimethylimidazolidine-2,4-dione (5.19).**



The title compound was obtained from the same reaction described for compound **5.18**.

Colorless glassy solid; yield 12% (6 mg, 0.02 mmol); TLC, R<sub>f</sub> 0.47 (cyclohexane/ethyl acetate: 50/50). <sup>1</sup>H NMR (400 MHz, METHANOL-*d*<sub>4</sub>) δ ppm 7.40 - 7.49 (m, 1 H), 7.08 - 7.19 (m, 2 H), 6.84 - 7.00 (m, 4 H), 4.87 - 4.94 (m, 1 H), 3.66 - 3.92 (m, 5 H), 3.22 (d, *J*=6.8 Hz, 3 H), 2.73 (s, 3 H), 1.72 (d, *J*=13.1 Hz, 3 H). <sup>13</sup>C NMR (101 MHz, METHANOL-*d*<sub>4</sub>) (mixture of diastereoisomers) δ ppm 177.2, 177.1, 163.1 - 165.8 (m), 161.6, 161.6, 161.3 - 164.1 (m), 157.4, 157.4, 130.9 - 131.2 (m), 129.5, 129.5, 128.7, 128.6, 122.8 - 123.2 (m), 115.5 - 115.6 (m), 112.8 - 113.2 (m), 104.8 (t, <sup>2</sup>*J*<sub>CF</sub>=25.6 Hz), 75.0, 74.7, 67.8, 67.8, 57.4 - 57.7 (m), 56.0, 44.1, 44.0, 25.5 - 25.7 (m), 20.2, 20.1. UPLC-MS (C) RT 1.28 min, *m/z* 405 [M+H]<sup>+</sup> (>95%).

**4-(4-Methoxyphenyl)-1H-imidazole (5.22).**

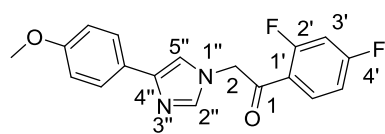


2-Bromo-4'-methoxyacetophenone (1.00 g, 4.37 mmol) was dissolved in formamide (10.0 mL, 252 mmol) and heated at 170 °C for 3 h. The reaction mixture was cooled to room temperature, diluted with H<sub>2</sub>O (40 mL) and basified using aqueous solution of NaHCO<sub>3</sub> (10%) until pH~10. The target compound was extracted with ethyl acetate (50 mL x 4) and the combined organic layers were evaporated under reduced pressure. The obtained residue was purified by NH functionalized silica gel column chromatography using an Isolute pre-packed column (25+1 g) and eluent ethyl acetate/cyclohexane gradient from 0-57%. The obtained

solid was dissolved in a mixture of ACN/H<sub>2</sub>O (1:1) (16 mL) and was lyophilized to give the target compound.

Salmon-colored solid; yield 33% (250 mg, 1.44 mmol); TLC, R<sub>f</sub> 0.54 (ethyl acetate/methanol: 90/10). <sup>1</sup>H NMR (400 MHz, DMSO-*d*<sub>6</sub>) δ ppm 12.05 (br. s., 1 H), 7.64 (d, *J*=0.8 Hz, 3 H), 7.43 (br. s., 1 H), 6.92 (d, *J*=8.6 Hz, 2 H), 3.76 (s, 3 H). <sup>1</sup>H NMR (400 MHz, CDCl<sub>3</sub>) δ ppm 10.22 (br. s., 1 H), 7.58 - 7.73 (m, 3 H), 7.24 (s, 1 H), 6.88 - 6.97 (m, 2 H), 3.82 (s, 3 H). <sup>13</sup>C NMR (101 MHz, CDCl<sub>3</sub>) δ ppm 158.9, 138.6, 135.4, 126.3, 126.0, 114.6, 114.3, 55.4. UPLC-MS (C) RT 0.74 min, *m/z* 175 [M+H]<sup>+</sup> (>95%).

**1-(2,4-Difluorophenyl)-2-(4-(4-methoxyphenyl)-1H-imidazol-1-yl)ethanone (5.23).**

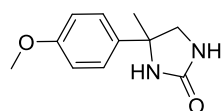


4-(4-Methoxyphenyl)-1*H*-imidazole (100 mg, 0.574 mmol) and cesium carbonate (Cs<sub>2</sub>CO<sub>3</sub>) (224 mg, 0.687 mmol) were suspended in *N,N*-Dimethylformamide (DMF) (2.5 mL). 2-

chloro-2',4'-difluoroacetophenone (219 mg, 1.15 mmol) was added to the reaction mixture and it was heated at 80 °C for 90 min. The reaction mixture was cooled down and poured into water (50 mL) and extracted with ethyl acetate (50 mL x 3). The combined organic layers were evaporated under reduced pressure. The residue was dissolved in DCM (1 mL) and loaded on a Merck silica gel pre-packed column (10 g) and it was purified using as eluent ethyl acetate/cyclohexane gradient from 20/80 to 80/20.

Off-white solid; yield 41% (77 mg, 0.24 mmol); TLC, R<sub>f</sub> 0.45 (ethyl acetate). <sup>1</sup>H NMR (400 MHz, DMSO-*d*<sub>6</sub>) δ ppm 8.06 (dd, *J*=8.6, 1.8 Hz, 1 H), 7.62 - 7.72 (m, 2 H), 7.60 (d, *J*=1.0 Hz, 1 H), 7.54 (ddd, *J*=11.6, 9.3, 2.4 Hz, 1 H), 7.42 (d, *J*=1.0 Hz, 1 H), 7.32 (td, *J*=8.4, 2.4 Hz, 1 H), 6.88 - 6.98 (m, 2 H), 5.58 (d, *J*=3.0 Hz, 2 H), 3.76 (s, 3 H). <sup>13</sup>C NMR (101 MHz, DMSO-*d*<sub>6</sub>) δ ppm 190.3 (d, <sup>3</sup>J<sub>CF</sub>=5.1 Hz), 165.6 (dd, <sup>1</sup>J<sub>CF</sub>=254.7 Hz, <sup>3</sup>J<sub>CF</sub>=12.4 Hz), 162.4 (dd, <sup>1</sup>J<sub>CF</sub>=258.3 Hz, <sup>3</sup>J<sub>CF</sub>=13.2 Hz), 157.8, 140.0, 138.6, 132.6 (dd, <sup>3</sup>J<sub>CF</sub>=11.0 Hz, <sup>3</sup>J<sub>CF</sub>=3.7 Hz), 127.4, 125.4, 119.9 (dd, <sup>2</sup>J<sub>CF</sub>=13.9 Hz, <sup>4</sup>J<sub>CF</sub>=3.7 Hz), 115.8, 113.9, 112.7 (dd, <sup>2</sup>J<sub>CF</sub>=22.0 Hz, <sup>4</sup>J<sub>CF</sub>=3.7 Hz), 105.4 (t, <sup>2</sup>J<sub>CF</sub>=26.8 Hz), 55.6 (d, <sup>4</sup>J<sub>CF</sub>=11.0 Hz), 55.0. UPLC-MS (C) RT 1.14 min, *m/z* 329 [M+H]<sup>+</sup> (>95%).

**4-(4-Methoxyphenyl)-4-methyl imidazolidin-2-one (5.24).**



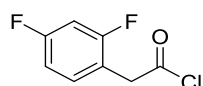
5-(4-Methoxyphenyl)-5-methyl-2,4-imidazolidinedione (300 mg, 1.36 mmol) was dissolved in anhydrous toluene (2 mL) and sodium bis(2-methoxyethoxy)aluminumhydride (Red-Al, 1.33 mL, 6.81 mmol) was added

to the solution under nitrogen atmosphere. The reaction mixture was heated at 120 °C for 2 h using an oil bath. The reaction mixture was cooled down and quenched by careful addition of

aqueous NaOH (1M, 7 mL) followed by addition of ethyl acetate (20 mL) and water (13 mL). The resulting biphasic system was separated and the organic layer was further washed with water (20 mL x 2) to remove the produced 2-methoxyethanol. The organic layer was evaporated under reduced pressure to give the desired product.

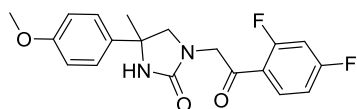
White solid; yield 62 % (173 mg, 0.839 mmol). <sup>1</sup>H NMR (400 MHz, DMSO-*d*<sub>6</sub>) δ ppm 7.27 - 7.32 (m, 2 H), 6.92 (s, 1 H), 6.87 - 6.91 (m, 2 H), 6.22 (s, 1 H), 3.74 (s, 3 H), 3.38 (dd, *J*=8.59, 0.51 Hz, 1 H), 3.23 (dd, *J*=8.59, 1.01 Hz, 1 H), 1.47 (s, 3 H). <sup>13</sup>C NMR (101 MHz, DMSO-*d*<sub>6</sub>) δ ppm 162.30, 157.88, 139.12, 125.96, 113.48, 59.06, 55.04, 54.32, 28.61. UPLC-MS (C) RT 1.16 min, *m/z*: 207 [M+H]<sup>+</sup> (>95%).

### 2-(2,4-Difluorophenyl)acetyl chloride (5.25).



2-(2,4-Difluorophenyl)acetic acid (200 mg, 1.16 mmol) was dissolved in anhydrous 1,2-dichloroethane (DCE, 2.5 mL) and anhydrous *N,N*-Dimethylformamide (DMF, 0.1 mL). Thionyl chloride (SOCl<sub>2</sub>, 2 mL, 27.4 mmol) was added to the solution and the reaction mixture was left stirring 3 days at room temperature. The volatiles were evaporated and the residue was directly used in the next step.

### 1-(2-(2,4-difluorophenyl)-2-oxoethyl)-4-(4-methoxyphenyl)-4-methylimidazolidin-2-one (5.26).



A solution of oxalyl chloride (6 μL, 0.07 mmol) (1 drop) in DCM (0.14 mL) was cooled to -78 °C. Dimethyl sulfoxide (DMSO) (9.9 μL, 0.14 mmol) (1 drop) was added and the mixture was allowed to stir for 5 min. 3-(2-(2,4-difluorophenyl)-2-hydroxyethyl)-5-(4-methoxyphenyl)-5-methyl imidazolidin-4-one (23 mg, 0.063 mmol) dissolved in DCM (1 mL) was added slowly and the reaction was stirred for 15 mins before addition of triethylamine (TEA, 0.04 mL, 0.3 mmol). The reaction mixture was left to warm to room temperature and stirred for 2 h. Then, the reaction mixture was diluted with water (50 mL) and organics were extracted with ethyl acetate (50 mL x 3). The combined organic layers were washed with brine (50 mL), dried over magnesium sulfate (MgSO<sub>4</sub>) and evaporated under reduced pressure. It was purified by preparative HPLC Agilent 1100 in: Chiralpak IC: Heptane/Methanol-Ethanol: 80/20, 45 min, flow: 18 mL/min to obtain both enantiomers (**E1** and **E2**).

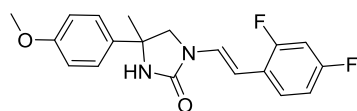
(**E1**): transparent colourless solid; yield 35 % (8 mg, 0.02 mmol); TLC, *R*<sub>f</sub> = 0.18 (cyclohexane/ethyl acetate: 50/50). <sup>1</sup>H NMR (400 MHz, CDCl<sub>3</sub>) δ ppm 8.01 (td, *J*=8.5, 6.6 Hz, 1 H), 7.38 - 7.46 (m, 2 H), 6.95 - 7.04 (m, 1 H), 6.85 - 6.94 (m, 3 H), 4.87 (s, 1 H), 4.64 (dd, *J*=18.7, 4.3 Hz, 1 H), 4.49 (dd, *J*=18.9, 4.0 Hz, 1 H), 3.82 (s, 3 H), 3.61 (dd, *J*=12.6, 8.3 Hz, 2 H), 1.77 (s, 3 H). <sup>13</sup>C NMR (101 MHz,



CDCl<sub>3</sub>)  $\delta$  ppm 191.6 (d,  $^3J_{CF}$ =6.6 Hz), 166.3 (dd,  $^1J_{CF}$ =258.3 Hz,  $^3J_{CF}$ =12.4 Hz), 163.1 (dd,  $^1J_{CF}$ =256.9 Hz,  $^3J_{CF}$ =12.4 Hz), 160.8, 158.9, 137.6, 132.8 (dd,  $^3J_{CF}$ =10.2 Hz,  $^3J_{CF}$ =5.1 Hz), 126.3, 119.9 (dd,  $^2J_{CF}$ =15.4 Hz,  $^4J_{CF}$ =3.7 Hz), 113.9, 112.6 (dd,  $^2J_{CF}$ =22.0 Hz,  $^4J_{CF}$ =2.9 Hz), 104.8 (t,  $^2J_{CF}$ =27.1 Hz), 60.6, 57.0, 55.3, 53.2 (d,  $^4J_{CF}$ =12.4 Hz), 28.1. UPLC-MS (C) RT 1.19 min,  $m/z$  361 [M+H]<sup>+</sup> (>95%)

**(E2):** transparent colourless solid; yield 32 % (7 mg, 0.02 mmol); TLC,  $R_f$  = 0.18 (cyclohexane/ethyl acetate: 50/50). <sup>1</sup>H NMR (400 MHz, CDCl<sub>3</sub>)  $\delta$  ppm 8.01 (td,  $J$ =8.5, 6.6 Hz, 1 H), 7.38 - 7.45 (m, 2 H), 6.96 - 7.03 (m, 1 H), 6.86 - 6.94 (m, 3 H), 4.87 (s, 1 H), 4.64 (dd,  $J$ =18.9, 4.0 Hz, 1 H), 4.49 (dd,  $J$ =18.7, 4.0 Hz, 1 H), 3.82 (s, 3 H), 3.61 (dd,  $J$ =12.4, 8.1 Hz, 2 H), 1.77 (s, 3 H). <sup>13</sup>C NMR (101 MHz, CDCl<sub>3</sub>)  $\delta$  ppm 191.6 (d,  $^3J_{CF}$ =5.9 Hz), 166.3 (dd,  $^1J_{CF}$ =258.3 Hz,  $^3J_{CF}$ =12.4 Hz), 163.1 (dd,  $^1J_{CF}$ =257.6 Hz,  $^3J_{CF}$ =12.4 Hz), 160.8, 158.9, 137.6, 132.8 (dd,  $^3J_{CF}$ =10.6 Hz,  $^3J_{CF}$ =4.8 Hz), 126.3, 119.9 (dd,  $^2J_{CF}$ =14.6 Hz,  $^4J_{CF}$ =4.4 Hz), 113.9, 112.6 (dd,  $^2J_{CF}$ =22.0 Hz,  $^4J_{CF}$ =2.9 Hz), 104.8 (t,  $^2J_{CF}$ =26.8 Hz), 60.6, 57.0, 55.3, 53.2 (d,  $^4J_{CF}$ =12.4 Hz), 28.1. UPLC-MS (C) RT 1.19 min,  $m/z$  361 [M+H]<sup>+</sup> (>95%).

**(E)-1-(2,4-difluorostyryl)-4-(4-methoxyphenyl)-4-methylimidazolidin-2-one (5.27).**

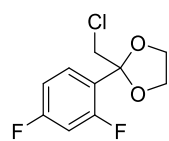


4-(4-Methoxyphenyl)-4-methylimidazolidin-2-one (48 mg, 0.23 mmol) and sodium hydride, 60% dispersion in mineral oil (NaH) (19 mg, 0.47 mmol) were suspended in anhydrous DMF (3 mL)

and left stirring at room temperature for 1 h. Subsequently, 2-(2,4-difluorophenyl) acetyl chloride (138 mg, 0.724 mmol) dissolved in anhydrous DMF (4 mL) was added to the mixture and heated at 50-60 °C for 6 h. The reaction mixture was left stirring overnight at room temperature. The crude product was partially purified by HPLC (X Bridge 19) using as eluent ACN/H<sub>2</sub>O (+ 0.1% NH<sub>4</sub>HCO<sub>3</sub>) gradient from 40/60 to 100/0. It was further purified by HPLC (X Bridge 19) using as eluent ACN/H<sub>2</sub>O (+ 0.1% TFA) gradient from 50/50 to 100/0 to deliver the title compound.

Brown oil; yield 3% (2.7 mg, 7.84  $\mu$ mol). <sup>1</sup>H NMR (400 MHz, DMSO-*d*<sub>6</sub>)  $\delta$  ppm 8.06 (s, 1 H), 7.43 - 7.56 (m, 2 H), 7.33 - 7.41 (m, 2 H), 7.17 (ddd,  $J$ =11.6, 9.2, 2.5 Hz, 1 H), 6.99 (td,  $J$ =8.6, 2.5 Hz, 1 H), 6.94 (m,  $J$ =8.8 Hz, 2 H), 5.58 (d,  $J$ =14.9 Hz, 1 H), 3.82 (d,  $J$ =10.1 Hz, 1 H), 3.75 (s, 3 H), 3.61 (d,  $J$ =10.1 Hz, 1 H), 1.58 (s, 3 H). LC-MS RT 1.27 min,  $m/z$  345 [M+H]<sup>+</sup> (>95%).

**2-(Chloromethyl)-2-(2,4-difluorophenyl)-1,3-dioxolane (5.28).**

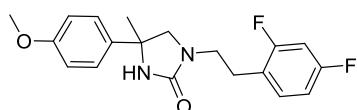


A mixture of 2-chloro-2',4'-difluoroacetophenone (1.00 g, 5.25 mmol), ethylene glycol (10.0 mL, 179 mmol) and *p*-toluene sulfonic acid monohydrate (14 mg, 0.08 mmol) was placed in a microwave tube, which was irradiated for 40 minutes at 100 °C. The reaction mixture was cooled to ambient temperature and poured into water (40 mL) and extracted with a mixture of cyclohexane/ethyl acetate (80/20, 50 mL x 3). The combined

organic layers were dried over magnesium sulfate ( $\text{MgSO}_4$ ) and then evaporated under reduced pressure. The residue was separated by HPLC using a Sunfire 30 column and as eluent ACN/ $\text{H}_2\text{O}$  (+ 0.1 %  $\text{NH}_4\text{HCO}_3$ ) gradient from 40/60 to 100/0 to deliver the target compound.

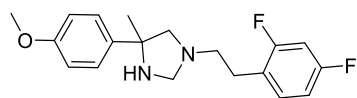
Colourless liquid; yield 35% (432 mg, 1.84 mmol).  $^1\text{H}$  NMR (400 MHz,  $\text{DMSO}-d_6$ )  $\delta$  ppm 7.56 (td,  $J=8.8, 6.8$  Hz, 1 H), 7.28 (ddd,  $J=11.5, 9.2, 2.5$  Hz, 1 H), 7.05 - 7.14 (m, 1 H), 4.06 - 4.18 (m, 2 H), 3.93 (s, 2 H), 3.85 - 3.92 (m, 2 H).  $^{13}\text{C}$  NMR (101 MHz,  $\text{DMSO}-d_6$ )  $\delta$  ppm 162.6 (dd,  $^1J_{\text{CF}}=245.2$  Hz,  $^3J_{\text{CF}}=9.5$  Hz), 159.6 (dd,  $^1J_{\text{CF}}=251.0$  Hz,  $^3J_{\text{CF}}=11.7$  Hz), 129.7 (dd,  $^3J_{\text{CF}}=9.9$  Hz,  $^3J_{\text{CF}}=5.5$  Hz), 122.8 (dd,  $^2J_{\text{CF}}=13.2$  Hz,  $^4J_{\text{CF}}=3.7$  Hz), 111.0 (dd,  $^2J_{\text{CF}}=21.2$  Hz,  $^4J_{\text{CF}}=3.7$  Hz), 106.1 (d,  $^3J_{\text{CF}}=3.7$  Hz), 104.8 (t,  $^2J_{\text{CF}}=26.3$  Hz), 65.5, 47.5 (d,  $^4J_{\text{CF}}=3.7$  Hz).

**1-(4-Fluorophenethyl)-4-(4-methoxyphenyl)-4-methylimidazolidin-2-one (5.31).**



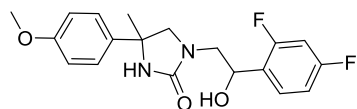
3-(4-Fluorophenethyl)-5-(4-methoxyphenyl)-5-methylimidazolidine-2,4-dione (104 mg, 0.304 mmol) was dissolved in anhydrous toluene (3 mL) and sodium bis(2-methoxyethoxy) aluminum hydride solution (Red-Al, 0.30 mL, 1.5 mmol) was added to the solution under nitrogen atmosphere. The reaction mixture was heated at 120 °C for 2 h using an oil bath. The reaction mixture was cooled down and quenched by careful addition of aqueous NaOH (2N, 5 mL) followed by addition of ethyl acetate (17 mL) and water (15 mL). The resulting biphasic system was separated and the organic layer was further washed with water (20 mL x 2) to get rid of the produced 2-methoxyethanol. The organic layer was evaporated under reduced pressure to provide the crude product which was separated by silica gel column chromatography using a Merck pre-packed column (9+1 g) and as eluent cyclohexane/ethyl acetate gradient from 100/0 to 0/100 and then, ethanol/ethyl acetate gradient from 0/100 to 25/75. Compound **5.32** was also obtained together with the title compound (**5.31**).

Off-white solid; yield 24% (25 mg, 0.072 mmol); TLC, 0.55 (ethyl acetate).  $^1\text{H}$  NMR (400 MHz,  $\text{DMSO}-d_6$ )  $\delta$  ppm 7.23 - 7.29 (m, 2 H), 7.16 - 7.23 (m, 2 H), 7.02 - 7.10 (m, 3 H), 6.86 - 6.92 (m, 2 H), 3.73 (s, 3 H), 3.41 (d,  $J=8.6$  Hz, 1 H), 3.28 - 3.38 (m, 1 H), 3.17 - 3.26 (m, 2 H), 2.70 (t,  $J=7.2$  Hz, 2 H), 1.40 (s, 3 H).  $^{13}\text{C}$  NMR (101 MHz,  $\text{DMSO}-d_6$ )  $\delta$  ppm 160.2, 160.7 (d,  $^1J_{\text{CF}}=241.5$  Hz), 157.9, 138.8, 135.4 (d,  $^4J_{\text{CF}}=3.7$  Hz), 130.4 (d,  $^3J_{\text{CF}}=8.1$  Hz), 126.0, 114.8 (d,  $^2J_{\text{CF}}=22.0$  Hz), 113.5, 58.5, 56.3, 55.0, 43.8, 32.4, 28.6. UPLC-MS (C) RT 1.18 min,  $m/z$  329  $[\text{M}+\text{H}]^+$  (>95%).

**1-(4-Fluorophenethyl)-4-(4-methoxyphenyl)-4-methylimidazolidine (5.32).**

The title compound was obtained from the same reaction described for compound **5.31** and it was observed that it was slowly degraded.

Off-white solid; yield 39% (43 mg, 0.12 mmol); TLC,  $R_f$  0.17 (ethyl acetate/methanol: 90/10).  $^1\text{H}$  NMR (400 MHz,  $\text{DMSO-}d_6$ )  $\delta$  ppm 8.27 (s, 1 H), 7.38 (d,  $J=8.8$  Hz, 2 H), 7.24 (dd,  $J=8.5, 5.7$  Hz, 2 H), 7.07 (t,  $J=8.8$  Hz, 2 H), 6.80 - 6.87 (m, 2 H), 3.78 (d,  $J=6.8$  Hz, 1 H), 3.72 (s, 3 H), 3.22 (d,  $J=7.1$  Hz, 1 H), 2.96 (d,  $J=8.8$  Hz, 1 H), 2.53 - 2.74 (m, 5 H), 1.37 (s, 3 H).  $^{13}\text{C}$  NMR (151 MHz,  $\text{DMSO-}d_6$ )  $\delta$  ppm 160.6 (d,  $^1J_{\text{CF}}=240.5$  Hz), 157.4, 141.3, 136.5 (d,  $^4J_{\text{CF}}=2.3$  Hz), 130.3 (d,  $^3J_{\text{CF}}=8.1$  Hz), 126.4, 114.7 (d,  $^2J_{\text{CF}}=20.7$  Hz), 113.2, 70.4, 66.5, 63.4, 55.4, 54.9, 34.1, 30.4. UPLC-MS (C) RT 1.18 min,  $m/z$  329  $[\text{M}+\text{H}]^+$  (85%). It

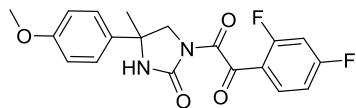
**1-(2-(2,4-Difluorophenyl)-2-hydroxyethyl)-4-(4-methoxyphenyl)-4-methylimidazolidin-2-one (5.33).**

3-(2-(2,4-Difluorophenyl)-2-oxoethyl)-5-(4-methoxyphenyl)-5-methylimidazolidine-2,4-dione (100 mg, 0.267 mmol) was

dissolved in anhydrous toluene (50 mL) and sodium bis(2-methoxyethoxy)aluminum hydride solution (Red-Al, 0.16 mL, 0.53 mmol) was added to the solution under nitrogen atmosphere. The reaction mixture was heated at 120 °C for 2 h 15 min using an oil bath. The reaction mixture was cooled down and quenched by careful addition of aqueous NaOH (2N, 2 mL) followed by addition of EtOAc (20 mL) and water (70 mL). The resulting biphasic system was separated and the organic layer was further washed with water (50 mL x 2) to get rid of the produced 2-methoxyethanol. The organic layer was evaporated under reduced pressure to provide the crude product which was separated by silica gel column chromatography using a pre-packed Merck column (9+1g) and as eluent cyclohexane/ethyl acetate gradient from 100/0 to 0/100 to give the title compound.

Colorless glassy solid; yield 48% (46 mg, 0.13 mmol); TLC,  $R_f$  0.38 (ethyl acetate).  $^1\text{H}$  NMR (400 MHz,  $\text{DMSO-}d_6$ )  $\delta$  ppm 7.38 - 7.56 (m, 1 H), 7.24 (dd,  $J=8.8, 1.5$  Hz, 2 H), 6.95 - 7.17 (m, 3 H), 6.84 - 6.91 (m, 2 H), 5.59 (dd,  $J=4.8, 2.5$  Hz, 1 H), 4.93 (q,  $J=5.5$  Hz, 1 H), 3.74 (d,  $J=4.3$  Hz, 3 H), 3.47 (dd,  $J=46.7, 8.6$  Hz, 1 H), 3.15 - 3.38 (m, 3 H), 1.40 (d,  $J=2.5$  Hz, 3 H).  $^{13}\text{C}$  NMR (101 MHz,  $\text{CDCl}_3$ ) (mixture of diastereoisomers)  $\delta$  ppm 162.5, 160.9 - 163.6 (m), 158.95, 158.93, 159.2 (dd,  $^1J_{\text{CF}}=247.4$  Hz,  $^3J_{\text{CF}}=11.7$  Hz), 137.1, 136.9, 128.7 - 129.2 (m), 125.9, 125.8, 124.8 - 125.3 (m), 114.0, 113.9, 111.2 (dd,  $^2J_{\text{CF}}=20.5$  Hz,  $^4J_{\text{CF}}=3.7$  Hz), 103.32 (t,  $^2J_{\text{CF}}=25.6$  Hz), 103.26 (t,  $^2J_{\text{CF}}=25.6$  Hz), 67.71, 67.66, 62.3, 62.0, 57.8, 57.7, 55.3, 51.1, 50.8, 28.0. UPLC-MS (C) RT 1.20 min,  $m/z$  363  $[\text{M}+\text{H}]^+$  (>95%).

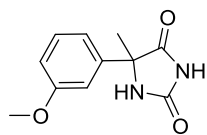
**1-(2,4-Difluorophenyl)-2-(4-(4-methoxyphenyl)-4-methyl-2-oxoimidazolidin-1-yl)ethane-1,2-dione (5.34).**



1-(2-(2,4-Difluorophenyl)-2-hydroxyethyl)-4-(4-methoxyphenyl)-4-methylimidazolidin-2-one (5 mg, 0.01 mmol) was dissolved in anhydrous dichloromethane (DCM, 2 mL) and excess of manganese dioxide ( $\text{MnO}_2$ , 20 mg, 0.23 mmol) was added to the solution. The reaction mixture was left stirring at room temperature for 6 h. The reaction mixture was passed through a syringe filter in order to remove  $\text{MnO}_2$  and DCM was evaporated under reduced pressure. The obtained residue was purified by silica gel column chromatography using a Merck pre-packed column (10 g) and as eluent cyclohexane/EtOAc gradient from 100/0 to 50/50 to deliver the pure product.

Transparent colourless solid; yield 12% (0.6 mg, 1.603  $\mu\text{mol}$ ).  $^1\text{H}$  NMR (400 MHz,  $\text{DMSO}-d_6$ )  $\delta$  ppm 8.94 (s, 1 H), 7.97 - 8.09 (m, 1 H), 7.46 - 7.55 (m, 1 H), 7.27 - 7.41 (m, 3 H), 6.92 - 7.03 (m, 2 H), 4.08 (d,  $J=11.4$  Hz, 1 H), 3.83 (d,  $J=11.4$  Hz, 1 H), 3.76 (s, 3 H), 1.63 (s, 3 H). UPLC-MS (C) RT 1.29 min,  $m/z$  375  $[\text{M}+\text{H}]^+$  (>95%).

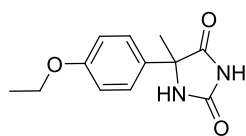
**5-(3-Methoxyphenyl)-5-methylimidazolidine-2,4-dione (5.36).**



The title compound was prepared according to the general method B using 1-(3-methoxyphenyl)ethanone (500 mg, 3.33 mmol), ammonium carbonate (2.88 g, 30.0 mmol) and potassium cyanide (434 mg, 6.66 mmol) in a mixture of ethanol/water (50/50) (14 mL). The mixture was microwave irradiated at 70 °C for 6 h.

White solid; yield 90% (662 mg, 3.00 mmol); TLC,  $R_f$  0.47 (cyclohexane/ethyl acetate: 50/50).  $^1\text{H}$  NMR (400 MHz,  $\text{DMSO}-d_6$ )  $\delta$  ppm 10.74 (s, 1 H), 8.60 (s, 1 H), 7.31 (t,  $J=8.0$  Hz, 1 H), 7.02 - 7.07 (m, 1 H), 7.00 (t,  $J=2.1$  Hz, 1 H), 6.88 - 6.93 (m, 1 H), 3.76 (s, 3 H), 1.63 (s, 3 H).  $^{13}\text{C}$  NMR (101 MHz,  $\text{DMSO}-d_6$ )  $\delta$  ppm 176.7, 159.2, 156.1, 141.5, 129.6, 117.5, 112.8, 111.4, 63.8, 55.1, 25.2. UPLC-MS (C) RT 0.94 min,  $m/z$  219  $[\text{M}+\text{H}]^+$  (>95%)

**5-(4-Ethoxyphenyl)-5-methylimidazolidine-2,4-dione (5.37).**

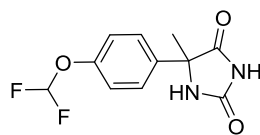


The title compound was prepared according to the general procedure B, using 1-(4-ethoxyphenyl)ethanone (500 mg, 3.05 mmol), ammonium carbonate (2.63 g, 27.4 mmol) and potassium cyanide (397 mg, 6.09 mmol) in a mixture of ethanol/water (50/50) (14 ml). The mixture was microwave irradiated at 70 °C for 12 h.

White solid; yield 65% (461 mg, 1.97 mmol); TLC,  $R_f$  0.24 (cyclohexane/ethyl acetate: 50/50).  $^1\text{H}$  NMR (400 MHz,  $\text{DMSO}-d_6$ )  $\delta$  ppm 10.69 (s, 1 H), 8.52 (s, 1 H), 7.31 - 7.38 (m, 2 H), 6.88 - 6.96 (m,

2 H), 4.01 (q,  $J=7.0$  Hz, 2 H), 1.61 (s, 3 H), 1.31 (t,  $J=6.9$  Hz, 3 H).  $^{13}\text{C}$  NMR (101 MHz,  $\text{DMSO-}d_6$ )  $\delta$  ppm 177.2, 158.1, 156.2, 131.7, 126.5, 114.2, 63.5, 63.0, 24.9, 14.6. UPLC-MS (C) RT 1.04 min,  $m/z$  235  $[\text{M}+\text{H}]^+$  (>95%).

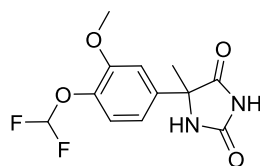
**5-(4-(Difluoromethoxy)phenyl)-5-methylimidazolidine-2,4-dione (5.38).**



The title compound was prepared according to the general method B, using 1-(4-(difluoromethoxy)phenyl)ethanone (500 mg, 2.69 mmol), potassium cyanide (0.350 g, 5.37 mmol) and ammonium carbonate (2.323 g, 24.17 mmol) in a mixture of ethanol/water (50/50) (14 mL). The mixture was microwave irradiated at 70 °C for 5 h.

White solid; yield 95% (651 mg, 2.54 mmol).  $^1\text{H}$  NMR (400 MHz,  $\text{DMSO-}d_6$ )  $\delta$  ppm 10.79 (br. s., 1 H), 8.62 (s, 1 H), 7.48 - 7.54 (m, 2 H), 7.03 - 7.43 (m, 3 H), 1.64 (s, 3 H).  $^{13}\text{C}$  NMR (101 MHz,  $\text{DMSO-}d_6$ )  $\delta$  ppm 176.8, 156.1, 150.5 (t,  $^3J_{\text{CF}}=3.3$  Hz), 136.8, 127.1, 118.7, 116.3 (t,  $^1J_{\text{CF}}=258.3$  Hz), 63.5, 25.0. UPLC-MS (C) RT 1.07 min,  $m/z$  255  $[\text{M}-\text{H}]^-$  (>95%).

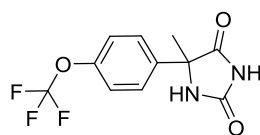
**5-(4-(Difluoromethoxy)-3-methoxyphenyl)-5-methylimidazolidine-2,4-dione (5.39).**



The title compound was prepared according to the general procedure B, using 1-(4-(difluoromethoxy)-3-methoxyphenyl)ethanone (500 mg, 2.31 mmol), ammonium carbonate (2000 mg, 20.82 mmol) and potassium cyanide (301 mg, 4.63 mmol) in a mixture of ethanol/water (50/50) (14 ml). The mixture was microwave irradiated at 70 °C for 12 h.

White solid; yield 99% (655 mg, 2.29 mmol); TLC,  $R_f$  0.21 (cyclohexane/ethyl acetate: 50/50).  $^1\text{H}$  NMR (400 MHz,  $\text{DMSO-}d_6$ )  $\delta$  ppm 10.80 (s, 1 H), 8.65 (s, 1 H), 6.84 - 7.26 (m, 4 H), 3.84 (s, 3 H), 1.65 (s, 3 H).  $^{13}\text{C}$  NMR (101 MHz,  $\text{DMSO-}d_6$ )  $\delta$  ppm 176.6, 156.1, 150.4, 139.0 (t,  $^3J_{\text{CF}}=3.3$  Hz), 138.5, 121.0, 117.6, 116.6 (t,  $^1J_{\text{CF}}=258.3$  Hz), 110.4, 63.7, 55.9, 25.6. UPLC (C) RT 0.99 min,  $m/z$  285  $[\text{M}+\text{H}]^+$  (>95%)

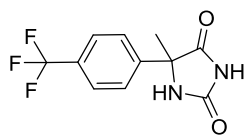
**5-Methyl-5-(4-(trifluoromethoxy)phenyl)imidazolidine-2,4-dione (5.40).**



The title compound was prepared according to the general method B, using 1-(4-(trifluoromethoxy)phenyl)ethanone (500 mg, 2.45 mmol), ammonium carbonate (2118 mg, 22.04 mmol) and potassium cyanide (207 mg, 3.18 mmol) in a mixture of ethanol/water (50/50) (16 mL) and the reaction mixture was stirred at 55-65 °C overnight.

Glassy colorless solid; yield 68% (454 mg, 1.66 mmol).  $^1\text{H}$  NMR (400 MHz,  $\text{DMSO-}d_6$ )  $\delta$  ppm 10.84 (s, 1 H), 8.66 (s, 1 H), 7.60 (d,  $J=8.8$  Hz, 2 H), 7.40 (d,  $J=8.8$  Hz, 2 H), 1.66 (s, 3 H). UPLC (C) RT 1.30 min,  $m/z$  275.10  $[\text{M}+\text{H}]^+$  (>95%).

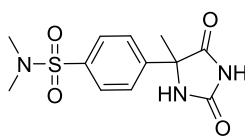
**5-Methyl-5-(4-(trifluoromethyl)phenyl)imidazolidine-2,4-dione (5.41).**



The title compound was prepared according to the general method B, using 1-(4-(trifluoromethyl)phenyl)ethanone (500 mg, 2.66 mmol), ammonium carbonate (2298 mg, 23.92 mmol) and potassium cyanide (346 mg, 5.32 mmol) in a mixture of ethanol/water (50/50) (14 mL). The mixture was microwave irradiated at 70 °C for 6 h.

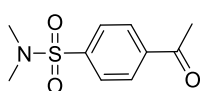
White foamy solid; yield 94% (644 mg, 2.49 mmol); TLC,  $R_f$  0.34 (cyclohexane/ethyl acetate: 50/50).  $^1\text{H}$  NMR (400 MHz,  $\text{DMSO-}d_6$ )  $\delta$  ppm 10.89 (s, 1 H), 8.72 (s, 1 H), 7.78 (d,  $J=8.6$  Hz, 2 H), 7.71 (d,  $J=8.6$  Hz, 2 H), 1.69 (s, 3 H).  $^{13}\text{C}$  NMR (101 MHz,  $\text{DMSO-}d_6$ )  $\delta$  ppm 176.3, 156.1, 144.5, 128.5 (q,  $^2J_{\text{CF}}=31.8$  Hz), 126.3, 125.4 (q,  $^3J_{\text{CF}}=3.7$  Hz), 124.1 (q,  $^1J_{\text{CF}}=271.8$  Hz), 63.9, 25.1. UPLC-MS (C) RT 1.06 min,  $m/z$  257  $[\text{M}+\text{H}]^+$  (>95%).

***N,N*-dimethyl-4-(4-methyl-2,5-dioximidazolidin-4-yl)benzenesulfonamide (5.42).**



The title compound was prepared according to the general method B, using 4-acetyl-*N,N*-dimethylbenzenesulfonamide (150 mg, 0.660 mmol), ammonium carbonate (571 mg, 5.94 mmol) and potassium cyanide (86 mg, 1.3 mmol) in a mixture of ethanol/water (50/50) (10 mL). The mixture was microwave irradiated at 70 °C for 6 h.

White solid; yield (75%, 147 mg, 0.494 mmol).  $^1\text{H}$  NMR (400 MHz,  $\text{DMSO-}d_6$ )  $\delta$  ppm 10.90 (s, 1 H), 8.73 (s, 1 H), 7.57 - 7.96 (m, 4 H), 2.61 (s, 6 H), 1.69 (s, 3 H). UPLC (C) RT 1.02 min,  $m/z$  298  $[\text{M}+\text{H}]^+$  (>95%).

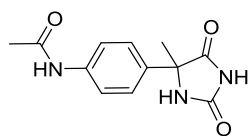


The 4-acetyl-*N,N*-dimethylbenzenesulfonamide was prepared according to Hinsberg reaction. A solution of dimethylamine in THF (2.0 M, 3.43 mL, 6.86 mmol) was added to a solution of 4-acetylbenzenesulfonyl chloride (500 mg, 2.29 mmol) in anhydrous tetrahydrofuran (THF) (13 mL) and the resulting mixture was stirred at room temperature overnight. THF was evaporated and the residue was dissolved in water (80 mL). The pH was adjusted to 7 using an aqueous solution of  $\text{Na}_2\text{CO}_3$  (10%). The target compound was extracted with ethyl acetate (80 mL x 3). The combined organic layers were dried over magnesium sulfate ( $\text{MgSO}_4$ ) and evaporated under reduced pressure. The obtained residue was purified by

column chromatography using a pre-packed Merck silica gel column (27+3 g) and as eluent ethyl acetate/cyclohexane gradient from 0/100 to 0/60 to deliver 156 mg of the target compound.

White solid; yield 30% (156 mg, 0.686 mmol).  $^1\text{H}$  NMR (400 MHz,  $\text{DMSO-}d_6$ )  $\delta$  ppm 8.18 (m, 2 H), 7.85-7.92 (m, 2 H), 2.65 (s, 3 H), 2.64 (s, 6 H). UPLC-MS (C) RT 2.45 min,  $m/z$  228.10  $[\text{M}+\text{H}]^+$  (>95%).

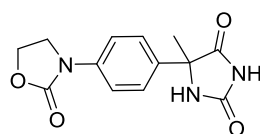
***N*-(4-(4-methyl-2,5-dioxoimidazolidin-4-yl)phenyl)acetamide (5.43).**



The title compound was prepared according to the general method B, using 4-acetamidoacetophenone (500 mg, 2.82 mmol), ammonium carbonate (2.44 g, 25.4 mmol) and potassium cyanide (367 mg, 5.64 mmol) in a mixture of ethanol/water (50/50) (14 mL). The mixture was microwave irradiated at 70 °C for 6 h.

White solid; yield 80 % (557 mg, 2.25 mmol).  $^1\text{H}$  NMR (400 MHz,  $\text{DMSO-}d_6$ )  $\delta$  ppm 10.69 (br. s., 1 H), 9.97 (s, 1 H), 8.52 (s, 1 H), 7.57 (d,  $J=8.8$  Hz, 2 H), 7.36 (d,  $J=8.8$  Hz, 2 H), 2.03 (s, 3 H), 1.62 (s, 3 H). UPLC-MS (C) RT 0.89 min,  $m/z$  248  $[\text{M}+\text{H}]^+$  (>95%).

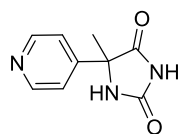
***5*-Methyl-5-(4-(2-oxooxazolidin-3-yl)phenyl)imidazolidine-2,4-dione (5.44).**



The title compound was prepared according to the general method B, using 3-(4-acetylphenyl)oxazolidin-2-one (300 mg, 1.46 mmol), ammonium carbonate (1264 mg, 13.16 mmol) and potassium cyanide (190 mg, 2.92 mmol) in a mixture of ethanol/water (50/50) (12 mL). The mixture was microwave irradiated at 70 °C for 6 h.

White solid, yield 54% (218 mg, 0.792 mmol).  $^1\text{H}$  NMR (400 MHz,  $\text{DMSO-}d_6$ )  $\delta$  ppm 10.74 (s, 1 H), 8.58 (s, 1 H), 7.54 - 7.60 (m, 2 H), 7.44 - 7.50 (m, 2 H), 4.44 (t,  $J=7.6$  Hz, 2 H), 4.05 (m,  $J=8.6$  Hz, 2 H), 1.64 (s, 3 H). UPLC-MS (C) RT 0.94 min,  $m/z$  276  $[\text{M}+\text{H}]^+$  (>95%).

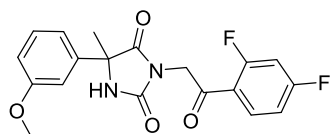
***5*-Methyl-5-(pyridin-4-yl)imidazolidine-2,4-dione (5.45).**



The title compound was prepared according to the general method B, using 1-(pyridin-4-yl)ethanone (200 mg, 0.183 mL, 1.65 mmol), ammonium carbonate (1428 mg, 14.86 mmol) and potassium cyanide (140 mg, 2.15 mmol) in a mixture of ethanol/water (50/50, 6 mL). The mixture was heated at 55 °C and the reaction time was 1 d.

White solid, yield 87% (275 mg, 1.44 mmol).  $^1\text{H}$  NMR (400 MHz,  $\text{DMSO-}d_6$ )  $\delta$  ppm 10.89 (br. s., 1 H), 8.71 (s, 1 H), 8.56 - 8.63 (m, 2 H), 7.45 - 7.51 (m, 2 H), 1.66 (s, 3 H).  $^{13}\text{C}$  NMR (101 MHz,  $\text{DMSO-}d_6$ )  $\delta$  ppm 175.83, 156.10, 149.90, 148.45, 120.40, 63.42, 24.65. UPLC-MS (C) RT 0.75 min,  $m/z$  192  $[\text{M}+\text{H}]^+$  (>95%).

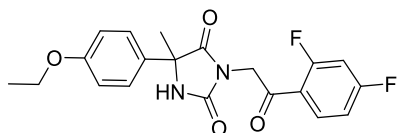
**3-(2-(2,4-Difluorophenyl)-2-oxoethyl)-5-(3-methoxyphenyl)-5-methylimidazolidine-2,4-dione (5.46).**



The title compound was prepared according to the general method A, using 5-(3-methoxyphenyl)-5-methylimidazolidine-2,4-dione (100 mg, 0.454 mmol), 2-chloro-2',4'-difluoroacetophenone (130 mg, 0.682 mmol) and  $K_2CO_3$  (75 mg, 0.545 mmol) in DMF (3 mL) and the reaction time was 24 h.

White foamy solid; yield 26% (43 mg, 0.12 mmol); TLC,  $R_f$  0.68 (cyclohexane/ethyl acetate: 50/50).  $^1H$  NMR (400 MHz,  $DMSO-d_6$ )  $\delta$  ppm 9.06 (s, 1 H), 8.00 (td,  $J=8.6, 6.8$  Hz, 1 H), 7.50 (ddd,  $J=11.6, 9.2, 2.4$  Hz, 1 H), 7.34 (t,  $J=8.0$  Hz, 1 H), 7.28 (td,  $J=8.4, 2.4$  Hz, 1 H), 7.06 - 7.15 (m, 2 H), 6.94 (dd,  $J=8.2, 1.9$  Hz, 1 H), 4.80 (d,  $J=2.8$  Hz, 2 H), 3.79 (s, 3 H), 1.74 (s, 3 H).  $^{13}C$  NMR (101 MHz,  $DMSO-d_6$ )  $\delta$  ppm 189.2 (d,  $^3J_{CF}=5.1$  Hz), 175.0, 165.7 (dd,  $^1J_{CF}=255.4$  Hz,  $^3J_{CF}=13.2$  Hz), 162.4 (dd,  $^1J_{CF}=257.6$  Hz,  $^3J_{CF}=13.2$  Hz), 159.3, 155.0, 140.9, 132.6 (dd,  $^3J_{CF}=10.6$  Hz,  $^3J_{CF}=3.3$  Hz), 129.6, 119.5 (dd,  $^2J_{CF}=13.2$  Hz,  $^4J_{CF}=3.7$  Hz), 117.7, 113.2, 112.8 (dd,  $^2J_{CF}=22.0$  Hz,  $^4J_{CF}=2.9$  Hz), 111.7, 105.4 (t,  $^2J_{CF}=26.3$  Hz), 63.2, 55.1, 47.1 (d,  $^4J_{CF}=11.0$  Hz), 24.9. UPLC-MS (C) RT 1.18 min,  $m/z$  375  $[M+H]^+$  (>95%).

**3-(2-(2,4-Difluorophenyl)-2-oxoethyl)-5-(4-ethoxyphenyl)-5-methylimidazolidine-2,4-dione (5.47).**

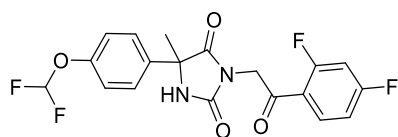


The title compound was prepared according to the general method A, using 5-(4-ethoxyphenyl)-5-methylimidazolidine-2,4-dione (88 mg, 0.38 mmol), 2-chloro-1-(2,4-difluorophenyl)ethanone (107 mg, 0.563 mmol) and  $K_2CO_3$  (62 mg, 0.45 mmol) in DMF (2 mL) and the reaction time was 40 h.

Yellowish solid; yield 22% (32 mg, 0.082 mmol); TLC,  $R_f$  0.57 (cyclohexane/ethyl acetate: 50/50).  $^1H$  NMR (400 MHz,  $DMSO-d_6$ )  $\delta$  ppm 8.99 (s, 1 H), 8.00 (td,  $J=8.6, 6.8$  Hz, 1 H), 7.50 (ddd,  $J=11.6, 9.2, 2.4$  Hz, 1 H), 7.39 - 7.46 (m, 2 H), 7.29 (td,  $J=8.5, 2.3$  Hz, 1 H), 6.92 - 7.00 (m, 2 H), 4.79 (d,  $J=2.5$  Hz, 2 H), 4.03 (q,  $J=7.1$  Hz, 2 H), 1.72 (s, 3 H), 1.33 (t,  $J=6.9$  Hz, 3 H).  $^{13}C$  NMR (101 MHz,  $DMSO-d_6$ )  $\delta$  ppm 189.2 (d,  $^3J_{CF}=5.1$  Hz), 175.5, 165.7 (dd,  $^1J_{CF}=255.4$  Hz,  $^3J_{CF}=13.2$  Hz), 162.4 (dd,  $^1J_{CF}=259.8$  Hz,  $^3J_{CF}=13.2$  Hz), 158.2, 155.0, 132.6 (dd,  $^3J_{CF}=11.7$  Hz,  $^3J_{CF}=3.7$  Hz), 131.1, 126.9, 119.5 (dd,  $^2J_{CF}=13.2$  Hz,  $^4J_{CF}=3.7$  Hz), 114.3, 112.8 (dd,  $^2J_{CF}=22.0$  Hz,  $^4J_{CF}=2.9$  Hz), 105.4 (t,  $^2J_{CF}=26.3$  Hz), 63.1, 62.9, 47.1 (d,  $^4J_{CF}=10.2$  Hz), 24.8, 14.6. UPLC-MS (C) RT 1.27 min,  $m/z$  389  $[M+H]^+$  (>95%). HRMS (ESI)  $m/z$  calcd for  $C_{20}H_{19}F_2N_2O_4$   $[M+H]^+$ : 389.1307; found: 389.1303.



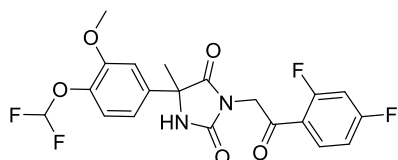
**5-(4-(Difluoromethoxy)phenyl)-3-(2-(2,4-difluorophenyl)-2-oxoethyl)-5-methylimidazolidine-2,4-dione (5.48).**



The title compound was prepared according to the general method A, using 5-(4-(difluoromethoxy)phenyl)-5-methylimidazolidine-2,4-dione (100 mg, 0.390 mmol), 2-chloro-2',4'-difluoroacetophenone (112 mg, 0.585 mmol) and  $K_2CO_3$  (65 mg, 0.47 mmol) in DMF (3 mL) and the reaction time was 24 h.

Off-white foamy solid; yield 59% (95 mg, 0.23 mmol); TLC,  $R_f$  0.55 (cyclohexane/ethyl acetate: 50/50).  $^1H$  NMR (400 MHz,  $DMSO-d_6$ )  $\delta$  ppm 9.09 (s, 1 H), 8.00 (td,  $J=8.6, 6.8$  Hz, 1 H), 7.56 - 7.62 (m, 2 H), 7.50 (ddd,  $J=11.6, 9.3, 2.4$  Hz, 1 H), 7.06 - 7.45 (m, 4 H), 4.80 (d,  $J=2.8$  Hz, 2 H), 1.75 (s, 3 H).  $^{13}C$  NMR (101 MHz,  $DMSO-d_6$ )  $\delta$  ppm 189.1, 175.0, 165.7 (dd,  $^1J_{CF}=255.4$  Hz,  $^3J_{CF}=12.4$  Hz), 162.4 (dd,  $^1J_{CF}=257.6$  Hz,  $^3J_{CF}=13.2$  Hz), 155.0, 150.7 (t,  $^3J_{CF}=3.2$  Hz), 136.2, 132.6 (dd,  $^3J_{CF}=10.6$  Hz,  $^3J_{CF}=4.0$  Hz), 127.4, 119.5 (dd,  $^2J_{CF}=13.2$  Hz,  $^4J_{CF}=3.7$  Hz), 118.7, 116.3 (t,  $^1J_{CF}=257.6$  Hz), 112.8 (dd,  $^2J_{CF}=22.0$  Hz,  $^4J_{CF}=3.2$  Hz), 105.4 (t,  $^2J_{CF}=27.1$  Hz), 62.9, 47.2 (d,  $^4J_{CF}=10.2$  Hz), 24.9. UPLC-MS (C) RT 1.28 min,  $m/z$  411  $[M+H]^+$  (>95%). HRMS (ESI)  $m/z$  calcd for  $C_{19}H_{15}F_4N_2O_4$   $[M+H]^+$ : 411.0962; found: 411.0950.

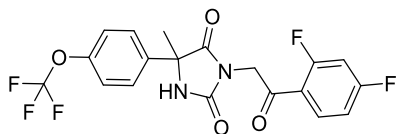
**5-(4-(Difluoromethoxy)-3-methoxyphenyl)-3-(2-(2,4-difluorophenyl)-2-oxoethyl)-5-methylimidazolidine-2,4-dione (5.49).**



The title compound was prepared according to the general method A, using 5-(4-(difluoromethoxy)-3-methoxyphenyl)-5-methylimidazolidine-2,4-dione (70 mg, 0.25 mmol), 2-chloro-1-(2,4-difluorophenyl)ethanone (70 mg, 0.37 mmol) and  $K_2CO_3$  (41 mg, 0.29 mmol) in DMF (2 mL) and the reaction time was 40 h.

Off-white solid, yield 49% (53 mg, 0.12 mmol); TLC,  $R_f$  0.48 (cyclohexane/ethyl acetate: 50/50).  $^1H$  NMR (400 MHz,  $DMSO-d_6$ )  $\delta$  ppm 9.11 (s, 1 H), 8.00 (td,  $J=8.6, 6.8$  Hz, 1 H), 7.50 (ddd,  $J=11.6, 9.3, 2.4$  Hz, 1 H), 6.87 - 7.34 (m, 5 H), 4.81 (d,  $J=2.5$  Hz, 2 H), 3.88 (s, 3 H), 1.76 (s, 3 H).  $^{13}C$  NMR (101 MHz,  $DMSO-d_6$ )  $\delta$  ppm 189.2 (d,  $^3J_{CF}=4.4$  Hz), 174.9, 165.7 (dd,  $^1J_{CF}=255.4$  Hz,  $^3J_{CF}=12.4$  Hz), 162.4 (dd,  $^1J_{CF}=258.3$  Hz,  $^3J_{CF}=13.9$  Hz), 155.0, 150.5, 139.2, 137.9, 132.6 (dd,  $^3J_{CF}=11.0$  Hz,  $^3J_{CF}=4.4$  Hz), 120.9, 119.5 (dd,  $^2J_{CF}=13.2$  Hz,  $^4J_{CF}=3.7$  Hz), 117.9, 116.6 (t,  $^1J_{CF}=259.1$  Hz), 112.8 (dd,  $^2J_{CF}=22.0$  Hz,  $^4J_{CF}=2.9$  Hz), 110.8, 105.4 (t,  $^2J_{CF}=27.1$  Hz), 63.1, 55.9, 47.2 (d,  $^4J_{CF}=11.0$  Hz), 24.9. UPLC-MS (C) RT 1.26 min,  $m/z$  441  $[M+H]^+$  (>95%).

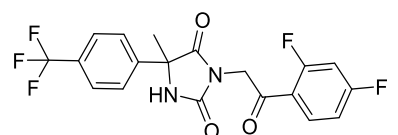
**3-(2-(2,4-Difluorophenyl)-2-oxoethyl)-5-methyl-5-(4-(trifluoromethoxy)phenyl)imidazolidine-2,4-dione (5.50).**



The title compound was prepared according to the general method A, using 5-methyl-5-(4-(trifluoromethoxy) phenyl) imidazolidine-2,4-dione (80 mg, 0.29 mmol), 2-chloro-2',4'-difluoroacetophenone (83 mg, 0.44 mmol) and  $K_2CO_3$  (48 mg, 0.35 mmol) in DMF (3 mL) and the reaction time was 1 d.

Off-white solid; Yield 59% (74 mg, 0.17 mmol); TLC,  $R_f$  0.52 (cyclohexane/ethyl acetate: 50/50).  $^1H$  NMR (400 MHz,  $DMSO-d_6$ )  $\delta$  ppm 9.14 (s, 1 H), 7.94 - 8.05 (m, 1 H), 7.63 - 7.71 (m, 2 H), 7.40 - 7.53 (m, 3 H), 7.28 (td,  $J=8.5, 2.5$  Hz, 1 H), 4.81 (d,  $J=2.8$  Hz, 2 H), 1.77 (s, 3 H).  $^{13}C$  NMR (101 MHz,  $DMSO-d_6$ )  $\delta$  ppm 189.1 (d,  $^3J_{CF}=5.1$  Hz), 174.8, 165.7 (dd,  $^1J_{CF}=255.4$  Hz,  $^3J_{CF}=12.4$  Hz), 162.4 (dd,  $^1J_{CF}=257.6$  Hz,  $^3J_{CF}=13.2$  Hz), 155.0, 148.0, 138.7, 132.6 (dd,  $^3J_{CF}=11.3$  Hz,  $^3J_{CF}=4.0$  Hz), 127.8, 121.1, 120.0 (q,  $^1J_{CF}=256.1$  Hz), 119.5 (dd,  $^2J_{CF}=13.2$  Hz,  $^4J_{CF}=3.7$  Hz), 112.8 (dd,  $^2J_{CF}=22.0$  Hz,  $^4J_{CF}=3.7$  Hz), 105.4 (t,  $^2J_{CF}=26.4$  Hz), 62.9, 47.2 (d,  $^4J_{CF}=10.2$  Hz), 25.0. UPLC-MS (C) RT 1.32 min,  $m/z$  429  $[M+H]^+$  (>95%).

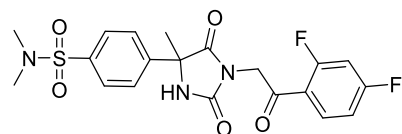
**3-(2-(2,4-Difluorophenyl)-2-oxoethyl)-5-methyl-5-(4-(trifluoromethyl)phenyl)imidazolidine-2,4-dione (5.51).**



The title compound was prepared according to the general method A, using 5-methyl-5-(4-(trifluoromethyl) phenyl) imidazolidine-2,4-dione (100 mg, 0.387 mmol), 2-chloro-2',4'-difluoroacetophenone (111 mg, 0.581 mmol) and  $K_2CO_3$  (64 mg, 0.47 mmol) in DMF (3 mL) and the reaction time was 24 h.

White foamy solid; yield 61% (97 mg, 0.24 mmol); TLC,  $R_f$  0.78 (cyclohexane/ethyl acetate: 50/50).  $^1H$  NMR (400 MHz,  $DMSO-d_6$ )  $\delta$  ppm 9.21 (s, 1 H), 7.99 (td,  $J=8.6, 6.6$  Hz, 1 H), 7.80 (q,  $J=8.7$  Hz, 4 H), 7.49 (ddd,  $J=11.7, 9.3, 2.5$  Hz, 1 H), 7.28 (td,  $J=8.5, 2.3$  Hz, 1 H), 4.81 (d,  $J=2.8$  Hz, 2 H), 1.79 (s, 3 H).  $^{13}C$  NMR (101 MHz,  $DMSO-d_6$ )  $\delta$  ppm 189.0 (d,  $^3J_{CF}=5.1$  Hz), 174.5, 165.7 (dd,  $^1J_{CF}=255.4$  Hz,  $^3J_{CF}=13.2$  Hz), 162.4 (dd,  $^1J_{CF}=257.6$  Hz,  $^3J_{CF}=13.2$  Hz), 155.0, 143.9, 132.6 (dd,  $^3J_{CF}=10.6$  Hz,  $^3J_{CF}=4.0$  Hz), 128.7 (q,  $^2J_{CF3}=31.8$  Hz), 126.6, 125.5 (q,  $^3J_{CF3}=3.6$  Hz), 124.1 (q,  $^1J_{CF3}=272.2$  Hz), 119.5 (dd,  $^2J_{CF}=13.2$  Hz,  $^4J_{CF}=3.7$  Hz), 112.8 (dd,  $^2J_{CF}=22.0$  Hz,  $^4J_{CF}=3.7$  Hz), 105.4 (t,  $^2J_{CF}=27.0$  Hz), 63.2, 47.2 (d,  $^4J_{CF}=11.0$  Hz), 25.0. UPLC-MS (C) RT 1.26 min,  $m/z$  412  $[M+H]^+$  (>95%). HRMS (ESI)  $m/z$  calcd for  $C_{19}H_{14}F_5N_2O_3$   $[M+H]^+$ : 413.0919; found: 413.0911.

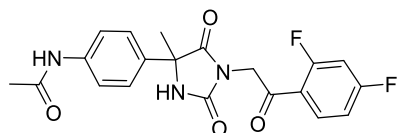
**4-(1-(2-(2,4-Difluorophenyl)-2-oxoethyl)-4-methyl-2,5-dioximidazolidin-4-yl)-N,N-dimethylbenzenesulfonamide (5.52).**



The title compound was prepared according to the general method A, using *N,N*-dimethyl-4-(4-methyl-2,5-dioximidazolidin-4-yl)benzenesulfonamide (70 mg, 0.24 mmol), 2-chloro-2',4'-difluoroacetophenone (67 mg, 0.35 mmol) and  $K_2CO_3$  (39 mg, 0.28 mmol) in DMF (3 mL) and the reaction time was 20 h.

White solid; yield 64% (68 mg, 0.15 mmol); TLC,  $R_f$  0.28 (cyclohexane/ethyl acetate: 50/50).  $^1H$  NMR (400 MHz,  $DMSO-d_6$ )  $\delta$  ppm 9.21 (s, 1 H), 8.00 (td,  $J=8.6$ , 6.6 Hz, 1 H), 7.78 - 7.89 (m, 4 H), 7.51 (ddd,  $J=11.6$ , 9.2, 2.4 Hz, 1 H), 7.29 (td,  $J=8.4$ , 2.4 Hz, 1 H), 4.82 (d,  $J=2.5$  Hz, 2 H), 2.63 (s, 6 H), 1.80 (s, 3 H).  $^{13}C$  NMR (101 MHz,  $DMSO-d_6$ )  $\delta$  ppm 189.0 (d,  $^3J_{CF}=5.1$  Hz), 174.5, 165.7 (dd,  $^1J_{CF}=254.7$  Hz,  $^3J_{CF}=12.4$  Hz), 162.4 (dd,  $^1J_{CF}=256.9$  Hz,  $^3J_{CF}=13.9$  Hz), 155.0, 144.1, 134.7, 132.6 (dd,  $^3J_{CF}=11.0$  Hz,  $^3J_{CF}=4.4$  Hz), 127.8, 126.7, 119.5 (dd,  $^2J_{CF}=13.2$  Hz,  $^4J_{CF}=3.7$  Hz), 112.8 (dd,  $^2J_{CF}=22.0$  Hz,  $^4J_{CF}=2.9$  Hz), 105.4 (t,  $^3J_{CF}=26.7$  Hz), 63.2, 47.3 (d,  $^4J_{CF}=11.7$  Hz), 37.5, 25.1. UPLC-MS (C) RT 1.23 min,  $m/z$  452  $[M+H]^+$  (>95%).

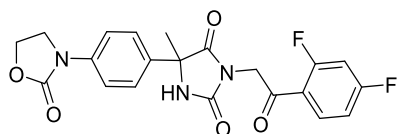
***N*-(4-(1-(2-(2,4-difluorophenyl)-2-oxoethyl)-4-methyl-2,5-dioximidazolidin-4-yl)phenyl)acetamide (5.53).**



The title compound was prepared according to the general method A, using *N*-(4-(4-methyl-2,5-dioximidazolidin-4-yl)phenyl)acetamide (200 mg, 0.809 mmol) and 2-chloro-2',4'-difluoroacetophenone (231 mg, 1.21 mmol) and  $K_2CO_3$  (134 mg, 0.971 mmol) in DMF (3 mL) and the reaction time was 42 h.

White solid, yield 40% (131 mg, 0.326 mmol); TLC,  $R_f$  0.53 (ethyl acetate).  $^1H$  NMR (400 MHz,  $DMSO-d_6$ )  $\delta$  ppm 10.01 (s, 1 H), 9.00 (s, 1 H), 8.00 (td,  $J=8.6$ , 6.8 Hz, 1 H), 7.60 (d,  $J=8.6$  Hz, 2 H), 7.50 (ddd,  $J=11.6$ , 9.2, 2.4 Hz, 1 H), 7.44 (d,  $J=8.8$  Hz, 2 H), 7.28 (td,  $J=8.5$ , 2.3 Hz, 1 H), 4.79 (d,  $J=2.5$  Hz, 2 H), 3.32 (s, 1 H), 2.04 (s, 3 H), 1.73 (s, 3 H).  $^{13}C$  NMR (101 MHz,  $DMSO-d_6$ )  $\delta$  ppm 189.2 (d,  $^3J_{CF}=4.4$  Hz), 175.3, 168.3, 165.7 (dd,  $^1J_{CF}=255.4$  Hz,  $^3J_{CF}=12.4$  Hz), 162.4 (dd,  $^1J_{CF}=258.3$  Hz,  $^3J_{CF}=13.9$  Hz), 155.1, 139.1, 133.6, 132.6 (dd,  $^3J_{CF}=11.0$  Hz,  $^3J_{CF}=4.4$  Hz), 126.0, 119.5 (dd,  $^2J_{CF}=13.9$  Hz,  $^4J_{CF}=3.7$  Hz), 118.9, 112.8 (dd,  $^2J_{CF}=22.0$  Hz,  $^4J_{CF}=2.9$  Hz), 105.4 (t,  $^2J_{CF}=27.1$  Hz), 63.0, 47.1 (d,  $^4J_{CF}=10.2$  Hz), 24.6, 24.0. UPLC-MS (C) RT 3.31 min,  $m/z$  402  $[M+H]^+$  (>95%).

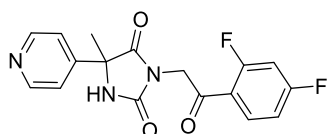
**3-(2-(2,4-Difluorophenyl)-2-oxoethyl)-5-methyl-5-(4-(2-oxooxazolidin-3-yl)phenyl)imidazolidine-2,4-dione (5.54).**



The title compound was prepared according to the general method A using 5-methyl-5-(4-(2-oxooxazolidin-3-yl)phenyl)imidazolidine-2,4-dione (80 mg, 0.29 mmol), 2-chloro-2,4-difluoroacetophenone (138 mg, 0.727 mmol) and  $K_2CO_3$  (48 mg, 0.35 mmol) in DMF (3 mL) and the reaction time was 24 h.

White solid, yield 58% (72 mg, 0.17 mmol); TLC,  $R_f$  0.48 (ethyl acetate).  $^1H$  NMR (400 MHz,  $DMSO-d_6$ )  $\delta$  ppm 9.06 (s, 1 H), 8.00 (td,  $J=8.6, 6.8$  Hz, 1 H), 7.46 - 7.66 (m, 5 H), 7.28 (td,  $J=8.4, 2.4$  Hz, 1 H), 4.80 (d,  $J=2.5$  Hz, 2 H), 4.45 (t,  $J=8.0$  Hz, 2 H), 4.03 - 4.11 (m, 2 H), 1.75 (s, 3 H).  $^{13}C$  NMR (101 MHz,  $DMSO-d_6$ )  $\delta$  ppm 189.1 (d,  $^3J_{CF}=5.1$  Hz), 175.2, 165.7 (dd,  $^1J_{CF}=256.1$  Hz,  $^3J_{CF}=13.2$  Hz), 162.4 (dd,  $^1J_{CF}=257.6$  Hz,  $^3J_{CF}=13.9$  Hz), 155.1, 154.9, 138.3, 134.2, 132.6 (dd,  $^3J_{CF}=11.7$ ,  $^3J_{CF}=3.7$  Hz), 126.2, 119.5 (dd,  $^2J_{CF}=13.2$  Hz,  $^4J_{CF}=3.7$  Hz), 117.9, 112.8 (dd,  $^2J_{CF}=22.0$  Hz,  $^4J_{CF}=2.9$  Hz), 105.4 (t,  $^2J_{CF}=27.1$  Hz), 62.9, 61.5, 47.1 (d,  $^4J_{CF}=10.2$  Hz), 44.7, 24.7. UPLC-MS (C) RT 1.19 min,  $m/z$  430  $[M+H]^+$  (>95%). HRMS (ESI)  $m/z$  calcd for  $C_{21}H_{17}F_2N_3O_5Na$   $[M+Na]^+$ : 452.1028; found: 452.1030.

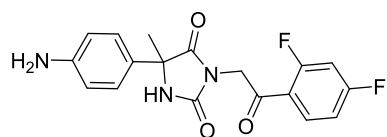
**3-(2-(2,4-Difluorophenyl)-2-oxoethyl)-5-methyl-5-(pyridin-4-yl)imidazolidine-2,4-dione (5.55).**



The compound was prepared according to the general method A, using 5-methyl-5-(pyridin-4-yl)imidazolidine-2,4-dione (100 mg, 0.523 mmol), 2-chloro-2',4'-difluoroacetophenone (100 mg, 0.523 mmol) and  $K_2CO_3$  (87 mg, 0.63 mmol) in DMF (4 mL) and the reaction time was 1 d.

White solid Yield 39% (71 mg, 0.20 mmol); TLC,  $R_f$  0.69 (ethyl acetate, functionalized NH silica gel TLC plate ( $NH_2F_{254}$ s) was used).  $^1H$  NMR (400 MHz,  $DMSO-d_6$ )  $\delta$  ppm 9.19 (s, 1 H), 8.58 - 8.71 (m, 2 H), 8.00 (td,  $J=8.6, 6.8$  Hz, 1 H), 7.53 - 7.57 (m, 2 H), 7.43 - 7.53 (m, 1 H), 7.28 (td,  $J=8.5, 2.5$  Hz, 1 H), 4.81 (d,  $J=2.8$  Hz, 2 H), 1.76 (s, 3 H).  $^{13}C$  NMR (101 MHz,  $DMSO-d_6$ )  $\delta$  ppm 189.0 (d,  $^3J_{CF}=4.4$  Hz), 174.1, 165.7 (dd,  $^1J_{CF}=253.2$  Hz,  $^3J_{CF}=13.2$  Hz), 162.4 (dd,  $^1J_{CF}=257.6$  Hz,  $^3J_{CF}=13.2$  Hz), 155.0, 150.0, 147.9, 132.6 (dd,  $^3J_{CF}=11.7$  Hz,  $^3J_{CF}=4.4$  Hz), 120.6, 119.4 (dd,  $^2J_{CF}=13.2$  Hz,  $^4J_{CF}=3.7$  Hz), 112.8 (dd,  $^2J_{CF}=22.0$  Hz,  $^4J_{CF}=2.9$  Hz), 105.4 (t,  $^2J_{CF}=26.3$  Hz), 62.8, 47.3 (d,  $^4J_{CF}=11.0$  Hz), 24.5. UPLC-MS (C) RT 1.04 min,  $m/z$  346  $[M+H]^+$  (>95%).

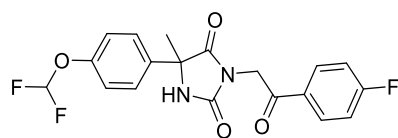
**5-(4-Aminophenyl)-3-(2-(2,4-difluorophenyl)-2-oxoethyl)-5-methylimidazolidine-2,4-dione (5.57).**



*N*-(4-(1-(2-(2,4-difluorophenyl)-2-oxoethyl)-4-methyl-2,5-dioxoimidazolidin-4-yl)phenyl) acetamide (51 mg, 0.13 mmol) was dissolved in ethanol (4 mL) and subsequently hydrochloric acid (HCl) (1 M, 2 mL) was added to the solution. The reaction mixture was left stirring at 65 °C over weekend. Then, ethanol was evaporated under reduced pressure and the residue was diluted with water (30 mL), neutralized using sodium carbonate (Na<sub>2</sub>CO<sub>3</sub>) (1N) and the target compound was extracted with EtOAc (30 mL x 2). The combined organic layers were dried over Na<sub>2</sub>SO<sub>4</sub> and evaporated under reduced pressure to give the title compound.

White solid; yield 94% (43 mg, 0.12 mmol); mp 218-221 °C; TLC, R<sub>f</sub> = 0.89 (ethyl acetate). <sup>1</sup>H NMR (400 MHz, DMSO-*d*<sub>6</sub>) δ ppm 8.83 (s, 1 H), 8.00 (td, *J*=8.6, 6.8 Hz, 1 H), 7.51 (ddd, *J*=11.6, 9.3, 2.4 Hz, 1 H), 7.29 (td, *J*=8.5, 2.3 Hz, 1 H), 7.06 - 7.19 (m, 2 H), 6.51 - 6.62 (m, 2 H), 5.17 (s, 2 H), 4.77 (d, *J*=2.3 Hz, 2 H), 1.66 (s, 3 H). <sup>13</sup>C NMR (101 MHz, DMSO-*d*<sub>6</sub>) δ ppm 189.3 (d, <sup>3</sup>*J*<sub>CF</sub>=5.1 Hz), 175.9, 165.6 (dd, <sup>1</sup>*J*<sub>CF</sub>=255.4 Hz, <sup>3</sup>*J*<sub>CF</sub>=13.2 Hz), 162.4 (dd, <sup>1</sup>*J*<sub>CF</sub>=256.9 Hz, <sup>3</sup>*J*<sub>CF</sub>=13.2 Hz), 155.1, 148.5, 132.6 (dd, <sup>3</sup>*J*<sub>CF</sub>=10.6 Hz, <sup>3</sup>*J*<sub>CF</sub>=4.0 Hz), 126.3, 125.9, 119.6 (dd, <sup>2</sup>*J*<sub>CF</sub>=13.9 Hz, <sup>4</sup>*J*<sub>CF</sub>=3.7 Hz), 113.5, 112.8 (dd, <sup>2</sup>*J*<sub>CF</sub>=22.0 Hz, <sup>4</sup>*J*<sub>CF</sub>=2.9 Hz), 105.4 (t, <sup>2</sup>*J*<sub>CF</sub>=26.3 Hz), 62.9, 47.0 (d, <sup>4</sup>*J*<sub>CF</sub>=10.2 Hz), 24.4. UPLC-MS (C) RT 1.04 min, *m/z* 360 [M+H]<sup>+</sup> (>95%). HRMS (ESI) *m/z* calcd for C<sub>18</sub>H<sub>16</sub>F<sub>2</sub>N<sub>3</sub>O<sub>3</sub> [M+H]<sup>+</sup>: 360.1154; found: 3601156.

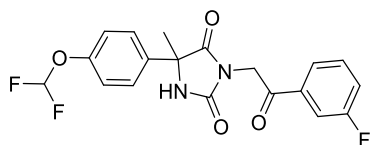
**5-(4-(Difluoromethoxy)phenyl)-3-(2-(4-fluorophenyl)-2-oxoethyl)-5-methylimidazolidine-2,4-dione (5.72).**



The title compound was prepared according to the general method A, starting from 5-(4-(difluoromethoxy)phenyl)-5-methylimidazolidine-2,4-dione (50 mg, 0.20 mmol), 2-chloro-1-(4-fluorophenyl)ethanone (51 mg, 0.29 mmol) and K<sub>2</sub>CO<sub>3</sub> (32 mg, 0.23 mmol) in DMF (2 mL) and the reaction time was 24 h.

White foamy solid; yield 72% (55 mg, 0.14 mmol); TLC, R<sub>f</sub> 0.50 (cyclohexane/ethyl acetate: 50/50). <sup>1</sup>H NMR (400 MHz, DMSO-*d*<sub>6</sub>) δ ppm 9.10 (s, 1 H), 8.13 (m, *J*=8.8, 5.6 Hz, 2 H), 7.60 (d, *J*=8.8 Hz, 2 H), 7.06 - 7.47 (m, 5 H), 4.98 (s, 2 H), 1.76 (s, 3 H). <sup>13</sup>C NMR (101 MHz, DMSO-*d*<sub>6</sub>) δ ppm 190.9, 175.2, 165.5 (d, <sup>1</sup>*J*<sub>CF</sub>=253.2 Hz), 155.1, 150.7 (t, <sup>3</sup>*J*<sub>CF</sub>=2.9 Hz), 136.3, 131.3 (d, <sup>3</sup>*J*<sub>CF</sub>=9.5 Hz), 130.7 (d, <sup>4</sup>*J*<sub>CF</sub>=2.9 Hz), 127.4, 118.7, 116.1 (d, <sup>2</sup>*J*<sub>CF</sub>=22.0 Hz), 116.3 (t, <sup>1</sup>*J*<sub>CF</sub>=257.6 Hz), 62.9, 44.5, 25.0. UPLC-MS (C) RT 1.21 min, *m/z* 391 [M+H]<sup>+</sup> (>95%). HRMS (ESI) *m/z* calcd for C<sub>19</sub>H<sub>16</sub>F<sub>3</sub>N<sub>2</sub>O<sub>4</sub> [M+H]<sup>+</sup>: 393.1057; found: 393.1052.

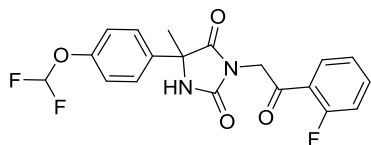
**5-(4-(Difluoromethoxy)phenyl)-3-(2-(3-fluorophenyl)-2-oxoethyl)-5-methylimidazolidine-2,4-dione (5.73).**



The title compound was prepared according to the general method A, using 5-(4-(difluoromethoxy)phenyl)-5-methylimidazolidine-2,4-dione (50 mg, 0.20 mmol), 2-bromo-1-(3-fluorophenyl)ethanone (64 mg, 0.29 mmol) and  $K_2CO_3$  (32 mg, 0.23 mmol) in DMF (3 mL) and the reaction time was 24 h.

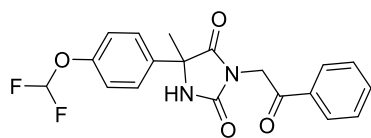
White foamy solid; yield 81% (62 mg, 0.16 mmol); mp 56-58 °C; TLC,  $R_f$  0.48 (cyclohexane/ethyl acetate: 50/50).  $^1H$  NMR (400 MHz,  $DMSO-d_6$ )  $\delta$  ppm 9.11 (s, 1 H), 7.90 (dt,  $J=7.6, 1.0$  Hz, 1 H), 7.85 (dt,  $J=9.5, 1.9$  Hz, 1 H), 7.55 - 7.69 (m, 4 H), 7.05 - 7.50 (m, 3 H), 5.00 (s, 2 H), 1.76 (s, 3 H).  $^{13}C$  NMR (101 MHz,  $DMSO-d_6$ )  $\delta$  ppm 191.5, 175.1, 162.1 (d,  $^1J_{CF}=245.9$  Hz), 155.1, 150.7 (t,  $^3J_{CF}=3.3$  Hz), 136.2, 136.0 (d,  $^3J_{CF}=6.6$  Hz), 131.2 (d,  $^3J_{CF}=8.1$  Hz), 127.4, 124.4 (d,  $^4J_{CF}=2.9$  Hz), 121.2 (d,  $^2J_{CF}=22.7$  Hz), 118.7, 114.8 (d,  $^2J_{CF}=22.7$  Hz), 116.3 (t,  $^1J_{CF}=258.3$  Hz), 62.9, 44.7, 24.9. UPLC-MS (C) RT 4.05 min,  $m/z$  391  $[M-H]^-$  (>95%). HRMS (ESI)  $m/z$  calcd for  $C_{19}H_{16}F_3N_2O_4$   $[M + H]^+$ : 393.1057; found: 393.1070.

**5-(4-(Difluoromethoxy)phenyl)-3-(2-(2-fluorophenyl)-2-oxoethyl)-5-methylimidazolidine-2,4-dione (5.74).**



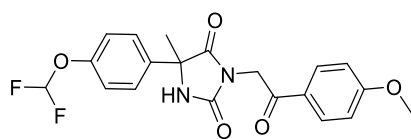
The title compound was prepared according to the general method A, using 5-(4-(difluoromethoxy)phenyl)-5-methylimidazolidine-2,4-dione (50 mg, 0.12 mmol), 2-bromo-1-(2-fluorophenyl)ethanone (64 mg, 0.29 mmol) and  $K_2CO_3$  (32 mg, 0.23 mmol) in DMF (2 mL) and the reaction time was 20 h.

Light orange foamy solid; yield 73% (56 mg, 0.14 mmol); TLC,  $R_f$  0.48 (cyclohexane/ethyl acetate: 50/50).  $^1H$  NMR (400 MHz,  $DMSO-d_6$ )  $\delta$  ppm 9.09 (s, 1 H), 7.90 (td,  $J=7.6, 1.8$  Hz, 1 H), 7.71 - 7.80 (m, 1 H), 7.56 - 7.62 (m, 2 H), 7.06 - 7.48 (m, 5 H), 4.81 (d,  $J=2.5$  Hz, 2 H), 1.75 (s, 3 H).  $^{13}C$  NMR (101 MHz,  $DMSO-d_6$ )  $\delta$  ppm 190.3 (d,  $^3J_{CF}=4.4$  Hz), 175.0, 161.5 (d,  $^1J_{CF}=254.7$  Hz), 155.0, 150.7 (t,  $^3J_{CF}=2.9$  Hz), 136.3 (d,  $^3J_{CF}=9.5$  Hz), 136.2, 130.3 (d,  $J_{CF}=2.9$  Hz), 127.4, 125.1 (d,  $J_{CF}=3.7$  Hz), 122.4 (d,  $^2J_{CF}=13.2$  Hz), 118.7, 117.0 (d,  $^2J_{CF}=22.7$  Hz), 116.3 (t,  $^1J_{CF}=257.6$  Hz), 62.9, 47.3 (d,  $^4J_{CF}=11.0$  Hz), 24.9. UPLC-MS (C) RT 1.27 min,  $m/z$  393  $[M+H]^+$  (>95%). HRMS (ESI)  $m/z$  calcd for  $C_{19}H_{16}F_3N_2O_4$   $[M+H]^+$ : 393.1057; found: 393.1072.

**5-(4-(Difluoromethoxy)phenyl)-5-methyl-3-(2-oxo-2-phenylethyl)imidazolidine-2,4-dione (5.75).**

The title compound was prepared according to the general method A, starting from 5-(4-(difluoromethoxy)phenyl)-5-methylimidazolidine-2,4-dione (50 mg, 0.20 mmol), 2-chloroacetophenone (45 mg, 0.29 mmol) and  $K_2CO_3$  (32 mg, 0.23 mmol) in DMF (2 mL) and the reaction time was 20 h.

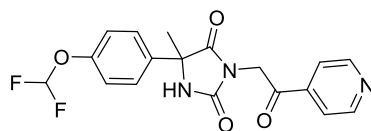
White foamy solid; yield 61% (45 mg, 0.12 mmol); TLC,  $R_f$  0.37 (cyclohexane/ethyl acetate: 50/50).  $^1H$  NMR (400 MHz,  $DMSO-d_6$ )  $\delta$  ppm 9.09 (s, 1 H), 8.00 - 8.08 (m, 2 H), 7.69 - 7.75 (m, 1 H), 7.54 - 7.64 (m, 4 H), 7.06 - 7.47 (m, 3 H), 4.98 (s, 2 H), 1.76 (s, 3 H).  $^{13}C$  NMR (101 MHz,  $DMSO-d_6$ )  $\delta$  ppm 192.2, 175.2, 155.2, 150.6 (t,  $^3J_{CF}=2.9$  Hz), 136.3, 134.2, 134.0, 129.0, 128.1, 127.4, 118.7, 116.3 (t,  $^1J_{CF}=259.1$  Hz), 62.9, 44.6, 25.0. UPLC-MS (C) RT 1.21 min,  $m/z$  375  $[M+H]^+$  (>95%). HRMS (ESI)  $m/z$  calcd for  $C_{19}H_{17}F_2N_2O_4$   $[M+H]^+$ : 375.1151; found: 375.1147.

**5-(4-(Difluoromethoxy)phenyl)-3-(2-(4-methoxyphenyl)-2-oxoethyl)-5-methylimidazolidine-2,4-dione (5.76).**

The title compound was prepared according to the general method A, using 5-(4-(difluoromethoxy)phenyl)-5-methylimidazolidine-2,4-dione (50 mg, 0.20 mmol), 2-bromo-1-(4-methoxyphenyl)ethanone (67 mg, 0.29 mmol) and  $K_2CO_3$  (32 mg, 0.23 mmol) in DMF

(2 mL) and the reaction time was 20 h.

White foamy solid; yield 66% (52 mg, 0.13 mmol); TLC,  $R_f$  0.33 (cyclohexane/ethyl acetate: 50/50).  $^1H$  NMR (400 MHz,  $DMSO-d_6$ )  $\delta$  ppm 9.06 (s, 1 H), 7.94 - 8.09 (m, 2 H), 7.56 - 7.64 (m, 2 H), 7.03 - 7.47 (m, 5 H), 4.90 (s, 2 H), 3.86 (s, 3 H), 1.76 (s, 3 H).  $^{13}C$  NMR (101 MHz,  $DMSO-d_6$ )  $\delta$  ppm 190.3, 175.3, 163.8, 155.3, 150.6 (t,  $^3J_{CF}=2.9$  Hz), 136.3, 130.5, 127.4, 126.9, 118.7, 114.2, 116.3 (t,  $^1J_{CF}=257.6$  Hz), 62.8, 55.6, 44.2, 24.9. UPLC-MS (C) RT 1.28 min,  $m/z$  405  $[M+H]^+$  (>95%).

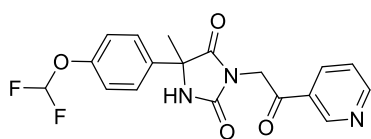
**5-(4-(Difluoromethoxy)phenyl)-5-methyl-3-(2-oxo-2-(pyridin-4-yl)ethyl)imidazolidine-2,4-dione (5.77).**

The title compound was prepared according to the general method A, using 5-(4-(difluoromethoxy)phenyl)-5-methylimidazolidine-2,4-dione (80 mg, 0.31 mmol), 2-bromo-

1-(pyridin-4-yl)ethanone hydrobromide (132 mg, 0.468 mmol) and  $Cs_2CO_3$  (173 mg, 0.531 mmol) in DMF (2 mL) and the reaction time was 1 d.

Colorless transparent solid; yield 10% (12 mg, 0.032 mmol); mp 171-173 °C; TLC,  $R_f$  0.51(ethyl acetate).  $^1\text{H}$  NMR (400 MHz,  $\text{CDCl}_3$ )  $\delta$  ppm 8.86 (d,  $J=5.1$  Hz, 2 H), 7.68 - 7.76 (m, 2 H), 7.54 - 7.63 (m, 2 H), 7.13 - 7.22 (m, 2 H), 6.30 - 6.76 (m, 2 H), 4.85 - 4.97 (ABq,  $\Delta\delta_{AB}=0.05$ ,  $J_{AB}=17.7$  Hz, 2 H), 1.94 (s, 3 H).  $^{13}\text{C}$  NMR (101 MHz,  $\text{CDCl}_3$ )  $\delta$  ppm 190.6, 174.8, 155.7, 151.3 (t,  $^3J_{CF}=2.9$  Hz), 151.2, 140.0, 135.2, 127.2, 120.8, 119.9, 115.6 (t,  $^1J_{CF}=261.3$  Hz), 63.9, 44.8, 25.3. UPLC-MS (C) RT 1.27 min,  $m/z$  376  $[\text{M}+\text{H}]^+$  (>95%). HRMS (ESI)  $m/z$  calcd for  $\text{C}_{18}\text{H}_{16}\text{F}_2\text{N}_3\text{O}_4$   $[\text{M}+\text{H}]^+$ : 376.1103; found: 376.1118.

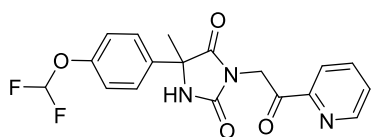
**5-(4-(Difluoromethoxy)phenyl)-5-methyl-3-(2-oxo-2-(pyridin-3-yl)ethyl)imidazolidine-2,4-dione (5.78).**



The title compound was prepared according to the general method A, using 5-(4-(difluoromethoxy)phenyl)-5-methylimidazolidine-2,4-dione (50 mg, 0.20 mmol), 2-bromo-1-(pyridin-3-yl)ethanone (59 mg, 0.29 mmol) and  $\text{K}_2\text{CO}_3$  (32 mg, 0.23 mmol) in anhydrous DMF (2 mL) and the reaction time was 24 h.

White foamy solid; yield 34% (25 mg, 0.067 mmol); TLC,  $R_f$  0.26 (ethyl acetate).  $^1\text{H}$  NMR (400 MHz,  $\text{DMSO}-d_6$ )  $\delta$  ppm 9.21 (d,  $J=1.5$  Hz, 1 H), 9.12 (s, 1 H), 8.86 (dd,  $J=4.8$ , 1.8 Hz, 1 H), 8.37 (dt,  $J=8.0$ , 1.9 Hz, 1 H), 7.60 (m,  $J=8.8$  Hz, 3 H), 7.06 - 7.46 (m, 3 H), 5.06 (s, 2 H), 1.76 (s, 3 H).  $^{13}\text{C}$  NMR (101 MHz,  $\text{DMSO}-d_6$ )  $\delta$  ppm 192.1, 175.1, 155.1, 154.3, 150.7 (t,  $^3J_{CF}=2.9$  Hz), 149.3, 136.2, 135.7, 129.5, 127.4, 124.0, 118.8, 116.3 (t,  $^1J_{CF}=257.6$  Hz), 62.9, 44.7, 24.9. UPLC-MS (C) RT 1.09 min,  $m/z$  376  $[\text{M}+\text{H}]^+$  (>95%).

**5-(4-(Difluoromethoxy)phenyl)-5-methyl-3-(2-oxo-2-(pyridin-2-yl)ethyl)imidazolidine-2,4-dione (5.79).**



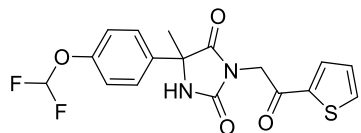
The title compound was prepared according to the general method A, using 5-(4-(difluoromethoxy)phenyl)-5-methylimidazolidine-2,4-dione (50 mg, 0.20 mmol), 2-bromo-1-(pyridin-2-yl)ethanone (59 mg, 0.29 mmol) and  $\text{K}_2\text{CO}_3$  (32 mg, 0.23 mmol) in anhydrous DMF (2 mL) and the reaction time was 4 d.

Off-white solid; yield 28% (21 mg, 0.055 mmol); TLC,  $R_f$  0.44 (cyclohexane/ethyl acetate: 50/50).  $^1\text{H}$  NMR (400 MHz,  $\text{DMSO}-d_6$ )  $\delta$  ppm 9.11 (s, 1 H), 8.75 - 8.81 (m, 1 H), 8.07 (td,  $J=7.6$ , 1.5 Hz, 1 H), 7.95 - 8.00 (m, 1 H), 7.75 (ddd,  $J=7.3$ , 4.8, 1.3 Hz, 1 H), 7.57 - 7.65 (m, 2 H), 7.04 - 7.49 (m, 3 H), 5.04 (s, 2 H), 1.76 (s, 3 H).  $^{13}\text{C}$  NMR (101 MHz,  $\text{DMSO}-d_6$ )  $\delta$  ppm 193.3, 175.2, 155.2, 150.9, 150.7 (t,  $^3J_{CF}=2.9$  Hz), 149.5, 138.0, 136.3, 128.8, 127.5, 121.9, 118.8, 116.3 (t,  $^1J_{CF}=257.6$  Hz), 62.9, 44.2,



25.0. UPLC-MS (C) RT 1.19 min,  $m/z$  376  $[M+H]^+$  (>95%). HRMS (ESI)  $m/z$  calcd for  $C_{18}H_{16}F_2N_3O_4$   $[M+H]^+$ : 376.1103; found: 376.1100.

**5-(4-(Difluoromethoxy)phenyl)-5-methyl-3-(2-oxo-2-(thiophen-2-yl)ethyl)imidazolidine-2,4-dione (5.80).**

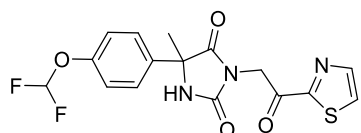


The title compound was prepared according to the general method A, using 5-(4-(difluoromethoxy)phenyl)-5-methylimidazolidine-2,4-dione (55 mg, 0.22 mmol), 2-bromo-1-

(thiophen-2-yl)ethanone (66 mg, 0.32 mmol) and  $K_2CO_3$  (36 mg, 0.26 mmol) in anhydrous DMF (5 mL) and the reaction time was 20 h.

White solid; yield 64% (52 mg, 0.14 mmol); TLC,  $R_f$  0.47 (cyclohexane/ethyl acetate: 50/50).  $^1H$  NMR (400 MHz,  $DMSO-d_6$ )  $\delta$  ppm 9.09 (s, 1 H), 8.17 (dd,  $J=3.8, 1.0$  Hz, 1 H), 8.13 (dd,  $J=4.9, 0.9$  Hz, 1 H), 7.56 - 7.63 (m, 2 H), 7.32 (dd,  $J=4.8, 3.8$  Hz, 1 H), 7.06 - 7.46 (m, 3 H), 4.92 (s, 2 H), 1.75 (s, 3 H).  $^{13}C$  NMR (101 MHz,  $DMSO-d_6$ )  $\delta$  ppm 185.3, 175.2, 155.1, 150.7 (t,  $^3J_{CF}=3.7$  Hz), 140.1, 136.2, 136.1, 134.5, 129.1, 127.4, 118.7, 116.3 (t,  $^1J_{CF}=257.6$  Hz), 62.9, 44.2, 24.8. UPLC-MS (C) RT 1.17 min,  $m/z$  381  $[M+H]^+$  (>95%). HRMS (ESI)  $m/z$  calcd for  $C_{17}H_{15}F_2N_2O_4S$   $[M+H]^+$ : 381.0715; found: 381.0724.

**5-(4-(Difluoromethoxy)phenyl)-5-methyl-3-(2-oxo-2-(thiazol-2-yl)ethyl)imidazolidine-2,4-dione (5.81).**

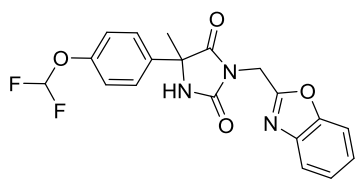


The title compound was prepared according to the general method A, using 5-(4-(difluoromethoxy)phenyl)-5-methylimidazolidine-2,4-dione (50 mg, 0.20 mmol), 2-bromo-1-

(thiazol-2-yl)ethanone (60 mg, 0.29 mmol) and  $K_2CO_3$  (32 mg, 0.23 mmol) in anhydrous DMF (2 mL) and the reaction time was 70 h.

Off-white solid; yield 20% (15 mg, 0.038 mmol); TLC,  $R_f$  = 0.27 (cyclohexane/ethyl acetate: 50/50).  $^1H$  NMR (400 MHz,  $DMSO-d_6$ )  $\delta$  ppm 9.13 (s, 1 H), 8.34 (d,  $J=3.0$  Hz, 1 H), 8.23 (d,  $J=3.0$  Hz, 1 H), 7.54 - 7.64 (m, 2 H), 7.01 - 7.47 (m, 3 H), 5.00 (s, 2 H), 1.75 (s, 3 H).  $^{13}C$  NMR (101 MHz,  $DMSO-d_6$ )  $\delta$  ppm 186.0, 175.0, 163.3, 154.9, 150.7 (t,  $^3J_{CF}=3.3$  Hz), 145.6, 136.2, 129.0, 127.4, 118.8, 116.3 (t,  $^1J_{CF}=257.6$  Hz), 63.0, 44.1, 24.8. UPLC-MS (C) RT 1.16 min,  $m/z$  382  $[M+H]^+$  (>95%). HRMS (ESI)  $m/z$  calcd for  $C_{16}H_{14}F_2N_3O_4S$   $[M+H]^+$ : 382.0668; found: 382.0669.

**3-(Benzo[d]oxazol-2-ylmethyl)-5-(4-(difluoromethoxy)phenyl)-5-methylimidazolidine-2,4-dione (5.82).**



The title compound was prepared according to the general method A, using 5-(4-(difluoromethoxy)phenyl)-5-methylimidazolidine-2,4-dione (50 mg, 0.20 mmol), 2-(chloromethyl)-1,3-benzoxazole (49 mg, 0.29 mmol) and  $K_2CO_3$  (32 mg, 0.23 mmol) in anhydrous DMF (2 mL) and the reaction time was 72 h.

White solid; yield 66% (50 mg, 0.13 mmol); TLC,  $R_f$  0.31 (cyclohexane/ethyl acetate: 50/50).  $^1H$  NMR (400 MHz,  $DMSO-d_6$ )  $\delta$  ppm 9.18 (s, 1 H), 7.68 - 7.75 (m, 2 H), 7.57 - 7.64 (m, 2 H), 7.04 - 7.48 (m, 5 H), 4.93 (s, 2 H), 1.77 (s, 3 H).  $^{13}C$  NMR (101 MHz,  $DMSO-d_6$ )  $\delta$  ppm 174.7, 161.1, 154.6, 150.7 (t,  $^3J_{CF}=3.3$  Hz), 150.2, 140.3, 136.1, 127.5, 125.3, 124.7, 119.7, 118.8, 116.3 (t,  $^1J_{CF}=257.6$  Hz), 110.9, 62.9, 35.5, 24.7. UPLC-MS (C) RT 1.18 min,  $m/z$  388  $[M+H]^+$  (>95%).

### 5.11.3. Enzyme Assay for DprE1

Oxidation of farnesylphosphoryl- $\beta$ -D-ribose (FPR) to farnesylphosphoryl- $\beta$ -D-2'-keto-erythro-pentafuranose (FPX) by DprE1 enzyme results in the formation of a two-electron reduced flavin intermediate ( $FADH_2$ ). To complete the catalytic cycle, the  $FADH_2$  has to be reoxidized to FAD. In the present assay, this can be accomplished by resazurin, which upon reduction generates the highly fluorescent product resorufin. Reactions were monitored by following an increase in fluorescence intensity ( $\lambda_{ex} = 530$  nm,  $\lambda_{em} = 595$  nm) associated with the formation of resorufin. Assays were carried out in black 384-well low-volume microplates (Greiner Bio-one, Stonehouse, UK; catalog no. 78076) and contained 50 mM HEPES, pH 7.5, 100 mM NaCl, 1.5% (v/v) DMSO, 100  $\mu$ M Tween-20, 2  $\mu$ M FAD, and 50  $\mu$ M resazurin, with variable concentrations of FPR and DprE1 in a total reaction volume of 10  $\mu$ L. Measurements were made using a Tecan Safire2 instrument (Tecan Group Ltd., Seestrasse, Switzerland). Enzymatic rates in arbitrary fluorescence units per unit time were converted to quantity of product formed per unit time using a resorufin standard curve.

### 5.11.4. General antimicrobial activity assay

Whole-cell antimicrobial activity was determined by broth microdilution using the Clinical and Laboratory Standards Institute (CLSI) recommended procedure, Document M7-A7, "Methods for Dilution Susceptibility Tests for Bacteria that Grow Aerobically". Some compounds were evaluated against a panel of Gram-positive and Gram-negative organisms, including *Acinetobacter baumannii*, *Escherichia coli*, *Enterobacter cloacae*, *Haemophilus influenzae*, *Klebsiella*

*pneumoniae*, *Pseudomonas aeruginosa*, *Staphylococcus aureus*, *Streptococcus pneumoniae* and *Streptococcus pyogenes*. Minimum inhibitory concentration (MIC) values were determined as the lowest concentration of compound producing >80 or 90% decrease in fluorescence observed.

#### 5.11.5. DprE1 overexpressor strain

Expression and purification of Mt-DprE1 and cloning of Mt-DprE1 into plasmid pMV261 were performed as described by Batt *et al.*<sup>147</sup>

*M. tuberculosis* DprE1 was cloned into the plasmid pMV261<sup>188</sup> to generate pMV261:dprE1 and introduced into *M. tuberculosis* (H37Rv). This host-plasmid system permitted constitutive expression of target proteins. After the bacteria had been incubated in the presence of the tested compound for 7 days, cell viability was assessed by the ability of endogenous reductases to reduce resazurin to resorufin.<sup>189</sup> As a proof of concept, cells transformed with pMV261:dprE1 grew in the presence of BTZ043 and TCA-1 with an MIC  $\geq$ 64-fold than that when cells were transformed with empty vector in both cases. Cells transformed with pMV261:dprE1 did not confer any growth advantage over cells transformed with vector alone when cells were grown in the presence of ethambutol or isoniazid, two anti-mycobacterial-specific compounds that do not inhibit Mt-DprE1.<sup>30</sup>

#### 5.11.6. Generation of *M. tuberculosis* DprE1 spontaneous mutants

The protocol to generate the H37Rv mutants by recombineering is described by Murphy K.C. *et al.*<sup>190</sup> More details about E221Q and G248S mutant strains are given by Batt *et al.*,<sup>147</sup> about C387S mutant strain by Makarov *et al.*,<sup>191</sup> about L368P and G17C mutant strains by Neres *et al.*<sup>192</sup> and about Y314H mutant strain by Shirude *et al.*<sup>154</sup>

#### 5.11.7. Time courses

The assay contained 100 mM Hepes pH 7.5, 100 mM NaCl, 100  $\mu$ M Tween-20, 4  $\mu$ M BSA, 2  $\mu$ M FAD, 50  $\mu$ M Resazurin, 150  $\mu$ M E-GGPR, 50 nM Mtb-DprE1, and increasing concentrations of the tested compounds. More information about the experimental details are given by Batt *et al.*<sup>147</sup>

#### 5.11.8. Therapeutic efficacy

Specific pathogen-free, 8-10 week-old female C57BL/6 mice were purchased from Harlan Laboratories and were allowed to acclimate for one week. Mice were intratracheally infected with 100,000 CFU/mouse (*M. tuberculosis* H37Rv strain). Compounds were orally administered for four consecutive days starting five days after the infection. Moxifloxacin was used as an interassay control and was administered for four consecutive days starting five days after the infection. Lungs

were harvested on day 9, 24 hours after the last administration. All lung lobes were aseptically removed, homogenized and frozen. Homogenates were plated in 10% OADC-7H11 medium supplemented with activated charcoal 0.4% for 18 days at 37°C. Blood samples were obtained at different time points from infected mice to measure the levels of the tested compounds. All animal studies were ethically reviewed and carried out in accordance with European Directive 2010/63/EU and the GSK Policy on the Care, Welfare and Treatment of Animals.

*Quality controls:* In this experiment, moxifloxacin (100 mg/kg) was administered for 4 days starting on day 5 after the infection as an interassay control. It reduced 4.1 logCFU the bacterial lung number respect to untreated mice. This quality control value is included in the accepted interval. CFU number in lungs of untreated mice: 7.4 logCFU. This value is included in the interval mean  $\pm$  2 SD of the values of the last experiments.

# Chapter 6

---

*Conclusions and outlook*



## 6. Conclusions and outlook

The primary goal of this PhD was the exploration of the primary hits identified by HTS with the aim to identify potent compounds against *M. tuberculosis* (H37Rv). Two series of compounds, namely quinoloxycetamides and hydantoin, with very good cellular potency in the low micromolar range were obtained. Furthermore, the best compounds in these series were found to possess good physicochemical properties without cytotoxic effects. The best compound that belongs in the hydantoin series demonstrated a statistical significant reduction in bacterial load in mice offering an *in vivo* proof of concept about the potential of this series.

## 6. Outlook

### 6.1. Quinoloxycetamide series

#### 6.1.1. Additional SAR

Although a large number of compounds has already been made during the course of this PhD around the quinoloxycetamides series, a number of structures would still be very interesting to make. Since the benzoxazole analogue **3.159** showed good blood stability and the *para*-methoxyphenyl analogue **3.130** showed the best potency and a good physicochemical profile, a combination of this two groups, as shown in Figure 6.1(A) could possibly offer a compound which ideally would demonstrate high potency, good physicochemical properties and blood stability.

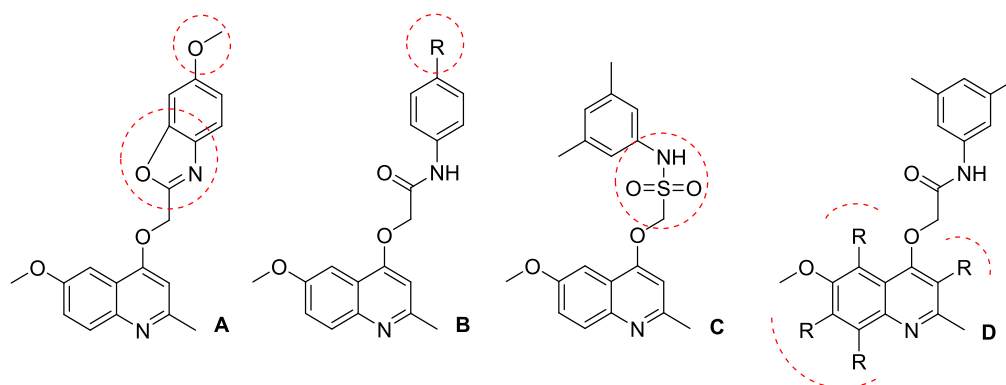


**Figure 6.1. Interesting modifications of the quinoloxycetamides series. (A) Combination of benzoxazole ring and *para*-methoxy substitution, (B) *para*-phenyl exploration, (C) further linker modifications, (D) quinoline substitution and ring replacement.**

Further exploration of the *para*-phenyl substitution (Figure 6.1B) could possibly deliver even more potent inhibitors. Furthermore, even if the benzoxazole derivative was found to possess good blood stability, the amide bond replacements were only limited to three groups. Therefore, further exploration of alternative groups on the linker could possibly offer a better replacement.

Possible groups could be for example a sulphonamide as shown in Figure 6.1(C) or other 5- and 6-membered heterocyclic rings. Exploration of the quinoline substitution pattern included a number of groups mainly focused on positions 6 and 2. However, introduction of additional substituents at positions 3, 5, 7 and 8 on the quinoline ring, preferably more hydrophilic, would be interesting to prepare (Figure 6.1(D)). Also, replacement of the quinoline core with other bicyclic systems such as indole, benzoimidazole etc. could offer better alternatives.

Lastly, a number of quinoline derivatives exist in literature possessing antimycobacterial properties. It would be interesting to continue the hybridization approach (already initiated by replacing the northern phenyl of the initial hit with some known antimycobacterial molecules), using the most promising examples. In this investigation, the most interesting known substituted quinolines could replace our 2-methyl-6-methoxy-quinoline moiety.

### 6.1.2. Mode of action

Identification of the mode of action can offer all the benefits of structural biology feedback. Once the target is identified, computational approaches, including molecular docking techniques, can be used to provide an insight at the molecular level of the binding mode.

As recently published by Phummarin *et al.* that are working on the same series of compounds, an *M. tuberculosis* cytochrome bd oxidase deletion mutant (cydKO) was found to be hypersensitive to most members of their compound library, while strains carrying single-nucleotide polymorphisms of the qcrB gene, which encodes a subunit of the menaquinol cytochrome c oxidoreductase (bc1) complex, were resistant to their library. These results identify that the 2-(quinolin-4-yloxy)acetamide class likely target the *M. tuberculosis* bc1 complex.<sup>193</sup>

Future work could include molecular docking studies to explore the possible binding mode and interactions in the target enzyme to assist future design of compounds.



## 6.2. Hydantoin series

### 6.2.1. More inhibitors

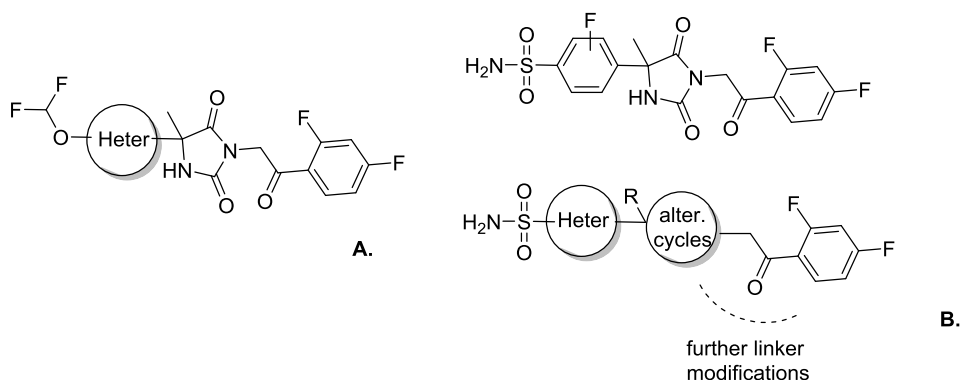


**Figure 6.2. Interesting modifications of the hydantoin series. A) difluoromethoxy subseries, B) sulfonamide subseries.**

With respect to the difluoromethoxy subseries (Figure 6.2, A), of which compound **5.48** was found to be the most promising representative, future work could include the exploration of other parts of the molecule in an effort to reduce the overall lipophilicity of the molecule (chromlogD) with the goal to improve LLE of the molecule. The phenyl ring at the left-hand side part of the molecule could be a possible alternative region.

Optimization of the second subseries (Figure 6.2, B), represented by sulfonamide **5.69**, has already been initiated by the other members of the OpenMedChem group. As described, mono- or dimethylation led to drop of activity. Additional medicinal chemistry effort could focus on the strategic decoration of the phenyl ring with, for example, fluorine atoms in order to influence the  $pK_a$  of the mildly acidic sulfonamide and the electron density in the phenyl ring. Moreover, efforts to introduce a heterocycle instead of the left-hand side phenyl or to decorate it with additional substituents are ongoing. Further exploration of the R group, substitution of the core hydantoin (scaffold hopping) and linker modifications are planned in order to gain more profound insight in the SAR of this central part.

### 6.2.2. Docking studies

Docking studies on the crystal structure of the DprE<sub>1</sub> enzyme have also been initiated in order to give a better understanding of the key interactions with the enzyme and to offer guidance for further chemistry efforts. Preliminary results are in agreement with the obtained SAR so far.



# Chapter 7

---

*Summary*



## 7. Summary

### 7.1. Introduction

TB represents an escalating threat for global health, with the increasing prevalence of MDR- and XDR-TB strains.<sup>194</sup> The re-emergence of TB in recent years led the WHO to launch the Stop TB Strategy program.<sup>157</sup>

The present thesis about antimycobacterial drug discovery was performed as part of the OpenMedChem project at the University of Antwerp (Antwerp, Belgium) and GlaxoSmithKline DDW (Tres Cantos, Spain) funded by Marie Skłodowska-Curie Innovative Training Networks. The OpenMedChem project comprised collaboration between a major industrial R&D unit and academia with common goal to find new chemical entities to battle *M. tuberculosis*.

The research performed during my PhD studies can be summarized into two distinct Hit-to-Lead optimization projects of two novel classes of anti-mycobacterial compounds discovered by HTS campaigns performed by GSK.<sup>76</sup>

### 7.2. Discovery and SAR exploration of QOA-based antimycobacterial compounds

As a result of a whole-cell HTS campaign, QOA were identified as an interesting family with potent antimycobacterial profile. Thus, the most active hit compounds were selected for further SAR studies and optimization of their properties during the academic part of my PhD studies at University of Antwerp. The main goal of this project was to identify even more potent compounds than the primary hits and to improve their physicochemical properties such as solubility and permeability. Furthermore, modifications which would allow intracellular activity were desired. Cytotoxicity was also taken into account.

As part of this study, modifications that were investigated could be divided into three categories: (1) the quinoline, (2) the linker and (3) the northern aryl part. This was done by preparing three compound sub-series in which each of the substructures was modified separately, while keeping the rest of the molecule identical to the reference compound.

The schematic results of the SAR screening performed can be found in Figure 7.1.

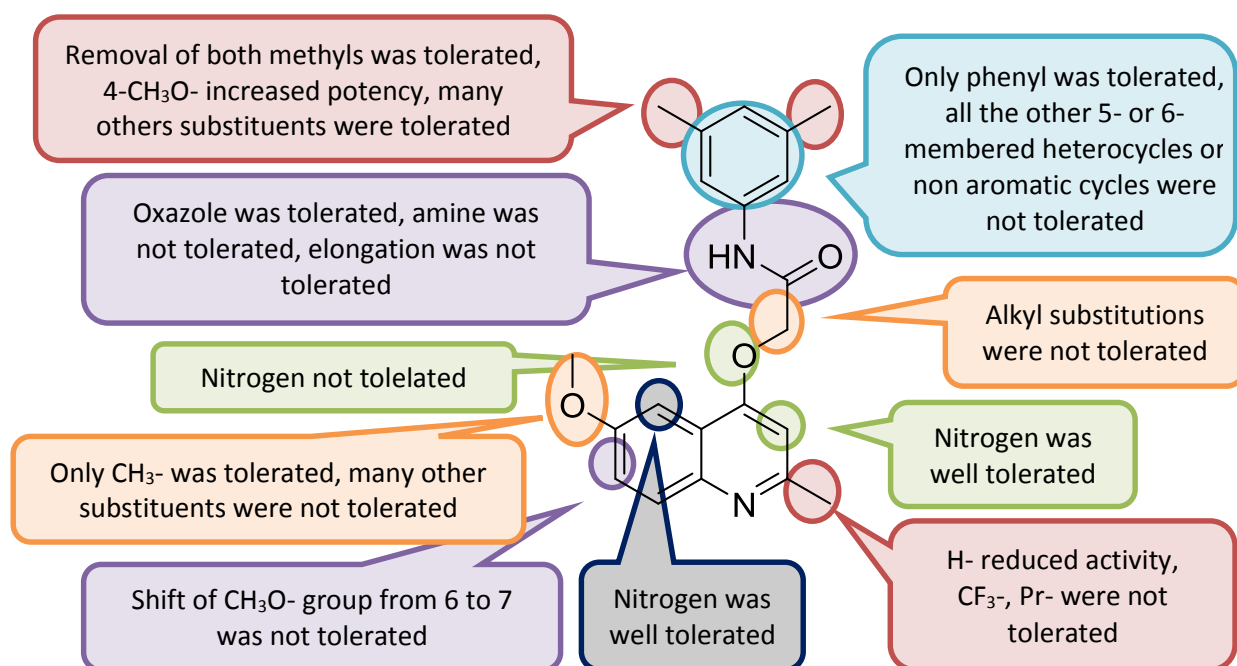


**Figure 7.1. SAR exploration of the initial hit compound 2.1.**

During our antimycobacterial research on quinoloxacetamides, several synthetic routes were explored. Furthermore, we studied the alkylation of heterocyclic *N/O*-ambident nucleophilic scaffolds such as quinolin-4-ol, naphthyridin-4-ol and quinazolin-4-ol. When *N*-alkylated products were obtained, the desired alkoxy- analogues were prepared via alternative methods. Given the lack of commonly applied methods for the unambiguous assignment of *N/O*-ambident alkylation reaction products in the literature, three NMR methods (<sup>13</sup>C-NMR chemical shifts, 2D HSQC/HMBC and 1D NOE) were applied for structure determination.

All these medicinal chemistry efforts resulted in compound **3.130** which exhibited improved potency (MIC = 0.6 μM) in comparison with the reference compound **2.1** (MIC = 1.9 μM), excellent intracellular activity comparable with the primary hit **2.1**, no cytotoxicity in hepG2 assay, increased solubility and more than 2 times enhancement of permeability than **2.1** (Figure 7.2).

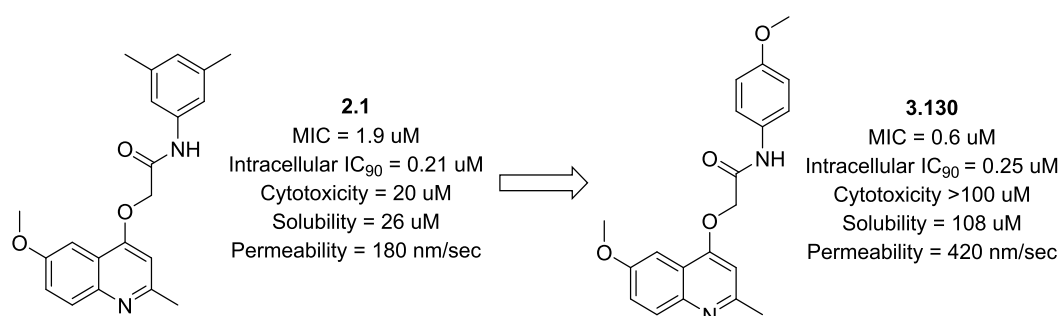


**Figure 7.2. Potency and physicochemical properties optimization resulted in compound 3.130.**

In view of the fact that microsomal instability was identified as a possible liability of the initial hits, six compounds were selected and the stability in murine and human microsomal fractions was evaluated before continuing with further synthetic efforts. The selection of compounds was driven by structural criteria in an attempt to identify the metabolic liabilities of the series. Four possible metabolic sites were explored: the methoxy group, the amide bond, the methylene linker, and the phenyl ring of the reference compound **2.1**.

All the tested compounds proved to be highly unstable, especially when incubated with murine microsomal fractions. Comparison of the obtained data with and without co-factor indicated that cytochrome P-450 metabolism was not determinant for all tested compounds possessing an amide bond, signifying that this group is the most susceptible one of the series and that an esterase hydrolysis might be involved. In order to confirm that esterases are responsible for the rapid metabolism of the compounds, the selected compounds were incubated in fresh whole CD1 murine blood. A parallel run, after pretreatment of the blood with pan-esterase inhibitor sodium fluoride (NaF), was performed. Nearly all the compounds possessing an amide bond were highly unstable. In addition, the instability is mitigated after NaF pretreatment suggesting that it is mainly due to the hydrolysis of the amide.

In the light of this evidence, further medicinal chemistry efforts were focused on the amide bond replacement. A ring closure giving an oxazole lead to compound **3.159** which proved to be very stable when incubated in murine blood with half-life time more than 240 min (Figure 7.3).

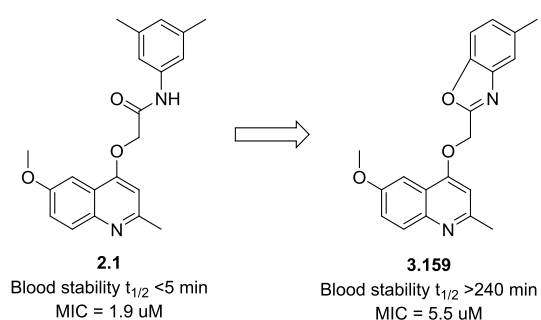


**Figure 7.3. Blood stability optimization.**

Although this compound is not as potent as compounds **2.1** and **3.130**, it possessed a reasonable MIC value indicating that further amide replacements could give more opportunities for the development of the series.

Lastly, a preliminary safety evaluation of the cardiovascular risk of the series was performed by measuring the human Ether-à-go-go-Related Gene (hERG) binding of selected compounds. Unfortunately, the most potent compound **3.130** exhibited some interaction with the ion channels

while compound **3.159** and the primary hit compound **2.1** did not show any activity in the assay. The obtained results indicated that there might be a connection between the methoxy substituent at the northern aryl part and hERG liability. However, the small size of the dataset does not allow definitive conclusions about a correlation between the presence of a methoxy group and hERG channel inhibition.

### 7.3. Identification and exploration of the hydantoin series as DprE1 inhibitors

The hydantoin series was identified as a novel class of DprE1 inhibitors during a target-based HTS performed by GSK. DprE1 enzyme is a new promising target for antimycobacterial drug discovery. More specifically, inhibition of the DprE<sub>1</sub> enzyme interrupts the essential cell wall biosynthesis leading to mycobacteria death. The vulnerability of DprE<sub>1</sub> and the remarkable potency of the best inhibitors set this enzyme a promising drug target for the discovery of new drugs to combat TB.

The aim of this project was to prepare novel compounds with high DprE1 inhibitory activity that could be translated into good cellular potency. Furthermore, balanced physicochemical properties and toxicity was taken into account. The ultimate goal of this project was an *in vivo* proof of concept in mice.

#### 7.3.1. First round of Hit-to-Lead optimization

During the first round of optimization our main focus was: (1) exploration of the linker, (2) replacement of the hydantoin core and (3) investigation of the left-hand side phenyl substitution.

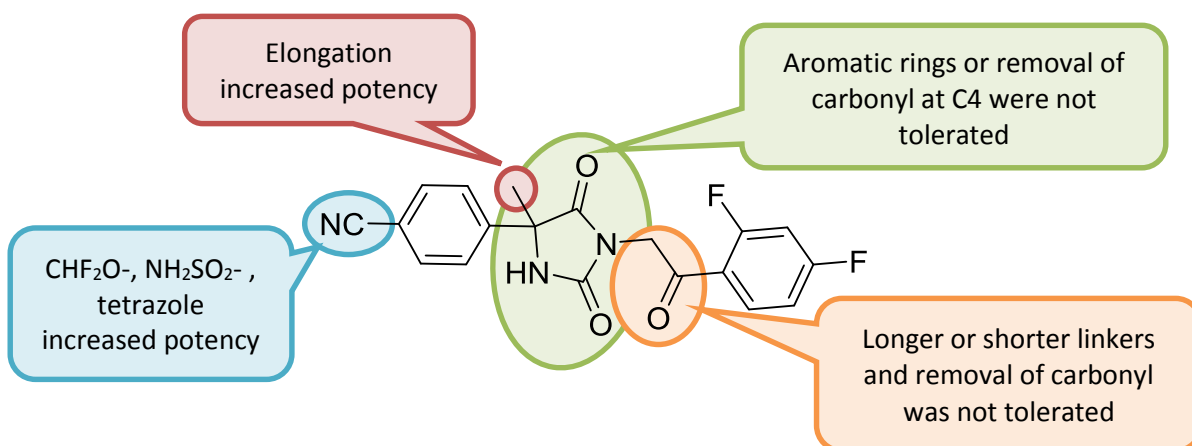
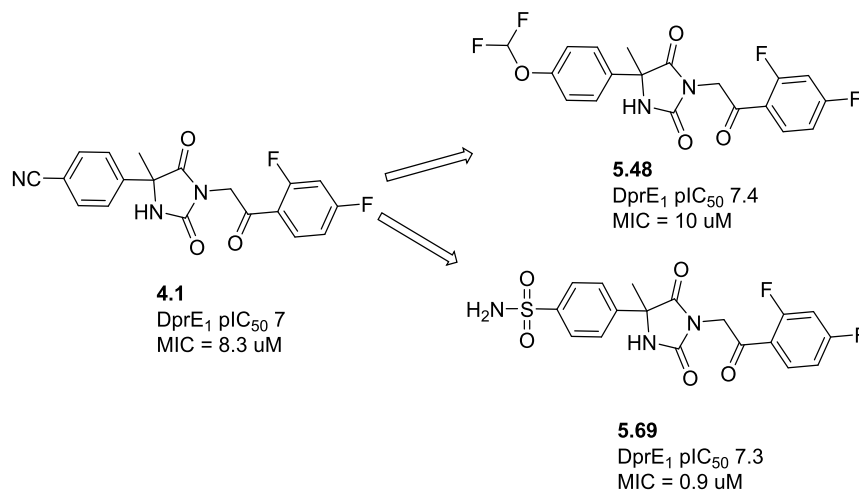


Figure 7.4 SAR summary.

During this SAR study, some very potent inhibitors were identified possessing various substituents at position 4 of the left-hand side of the molecule. The most active compounds obtained with



enzymatic inhibitory activities of  $pIC_{50} = 7.3-7.4$  are shown in Figure 7.5. However, these high inhibitory activities were translated into sub-micromolar cellular potency only in case of compound **5.69** (MIC = 0.9  $\mu$ M).



**Figure 7.5. Potency optimization of DprE1 inhibitors.**

It was found that not only high enzymatic affinity is necessary for cellular potency, but lipophilicity (chromlogD) played an important role for activity. Calculating LLE was found to be a helpful parameter that gave a reasonable correlation with MIC values. More specifically, values of LLE more than 3, ideally 4-5, were desirable.

### 7.3.2. Second round of Hit-to-Lead optimization

The second round of optimization was around the right-hand phenyl ring, having selected the difluoromethoxy group as fixed substituent at position 4 of the left-hand side aryl (as compound **5.48**). Compound **5.69** had been followed by other members of the OpenMedChem group. In the present thesis, the aim of this second round of H2L optimization was to reduce the lipophilicity of compound **5.48** in an attempt to improve the LLE, with the goal to improve its cellular activity (MIC). However, none of the synthesized compounds achieved the desired LLE value  $>3$ . In all cases where some improvement of the chromlogD was achieved, a simultaneous reduction of the enzymatic affinity was observed. This might be because of the lipophilic nature of the pocket where the right-hand phenyl lies on.

### 7.3.3. Further evaluation of selected compounds

The best examples of this series were selected for further evaluation of their properties. Therefore, the intramacrophage activity was measured with good activity obtained. Furthermore, the *in vitro* intrinsic clearance was evaluated using human and murine liver hepatocytes, indicating

that all tested compounds possessed satisfactory metabolic stability. Unfortunately, the hERG binding assay revealed interactions for some compounds including the difluoromethoxy substituted subseries. Four selected compounds were evaluated for their antimicrobial activity against a panel of Gram-positive and Gram-negative bacteria indicating that our series is very specific for mycobacteria.

Shifts in MIC values caused by target overexpression can provide a simple measure of target engagement at cellular level, which is extremely valuable information for drug discovery programs.<sup>186</sup> During our project, this approach was used to validate DprE1 as the target enzyme of this series. Furthermore, MIC modulation against mutant strains that include some mutations of the DprE1 enzyme confirm our target. Time course curves showed that both tested compounds behaved like normal reversible inhibitors, and there was no evidence of time-dependent inhibition.

Lastly, the two most potent derivatives obtained (**5.69** and **5.71**) were selected for *in vivo* studies in an acute murine model of intratracheal infection. The therapeutic efficacy against *M. tuberculosis* (H37Rv) was determined using a model of C57BL/6J infected mice. The blood exposure levels and the differences in the lung microorganism burden ( $\log_{10}$ CFUs/lungs) obtained in the treated mice with respect to untreated controls (day 9 after infection) were measured. Compound **5.69** demonstrated the best blood exposure with a C<sub>max</sub> value of 6380 ng/mL and an AUC value of 31.400 h\*ng/mL. Moreover, the same compound showed the highest reduction of logCFU units (0.5) among the tested compounds. Although this value reflects limited *in vivo* activity compared to reference moxifloxacin, it demonstrates that the hydantoin series is capable of delivering statistically significant efficacy in the *in vivo* murine model.

# Chapter 8

---

*Samenvatting*



## 8. Samenvatting

### 8.1. Inleiding

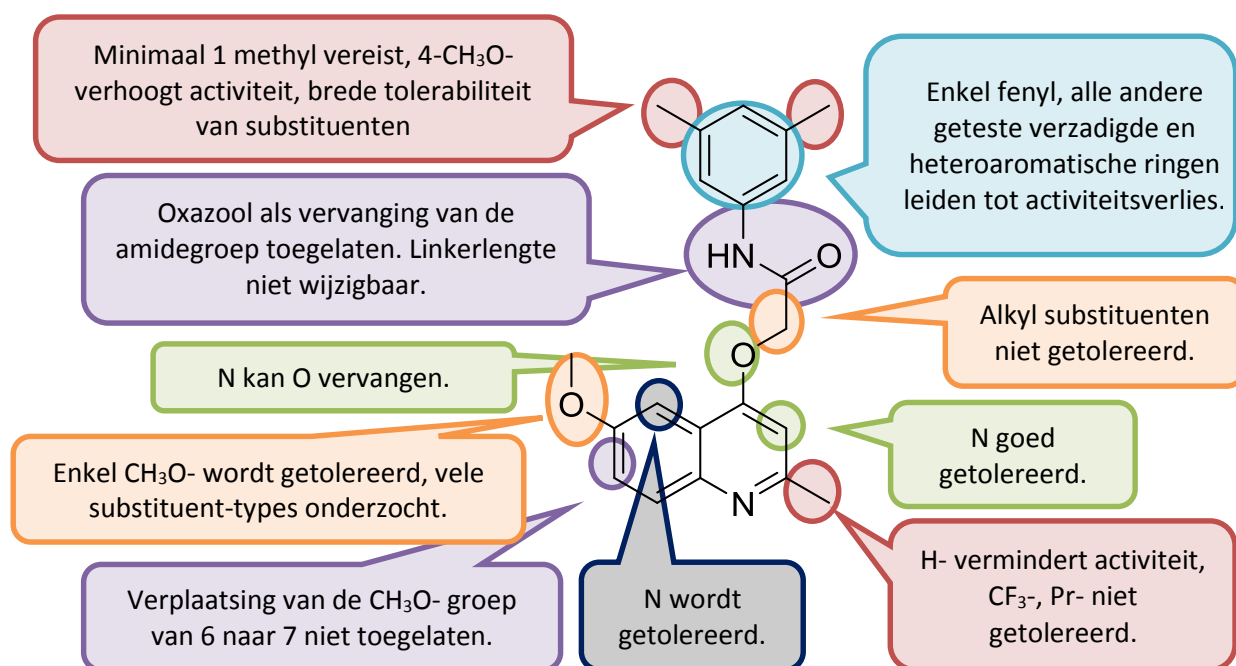
Tuberculose vormt een moeilijk te onderschatten bedreiging voor de volksgezondheid in de wereld, de stijgende prevalentie van Multidrug-resistente (MDR) en Extensief-resistente (XDR) mycobacteriële stammen draagt daar in belangrijke mate toe bij. Om deze zorgwekkende evolutie tegen te gaan, heeft de *Wereldgezondheidsorganisatie (World Health Organization, WHO)* in 2014 het *End TB Strategy* programma goedgekeurd, dat ondermeer wil inzetten op doorgedreven onderzoek en ontwikkeling van nieuwe geneesmiddelen en diagnostica die kunnen ingezet worden in de strijd tegen TB.

Deze thesis handelt over drug discovery van nieuwe antimycobacteriële middelen. Het beschreven onderzoek werd uitgevoerd in het kader van het FP7-Marie Curie project *OpenMedChem*, een open-innovatie samenwerkingsverband tussen de Universiteit Antwerpen en *GlaxoSmithKline-Drugs of the Developing World (GSK-DDW, Tres Cantos, Spanje)*. Twee duidelijk onderscheidbare onderzoeksbenaderingen (fenotypisch gestuurde en target-gebonden drug discovery) werden gebruikt en toegepast voor de Hit-to-Lead optimalisatie van twee nieuwe antimycobacteriële families die bij GSK-DDW ontdekt werden door middel van High Throughput Screening (HTS).

### 8.2 Discovery en Structuur-Activiteitsrelatie (SAR) onderzoek op quinoloxycetamide-gebaseerde antimycobacteriële verbindingen.

Quinoloxycetamide-gebaseerde verbindingen (QOAs) werden geïdentificeerd als een chemische familie met een interessant antimycobacterieel profiel. De meest actieve vertegenwoordigers in de “hit-set” werden geselecteerd voor verder SAR-onderzoek en optimalisatie. Het uiteindelijke doel was de identificatie van nieuwe analogen met hogere antimycobacteriële activiteit en verbeterde fysicochemische eigenschappen, in het bijzonder oplosbaarheid en permeabiliteit. Bijkomende aandachtspunten waren de intracellulaire activiteit en de cytotoxiciteit van deze reeks.

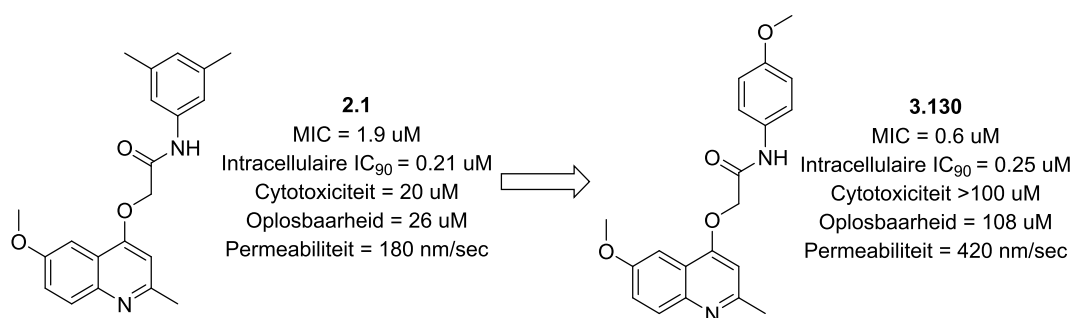
Drie onderdelen van de basisstructuur werden onderzocht: het (1) quinoline-gedeelte, (2) de linker en (3) het “noordelijke” aryl fragment. Deze substructuren werden grondig afzonderlijk bestudeerd met drie verschillende reeksen verbindingen, waarbij de rest van de molecule telkens constant gehouden werd. Schematisch weergegeven resultaten zijn terug te vinden in Figuur 8.1



**Figuur 8.1. SAR exploratie van referentie-QOA 2.1**

Gedurende dit deel van het doctoraatsonderzoek werden verschillende chemische synthesemethoden geëxploreerd. Ook alkylering van heterocyclische, ambidente *N/O*-nucleofielen als quinolin-4-ol, naphthyridin-4-ol en quinazolin-4-ol werd bestudeerd. In gevallen waar *N*-gealkyleerde producten bekomen werden, konden telkens ook de *O*-gealkyleerde analogen aangemaakt worden via een alternatieve syntheseroute. Gezien het gebrek aan algemeen gebruikte methodologieën voor de ondubbelzinnige structurele toewijzing van alkyleringsreactieproducten van ambidente alkyleringsreactieproducten, werden hiertoe de performantie van drie NMR-methodologieën ( $^{13}\text{C}$ -NMR, 2D-HSQC/HMBC en 1D-NOE) vergeleken.

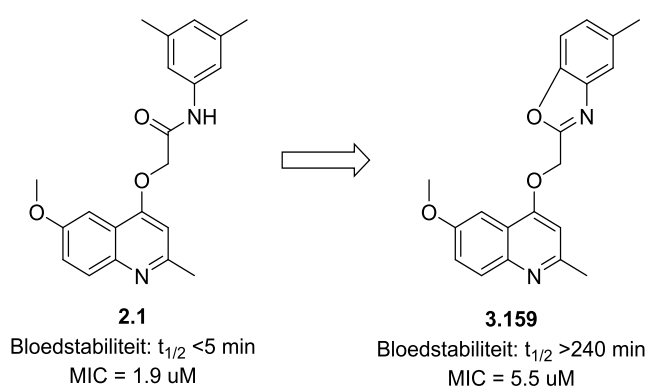
Dit deel van het onderzoek resulteerde in, onder andere, verbinding **3.130** die gekenmerkt werd door een verbeterde antimycobacteriële activiteit (MIC= 0.6  $\mu\text{M}$ ) vergeleken met referentie **2.1** (MIC= 2.1  $\mu\text{M}$ ). Bovendien bleek **3.130** niet cytotoxisch te zijn in hepG2 cellen, een hogere oplosbaarheid en hogere permeabiliteit te hebben dan **2.1** en daarnaast ook te beschikken over een bevredigend intramacrofaag activiteitsprofiel (Figuur 8.2).



**Figuur 8.2. Optimalisatie van activiteit en fysicochemische eigenschappen resulteerde in verbinding 3.130.**

Omdat ook microsomale instabiliteit als een potentieel probleem geïdentificeerd werd bij de initiële “hit-set”, werden zes nieuwe verbindingen geselecteerd en onderzocht op stabiliteit in muis- en humane microsomale fracties. De selectie van deze verbindingen was gebaseerd op structurele criteria. Drie potentieel metaboliseerbare posities konden op die manier onderzocht worden: de methoxygroep, de methyleenlinker, de amidebinding en de fenyling. Alle geteste moleculen bleken zeer onstabiel, vooral in aanwezigheid van de muis-microsomale fracties. Vergelijking van resultaten in aan- of afwezigheid van oxidatieve cofactor, toonde aan dat cytochroom P-450 gemedieerde transformatie niet bepalend was bij de omzetting van de verbindingen. Op basis van deze bevinding werd als hypothese naar voor geschoven dat een snelle hydrolyse van de amidebinding door esterasen/proteasen het halfleven negatief beïnvloedt. Ter bevestiging werden de verbindingen geïncubeerd in vers CD1 muisbloed in aan- of afwezigheid van de pan-hydrolase inhibitor natriumfluoride (NaF). Dit experiment bleek inderdaad aan te tonen dat gevoeligheid voor hydrolase-activiteit het belangrijkste probleem is bij de metabolisatie van de verbindingen.

Om deze reden werd geïnvesteerd in de aanmaak van bijkomende analogen waarin de amidegroep vervangen of weggelaten werd. Een oxazool-bevattend analoog (**3.159**) bleek zeer stabiel te zijn na incubatie in muisbloed (halfleven > 240 minuten) (Figuur 8.3).



**Figuur 8.3. Optimalisatie van bloedstabiliteit.**

Hoewel de antimycobacteriële activiteit van **3.159** iets lager bleek dan die van referentie **2.1**, bleek deze benadering toch ruimte te laten voor synthese van bijkomende, geoptimaliseerde analogen.

Tenslotte werd de QOA-familie preliminair onderzocht op mogelijke hERG inhibitie. Verbinding **3.130** bleek bij hogere concentraties inderdaad te interfereren met hERG, terwijl zowel referentie **2.1** als **3.159** geen enkele affiniteit bleken te vertonen.

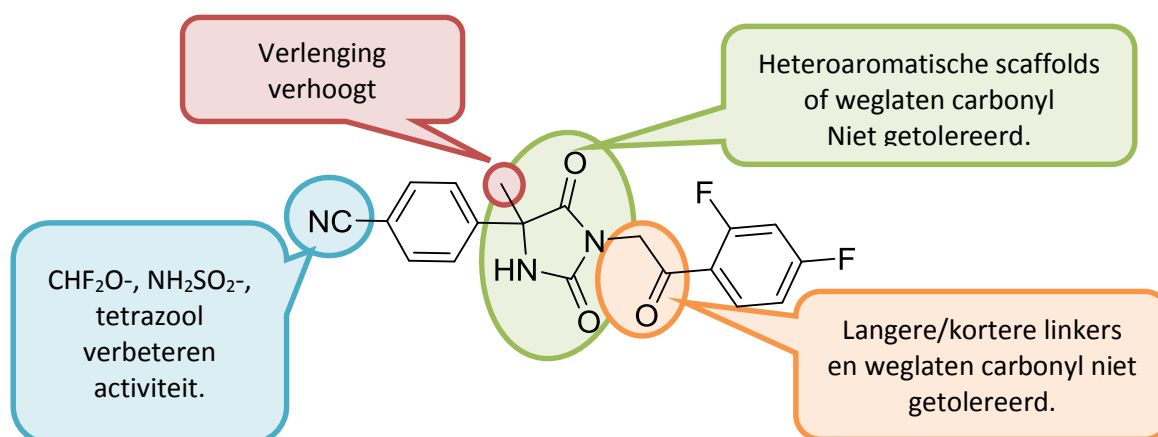
### 8.3. Identificatie en exploratie van een hydantoïne-gebaseerde serie DprE1 inhibitoren.

#### 8.3.1. Eerste cyclus van Hit-to-Lead optimalisatie.

Gedurende een target-gebaseerde HTS-campagne van GSK-DDW, werd een reeks hydantoïnes geïdentificeerd als een nieuwe structurele klasse van DprE1 remmers. DprE1 is een nieuw en veelbelovend doelwit voor ontwikkeling van antimycobacteriële geneesmiddelen. Inhibitie van dit enzym verstoort de aanmaak van de mycobacteriële celwand en leidt tot celdood. De kwaliteit van DprE1 als doelwit en de antimycobacteriële activiteit van de verbindingen in de “hit-set” waren bepalend om dit deel van het onderzoek te starten.

Het doel van dit project was enerzijds om nieuwe verbindingen te bekommen die hoge affiniteit voor DprE1 combineren met overtuigende antimycobacteriële eigenschappen. Andere aandachtspunten waren fysico-chemische parameters (oplosbaarheid, permeabiliteit) en cytotoxiciteit. Het uiteindelijke doel van dit subproject was het bekomen van een *in vivo proof-of-concept* in muismodel van longtuberculose.

Tijdens het SAR-onderzoek werden zeer krachtige DprE1 inhibitoren bekomen door specifieke substituenten in te voeren ter hoogte van de 4-positie van de linker-aryring van de molecule. (Figuur 8.4) De meest krachtige verbindingen bleken  $pIC_{50}$ -waarden rond 7.3-7.4 te hebben en worden getoond in Figuur 8.5. De cellulaire antimycobacteriële activiteit bleek laag micromolair te zijn ( $MIC=0.9 \mu M$ ).



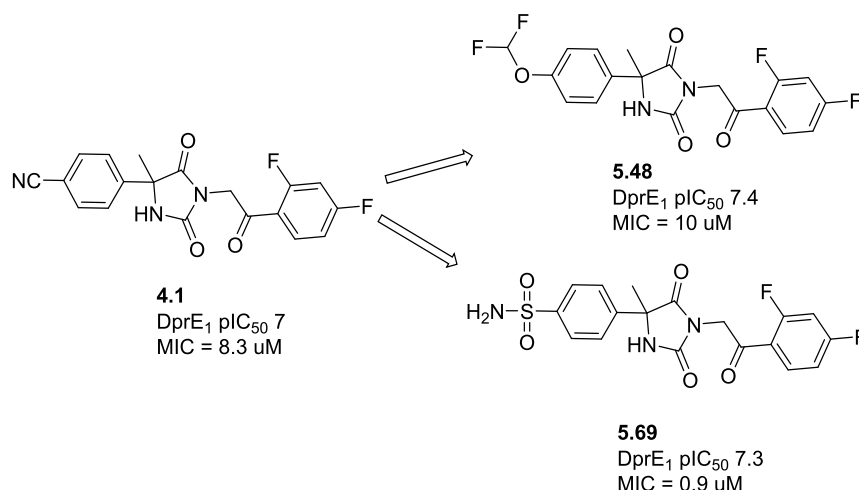
**Figuur 8.4** Overzicht van bekomen SAR-informatie voor de hydantoïne-reeks.



Niet enkel de aanwezigheid van voldoende enzymaffiniteit bleek noodzakelijk voor significante activiteit op mycobacterieën, maar ook de lipofiliciteit (ChromLogD) bleek een bepalende factor. De *lipophilic ligand efficiency* (LLE) was voor deze verbindingen een nuttige descriptor die correleerde met de experimentele MIC-waarden. LLE-waarden tussen 4 en 5 bleken binnen de geëvalueerde serie optimaal te zijn.

### 8.3.2 Tweede cyclus van Hit-to-Lead optimalisatie

De tweede cyclus was geconcentreerd op de optimalisatie van de rechter-aryl ring, waarbij de difluormethoxygroep gefixeerd werd als 4-substituent op de linker arylring (zoals bijvoorbeeld in verbinding **5.48**). Tegelijkertijd werd door collega-onderzoekers gefocust op rechter-arylring gemodificeerde analogen van **5.69**.



**Figuur 8.5. Verdere optimalisatie van DprE1 inhibitoren.**

Een belangrijke doelstelling van dit deel van het onderzoek was om de LLE verder te verbeteren. Geen enkele van de nieuwe analogen van **5.48** bleek echter in staat om een ratio > 3 te behalen. In alle gevallen waar een verbetering van de chromlogD-waarde werd vastgesteld, kon een gelijktijdige daling van de enzymaffiniteit geobserveerd worden. Mogelijk ligt het lipofiel karakter van de DprE1-pocket waarin de rechter-arylring bindt, aan de basis van deze bevindingen.

### 8.3.3. Uitgebreide evaluatie van geselecteerde verbindingen

Voor de beste vertegenwoordigers van deze chemische familie werd het intramacrofaag activiteitsprofiel verder onderzocht. Hierbij werden bevredigende resultaten bekomen. Daarnaast werd de *in vitro* intrinsieke klaring geëvalueerd met behulp van muis- en humane hepatocyten. Ook op dit vlak konden geen problemen vastgesteld worden binnen de onderzochte set.

Daartegenover bleek wel een risico op hERG-interferentie te bestaan voor, ondermeer, producten met een difluormethoxygroep op de linker-arylring. Daarnaast werden geselecteerde moleculen getest tegenover een panel van Gram-positieve en Gram-negatieve kiemen, waarbij een duidelijke selectiviteit voor mycobacteriën bleek. Door middel van een DprE1-overexpressor assay werd gevalideerd dat de verbindingen hun antimycobacteriële activiteit inderdaad ontlenen aan de inhibitie van DprE1. Verder bleken ze klassieke, niet-irreversibele remmers te zijn van het enzym en geen tijdsafhankelijke remming te vertonen.

Tenslotte werd voor de twee beste vertegenwoordigers van de reeks (**5.69** en **5.71**) het *in vivo* potentieel onderzocht in een muismodel van acute intratracheale besmetting met de H37Rv-stam van *M. tuberculosis*. Zowel de farmacokinetiek van de twee remmers, als hun therapeutische efficaciteit werden onderzocht. Verbinding **5.69** bleek de beste biobeschikbaarheid te hebben en de hoogste efficaciteit, met een daling van de mycobacteriële burden van 0.5 logCFU-units tenopzichte van controledieren (t = negen dagen post-infectie). Hoewel deze daling veel kleiner is dan in geval van toedoeing van referentieproduct moxifloxacin, kan toch besloten worden dat hydantoïne-gebaseerde producten een statistisch significante activiteit hebben in het gebruikte *in vivo* model.

# Acknowledgements

---



## Acknowledgements

I would like to thank the OpenMedChem project board for accepting me and giving me the opportunity to conduct my doctoral research in the frame of the Marie Skłodowska-Curie actions, at the University of Antwerp and at GlaxoSmithKline (GSK) in Tres Cantos. This PhD experience was a life dream for me that I accomplished due to this decision.

I am grateful to my academic supervisor, Prof. Pieter Van der Veken and my industrial supervisor Dr. Robert Bates for their invaluable help, continuous support, confidence in my abilities and guidance on each step of my work. This PhD broadened my horizons in scientific world, gave me invaluable international exposure as well as provided a great springboard for my future research career.

I am thankful to each and every member of the research groups in Tres Cantos and Antwerp for their constant help, encouragement and valuable suggestions as well as the pleasant working environment. Special thanks to my research project fellows, Olga Balabon and Maciej Rogacki together with Fraser Cunningham who made the time in the lab not only productive but also highly enjoyable. They are the people that I shared most of my time during this doctoral program and they are part of my pleasant memories.

I owe my whole-hearted thanks to my family and my friends for being an important part of my life, and for their encouragement, constant support and faith in me. All my successes and victories would have been pointless and impossible without them.



# References

---





---

## References

- (1) Kumar, V.; Abbas, A. K.; Fausto, N.; Mitchell, R. *Robbins Basic Pathology*, 8th ed.; Saunders Elsevier, **2007**.
- (2) Daniel, T. M. The History of Tuberculosis. *Respir. Med.* **2006**, *100* (11), 1862–1870.
- (3) Lawn, S. D.; Zumla, A. I. Tuberculosis. *Lancet* **2011**, *378*, 57–72.
- (4) Zumla, A.; Raviglione, M.; Hafner, R.; Fordham von Reyn, C. Tuberculosis. *N. Engl. J. Med.* **2013**, *368*, 745–755.
- (5) Nachega, J. B.; Chaisson, R. E. Tuberculosis Drug Resistance: A Global Threat. *Clin. Infect. Dis.* **2003**, *36* (Suppl 1), S24–S30.
- (6) Raviglione, M. C. Global Epidemiology of Tuberculosis. *JAMA* **1995**, *273* (3), 220.
- (7) Raviglione, M. C.; Narain, J. P.; Kochi, A. HIV-Associated Tuberculosis in Developing Countries: Clinical Features, Diagnosis, and Treatment. *Bull. World Health Organ.* **1992**, *70* (4), 515–526.
- (8) World Health Organisation. Global Tuberculosis Report 2014 (WHO/HTM/TB/2014.08). **2014**, 171.
- (9) Skolnik, R. *Global Health 101*, 2nd ed.; Jones & Bartlett Publishers, **2011**.
- (10) World Health Organisation. *Global Tuberculosis Report 2016*; **2016**.
- (11) Talbot, E. A.; Raffa, B. J. *Molecular Medical Microbiology*; **2015**.
- (12) Olsen, C. H.; Olsen, C. H. Mycobacterium Tuberculosis in the Extracellular Compartment: An Underestimated Adversary. *Stat. Methods Med. Res.* **2003**, *71* (3), 6689–6692.
- (13) Dartois, V. The Path of Anti-Tuberculosis Drugs: From Blood to Lesions to Mycobacterial Cells. *Nat. Rev. Microbiol.* **2014**, *12* (3), 159–167.
- (14) Glickman, M. S.; Jacobs, W. R. Microbial Pathogenesis of Mycobacterium Tuberculosis: Dawn of a Discipline. *Cell* **2001**, *104* (4), 477–485.
- (15) Smith, I. *Mycobacterium Tuberculosis* Pathogenesis and Molecular Determinants of Virulence. *Clin. Microbiol. Rev.* **2003**, *16* (3), 463–496.
- (16) Houben, E. N. G.; Nguyen, L.; Pieters, J. Interaction of Pathogenic Mycobacteria with the Host Immune System. *Curr. Opin. Microbiol.* **2006**, *9*, 76–85.
- (17) Russell, D. G. Who Puts the Tubercle in Tuberculosis? *Nat. Rev. Microbiol.* **2007**, *5*, 39–47.

- (18) Doherty, T. M.; Andersen, P. Vaccines for Tuberculosis : Novel Concepts and Recent Progress Vaccines for Tuberculosis : Novel Concepts and Recent Progress. *Clin. Microbiol. Rev.* **2005**, *18* (4), 687–702.
- (19) Leong, F. J.; Dartois, V.; Dick, T. *A Color Atlas of Comparative Pathology of Pulmonary Tuberculosis*; CRC Press, **2010**.
- (20) Paige, C.; Bishai, W. R. Penitentiary or Penthouse Condo: The Tuberculous Granuloma from the Microbe’s Point of View. *Cell. Microbiol.* **2010**, *12* (3), 301–309.
- (21) Penchovsky, R.; Traykovska, M. Designing Drugs That Overcome Antibacterial Resistance: Where Do We Stand and What Should We Do? *Expert Opin. Drug Discov.* **2015**, *10* (6), 631–650.
- (22) Pyle, M. M. Relative Numbers of Resistant Tubercle Bacilli in Sputa of Patients before and during Treatment with Streptomycin. *Proc. Staff Meet. Mayo Clin.* **1947**, *22* (21), 465–473.
- (23) Medical Research Council. Treatment of Pulmonary Tuberculosis with Streptomycin and Para-Aminosalicylic Acid. *Br. Med. J.* **1950**, *2* (4688), 1073–1085.
- (24) Frieden, T. R.; Sterling, T.; Pablos-Mendez, A.; Kilburn, J. O.; Cauthen, G. M.; Dooley, S. W. The Emergence of Drug-Resistant Tuberculosis in New York City. *N. Engl. J. Med.* **1993**, *328* (8), 521–526.
- (25) Zhang, Y.; Yew, W. Mechanisms of Drug Resistance in Mycobacterium Tuberculosis. *Int J Tuberc Lung Dis* **2009**, *13* (11), 1320–1330.
- (26) Ramaswamy, S.; Musser, J. M. Molecular Genetic Basis of Antimicrobial Agent Resistance in Mycobacterium Tuberculosis: 1998 Update. *Tuber Lung Dis* **1998**, *79* (1), 3–29.
- (27) Zhang, Y.; Young, D. Molecular Genetics of Drug Resistance in Mycobacterium Tuberculosis. *J. Antimicrob. Chemother.* **1994**, *34* (3), 313–319.
- (28) WHO Treatment Guidelines for Drug-Resistant Tuberculosis 2016, **2016**.
- (29) Report. American Thoracic Society/Centers for Disease Control and Prevention/Infectious Diseases Society of America: Treatment of Tuberculosis. *Am. J. Respir. Crit. Care Med.* **2003**, *167* (4), 603–662.
- (30) Zumla, A.; Nahid, P.; Cole, S. T. Advances in the Development of New Tuberculosis Drugs and Treatment Regimens. *Nat. Rev. Drug Discov.* **2013**, *12* (5), 388–404.
- (31) World Health Organisation. *Global Tuberculosis Report 2015*; **2015**.
- (32) Ma, Z.; Lienhardt, C.; McIlleron, H.; Nunn, A. J.; Wang, X. Global Tuberculosis Drug

- Development Pipeline: The Need and the Reality. *Lancet* **2010**, 375 (9731), 2100–2109.
- (33) Bloom, B. R.; Murray, C. J. Tuberculosis: Commentary on a Reemergent Killer. *Science* **1992**, 257 (5073), 1055–1064.
- (34) Fätkenheuer, G.; Taelman, H.; Lepage, P.; Schwenk, A.; Wenzel, R. The Return of Tuberculosis. *Diagn. Microbiol. Infect. Dis.* **1999**, 34 (2), 139–146.
- (35) Koul, A.; Arnoult, E.; Lounis, N.; Guillemont, J.; Andries, K. The Challenge of New Drug Discovery for Tuberculosis. *Nature* **2011**, 469 (7331), 483–490.
- (36) Jnawali, H. N.; Ryoo, S. First – and Second – Line Drugs and Drug Resistance. *Tuberc. issues diagnosis Manag.* **2013**, 163–180.
- (37) Suarez, J.; Rangelova, K.; Jarzecki, A. A.; Manzerova, J.; Krymov, V.; Zhao, X.; Yu, S.; Metlitsky, L.; Gerfen, G. J.; Magliozzo, R. S. An Oxyferrous Heme/protein-Based Radical Intermediate Is Catalytically Competent in the Catalase Reaction of Mycobacterium Tuberculosis Catalase-Peroxidase (KatG). *J. Biol. Chem.* **2009**, 284 (11), 7017–7029.
- (38) Bardou, F.; Raynaud, C.; Ramos, C.; Lanéelle, M. A.; Lanéelle, G. Mechanism of Isoniazid Uptake in Mycobacterium Tuberculosis. *Microbiology* **1998**, 144 (9), 2539–2544.
- (39) Rana, F. Rifampicin-an Overview. *IJRPC* **2013**, 3 (1), 83–87.
- (40) Riva, M. A. From Milk to Rifampicin and Back Again: History of Failures and Successes in the Treatment for Tuberculosis. *J. Antibiot. (Tokyo)*. **2014**, 67 (9), 661–665.
- (41) Campbell, E. A.; Korzheva, N.; Mustaev, A.; Murakami, K.; Nair, S.; Goldfarb, A.; Darst, S. A. Structural Mechanism for Rifampicin Inhibition of Bacterial Rna Polymerase. *Cell* **2001**, 104 (6), 901–912.
- (42) Rae, J. M.; Johnson, M. D.; Lippman, M. E.; Flockhart, D. A. Rifampin Is a Selective, Pleiotropic Inducer of Drug Metabolism Genes in Human Hepatocytes: Studies with cDNA and Oligonucleotide Expression Arrays. *J. Pharmacol. Exp. Ther.* **2001**, 299 (3), 849–857.
- (43) Zhang, Y.; Mitchison, D. The Curious Characteristics of Pyrazinamide: A Review. *Int. J. Tuberc. Lung Dis.* **2003**, 7 (1), 6–21.
- (44) Zhang, Y.; Wade, M. M.; Scorpio, A.; Zhang, H.; Sun, Z. Mode of Action of Pyrazinamide: Disruption of Mycobacterium Tuberculosis Membrane Transport and Energetics by Pyrazinoic Acid. *J. Antimicrob. Chemother.* **2003**, 52 (5), 790–795.
- (45) Takayama, K.; Kilburn, J. O. Inhibition of Synthesis of Arabinogalactan by Ethambutol in Mycobacterium Smegmatis. *Antimicrob. Agents Chemother.* **1989**, 33 (9), 1493–1499.

- (46) WHO Guideline. Ethambutol Efficacy and Toxicity: Literature Review and Recommendations for Daily and Intermittent Dosage in Children. *WHO Bull.* **2006**, 1–76.
- (47) Van Deun, A.; Monedero, I.; Rieder, H. L.; Heldal, E.; Alarcon, E.; Mace, C.; Dlodlo, R. A.; Fujiwara, P. I.; Chiang, C.-Y.; Harries, A. D.; Trebucq, A.; Armengol, R.; Perrin, C.; Cesari, G.; Enarson, D. A. *Guidelines for Clinical and Operational Management of Drug-Resistant Tuberculosis 2013*; **2013**.
- (48) Schluger, N. W. Fluoroquinolones in The Treatment of Tuberculosis: Which Is Best? *Am. J. Respir. Crit. Care Med.* **2013**, *188* (7), 768–769.
- (49) Park-Wyllie, L. Y.; Juurlink, D. N.; Kopp, A.; Shah, B. R.; Stukel, T. A.; Stumpo, C.; Dresser, L.; Low, D. E.; Mamdani, M. M. Outpatient Gatifloxacin Therapy and Dysglycemia in Older Adults. *N. Engl. J. Med.* **2006**, *354* (13), 1352–1361.
- (50) Gninafon, M.; Lo, M. B.; Mthiyane, T.; Sc, M.; Kassa, F.; Diaye, A. N.; Rustomjee, R.; Jong, B. C. De; Ph, D.; Horton, J.; Perronne, C.; Sismanidis, C.; Ph, D.; Lapujade, O.; Sc, B.; Merle, C. S.; Fielding, K.; Sow, O. B.; Gninafon, M.; Lo, M. B.; Mthiyane, T.; Odhiambo, J.; Amukoye, E.; Bah, B.; Kassa, F.; N'Diaye, A.; Rustomjee, R.; de Jong, B. C.; Horton, J.; Perronne, C.; Sismanidis, C.; Lapujade, O.; Olliaro, P. L.; Lienhardt, C. A Four-Month Gatifloxacin-Containing Regimen for Treating Tuberculosis. *N. Engl. J. Med.* **2014**, *371* (17), 1588–1598.
- (51) Reeves, A. Z.; Campbell, P. J.; Sultana, R.; Malik, S.; Murray, M.; Plikaytis, B. B.; Shinnick, T. M.; Posey, J. E. Aminoglycoside Cross-Resistance in Mycobacterium Tuberculosis due to Mutations in the 5' Untranslated Region of whiB7. *Antimicrob. Agents Chemother.* **2013**, *57* (4), 1857–1865.
- (52) De Jager, R.; Van Altena, R. Hearing Loss and Nephrotoxicity in Long-Term Aminoglycoside Treatment in Patients with Tuberculosis. *Int. J. Tuberc. Lung Dis.* **2002**, *6* (7), 622–627.
- (53) Bruning, J. B.; Murillo, A. C.; Chacon, O.; Barletta, R. G.; Sacchetti, J. C. Structure of the Mycobacterium Tuberculosis D-alanine:D-Alanine Ligase, a Target of the Antituberculosis Drug D-Cycloserine. *Antimicrob. Agents Chemother.* **2011**, *55* (1), 291–301.
- (54) Bozdogan, B.; Appelbaum, P. C. Oxazolidinones: Activity, Mode of Action, and Mechanism of Resistance. *Int. J. Antimicrob. Agents* **2004**, *23* (2), 113–119.
- (55) Lee, M.; Lee, J.; Carroll, M. W.; Choi, H.; Min, S.; Song, T.; Via, L. E.; Goldfeder, L. C.; Kang, E.; Jin, B.; Park, H.; Kwak, H.; Kim, H.; Jeon, H.-S.; Jeong, I.; Joh, J. S.; Chen, R. Y.; Olivier, K. N.; Shaw, P. a.; Follmann, D.; Song, S. D.; Lee, J.-K.; Lee, D.; Kim, C. T.; Dartois, V.; Park, S.-K.; Cho, S.-N.; Barry, C. E. Linezolid for Treatment of Chronic Extensively Drug-Resistant

- Tuberculosis. *N. Engl. J. Med.* **2012**, *367* (16), 1508–1518.
- (56) Grosset, J. H.; Tyagi, S.; Almeida, D. V.; Converse, P. J.; Li, S. Y.; Ammerman, N. C.; Bishai, W. R.; Enarson, D.; Trebucq, A. Assessment of Clofazimine Activity in a Second-Line Regimen for Tuberculosis in Mice. *Am. J. Respir. Crit. Care Med.* **2013**, *188* (5), 608–612.
- (57) World Health Organisation, G. *Companion Handbook to the WHO Guidelines for the Programmatic Management of Drug-Resistant Tuberculosis*; **2014**.
- (58) Andries, K.; Verhasselt, P.; Guillemont, J.; Göhlmann, H. W. H.; Neefs, J.-M.; Winkler, H.; Van Gestel, J.; Timmerman, P.; Zhu, M.; Lee, E.; Williams, P.; de Chaffoy, D.; Huitric, E.; Hoffner, S.; Cambau, E.; Truffot-Pernot, C.; Lounis, N.; Jarlier, V. A Diarylquinoline Drug Active on the ATP Synthase of Mycobacterium Tuberculosis. *Science* **2005**, *307* (5707), 223–227.
- (59) Koul, A.; Vranckx, L.; Dendouga, N.; Balemans, W.; Van Den Wyngaert, I.; Vergauwen, K.; Göhlmann, H. W. H.; Willebrords, R.; Poncelet, A.; Guillemont, J.; Bald, D.; Andries, K. Diarylquinolines Are Bactericidal for Dormant Mycobacteria as a Result of Disturbed ATP Homeostasis. *J. Biol. Chem.* **2008**, *283* (37), 25273–25280.
- (60) Cabrera-rivero, J. L.; Vargas-vasquez, D. E.; Gao, M.; Ph, D.; Awad, M.; Ch, B.; Park, S.; Shim, T. S.; Suh, G. Y. The Diarylquinoline TMC207 for Multidrug-Resistant Tuberculosis. *N. Engl. J. Med.* **2009**, *360* (23), 2397–2405.
- (61) Lakshmanan, M.; Xavier, A. S. Bedaquiline - The First ATP Synthase Inhibitor against Multi Drug Resistant Tuberculosis. *J. Young Pharm.* **2013**, *5* (4), 112–115.
- (62) Lounis, N.; Gevers, T.; Van Den Berg, J.; Verhaeghe, T.; Van Heeswijk, R.; Andries, K. Prevention of Drug Carryover Effects in Studies Assessing Antimycobacterial Efficacy of TMC207. *J. Clin. Microbiol.* **2008**, *46* (7), 2212–2215.
- (63) Cohen, J. Approval of Novel TB Drug Celebrated-With Restraint. *Science*. **2013**, *339* (6116), 130–130.
- (64) Mukherjee, T.; Boshoff, H. Nitroimidazoles for the Treatment of TB: Past, Present and Future. *Future Med. Chem.* **2011**, *3* (11), 1427–1454.
- (65) Manjunatha, U. H.; Boshoff, H.; Dowd, C. S.; Zhang, L.; Albert, T. J.; Norton, J. E.; Daniels, L.; Dick, T.; Pang, S. S.; Barry, C. E. Identification of a Nitroimidazo-Oxazine-Specific Protein Involved in PA-824 Resistance in Mycobacterium Tuberculosis. *Proc. Natl. Acad. Sci. U. S. A.* **2006**, *103* (2), 431–436.

- (66) Matsumoto, M.; Hashizume, H.; Tomishige, T.; Kawasaki, M.; Tsubouchi, H.; Sasaki, H.; Shimokawa, Y.; Komatsu, M. OPC-67683, a Nitro-Dihydro-Imidazooxazole Derivative with Promising Action against Tuberculosis in Vitro and in Mice. *PLoS Med.* **2006**, *3* (11), 2131–2144.
- (67) Ryan, N. J.; Lo, J. H. Delamanid: First Global Approval. *Drugs* **2014**, *74*, 1041–1045.
- (68) Lee, M.; Song, T.; Kim, Y.; Jeong, I.; Cho, S. N.; Barry, C. E. Delamanid for Extensively Drug-Resistant Tuberculosis. *N. Engl. J. Med.* **2015**, *373* (3), 291–292.
- (69) Zheng, J.; Rubin, E. J.; Bifani, P.; Mathys, V.; Lim, V.; Au, M.; Jang, J.; Nam, J.; Dick, T.; Walker, J. R.; Pethe, K.; Camacho, L. R. Para-Aminosalicylic Acid Is a Prodrug Targeting Dihydrofolate Reductase in Mycobacterium Tuberculosis. *J. Biol. Chem.* **2013**, *288* (32), 23447–23456.
- (70) England, K.; Boshoff, H. I. M.; Arora, K.; Weiner, D.; Dayao, E.; Schimel, D.; Via, L. E.; Barry, C. E. Meropenem-Clavulanic Acid Shows Activity against Mycobacterium Tuberculosis in Vivo. *Antimicrob. Agents Chemother.* **2012**, *56* (6), 3384–3387.
- (71) Hugonnet, J.-E.; Tremblay, L. W.; Boshoff, H. I.; Barry, C. E.; Blanchard, J. S. Meropenem-Clavulanate Is Effective Against Extensively Drug-Resistant Mycobacterium Tuberculosis. *Science*, **2009**, *323* (5918), 1215–1218.
- (72) Brewer, T. F. Preventing Tuberculosis with Bacillus Calmette-Guérin Vaccine: A Meta-Analysis of the Literature. *Clin. Infect. Dis.* **2000**, *31*, Suppl 3, 64-7.
- (73) Keseru, G. M.; Makara, G. M. Hit Discovery and Hit-to-Lead Approaches. *Drug Discov. Today* **2006**, *11* (15/16), 741–748.
- (74) Copeland, R. A. *Evaluation of Enzyme Inhibitors in Drug Discovery: A Guide for Medicinal Chemists and Pharmacologists*; John Wiley & Sons, **2013**.
- (75) An, W. F.; Tolliday, N. Cell-Based Assays for High-Throughput Screening. *Mol. Biotechnol.* **2010**, *45* (2), 180–186.
- (76) Ballell, L.; Bates, R. H.; Young, R. J.; Alvarez-Gomez, D.; Alvarez-Ruiz, E.; Barroso, V.; Blanco, D.; Crespo, B.; Escribano, J.; González, R.; Lozano, S.; Huss, S.; Santos-Villarejo, A.; Martín-Plaza, J.; Mendoza, A.; Rebollo-Lopez, M. J.; Remuiñan-Blanco, M.; Lavandera, J. L.; Pérez-Herran, E.; Gamo-Benito, F. J.; García-Bustos, J. F.; Barros, D.; Castro, J. P.; Cammack, N.; Fueling Open-Source Drug Discovery: 177 Small-Molecule Leads against Tuberculosis. *ChemMedChem* **2013**, *8* (2), 313–321.

- (77) Marella, A.; Tanwar, O. P.; Saha, R.; Ali, M. R.; Srivastava, S.; Akhter, M.; Shaquiquzzaman, M.; Alam, M. M. Quinoline: A Versatile Heterocyclic. *Saudi Pharm. J. SPJ Off. Publ. Saudi Pharm. Soc.* **2013**, *21* (1), 1–12.
- (78) Boteva, A. A.; Krasnykh, O. P. The Methods of Synthesis, Modification, and Biological Activity of 4-Quinolones (Review). *Chem. Heterocycl. Compd.* **2009**, *45* (7), 757–785.
- (79) Wolfson, J. S.; Hooper, D. C. The Fluoroquinolones: Structures, Mechanisms of Action and Resistance, and Spectra of Activity in Vitro. *Antimicrob. Agents Chemother.* **1985**, *28* (4), 581–586.
- (80) Foley, M.; Tilley, L. Quinoline Antimalarials: Mechanisms of Action and Resistance. *Int. J. Parasitol.* **1997**, *27* (2), 231–240.
- (81) Musiol, R.; Serda, M.; Hensel-Bielowka, S.; Polanski, J. Quinoline-Based Antifungals. *Curr. Med. Chem.* **2010**, *17* (18), 1960–1973.
- (82) Lilienkamp, A.; Jialin, M.; Baojie, W.; Yuehong, W.; Franzblau, S. G.; Kozikowski, A. P. Structure-Activity Relationships for a Series of Quinoline-Based Compounds Active against Replicating and Nonreplicating Mycobacterium Tuberculosis. *J. Med. Chem.* **2009**, *52* (7), 2109–2118.
- (83) Eswaran, S.; Adhikari, A. V.; Pal, N. K.; Chowdhury, I. H. Design and Synthesis of Some New Quinoline-3-Carbohydrazone Derivatives as Potential Antimycobacterial Agents. *Bioorg. Med. Chem. Lett.* **2010**, *20* (3), 1040–1044.
- (84) Tukulula, M.; Little, S.; Gut, J.; Rosenthal, P. J.; Wan, B.; Franzblau, S. G.; Chibale, K. The Design, Synthesis, in Silico ADME Profiling, Antiplasmodial and Antimycobacterial Evaluation of New Arylamino Quinoline Derivatives. *Eur. J. Med. Chem.* **2012**, *57*, 259–267.
- (85) Koul, A.; Dendouga, N.; Vergauwen, K.; Molenberghs, B.; Vranckx, L.; Willebrords, R.; Ristic, Z.; Lill, H.; Dorange, I.; Guillemont, J.; Bald, D.; Andries, K. Diarylquinolines Target Subunit c of Mycobacterial ATP Synthase. *Nat. Chem. Biol.* **2007**, *3* (6), 323–324.
- (86) Moadebi, S.; Harder, C. K.; Fitzgerald, M. J.; Elwood, K. R.; Marra, F. Fluoroquinolones for the Treatment of Pulmonary Tuberculosis. *Drugs* **2007**, *67* (14), 2077–2099.
- (87) Singh, S.; Kaur, G.; Mangla, V.; Gupta, M. K. Quinoline and Quinolones: Promising Scaffolds for Future Antimycobacterial Agents. *J. Enzyme Inhib. Med. Chem.* **2014**, *6366* (3), 1–13.
- (88) Ho, T.-L. *Hard and Soft Acids and Bases Principle in Organic Chemistry*; Elsevier, 2012.
- (89) Frank, J.; Katritzky, A. R. Tautomeric Pyridines. Part XV. Pyridone–hydroxypyridine

- Equilibria in Solvents of Differing Polarity. *J. Chem. Soc., Perkin Trans. 2* **1976**, 584 (12), 1428–1431.
- (90) Comins, D. L.; Jianhua, G. N- vs. O-Alkylation in the Mitsunobu Reaction of 2-Pyridone. *Tetrahedron Lett.* **1994**, 35 (7), 968.
- (91) Torhan, M. C.; Peet, N. P.; Williams, J. D. A Comparison of N- versus O-Alkylation of Substituted 2-Pyridones under Mitsunobu Conditions. *Tetrahedron Lett.* **2013**, 54 (30), 3926–3928.
- (92) Hori, M.; Ohtaka, H. Effects of a 2-Substituent on the Ratio of N-and O-Alkylation of 4(3H)-Quinazolinones. *Chem. Pharm. Bull.* **1993**, 41 (6), 1114–1117.
- (93) Pearson, R. G. Hard and Soft Acids and Bases. *J. Am. Chem. Soc.* **1963**, 85 (22), 3533–3539.
- (94) Shevelev, S. A. Dual Reactivity of Ambident Anions. *Russ. Chem. Rev.* **1970**, 39 (10), 844–858.
- (95) Klopman, G. Chemical Reactivity and the Concept of Charge- and Frontier-Controlled Reactions. *J. Am. Chem. Soc.* **1968**, 90 (2), 223–234.
- (96) Salem, L. Intermolecular Orbital Theory of the Interaction between Conjugated Systems. I. General Theory. *J. Am. Chem. Soc.* **1968**, 90 (3), 543–552.
- (97) Gompper, R.; Wagner, H.-U. The Concept of Allopolarization. Effects of Substituents on the Reactions of Ambifunctional Anions. *Angew. Chemie Int. Ed. English* **1976**, 15 (6), 321–333.
- (98) Mayr, H.; Breugst, M.; Ofial, A. R. Farewell to the HSAB Treatment of Ambident Reactivity. *Angew. Chemie - Int. Ed.* **2011**, 50 (29), 6470–6505.
- (99) Breugst, M.; Zipse, H.; Guthrie, J. P.; Mayr, H. Marcus Analysis of Ambident Reactivity. *Angew. Chemie - Int. Ed.* **2010**, 49 (30), 5165–5169.
- (100) Young, R. J.; Green, D. V. S. S.; Luscombe, C. N.; Hill, A. P. Getting Physical in Drug Discovery II: The Impact of Chromatographic Hydrophobicity Measurements and Aromaticity. *Drug Discov. Today* **2011**, 16 (17–18), 822–830.
- (101) Hill, A. P.; Young, R. J. Getting Physical in Drug Discovery: A Contemporary Perspective on Solubility and Hydrophobicity. *Drug Discov. Today* **2010**, 15 (15–16), 648–655.
- (102) Brouet, J.-C.; Gu, S.; Peet, N. P.; Williams, J. D. A Survey of Solvents for the Conrad-Limpach Synthesis of 4-Hydroxyquinolones. *Synth. Commun.* **2009**, 39 (9), 5193–5196.
- (103) Escribano, J.; Rivero-Hernández, C.; Rivera, H.; Barros, D.; Castro-Pichel, J.; Pérez-Herrán, E.; Mendoza-Losana, A.; Angulo-Barturen, I.; Ferrer-Bazaga, S.; Jiménez-Navarro, E.; Ballell,



- L. 4-Substituted Thioquinolines and Thiazoloquinolines: Potent, Selective, and Tween-80 in Vitro Dependent Families of Antitubercular Agents with Moderate in Vivo Activity. *ChemMedChem* **2011**, *6* (12), 2252–2263.
- (104) Tsantrizos, Y. Inhibitors of Human Immunodeficiency Virus Replication. WO 2009/062285 A1, **2009**.
- (105) Ma, L.; Li, S.; Zheng, H.; Chen, J.; Lin, L.; Ye, X.; Chen, Z.; Xu, Q.; Chen, T.; Yang, J.; Qiu, N.; Wang, G.; Peng, A.; Ding, Y.; Wei, Y.; Chen, L. Synthesis and Biological Activity of Novel Barbituric and Thiobarbituric Acid Derivatives against Non-Alcoholic Fatty Liver Disease. *Eur. J. Med. Chem.* **2011**, *46* (6), 2003–2010.
- (106) Reitsema, R. H. The Chemistry of 4-Hydroxyquinolines. *Chem. Rev.* **1948**, *43* (1), 43–68.
- (107) Morgentin, R.; Pasquet, G.; Boutron, P.; Jung, F.; Lamorlette, M.; Maudet, M.; Plé, P. Strategic Studies in the Syntheses of Novel 6,7-Substituted Quinolones and 7- or 6-Substituted 1,6- and 1,7-Naphthyridones. *Tetrahedron* **2008**, *64* (12), 2772–2782.
- (108) Wang, T.-C.; Chen, Y.; Tzeng, C.; Liou, S.; Chang, Y.; Teng, C. Antiplatelet  $\alpha$ -Methylidene- $\gamma$ -Butyrolactones: Synthesis and Evaluation of Quinoline, Flavone, and Xanthone Derivatives. *Helv. Chim. Acta* **1996**, *79* (6), 1620–1626.
- (109) Oyama, T.; Negishi, E.; Onigahara, H.; Kusano, N.; Miyoshi, Y.; Mita, M.; Nakazono, M.; Ohtsuki, S.; Ojida, A.; Lindner, W.; Hamase, K. Design and Synthesis of a Novel Pre-Column Derivatization Reagent with a 6-Methoxy-4-Quinolone Moiety for Fluorescence and Tandem Mass Spectrometric Detection and Its Application to Chiral Amino Acid Analysis. *J. Pharm. Biomed. Anal.* **2015**, *116*, 71–79.
- (110) Pissinate, K.; Villela, A. D.; Rodrigues, V.; Giacobbo, B. C.; Grams, E. S.; Abbadi, B. L.; Trindade, R. V.; Roesler Nery, L.; Bonan, C. D.; Back, D. F.; Campos, M. M.; Basso, L. A.; Santos, D. S.; Machado, P. 2-(Quinolin-4-Yloxy)acetamides Are Active against Drug-Susceptible and Drug-Resistant Mycobacterium Tuberculosis Strains. *ACS Med. Chem. Lett.* **2016**, *7* (3), 235–239.
- (111) Maurya, S. K.; Gollapalli, D. R.; Kirubakaran, S.; Zhang, M.; Johnson, C. R.; Benjamin, N. N.; Hedstrom, L.; Cuny, G. D. Triazole Inhibitors of Cryptosporidium Parvum Inosine 5'-Monophosphate Dehydrogenase. *J. Med. Chem.* **2009**, *52* (15), 4623–4630.
- (112) Zhang, W.; Li, Z.; Zhou, M.; Wu, F.; Hou, X.; Luo, H.; Liu, H.; Han, X.; Yan, G.; Ding, Z.; Li, R. Synthesis and Biological Evaluation of 4-(1,2,3-Triazol-1-Yl)coumarin Derivatives as Potential Antitumor Agents. *Bioorg. Med. Chem. Lett.* **2014**, *24* (3), 799–807.

- (113) Hung, J. M.; Arabshahi, H. J.; Leung, E.; Reynisson, J.; Barker, D. Synthesis and Cytotoxicity of thieno[2,3-B]pyridine and furo[2,3-B]pyridine Derivatives. *Eur. J. Med. Chem.* **2014**, *86*, 420–437.
- (114) Zhou, Q.; Zhang, B.; Du, T.; Gu, H.; Ye, Y.; Jiang, H.; Chen, R. Copper-Catalyzed Highly Regioselective 2-Aryloxylation of 2,x-Dihalopyridines. *Tetrahedron* **2013**, *69* (1), 327–333.
- (115) Alexandre, F.-R.; Bercibar, A.; Besson, T. Microwave-Assisted Niementowski Reaction. Back to the Roots. *Tetrahedron Lett.* **2002**, *43* (21), 3911–3913.
- (116) Špulák, M.; Novák, Z.; Palát, K.; Kuneš, J.; Pourová, J.; Pour, M. The Unambiguous Synthesis and NMR Assignment of 4-Alkoxy and 3-Alkylquinazolines. *Tetrahedron* **2013**, *69* (6), 1705–1711.
- (117) Bodendiek, S. B.; Mahieux, C.; Hänsel, W.; Wulff, H. 4-Phenoxybutoxy-Substituted Heterocycles - A Structure-Activity Relationship Study of Blockers of the Lymphocyte Potassium Channel Kv1.3. *Eur. J. Med. Chem.* **2009**, *44* (5), 1838–1852.
- (118) Ullman, B. R.; Aja, T.; Chen, N.; Diaz, J. L.; Gu, X.; Herrmann, J.; Kalish, V. J.; Karanewsky, D. S.; Kodandapani, L.; Krebs, J. J.; Linton, S. D.; Meduna, S. P.; Nalley, K.; Robinson, E. D.; Roggo, S. P.; Sayers, R. O.; Schmitz, A.; Ternansky, R. J.; Tomaselli, K. J.; Wu, J. C. Structure-Activity Relationships within a Series of Caspase Inhibitors. Part 2: Heterocyclic Warheads. *Bioorganic Med. Chem. Lett.* **2005**, *15* (15), 3632–3636.
- (119) Peng, H.; Kumaravel, G.; Yao, G.; Sha, L.; Wang, J.; Van Vlijmen, H.; Bohnert, T.; Huang, C.; Vu, C. B.; Ensinger, C. L.; Chang, H.; Engber, T. M.; Whalley, E. T.; Petter, R. C. Novel Bicyclic Piperazine Derivatives of Triazolotriazine and Triazolopyrimidines as Highly Potent and Selective Adenosine A<sub>2A</sub> Receptor Antagonists. *J. Med. Chem.* **2004**, *47* (25), 6218–6229.
- (120) Gharat, L.A.; Banerjee, A.; Khairatkar-joshi, N.; Kattige, V. G. Bicyclic Compounds as mPGES-1 Inhibitors. US 9,006,257 B2, **2015**.
- (121) Kouznetsov, V.; Mendez, L.; Gomez, C. Recent Progress in the Synthesis of Quinolines. *Curr. Org. Chem.* **2005**, *9* (2), 141–161.
- (122) Laplante, S. R.; Bilodeau, F.; Aubry, N.; Gillard, J. R.; O'Meara, J.; Coulombe, R. N- versus O-Alkylation: Utilizing NMR Methods to Establish Reliable Primary Structure Determinations for Drug Discovery. *Bioorganic Med. Chem. Lett.* **2013**, *23* (16), 4663–4668.
- (123) Silverstein, R. M.; Webster, F. X.; Kiemle, D. J.; Bryce, D. L. *Spectrometric Identification of Organic Compounds*, 8th ed.; Willey: New York, **2015**.

- 
- (124) Bodenhausen, G.; Ruben, D. J. Natural Abundance Nitrogen-15 NMR by Enhanced Heteronuclear Spectroscopy. *Chem. Phys. Lett.* **1980**, *69* (1), 185–189.
- (125) Reynolds, W. F.; McLean, S.; Tay, L.-L.; Yu, M.; Enriquez, R. G.; Estwick, D. M.; Pascoe, K. O. Comparison of <sup>13</sup>C Resolution and Sensitivity of HSQC and HMQC Sequences and Application of HSQC-Based Sequences to the Total <sup>1</sup>H and <sup>13</sup>C Spectral Assignment of Clonasterol. *Magn. Reson. Chem.* **1997**, *35* (7), 455–462.
- (126) Bax, A.; Summers, M. F. <sup>1</sup>H and <sup>13</sup>C Assignments from Sensitivity-Enhanced Detection of Heteronuclear Multiple-Bond Connectivity by 2D Multiple Quantum NMR. *J. Am. Chem. Soc.* **1986**, *108* (12), 2093–2094.
- (127) Summers, M. F.; Marzilli, L. G.; Bax, A. Complete Proton and Carbon-13 Assignments of Coenzyme B12 through the Use of New Two-Dimensional NMR Experiments. *J. Am. Chem. Soc.* **1986**, *108* (15), 4285–4294.
- (128) Dvorak, C. A.; Swanson, D. M.; Wong, V. D. Piperazinyl Derivatives Useful as Modulators of Neuropeptide Y2 Receptor. Patent US 2011/0046151 A1, **2011**.
- (129) Zhao, Y.; Duan, S.; Zeng, X.; Liu, C.; Davies, N. M.; Li, B.; Forrest, M. L. Prodrug Strategy for PSMA-Targeted Delivery of TGX-221 to Prostate Cancer Cells. *Mol. Pharm.* **2012**, *9* (6), 1705–1716.
- (130) Pešić, D.; Starčević, K.; Toplak, A.; Herreros, E.; Vidal, J.; Almela, M. J.; Jelić, D.; Alihodžić, S.; Spaventi, R.; Perić, M. Design, Synthesis, and in Vitro Activity of Novel 2'-O-Substituted 15-Membered Azalides. *J. Med. Chem.* **2012**, *55* (7), 3216–3227.
- (131) Huang, T.-S.; Kunin, C. M.; Yan, B.-S.; Chen, Y.-S.; Lee, S. S.-J.; Syu, W. Susceptibility of Mycobacterium Tuberculosis to Sulfamethoxazole, Trimethoprim and Their Combination over a 12 Year Period in Taiwan. *J. Antimicrob. Chemother.* **2012**, *67* (3), 633–637.
- (132) Kestranek, A.; Chervenak, A.; Longenberger, J.; Placko, S. Chemiluminescent Nitrogen Detection (CLND) to Measure Kinetic Aqueous Solubility. *Curr. Protoc. Chem. Biol.* **2013**, *5* (4), 269–280.
- (133) Leroux, F. R.; Manteau, B.; Vors, J.-P.; Pazenok, S. Trifluoromethyl Ethers--Synthesis and Properties of an Unusual Substituent. *Beilstein J. Org. Chem.* **2008**, *4*, 13.
- (134) Leiserowitz, L.; Hagler, A. T. The Generation of Possible Crystal Structures of Primary Amides. *Proc. R. Soc. A* **1983**, *388* (1794), 133–175.
- (135) Ayerst, E. M.; Duke, J. R. C. Refinement of the Crystal Structure of Oxamide. *Acta*

- Crystallogr.* **1954**, 7 (8), 588–590.
- (136) Smith, D. A.; van de Waterbeemd, H.; Walker, D. K. *Pharmacokinetics and Metabolism in Drug Design*; Mannhold, R., Kubinyi, H., Timmerman, H., Eds.; Methods and Principles in Medicinal Chemistry; Wiley-VCH Verlag GmbH: Weinheim, Germany, **2012**; 51.
- (137) Sorrentino, F.; Gonzalez del Rio, R.; Zheng, X.; Presa Matilla, J.; Torres Gomez, P.; Martinez Hoyos, M.; Perez Herran, M. E.; Mendoza Losana, A.; Av-Gay, Y. Development of an Intracellular Screen for New Compounds Able To Inhibit Mycobacterium Tuberculosis Growth in Human Macrophages. *Antimicrob. Agents Chemother.* **2016**, 60 (1), 640–645.
- (138) Griffin, J. E.; Gawronski, J. D.; DeJesus, M. A.; Ioerger, T. R.; Akerley, B. J.; Sasseti, C. M. High-Resolution Phenotypic Profiling Defines Genes Essential for Mycobacterial Growth and Cholesterol Catabolism. *PLoS Pathog.* **2011**, 7 (9), 1–10.
- (139) Redfern, W. S.; Carlsson, L.; Davis, A. S.; Lynch, W. G.; MacKenzie, I.; Palethorpe, S.; Siegl, P. K. S.; Strang, I.; Sullivan, A. T.; Wallis, R.; Camm, A. J.; Hammond, T. G. Relationships between Preclinical Cardiac Electrophysiology, Clinical QT Interval Prolongation and Torsade de Pointes for a Broad Range of Drugs: Evidence for a Provisional Safety Margin in Drug Development. *Cardiovasc. Res.* **2003**, 58 (1), 32–45.
- (140) De Bruin, M. L.; Pettersson, M.; Meyboom, R. H. B.; Hoes, A. W.; Leufkens, H. G. M. Anti-HERG Activity and the Risk of Drug-Induced Arrhythmias and Sudden Death. *Eur. Heart J.* **2005**, 26 (6), 590–597.
- (141) Xu, G. P.; Gilbertson, S. R. Development of Building Blocks for the Synthesis of N-Heterocyclic Carbene Ligands. *Org. Lett.* **2005**, 7 (2), 4605.
- (142) Kokatla, H. P.; Yoo, E.; Salunke, D. B.; Sil, D.; Ng, C. F.; Balakrishna, R.; Malladi, S. S.; Fox, L. M.; David, S. a. Toll-like Receptor-8 Agonistic Activities in C2, C4, and C8 Modified thiazolo[4,5-C]quinolines. *Org. Biomol. Chem.* **2013**, 11 (7), 1179–1198.
- (143) Margolis, B. J.; Long, K. a; Laird, D. L. T.; Ruble, J. C.; Pulley, S. R.; Lilly, E. Assembly of 4-Aminoquinolines via Palladium Catalysis : A Mild and Convenient Alternative to S N Ar Methodology 4-Aminoquinolines , Classically Prepared via S N Ar Chemistry from an Amine and 4-Haloquinoline , Are Important Scaffolds in Medicinal Chemistr. *J. Org. Chem.* **2007**, 72, 2232–2235.
- (144) Valentin, J. P. Reducing QT Liability and Proarrhythmic Risk in Drug Discovery and Development. *Br. J. Pharmacol.* **2010**, 159 (1), 5–11.
- (145) Mikušová, K.; Huang, H.; Yagi, T.; Holsters, M.; Vereecke, D.; D’Haeze, W.; Scherman, M. S.;

- Brennan, P. J.; McNeil, M. R.; Crick, D. C. Decaprenylphosphoryl Arabinofuranose, the Donor of the D-Arabinofuranosyl Residues of Mycobacterial Arabinan, Is Formed via a Two-Step Epimerization of Decaprenylphosphoryl Ribose. *J. Bacteriol.* **2005**, *187* (23), 8020–8025.
- (146) Wolucka, B. A. Biosynthesis of D-Arabinose in Mycobacteria - A Novel Bacterial Pathway with Implications for Antimycobacterial Therapy. *FEBS J.* **2008**, *275* (11), 2691–2711.
- (147) Batt, S. M.; Cacho Izquierdo, M.; Castro Pichel, J.; Stubbs, C. J.; Vela-Glez Del Peral, L.; Pérez-Herrán, E.; Dhar, N.; Mouzon, B.; Rees, M.; Hutchinson, J. P.; Young, R. J.; McKinney, J. D.; Barros Aguirre, D.; Ballell, L.; Besra, G. S.; Argyrou, A. Whole Cell Target Engagement Identifies Novel Inhibitors of Mycobacterium Tuberculosis Decaprenylphosphoryl- $\beta$ -D-Ribose Oxidase. *ACS Infect. Dis.* **2015**, *1* (12), 615–626.
- (148) Kolly, G. S.; Boldrin, F.; Sala, C.; Dhar, N.; Hartkoorn, R. C.; Ventura, M.; Serafini, A.; Mckinney, J. D.; Manganeli, R.; Cole, S. T. Assessing the Essentiality of the Decaprenyl-Phospho-D-Arabinofuranose Pathway in Mycobacterium Tuberculosis Using Conditional Mutants. *Mol. Microbiol.* **2014**, *92* (1), 194–211.
- (149) Brecik, M.; Centárová, I.; Mukherjee, R.; Kolly, G. S.; Huszár, S.; Bobovská, A.; Kilacsková, E.; Mokošová, V.; Svetlíková, Z.; Šarkan, M.; Neres, J.; Korduláková, J.; Cole, S. T.; Mikušová, K. DprE1 Is a Vulnerable Tuberculosis Drug Target Due to Its Cell Wall Localization. *ACS Chem. Biol.* **2015**, *10* (7), 1631–1636.
- (150) Batt, S. M.; Jabeen, T.; Bhowruth, V.; Quill, L.; Lund, P. a.; Eggeling, L.; Alderwick, L. J.; Futterer, K.; Besra, G. S. Structural Basis of Inhibition of Mycobacterium Tuberculosis DprE1 by Benzothiazinone Inhibitors. *Proc. Natl. Acad. Sci.* **2012**, *109* (28), 11354–11359.
- (151) Trefzer, C.; Škovierová, H.; Buroni, S.; Bobovská, A.; Nenci, S.; Molteni, E.; Pojer, F.; Pasca, M. R.; Makarov, V.; Cole, S. T.; Riccardi, G.; Mikušová, K.; Johnsson, K. Benzothiazinones Are Suicide Inhibitors of Mycobacterial Decaprenylphosphoryl- $\beta$ -D-Ribofuranose 2'-Oxidase DprE1. *J. Am. Chem. Soc.* **2012**, *134* (2), 912–915.
- (152) Wang, F.; Sambandan, D.; Halder, R.; Wang, J.; Batt, S. M.; Weinrick, B.; Ahmad, I.; Yang, P.; Zhang, Y.; Kim, J.; Hassani, M.; Huszar, S.; Trefzer, C.; Ma, Z.; Kaneko, T.; Mdluli, K. E.; Franzblau, S.; Chatterjee, A. K.; Johnsson, K.; Johnson, K.; Mikusova, K.; Besra, G. S.; Fütterer, K.; Robbins, S. H.; Barnes, S. W.; Walker, J. R.; Jacobs, W. R.; Schultz, P. G. Identification of a Small Molecule with Activity against Drug-Resistant and Persistent Tuberculosis. *Proc. Natl. Acad. Sci. U. S. A.* **2013**, *110* (27), E2510-7.

- (153) Shirude, P. S.; Shandil, R. K.; Manjunatha, M. R.; Sadler, C.; Panda, M.; Panduga, V.; Reddy, J.; Saralaya, R.; Nanduri, R.; Ambady, A.; Ravishankar, S.; Sambandamurthy, V. K.; Humnabadkar, V.; Jena, L. K.; Suresh, R. S.; Srivastava, A.; Prabhakar, K. R.; Whiteaker, J.; McLaughlin, R. E.; Sharma, S.; Cooper, C. B.; Mdluli, K.; Butler, S.; Iyer, P. S.; Narayanan, S.; Chatterji, M. Lead Optimization of 1,4-Azaindoles as Antimycobacterial Agents. *J. Med. Chem.* **2014**, *57* (13), 5728–5737.
- (154) Shirude, P. S.; Shandil, R.; Sadler, C.; Naik, M.; Hosagrahara, V.; Hameed, S.; Shinde, V.; Bathula, C.; Humnabadkar, V.; Kumar, N.; Reddy, J.; Panduga, V.; Sharma, S.; Ambady, A.; Hegde, N.; Whiteaker, J.; McLaughlin, R. E.; Gardner, H.; Madhavapeddi, P.; Ramachandran, V.; Kaur, P.; Narayan, A.; Guptha, S.; Awasthy, D.; Narayan, C.; Mahadevaswamy, J.; Vishwas, K. G.; Ahuja, V.; Srivastava, A.; Prabhakar, K. R.; Bharath, S.; Kale, R.; Ramaiah, M.; Choudhury, N. R.; Sambandamurthy, V. K.; Solapure, S.; Iyer, P. S.; Narayanan, S.; Chatterji, M. Azaindoles: Noncovalent DprE1 Inhibitors from Scaffold Morphing Efforts, Kill Mycobacterium Tuberculosis and Are Efficacious in Vivo. *J. Med. Chem.* **2013**, *56* (23), 9701–9708.
- (155) Naik, M.; Humnabadkar, V.; Tantry, S. J.; Panda, M.; Narayan, A.; Guptha, S.; Panduga, V.; Manjrekar, P.; Jena, L. K.; Koushik, K.; Shanbhag, G.; Jatheendranath, S.; Manjunatha, M. R.; Gorai, G.; Bathula, C.; Rudrapatna, S.; Achar, V.; Sharma, S.; Ambady, A.; Hegde, N.; Mahadevaswamy, J.; Kaur, P.; Sambandamurthy, V. K.; Awasthy, D.; Narayan, C.; Ravishankar, S.; Madhavapeddi, P.; Reddy, J.; Prabhakar, K. R. K.; Saralaya, R.; Chatterji, M.; Whiteaker, J.; McLaughlin, B.; Chiarelli, L. R.; Riccardi, G.; Pasca, M. R.; Binda, C.; Neres, J.; Dhar, N.; Signorino-Gelo, F.; McKinney, J. D.; Ramachandran, V.; Shandil, R.; Tommasi, R.; Iyer, P. S.; Narayanan, S.; Hosagrahara, V.; Kavanagh, S.; Dinesh, N.; Ghorpade, S. R. 4-Aminoquinolone Piperidine Amides: Noncovalent Inhibitors of DprE1 with Long Residence Time and Potent Antimycobacterial Activity. *J. Med. Chem.* **2014**, *57* (12), 5419–5434.
- (156) Panda, M.; Ramachandran, S.; Ramachandran, V.; Shirude, P. S.; Humnabadkar, V.; Nagalapur, K.; Sharma, S.; Kaur, P.; Guptha, S.; Narayan, A.; Mahadevaswamy, J.; Ambady, A.; Hegde, N.; Rudrapatna, S. S.; Hosagrahara, V. P.; Sambandamurthy, V. K.; Raichurkar, A. Discovery of Pyrazolopyridones as a Novel Class of Noncovalent DprE1 Inhibitor with Potent Anti-Mycobacterial Activity. *J. Med. Chem.* **2014**, *57* (11), 4761–4771.
- (157) Riccardi, G.; Pasca, M. R.; Chiarelli, L. R.; Manina, G.; Mattevi, A.; Binda, C. The DprE1 Enzyme, One of the Most Vulnerable Targets of Mycobacterium Tuberculosis. *Appl. Microbiol. Biotechnol.* **2013**, *97* (20), 8841–8848.

- (158) Leveridge, M.; Buxton, R.; Argyrou, A.; Francis, P.; Leavens, B.; West, A.; Rees, M.; Hardwicke, P.; Bridges, A.; Ratcliffe, S.; Chung, C. Demonstrating Enhanced Throughput of RapidFire Mass Spectrometry through Multiplexing Using the JmjD2d Demethylase as a Model System. *J. Biomol. Screen.* **2014**, *19* (2), 278–286.
- (159) Hutchinson, S. E.; Leveridge, M. V.; Heathcote, M. L.; Francis, P.; Williams, L.; Gee, M.; Munoz-Muriedas, J.; Leavens, B.; Shillings, A.; Jones, E.; Homes, P.; Baddeley, S.; Chung, C.-w.; Bridges, A.; Argyrou, A. Enabling Lead Discovery for Histone Lysine Demethylases by High-Throughput RapidFire Mass Spectrometry. *J. Biomol. Screen.* **2012**, *17* (1), 39–48.
- (160) Brown Nigel, Shull Gary, Kao John, Goulding Eugenia, F. S. Teratogenicity and Lethality of Hydantoin Derivatives in the Mouse: Structure-Toxicity Relationships. *Toxicol. Appl. Pharmacol.* **1982**, *64*, 271–288.
- (161) Hanson, J. W.; Buehler, B. A. Fetal Hydantoin Syndrome: Current Status. *J. Pediatr.* **1982**, *101* (5), 816–818.
- (162) Hill, D. S.; Wlodarczyk, B. J.; Palacios, A. M.; Finnell, R. H. Teratogenic Effects of Antiepileptic Drugs. *Expert Rev. Neurother.* **2010**, *10* (6), 943–959.
- (163) Zha, C.; Brown, G. B.; Brouillette, W. J. Synthesis and Structure-Activity Relationship Studies for Hydantoins and Analogues as Voltage-Gated Sodium Channel Ligands. *J. Med. Chem.* **2004**, *47* (26), 6519–6528.
- (164) Oballa, R. M.; Truchon, J. F.; Bayly, C. I.; Chauret, N.; Day, S.; Crane, S.; Berthelette, C. A Generally Applicable Method for Assessing the Electrophilicity and Reactivity of Diverse Nitrile-Containing Compounds. *Bioorganic Med. Chem. Lett.* **2007**, *17*, 998–1002.
- (165) Potashman, M. H.; Duggan, M. E. Covalent Modifiers: An Orthogonal Approach to Drug Design. *J. Med. Chem.* **2009**, *52* (5), 1231–1246.
- (166) Smith, D. A. *Metabolism, Pharmacokinetics, and Toxicity of Functional Groups: Impact of the Building Blocks of Medicinal Chemistry in ADMET*; Royal Society of Chemistry, 2010.
- (167) Young, R. J.; Green, D. V. S.; Luscombe, C. N.; Hill, A. P. Getting Physical in Drug Discovery II: The Impact of Chromatographic Hydrophobicity Measurements and Aromaticity. *Drug Discov. Today* **2011**, *16* (17–18), 822–830.
- (168) Malátková, P.; Wsól, V. Carbonyl Reduction Pathways in Drug Metabolism. *Drug Metab. Rev.* **2014**, *46* (1), 96–123.
- (169) von Kieseritzky, F.; Lindström, J. Aziridines in One Step from Hydantoins via Red-Al

- Mediated Ring-Contraction. *Tetrahedron Lett.* **2011**, *52* (35), 4558–4561.
- (170) Olimpieri, F.; Bellucci, M. C.; Volonterio, A.; Zanda, M. A Mild, Efficient Approach for the Synthesis of 1,5-Disubstituted Hydantoins. *European J. Org. Chem.* **2009**, *2009* (35), 6179–6188.
- (171) Colacino, E.; Lamaty, F.; Martinez, J.; Parrot, I. Microwave-Assisted Solid-Phase Synthesis of Hydantoin Derivatives. *Tetrahedron Lett.* **2007**, *48* (30), 5317–5320.
- (172) Stilz, H. U.; Guba, W.; Jablonka, B.; Just, M.; Klingler, O.; König, W.; Wehner, V.; Zoller, G. Discovery of an Orally Active Non-Peptide Fibrinogen Receptor Antagonist Based on the Hydantoin Scaffold. *J. Med. Chem.* **2001**, *44* (8), 1158–1176.
- (173) Safari, J.; Javadian, L. A One-Pot Synthesis of 5,5-Disubstituted Hydantoin Derivatives Using Magnetic Fe<sub>3</sub>O<sub>4</sub> Nanoparticles as a Reusable Heterogeneous Catalyst. *Comptes Rendus Chim.* **2013**, *16* (12), 1165–1171.
- (174) Mahmoodi, N. O.; Khodaei, Z. Evaluating the One-Pot Synthesis of Hydantoins. *ARKIVOC* **2007**, *2007* (iii), 29–36.
- (175) Safari, J.; Gandomi-Ravandi, S.; Javadian, L. Microwave-Promoted Facile and Rapid Synthesis Procedure for the Efficient Synthesis of 5,5-Disubstituted Hydantoins. *Synth. Commun.* **2013**, *43* (23), 3115–3120.
- (176) 5.2 Chemical Shift <https://www.chem.wisc.edu/areas/reich/nmr/05-hmr-02-delta.htm> (accessed Jun 1, 2016).
- (177) Meanwell, N. a. Synopsis of Some Recent Tactical Application of Bioisosteres in Drug Design. *J. Med. Chem.* **2011**, *54*, 2529–2591.
- (178) Gillis, E. P.; Eastman, K. J.; Hill, M. D.; Donnelly, D. J.; Meanwell, N. a. Applications of Fluorine in Medicinal Chemistry. *J. Med. Chem.* **2015**, 150722143650003.
- (179) Murray, C. W.; Erlanson, D. a; Hopkins, A. L.; Keseru, G. M.; Leeson, P. D.; Rees, D. C.; Reynolds, C. H.; Richmond, N. J. Validity of Ligand Efficiency Metrics. **2014**, 616–618.
- (180) Leeson, P. D.; Springthorpe, B. The Influence of Drug-like Concepts on Decision-Making in Medicinal Chemistry. *Nat. Rev. Drug Discov.* **2007**, *6* (11), 881–890.
- (181) Tarcsay, Á.; Nyíri, K.; Keserú, G. M. Impact of Lipophilic Efficiency on Compound Quality. *J. Med. Chem.* **2012**, *55* (3), 1252–1260.
- (182) Da Silva, P. E. A.; Palomino, J. C. Molecular Basis and Mechanisms of Drug Resistance in Mycobacterium Tuberculosis: Classical and New Drugs. *J. Antimicrob. Chemother.* **2011**, *66*



- (7), 1417–1430.
- (183) Fonseca, J. D.; Knight, G. M.; McHugh, T. D. The Complex Evolution of Antibiotic Resistance in Mycobacterium Tuberculosis. *Int. J. Infect. Dis.* **2015**, *32*, 94–100.
- (184) Guo, H.; Seet, Q.; Denkin, S.; Parsons, L.; Zhang, Y. Molecular Characterization of Isoniazid-Resistant Clinical Isolates of Mycobacterium Tuberculosis from the USA. *J. Med. Microbiol.* **2006**, *55* (11), 1527–1531.
- (185) Shi, W.; Zhang, X.; Jiang, X.; Yuan, H.; Lee, J. S.; Barry, C. E.; Wang, H.; Zhang, W.; Zhang, Y. Pyrazinamide Inhibits Trans-Translation in Mycobacterium Tuberculosis. *Science* **2011**, *333* (6049), 1630–1632.
- (186) Bunnage, M. E.; Chekler, E. L. P.; Jones, L. H. Target Validation Using Chemical Probes. *Nat. Chem. Biol.* **2013**, *9* (4), 195–199.
- (187) Rullas, J.; García, J. I.; Beltrán, M.; Cardona, P. J.; Cáceres, N.; García-Bustos, J. F.; Angulo-Barturen, I. Fast Standardized Therapeutic-Efficacy Assay for Drug Discovery against Tuberculosis. *Antimicrob. Agents Chemother.* **2010**, *54* (5), 2262–2264.
- (188) Stover, C. K.; de la Cruz, V. F.; Fuerst, T. R.; Burlein, J. E.; Benson, L. A.; Bennett, L. T.; Bansal, G. P.; Young, J. F.; Lee, M. H.; Hatfull, G. F. New Use of BCG for Recombinant Vaccines. *Nature* **1991**, *351* (6326), 456–460.
- (189) Franzblau, S. G.; Witzig, R. S.; Mclaughlin, J. C.; Torres, P.; Madico, G.; Hernandez, A.; Degnan, M. T.; Cook, M. B.; Quenzer, V. K.; Ferguson, R. M.; Gilman, R. H. Rapid, Low-Technology MIC Determination with Clinical Mycobacterium Tuberculosis Isolates by Using the Microplate Alamar Blue Assay. *J. Clin. Microbiol.* **1998**, *36* (2), 362–366.
- (190) Parish, T.; Stoker, N. G. Mycobacteria Protocols. *Methods Mol. Biol.* **2015**, *101*, 77–103.
- (191) Makarov, V.; Lechartier, B.; Zhang, M.; Neres, J.; van der Sar, A. M.; Raadsen, S. a; Hartkoorn, R. C.; Ryabova, O. B.; Vocat, A.; Decosterd, L. A.; Widmer, N.; Buclin, T.; Bitter, W.; Andries, K.; Pojer, F.; Dyson, P. J.; Cole, S. T. Towards a New Combination Therapy for Tuberculosis with next Generation Benzothiazinones. *EMBO Mol. Med.* **2014**, *6* (3), 372–383.
- (192) Neres, J.; Hartkoorn, R. C.; Chiarelli, L. R.; Gadupudi, R.; Pasca, M. R.; Mori, G.; Venturelli, A.; Savina, S.; Makarov, V.; Kolly, G. S.; Molteni, E.; Binda, C.; Dhar, N.; Ferrari, S.; Brodin, P.; Delorme, V.; Landry, V.; de Jesus Lopes Ribeiro, A. L.; Farina, D.; Saxena, P.; Pojer, F.; Carta, A.; Luciani, R.; Porta, A.; Zanoni, G.; De Rossi, E.; Costi, M. P.; Riccardi, G.; Cole, S. T. 2-Carboxyquinoxalines Kill Mycobacterium Tuberculosis through Noncovalent Inhibition of

- DprE1. *ACS Chem. Biol.* **2015**, *10* (3), 705–714.
- (193) Phummarin, N.; Boshoff, H. I.; Tsang, P. S.; Dalton, J.; Wiles, S.; Barry 3rd, C. E.; Copp, B. R. SAR and Identification of 2-(Quinolin-4-Yloxy)acetamides as Mycobacterium Tuberculosis Cytochrome Bc<sub>1</sub> Inhibitors. *Med. Chem. Commun.* **2016**.
- (194) Remuiñán, M. J.; Pérez-Herrán, E.; Rullás, J.; Alemparte, C.; Martínez-Hoyos, M.; Dow, D. J.; Afari, J.; Mehta, N.; Esquivias, J.; Jiménez, E.; Ortega-Muro, F.; Fraile-Gabaldón, M. T.; Spivey, V. L.; Loman, N. J.; Pallen, M. J.; Constantinidou, C.; Minick, D. J.; Cacho, M.; Rebollo-López, M. J.; González, C.; Sousa, V.; Angulo-Barturen, I.; Mendoza-Losana, A.; Barros, D.; Besra, G. S.; Ballell, L.; Cammack, N. Tetrahydropyrazolo[1,5-a]Pyrimidine-3-Carboxamide and N-Benzyl-6',7'-Dihydrospiro[Piperidine-4,4'-Thieno[3,2-c]Pyran] Analogues with Bactericidal Efficacy against Mycobacterium Tuberculosis Targeting MmpL3. *PLoS One* **2013**, *8* (4).

# Curriculum Vitae

---



# Eleni Pitta

---

Efesou 2, Block D, Flat 304, Pallouriotissa, 1041, Nicosia, Cyprus | eleni.p.pitta@gmail.com

## Education

### PH.D. | UNIVERSITY OF ANTWERP | 2013 – 2017

- Medicinal Chemistry, Department of Pharmaceutical Sciences
- Marie Sklodowska-Curie fellow within the OpenMedChem project
- Thesis titled “Structural investigation of two quinoloxycetamide- and hydantoin-based novel classes of antimycobacterials guided by phenotypic screening and targeted approaches”

### M.SC. | ARISTOTLE UNIVERSITY OF THESSALONIKI | 2008-2010

- Medicinal Chemistry, Department of Pharmaceutical Sciences
- Thesis titled “Design, synthesis and biological evaluation of novel 4-thiazolidinones as potential HIV-1 inhibitors”
- European program Erasmus Placement, Computational Chemistry, University of Siena, Italy

### B.SC. | ARISTOTLE UNIVERSITY OF THESSALONIKI | 2003-2008

- Pharmaceutical Sciences
- European program Socrates-Erasmus, Laboratory of Microwave-Assisted Chemistry, Catholic University of Leuven, Belgium

## Experience

### LECTURER | FREDERICK UNIVERSITY | 2016-PRESENT

- Teaching the following courses: Medicinal Chemistry, Natural Products Chemistry, Pharmacology, ADMET.
- Thesis supervising for Bachelor students
- Writing and applying for research grants

### RESEARCH SCIENTIST | UNIVERSITY OF ANTWERP | 2013-2014

#### GLAXOSMITHKLINE SPAIN | 2014-2016

- Design, synthesis, purification and full characterization of novel organic molecules
- Analysis and interpretation of biological data
- Decision making and future planning for the project
- Scientific writing and literature review

### CLINICAL PHARMACIST | MEDICAL CLINIC ‘MICHAEL AGGELIS’ | 2010-2012

- Establishing, organizing, and managing clinic’s pharmacy
- Working closely with medical and nursing staff to ensure patients receive the most appropriate treatments

- Inventory management of medicines, maintaining medication records, issuing insurance funds documentation, authoring regulatory documents, and reporting any adverse effects

**LABORATORY ASSISTANT | ARISTOTLE UNIVERSITY OF THESSALONIKI | 2009-2010**

- Assisting professors in running and maintaining the laboratory of the Medicinal Chemistry Department

**PHARMACY ASSISTANT | M. NATSOURA PHARMACY | 2008-2009**

- Management of pharmacy inventory and dispensing medicines

## **Skills & Abilities**

- Good written and verbal communication skills
- I.T. skills including experience in Microsoft Office (Word, Excel, Powerpoint) and scientific software (ChemDraw, MestReNova, ACD labs, Discovery Studio, MOE, AutoDock etc.)
- Strong analytical and problem-solving skills
- Good organization, with high attention to accuracy and detail
- Self-motivation and ability to take the initiative
- Team working skills
- Strong administration and co-ordination skills

## **Languages**

- Greek: native
- English: fluent
- Spanish: intermediate
- Italian: basic

## **Scientific achievements**

- 06/2015 | Participation at the 65<sup>th</sup> Lindau Nobel Laureate Meeting
- 01/2013 - 01/2016 | Marie Sklodowska-Curie Fellowship
- 07/2012 | Grant for my participation at the European School of Medicinal Chemistry
- 05/2012 | Award from the Department of European Educational Programs
- 09/2009 – 06/2010 | Scholarship from the Alexander Onassis Public Benefit Foundation
- 05/2009 | Award from the Panhellenic Pharmaceutical Association
- 02/2009 | Award from the Panhellenic Pharmaceutical Industry Association
- 09/2008 – 06/2009 | Scholarship from the Cyrillic Center of Youths
- 07/2008 | Award from the Aristotle University of Thessaloniki
- 09/2003 – 06/2005 | Scholarship from the State Scholarship Foundation of Greece

## Publications

- **Eleni Pitta** *et al.*, Differential characterization using readily accessible NMR experiments of novel *N*- and *O*-alkylated quinolin-4-ol, 1,5-naphthyridin-4-ol and quinazolin-4-ol derivatives with antimycobacterial activity, *J.Eur.Med.Chem.*, 2017; 125, 890-901.
- **Eleni Pitta** *et al.*, Searching for new leads for Tuberculosis: Design, synthesis, and biological evaluation of novel 2-quinolin-4-yloxyacetamides, *J.Med.Chem.*, 2016, 59 (14), 6709–6728.
- **Eleni Pitta** *et al.*, 4-Thiazolidinone derivatives as potent antimicrobial agents: microwave-assisted synthesis, biological evaluation and docking studies, *MedChemComm.*, 2015, 6, 319-326.
- Athina A. Geronikaki, **Eleni P. Pitta**, Konstantinos S. Liaras, Antioxidant activity of thiazole and thiazolidinone derivatives, *Curr Med Chem.*, 2013, 20 (36) 4460-80.
- **Eleni Pitta** *et al.*, Synthesis and HIV-1 RT inhibitory action of novel (4/6-substituted benzo[d]thiazol -2-yl)thiazolidin-4-ones. Divergence from the non-competitive inhibition mechanism, *J. Enzyme Inhib. Med. Chem.*, 2013, 28 (1), 113-22.
- Manas Chakrabarty, Ajanta Mukherji, Sulakshana, Ratna Mukherjee, Kenichiro Nagai, Athina Geronikaki, **Pitta Eleni**, An expedient synthesis of novel 2-substituted thiazolo[4,5-f]isoquinolines/quinolines and benzo[1,2-d:4,3-d']bisthiazoles and their potential as inhibitors of COX-1 and COX-2, *ARKIVOC*, 2010 (xi), 265-290.
- **Eleni Pitta** *et al.*, Novel thiazolidinone derivatives with an uncommon mechanism of inhibition towards HIV-1 Reverse Transcriptase, *L.D.D.D.*, 2010, 7 (4), 228-234.

## Oral presentation

- Hit to lead optimization of novel quinoloxycetamide derivatives against *M. tuberculosis*, II Simposio de jovenes investigadores de la SEQT, Madrid, 2015.

